AN EXPERIMENTAL STUDY OF THE THERMODYNAMIC PROPERTIES OF MOLECULARLY SIMPLE LIQUID MIXTURES

LÉLIO Q. LOBO

Wolfson College

BODLEIAN LIBRARY OXFORD
DEPOSITED
THESIS
25-7-79

This thesis is submitted in partial fulfilment of the requirements for the degree of Doctor of Philosophy in the University of Oxford

Inorganic Chemistry Laboratory

April, 1979

To

LUÍSA,

my wife.

CONTENTS

			Page
		PART 1	
		INTRODUCTION	1
CHAPTER	1	INTRODUCTION	2
	1.1	REFERENCES	11
		PART 2	
		EXPERIMENTAL	14
CHAPTER	2	PREPARATION OF GASES	15
	2.1	SOURCES	15
	2.2	PURIFICATION	17
	2.3	TRIPLE-POINTS	31
	2.4	REFERENCES	40
CHAPTER	3	VAPOUR PRESSURE AND MOLAR VOLUME MEASUREMENTS	42
	3.1	THE APPARATUS AND ITS ACCESSORIES	42
	3.2	VAPOUR PRESSURES. EXPERIMENTAL PROCEDURE	56
	3.3	MOLAR VOLUMES. EXPERIMENTAL PROCEDURE	63
	3.4	REFERENCES	67
CHAPTER	4	ENTHALPY OF MIXING MEASUREMENTS	68
	4.1	THE HEAT OF MIXING LOW-TEMPERATURE CALORIMETER	71
	4.2	EXPERIMENTAL PROCEDURE	89
	4.3	REFERENCES	99
		PART 3	
		CALCULATIONS	100
CHAPTER	5	CALCULATION OF THE EXCESS MOLAR GIBBS ENERGY G^E	100
	5.1	G^E FROM TOTAL VAPOUR PRESSURE MEASUREMENTS	101
	5.2	G^E AS A FUNCTION OF COMPOSITION	109
	5.3	CALCULATION OF THE COMPOSITIONS OF THE LIQUID AND VAPOUR PHASES	109
	5.4	REFERENCES	114

CONTENTS

(continued)

		Page
CHAPTER 6	CALCULATION OF THE EXCESS MOLAR VOLUME V^E	115
6.1	V^E FROM DENSITY MEASUREMENTS	115
6.2	V^E AS A FUNCTION OF COMPOSITION	117
6.4	REFERENCES	119
CHAPTER 7	CALCULATION OF THE EXCESS MOLAR ENTHALPY H^E	120
7.1	H^E FROM CALORIMETRIC MEASUREMENTS	120
7.2	H^E AS A FUNCTION OF COMPOSITION	125
7.3	CALCULATION OF THE COMPOSITIONS	126
7.4	H^E FOR TWO PARTIALLY MISCIBLE LIQUIDS	130
7.5	REFERENCES	133
	PART 4	
	RESULTS AND DISCUSSION	134
CHAPTER 8	THE SYSTEM ARGON + KRYPTON	135
8.1	INTRODUCTION	135
8.2	CALCULATION OF G^E AT 138 AND 143 K	136
8.3	DISCUSSION	141
8.4	REFERENCES	145
CHAPTER 9	THE SYSTEM XENON + HYDROGEN CHLORIDE	146
9.1	INTRODUCTION	146
9.2	DETERMINATION OF H^E AT 182.26 K	147
9.3	DISCUSSION	153
9.4	REFERENCES	158
CHAPTER 10	THE SYSTEM XENON + NITROUS OXIDE	159
10.1	INTRODUCTION	159
10.2	DETERMINATION OF G^E, V^E AND H^E	160
10.3	DISCUSSION	169
10.4	REFERENCES	173

CONTENTS

(continued)

		Page
CHAPTER 11	THE SYSTEM XENON + CARBON TETRAFLUORIDE	175
11.1	INTRODUCTION	175
11.2	DETERMINATION OF V^E AND H^E	175
11.3	DISCUSSION	182
11.4	REFERENCES	186
CHAPTER 12	THE SYSTEM XENON + HEXAFLUOROETHANE	187
12.1	INTRODUCTION	187
12.2	DETERMINATION OF H^E AT 175.00 K	188
12.3	DISCUSSION	191
12.4	REFERENCES	194
CHAPTER 13	THE SYSTEM HYDROGEN CHLORIDE + NITROUS OXIDE	195
13.1	INTRODUCTION	195
13.2	DETERMINATION OF G^E, V^E AND H^E	196
13.3	DISCUSSION	203
13.4	REFERENCES	205
CHAPTER 14	THE SYSTEM HYDROGEN CHLORIDE + CARBON TETRAFLUORIDE	206
14.1	INTRODUCTION	206
14.2	DETERMINATION OF G^E AT 159.01 K AND 173.08 K	207
14.3	COMPOSITION OF THE VAPOUR AND THE TWO LIQUID PHASES IN EQUILIBRIUM	211
14.4	DETERMINATION OF H^E AT 162.97 K	214
14.5	DISCUSSION	216
14.6	REFERENCES	220
CHAPTER 15	THE SYSTEM NITROUS OXIDE + ETHYLENE	221
15.1	INTRODUCTION	221
15.2	DETERMINATION OF G^E, V^E AND H^E	222
15.3	DISCUSSION	229
15 4	REFERENCES	234
CHAPTER 16	THE SYSTEM ETHYLENE + METHANE	236
16.1	INTRODUCTION	236
16.2	DETERMINATION OF H^E AT 115.77, 140.12 AND 150.00 K	237
16.3	DISCUSSION	244
16.4	REFERENCES	248

CONTENTS

(continued)

		Page
CHAPTER 17	THE VAPOUR PRESSURE OF CARBON TETRAFLUORIDE	249
17.1	INTRODUCTION	249
17.2	RESULTS AND DISCUSSION	251
17.3	REFERENCES	258
	PART 5	
	CONCLUSIONS	260
CHAPTER 18	FINAL COMMENTS	261
18.1	REFERENCES	265
	PART 6	
	APPENDICES	266
APPENDIX (A)	MERCURY CAPILLARY DEPRESSIONS	267
APPENDIC (B)	PRESSURE CONVERSION FACTORS	268
APPENDIX (C)	CALIBRATED VOLUMES IN THE G^E AND V^E APPARATUS	269
APPENDIX (D)	CALIBRATION OF TEXAS INSTRUMENTS PRESSURE GAUGES	270
APPENDIX (E)	ERROR IN THE OVERALL COMPOSITION OF THE MIXTURES	271
APPENDIX (F)	CALIBRATED VOLUMES IN THE H^E APPARATUS	273
APPENDIX (G)	CALIBRATION OF THE AUXILIARY COPPER RESISTANCE THERMOMETERS	274
APPENDIX (H)	CALIBRATION OF THE CALORIMETER COPPER RESISTANCE THERMOMETER	275
APPENDIX (I)	SOME PROPERTIES OF THE REDLICH-KISTER EQUATION (5.37)	276
APPENDIX (J)	BARKER'S METHOD FOR THE EVALUATION OF G^E	278
APPENDIX (K)	ERRORS IN G^E	282
APPENDIX (L)	ERRORS IN V^E	284
APPENDIX (M)	ERRORS IN H^E	286
APPENDIX (N)	ESTIMATION OF V^E FOR $CH_4 + C_2H_4$	290

AKNOWLEDGEMENTS

First and foremost I would like to express my deepest gratitude to my supervisor, Dr L.A.K. Staveley, for his kindness, constant interest and advice throughout the course of this work; but for him, none of it would have been.

I am also in debt to Professor K.E. Gubbins of Cornell University and his co-workers, especially Dr Paulette Clancy, for communications and discussion relating to the perturbation theory calculations which they have been (and are) carrying out on some of the systems I studied experimentally.

I should also like to acknowledge the help given by Mr J. Walton (Engineering Sciences Data Unit), working at the National Physical Laboratory, who fitted the Wagner equation to the experimental data on the vapour pressure of carbon tetrafluoride.

Thanks are also due to my colleague Mr Paul Clayton for his invaluable help on technical points, and to the laboratory staff for their prompt assistance whenever their expertise was required.

From January 1976 to January 1979 my stay in Oxford was made possible by the award of a research fellowship from Comissão Permanente Invotan (Junta Nacional de Investigação Científica e Tecnológica/Portugal).

AN EXPERIMENTAL STUDY OF THE THERMODYNAMIC PROPERTIES

OF MOLECULARLY SIMPLE LIQUID MIXTURES

LÉLIO Q. LOBO , WOLFSON COLLEGE

Thesis submitted for the degree of Doctor of Philosophy, University of Oxford

---

ABSTRACT

The object of this work was to provide accurate experimental values of the primary thermodynamic excess functions — the excess Gibbs energy G^E, the enthalpy of mixing H^E, and the excess volume V^E — of suitably chosen binary liquid mixtures, with which modern theories of solutions, especially those which take polarity into account, could be tested. All the systems studied, therefore, involve at least one (multi-)polar component, this being selected from the following substances: $HC\ell$, N_2O, C_2H_4, CH_4, CF_4 and C_2F_6. Xenon was used as the second, non-polar component in four of the binary mixtures. G^E was derived from vapour pressure measurements, H^E determined by calorimetry, and V^E obtained by a pyknometric technique. The experimental results obtained for each of the excess properties, M^E, where generally fitted to a Redlich-Kister-type equation.

$$M^E = x_1 (1 - x_1) [A_M + B_M (2 x_1 - 1) + C_M (2 x_1 - 1)^2]$$

with the following values of the coefficients (G^E and H^E in $J\,mol^{-1}$, and V^E in $cm^3\,mol^{-1}$):

Component 1	Component 2	Property	T/K	A_M	B_M	C_M
$HC\ell$	Xe	H^E / RT	182.26	2.1430	- 0.3178	- 0.3654
N_2O	Xe	G^E / RT	182.32	1.1829	0.0532	0.0425
		H^E / RT	184.05	2.3574	- 0.0273	0.5827
		V^E	182.32	2.617	- 0.878	0.100
Xe	CF_4	H^E / RT	163.01	2.8310	0.1597	-
		V^E	159.01	7.747	- 2.027	-
Xe	C_2F_6	H^E / RT	175.00	2.9654	0.7798	- 2.0862
$HC\ell$	N_2O	G^E / RT	182.32	0.3875	- 0.0171	0.0209
		H^E / RT	184.03	0.2757	- 0.0547	- 0.0461
		V^E	182.32	0.583	0.083	0.129
$HC\ell$	CF_4	G^E / RT	159.01	3.90	- 0.80	-
			173.08	3.35	- 1.20	-
		H^E / RT	162.97	(5.85)	(- 6.97)	-
N_2O	C_2H_4	G^E / RT	182.32	0.4457	0.0674	-
		H^E / RT	184.01	0.7082	0.0759	-
		V^E	182.32	-	-	-

Three other investigations were carried out: (1) G^E for the Ar + Kr system was calculated at two relatively high temperatures (138 and 143 K) from results which had recently been published in the literature. (2) H^E for $CH_4 + C_2H_4$ was measured at three temperatures (115.77, 140.12 and 150.00 K), so making it possible to derive a general expression for G^E as a function of both temperature and composition. (3) the vapour pressure of pure CF_4 was measured at several temperatures and the Wagner equation used to fit the experimental points.

Whenever possible, the experimental results for the binary mixtures were compared with the values calculated by Professor K.E.Gubbins and his group using the perturbation theory which they have recently been developing. Although their theory fails to reproduce the experimental H^E for $HC\ell + Xe$, it seems to be able to give results in agreement with experiment for all three excess functions of systems in which the polar component does not have a large dipole moment.

'... molecules ... are complicated
'individuals' whose 'personalities'
are sensitive to their environment.'

J.M. PRAUSNITZ

PART 1

INTRODUCTION

CHAPTER 1 - INTRODUCTION

CHAPTER 1

INTRODUCTION

For over a century the investigation and interpretation of the physical properties of liquid mixtures have been a major branch of Physical Chemistry. However, from the quantitative point of view, it is only in the past twenty five years or so that some progress has been achieved in attempting to explain the properties of solutions of non-electrolytes on a molecular basis, as a consequence of the enormous experimental and theoretical effort devoted to the study of liquids and liquid mixtures during this period. Despite the considerable advances made in understanding the factors which determine the magnitude of the thermodynamic properties of solutions, current theories of liquid mixtures are still far from making successful quantitative predictions, with the possible exception of the special case of polymer solutions.

It has become common practice, both in theory and experiment, to express the thermodynamic properties of a mixture in terms of its excess properties, an excess property M^E being defined as the difference between the value of the property M for an actual mixture and that of an ideal mixture of the same composition, M^{id}, under the same conditions of pressure and temperature, i.e.

$$M^E = M - M^{id} \qquad \ldots (1.1)$$

In the present work we shall follow this practice, which is due to SCATCHARD[1].

The failure, or at least only limited success, of the ability of the theories available at present to predict these excess properties has been regarded partly as a consequence of the imperfection of the theoretical models themselves, and partly as the result of our rather limited knowledge

of the forces between molecules. Moreover, lack of experimental information in some important areas has also hampered the progress of theory.

Modern theories can be broadly classified as follows†:

(i) Corresponding states methods[7]. These should, in principle, strictly apply to liquid mixtures of the rare gases and other nearly spherically symmetrical molecules (such as CH_4); therefore the main disadvantage in the use of these methods is the difficulty in extending them to mixtures involving components which do not conform to the basic principle. Guidelines have nevertheless been advanced for such an extension[8]. Agreement with experiment has been found to be moderate in more or less favourable cases, but one should not expect this when polar components are involved. The two-fluid version of this theory has not been found to be superior to the simpler, one-fluid model[9]. Recently, HAYNES, HIZA and McCARTY[10] found the van der Waals one-fluid method to reproduce the experimental values of the densities of quite complex LNG mixtures, with a total uncertainty of less than 0.1%. However, in their work a complete set of highly accurate density experimental data for the binary mixtures was available and an equation of state with no less than 33 parameters was used for the reference fluid (methane).

---

† The so-called 'chemical' theory of liquid mixtures[2] and those of regular[1,3] and polymer[4] solutions, which apply to particular classes of mixtures not relevant to the present work, have not been considered in the listing, nor has the 'average potential model' developed by PRIGOGINE and his collaborators[5], since this has been found to give results in poor agreement with experiment even for mixtures of molecularly simple components. Monte Carlo and Molecular Dynamics machine calculations[6] can be regarded more as computer experiments than as theories of liquid mixtures.

(ii) Methods based on equations of state[11-13]. These are mainly useful for interpolation between already existing experimental measurements. They can lead to serious errors when applied to mixtures (or regions) for which experimental results are not available[8], and even when such results do exist the asymmetry of the curves of the excess properties when plotted against composition is often incorrectly predicted[14]. [See also Appendix (N) of this thesis.] For many mixtures, the value of $H^E_{\frac{1}{2}}$ — the excess molar enthalpy for the equimolar mixture — is not correctly estimated even after adjusting $G^E_{\frac{1}{2}}$ and $V^E_{\frac{1}{2}}$ to the experimental results[15,16]. The equations of state most widely used are those which combine a hard-spheres-like term for repulsion with a van der Waals-like term for attraction. These methods can be considered as semi-theoretical. Both one- and two-fluid versions have been employed, with no clear advantage of one over the other.

(iii) Group contribution methods[17-20]. These methods aim at reducing the excess properties of mixtures to a combination of terms arising from the functional groups present in the species involved. This requires, of course, the knowledge of a wide range of experimental information from which group parameters can, in principle, be worked out. Although useful for many applications, this approach, which falls in the category of an application of Molecular Thermodynamics, cannot be considered as being on the same footing as the other methods listed here because it gives no insight into the fundamental phenomena at the molecular level which determine the different behaviour of different liquid mixtures. Moreover, mixtures involving the simpler molecules — such as those studied in the present work — fall outside the range of these methods.

(iv) Variational methods[21]. This approach has been, perhaps, the least explored among those listed here. It was applied with some success to binary liquid mixtures involving the rare gases and some of the simpler diatomic molecules. Although the agreement achieved between theory and experiment was only moderate, it could be regarded as encouraging since it was obtained when the method was only in the initial stages of its development. It is therefore somewhat surprising that no further work appears to have been published on this subject since then.

(v) Perturbation methods[22,23]. Although the application of these methods to the study of liquid mixtures is not new, their relative importance has been increased by the extension, made in recent years, to the treatment of liquid mixtures involving components with non-spherical, polar molecules. In two fundamental papers[24,25] GUBBINS and his co-workers showed how strongly anisotropic terms could be included in the intermolecular potential. Starting with argon + krypton as the reference ('unperturbed') system, they examined the consequences of the inclusion of such terms in the intermolecular pair potential. In other words, they studied the effect of adding point dipoles, quadrupoles and/or octupoles to the molecules of one or both of the components of the reference mixture as well as that resulting from an anistropic overlap (shape) potential. This model has been refined in subsequent work, and has proved to be able to reproduce very closely the experimental results for several strongly non-ideal liquid mixtures, as we shall see in later chapters of this thesis.

A common feature of all these methods is that they require the introduction of at least one and sometimes two adjustable quantities to account adequately for the interaction between pairs of unlike molecules†. Usually this has been accomplished by considering 'deviation parameters' j_{12} and k_{12} to the Lorentz-Berthelot combination rules for obtaining the cross-parameters σ_{12} and ε_{12} of the intermolecular pair potential,

$$\sigma_{12} = \tfrac{1}{2}(1 + j_{12})(\sigma_{11} + \sigma_{22}) \qquad \text{(LORENTZ)}$$

$$\varepsilon_{12} = (1 - k_{12})(\varepsilon_{11}\,\varepsilon_{22})^{\frac{1}{2}} \qquad \text{(BERTHELOT).}$$

Sometimes the introduction of j_{12} may be neglected, but failure to include a non-zero k_{12} parameter of appropriate magnitude almost always seriously weakens the quantitative value of every method of prediction, giving rise, in some cases, to the calculated excess thermodynamic functions of the wrong sign. The fact that different theories generally require different (sometimes quite different) values for the same parameter, is in itself an indication of their unequal reliabilities. Several more or less semi-empirical methods have been proposed to estimate k_{12} [26,27], each with its own shortcomings. In principle, it is possible to determine the k_{12} values from independent experimental sources by methods which rest on a sound theoretical basis. For example, k_{12} can be obtained from a knowledge of the intermolecular pair potential which can be derived from experimental data, for instance, second virial coefficients or transport properties.

There is little doubt that intermolecular potential functions will continue to play a fundamental role in the theoretical treatment of molecular solutions, and that accordingly special importance will continue to

---

† The 'group interaction parameters' a_{mn} in UNIFAC ('UNIversal quasi-chemical Functional-group Activity Coefficients'), an example of methods (iii), may be regarded as playing a similar role.

be attached to the study of systems involving small, relatively simple molecules for which the pair potential parameters are likely to be known most accurately. This is why so much prominence has already been given to the mixtures of the rare gases, in particular Ar + Kr and Kr + Xe, since these are the only two such mixtures that can be experimentally studied over the entire liquid composition range. STAVELEY and his collaborators[28] have contributed to these studies. Information recently made available on Ar + Kr [29,30] has enabled the author to make a small contribution (Chapter 8) to this effort by estimating the excess molar Gibbs energy G^E at two relatively high temperatures, and using these results together with a value of the enthalpy of mixing measured in this laboratory[31] to draw some semi-quantitative conclusions about the temperature dependence of H^E, the excess molar enthalpy, of this system.

The introduction of diatomic species in the systems to be studied necessarily implies the presence of quadrupoles (for homonuclear molecules) or both dipoles and quadrupoles (if heteronuclear diatomics are involved). Some systems in this class have already been studied[32] but in general the electric moments in the diatomic molecules were either insignificant, or at least small. An important exception is the system Xe + HCℓ [33] since the small hydrogen chloride molecule has a relatively large dipole moment.

At the start of the work described in this thesis recently published papers by GUBBINS and his co-workers[24,25] had drawn attention to the need for accurate experimental studies of liquid mixtures involving species simultaneously as strongly (multi-)polar and as simple as possible. From the experimental point of view, other requirements have also to be met if such studies are to be feasible: the two components of every mixture should be available or easily preparable in a high state of purity, they

must be chemically stable and have suitable overlapping liquid ranges, and possess relatively low vapour pressures in the temperature range of interest. Moreover, certain properties of the pure substances, notably liquid densities and the electric moments, should be known with sufficient accuracy in order to make the theoretical calculations worthwhile. These stringent constraints effectively limit the choice to a very small number of substances. Among these, xenon, hydrogen chloride, nitrous oxide, ethylene, methane and carbon tetrafluoride were judged to be suitable components for the systems to be studied. From the purely theoretical point of view some of these substances and their binary mixtures will, of course, leave something to be desired, but a compromise between the claims of theory and experiment had clearly to be reached. In practice, one cannot have, for instance, a dipolar species with no quadrupole, this being perhaps the simplest example of how different the situations of the experimentalist and of the theoretician really are: while the latter can vary the parameters in his equations more or less continuously, as he chooses, the experimentalist has to work with the materials nature provides. We are confident, however, that the model systems we have selected for the experimental work are adequate for our main purpose — i.e., to provide information on which current theories can be tested. The actual mixtures studied in the present work are shown in Table 1.1. They include examples where (multi-)polar interactions of almost every type can be found. In the dipolar-dipolar category, measurements of G^E and V^E for the system $HC\ell + HBr$ have recently been made[34]. (For technical reasons we did not attempt the measurement of H^E for this system.) A simple liquid binary mixture in the octupole-octupole group is $CH_4 + CF_4$ which was recently studied by LEWIS and STAVELEY[32d]. While this work was already in progress the surprising results of CALADO and AZEVEDO[35] on the system $Xe + C_2H_6$, for which the measured excess thermodynamic functions were found to be all negative, led us to study, for comparative

TABLE 1.1

BINARY MIXTURES STUDIED IN THIS WORK

NON-POLAR	DIPOLAR	QUADRUPOLAR	OCTUPOLAR	
Ar + Kr	HCℓ + Xe	N_2O + Xe	CF_4 + Xe	NON-POLAR
		N_2O + HCℓ	CF_4 + HCℓ	DIPOLAR
		$N_2O + C_2H_4$	$CH_4 + C_2H_4$	QUADRUPOLAR
				OCTUPOLAR

purposes, the molecularly similar mixture of Xe + C_2F_6 (not included in the table). Also the need for more accurate data on pure carbon tetrafluoride prompted the author to undertake a brief study of the vapour pressure of this substance, the results of which are reported in this thesis (Chapter 17). In this investigation use was made of the technique introduced by STAVELEY and his co-workers[36] for the determination of the composition dependence of the vapour pressure of liquid mixtures, namely to take the measurements at the triple-point temperatures of substances of high purity. It is believed that this is the first time that this method has been employed to study the temperature dependence of the vapour pressure of a pure substance.

Although it has been recognized for some time that the estimation of the excess enthalpy H^E is a more exacting test of a theory than that of any other of the primary excess thermodynamic functions, the comparison of theory and experiment has often had to be limited in the past to G^E and V^E, owing to the lack of experimental information on H^E [22]. In the present work special attention has been given to the determination of H^E wherever possible.

The length of this thesis could have been substantially increased by trying to apply the earlier theories (namely those listed under (i) and

(ii), above) to the systems experimentally studied, in particular by calculating the values of the deviation parameters, k_{12} and j_{12}, required to give the best fit with the experimental data. However, we believe this would have been a fruitless exercise, since, as already pointed out, the mixtures investigated were selected with the specific aim of testing theories which explicitly take polarity into account. The necessary low-temperature experimentation on the one hand, and the application of highly sophisticated modern theories on the other, are both specialized techniques, and it seems sensible for an experimental group and a theoretical group to join forces. Hence the alliance with the Cornell team, the results of whose calculations we shall compare with our experimental findings wherever possible.

1.1 REFERENCES

(1) SCATCHARD, G., Chem. Rev., 1949, 44, 7.

(2)(a) DOLEZALEK, F., Z. physik. Chem., 1908, 64, 727.

(b) McGLASHAN, M.L. and RASTOGI, R.P., Trans. Faraday Soc., 1958, 54, 496.

(c) RENON, H. and PRAUSNITZ, J.M., Chem. Eng. Sci., 1967, 22, 299.

(d) HARRIS, H.G. and PRAUSNITZ, J.M., Ind. & Eng. Chem. Fundamentals, 1969, 8, 180.

(3)(a) HILDEBRAND, J.H., J. Amer. Chem. Soc., 1929, 51, 66.

(b) HILDEBRAND, J.H., PRAUSNITZ, J.M. and SCOTT, R.L., 'Regular and Related Solutions', Van Nostrand Reinhold, New York (1970).

(4)(a) FLORY, P.J., J. Chem. Phys., 1941, 9, 660.

(b) FLORY, P.J., J. Chem. Phys., 1942, 10, 51.

(c) HUGGINS, M.L., J. Chem. Phys., 1941, 9, 440.

(5)(a) PRIGOGINE, I., BELLEMANS, A. and ENGLERT-CHOWLES, J. Chem. Phys., 1956, 24, 518.

(b) BELLEMANS, A., MATHOT, V. and SIMON, M., Adv. Chem. Phys., 1967, 11, 117.

(6)(a) METROPOLIS, N., ROSENBLUTH, A.W., ROSENBLUTH, M.N., TELLER, A.H. and TELLER, E., J. Chem. Phys., 1953, 21, 1087.

(b) ALDER, B.J. and WAINWRIGHT, T.E., J. Chem. Phys., 1957, 27, 1208.

(c) BARKER, J.A. and HENDERSON, D., Rev. Mod. Phys., 1976, 48, 587.

(7)(a) LELAND, T.W., ROWLINSON, J.S. and SATHER, G.A., Trans. Faraday Soc., 1968, 64, 1447.

(b) LELAND, T.W., ROWLINSON, J.S., SATHER, G.A. and WATSON, I.D., Trans. Faraday Soc., 1969, 65, 2034.

(c) ROWLINSON, J.S., 'Liquids and Liquid Mixtures', 2nd ed., Butterworth, London (1969).

(8) ROWLINSON, J.S. and WATSON, I.D., Chem. Eng. Sci., 1969, 24, 1565.

(9) GUNNING, A.J. and ROWLINSON, J.S., Chem. Eng. Sci., 1973, 28, 521.

(10) HAYNES, W.M., HIZA, M.J. and McCARTY, R.D., Proc. 5th Int. Conf. on LNG, (Dusseldorf, W.G.), Inst. Gas Technol., Chicago, I11. (1977).

(11)(a) SNIDER, N.S. and HERRINGTON, T.M., J. Chem. Phys., 1967, 47, 2248.

(b) BLINOWSKA, A., HERRINGTON, T.M. and STAVELEY, L.A.K., Cryogenics, 1973, 13, 85.

(12) MARSH, K.N., McGLASHAN, M.L. and WARR, C., Trans. Faraday Soc., 1970, 66, 2453.

(13) RODOSEVICH, J.B. and MILLER, R.C., Adv. Cryog. Eng., 1974, 19, 339.

(14) SOARES, V.A.M., 'Estudo Termodinâmico de Misturas Binárias Contendo Etileno', Tese de doutoramento, Inst. Sup. Técnico, Lisboa, (1976).

(15) McCLURE, D.W., LEWIS, K.L., MILLER, R.C. and STAVELEY, L.A.K., J. Chem. Thermodynamics, 1976, 8, 785.

(16) CALADO, J.C.G., AZEVEDO, E.J.S.G. and SOARES, V.A.M., communication to the 71st A.I.Ch.E. Annual Meeting, Miami, U.S.A, 19768.

(17) RONC, M. and RATCLIFF, G.A., Can. J. Chem. Eng., 1971, 49, 825.

(18) ABRAMS, D.S. and PRAUSNITZ, J.M., A.I.Ch.E. Journal, 1975, 21, 116.

(19) FREDENSLUND, A., JONES, R.L. and PRAUSNITZ, J.M., A.I.Ch.E. Journal, 1975, 21, 1086.

(20) KEHIAIAN, H.V., communication to the Conf. on Fluids and Fluid Mixtures, NPL, Teddington, U.K., 1978.

(21)(a) MANSOORI, G.A. and LELAND, T.W., J. Chem. Phys., 1970, 53, 1931.

(b) MANSOORI, G.A., J. Chem. Phys., 1972, 56, 5335.

(22) LEONARD, P.J., HENDERSON, D. and BARKER, J.A., Trans. Faraday Soc., 1970, 66, 2439.

(23)(a) GUBBINS, K.E., A.I.Ch.E. Journal, 1973, 19, 684.

(b) GUBBINS, K.E. and TWU, C.-H., communication to the Engineering Foundation Conf. on the Estimation and Correlation of Phase Equilibria and Fluid Properties in the Chemical Industry, Pacific Grove, California, U.S.A., 1977.

(24) TWU, C.-H., GUBBINS, K.E. and GRAY, C.G., Mol. Phys., 1975, 29, 713.

(25) FLYTZANI-STEPHANOPOULOS, M., GUBBINS, K.E. and GRAY, C.G., Mol. Phys., 1975, 30, 1649.

(26) HIZA, M.J. and DUNCAN, A.G., A.I.Ch.E. Journal, 1970, 16, 733.

(27) WORMALD, C.J., LEWIS, E.J. and HUTCHINGS, D.J., J. Chem. Thermodynamics, 1979, 11, 1.

(28)(a) DAVIES, R.H., DUNCAN, A.G., SAVILLE, G. and STAVELEY, L.A.K., Trans. Faraday Soc., 1967, 63, 855.

(b) CALADO, J.C.G. and STAVELEY, L.A.K., Trans. Faraday Soc., 1971, 67, 289.

(29) SCHOUTEN, J.A., DEERENBERG, A. and TRAPPENIERS, N.J., Physica, 1975, 81A, 151.

(30) CALIGARIS, R.E. and HENDERSON, D., Mol. Phys., 1975, 30, 1853.

(31) LEWIS, K.L., LOBO, L.Q. and STAVELEY, L.A.K., J. Chem. Thermodynamics, 1978, 10, 351.

(32)(a) POOLE, R.A.H., SAVILLE, G., HERRINGTON, T.M., SHIELDS, B.D.C. and STAVELEY, L.A.K., Trans. Faraday Soc., 1962, 58, 1692.

(b) DUNCAN, A.G. and STAVELEY, L.A.K., Trans. Faraday Soc., 1966, 62, 548.

(c) LEWIS, K.L., SAVILLE, G. and STAVELEY, L.A.K., J. Chem. Thermodynamics, 1975, 7, 389.

(d) LEWIS, K.L. and STAVELEY, L.A.K., J. Chem. Thermodynamics, 1975, 7, 855.

(33) CALADO, J.C.G., KOZDON, A.F., MORRIS, P.J., da PONTE, M.N., STAVELEY, L.A.K. and WOOLF, L.A., J. Chem. Soc., Faraday I, 1975, 71, 1372.

(34) CALADO, J.C.G., GRAY, C.G., GUBBINS, K.E., PALAVRA, A.M.F., SOARES, V.A.M., STAVELEY, L.A.K. and TWU, C.-H., J. Chem. Soc., Faraday I, 1978, 74, 893.

(35) CALADO, J.C.G., and AZEVEDO, E.J.S.G., communication to the 8th Experimental Thermodynamics Conference, Guildford, U.K., 1978.

(36) MATHOT, V., STAVELEY, L.A.K., YOUNG, J.A. and PARSONAGE, N.G., Trans. Faraday Soc., 1956, 52, 1488.

PART 2

EXPERIMENTAL

CHAPTER 2 PREPARATION OF GASES

CHAPTER 3 VAPOUR PRESSURE AND MOLAR VOLUME EXPERIMENTS

CHAPTER 4 HEAT OF MIXING EXPERIMENTS

CHAPTER 2

PREPARATION OF GASES

2.1 SOURCES

With the exception of methane, which was a Matheson 'research grade' product of purity $\geqslant$ 99.99% CH_4, and krypton (B.O.C., > 99.995% Kr) all the substances used throughout this work, either for the cryostat or for the mixtures to be studied, were finally purified by fractional distillation starting, as a rule, with the purest samples commercially available. Hydrogen chloride was prepared in the laboratory and the remaining gases were taken from cylinders, the initial purity ranging from better than 99.0% (N_2O) to > 99.995% (Xe). Ethane (Matheson, $\geqslant$ 99.96 % C_2H_6) was used without further purification in the calibration of the volume of the pyknometer.

The hydrogen chloride was prepared by the method of SWEENEY[1]. The apparatus, schematically shown in Fig.2.1, was first submitted to a thorough evacuation. Concentrated hydrochloric acid (B.D.H., 'Analar') in vessel (A) was carefully allowed to drip down a capillary (B) into flask (C) containing concentrated sulphuric acid (B.D.H., 'Analar'). The dropping rate was controlled using tap (1), and kept at a value of 20 to 30 drops per minute. The gaseous hydrogen chloride generated in the reaction bubbled through further concentrated sulphuric acid in vessel (D), at a rate adjusted by means of tap (2), in order to remove water vapour. Manometer (E) was used to monitor the pressure inside the apparatus upstream from tap (3). Any remaining water was frozen out in U-tube (F), immersed in a solid carbon dioxide and methanol slurry (T $\simeq$ 195 K). The rate of withdrawal of hydrogen chloride was controlled by tap (3), the substance being collected as a solid in vessel (I) surrounded by liquid nitrogen. Taps (5), (7) and (10) were left open during this stage of the preparation while taps (4), (6), (8), (9) and (11) remained shut. When sufficient HCl

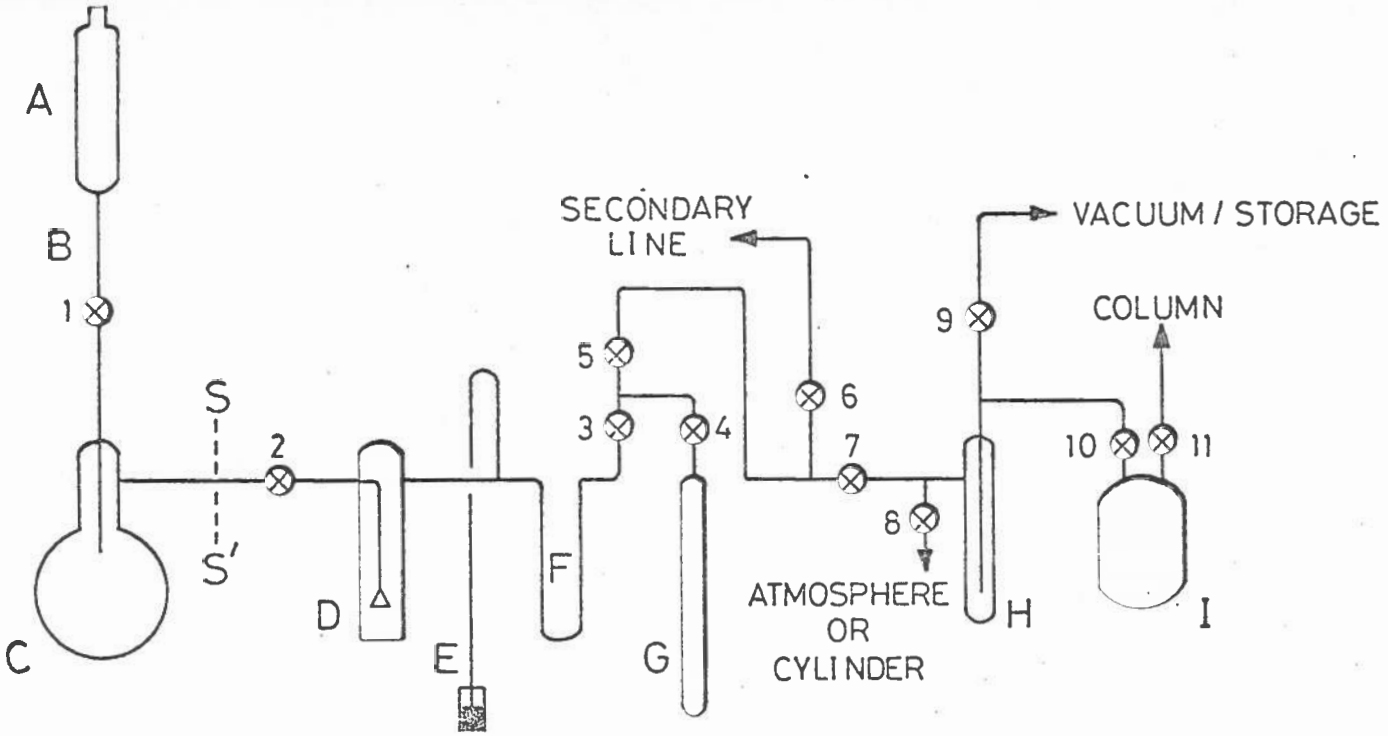

Fig. 2.1 - Preparation line

had been prepared, taps (1) and (10) were closed and trap (H) was surrounded by liquid nitrogen to freeze the residual gas, this fraction being discarded later. In this way about one mole of almost pure hydrogen chloride was prepared in less than an hour, starting from $\sim 100\,cm^3$ hydrochloric acid (and using an excess of H_2SO_4, $\sim 400\,cm^3$).

Even at this stage of the process, with the distillation of the material still to come, the HCℓ so prepared, exhibited a reddish pink colour in the solid state. This phenomenon was reported in the literature fifty years ago[2] but the origin of the colour is still not fully understood.

2.2 PURIFICATION

2.2.1 *INTRODUCTION*

Since considerable space is devoted in this chapter to the purification of the substances used, we will first briefly explain why so much importance was attached to this. In the first place, the basis of the control of the temperature at which the vapour pressure and the density measurements were made is simply that in a one-component system the temperature of co-existence of the solid, liquid and vapour phases is an invariant point. Any impurity, however, adds at least one more component, and in principle, the desired constancy and reproducibility of the triple-point temperature is lost. Accordingly, the substances to be used for this purpose must be as highly purified as possible.

As for the samples under examination, it is well known that the vapour pressure is particularly sensitive to the presence of impurities, especially if these differ considerably in volatility from the main component. The density (or molar volume) may be less susceptible to alteration by impurities, but it is clearly wise to take as little as possible for

granted in this matter. The calorimetric experiments make less severe demands on purity. As pointed out in papers describing previous work done in this laboratory[3], a purity of ~ 99% is probably adequate for the calorimetric determinations of enthalpies of mixing. However, only a few of these were actually carried out using substances less than 99.95% pure, since very pure samples were available.

2.2.2 *CHEMICAL PURIFICATION OF NITROUS OXIDE*

The main impurity in commercial nitrous oxide appears to be carbon dioxide which can be removed by reaction with an alkali. The two substances have similar physical properties which make it difficult to separate them by fractionation. In previous work done in this laboratory, the separation was attempted by simple distillation, but the triple-point pressure of the resulting nitrous oxide sample was found to be too high and to decrease by ~ 60 Pa (~ 0.5 torr) as melting proceeded, due to the preferential vaporization of the more volatile CO_2 during the first stages of melting.

To carry out the purification in the apparatus already described (Fig. 2.1) vessels (A) and (C) were put aside and the N_2O gas cylinder was connected to the glass tubing at section (SS′). The alkali — potassium hydroxide — was used both as pellets, in trap (G), and as an aqueous saturated solution, in vessel (D). The whole assembly was then evacuated until no further bubbling could be observed in (D), and a satisfactory response was obtained from a Tessla tube (U, in Fig. 2.3). Taps (4) and (7) were then closed and a small amount of the gas was allowed into the line. Tap (7) was opened and the apparatus thoroughly evacuated again. The assembly was flushed out two or three times in this way. Dewars containing solid carbon dioxide in methanol slurry and liquid nitrogen were put in place around (F) and (G) respectively. Tap (4) was opened, tap (5) closed and the cylinder

gas allowed to start flowing, the flow being carefully adjusted in such a way as to produce a moderate rate of bubbling through the KOH solution contained in (D). This was found to correspond to a flow rate of $\sim 10\,dm^3\,h^{-1}$. Pressure, as read in (E), gave an indication of the rate of condensation of N_2O in (G), and also (if it could not be kept at a steady low value) of the presence of non-condensable impurities. These, being mainly air, could be pumped out at any stage, by appropriate manipulation of the taps, since nitrous oxide is both harmless and inexpensive a gas, and the quantities involved were small. When enough material had been collected in (G), stopcocks (2) and (3) were closed, (5) was opened, the gas flow stopped, and any volatile impurities removed by pumping on the solid N_2O. The material was allowed to melt, re-frozen and pumped on again. After this cycle had been repeated several times, the nitrous oxide was sent either to the storage globes or to vessel (I) to be distilled.

2.2.3 *DISTILLATION COLUMN*

The distillation column used in the fractionation of the crude gases is shown in detail in Fig. 2.2, and in plan form, together with the rest of the line, in Fig. 2.3. It is a development of the CLUSIUS-RICCOBONI apparatus[4] with the rectification spiral replaced by a packed column, as in the apparatus described by PODBIELNIAK[5]. The apparatus makes it possible to operate with a refrigerant the boiling-point of which is below the solidus boundary of the mixture being fractionated.

The glass assembly (Fig. 2.2) consists of a boiler (M 1), of approximately $28\,cm^3$ capacity, fitted with an electrical heating coil of tungsten wire (M 2), of resistance $6.82\,\Omega$, in a groove at the bottom, thus allowing the distillation to be continued (if necessary) until a very small volume of liquid remains in the boiler. The internal surface of the lower part of the boiler is roughened to prevent bumping. The heating

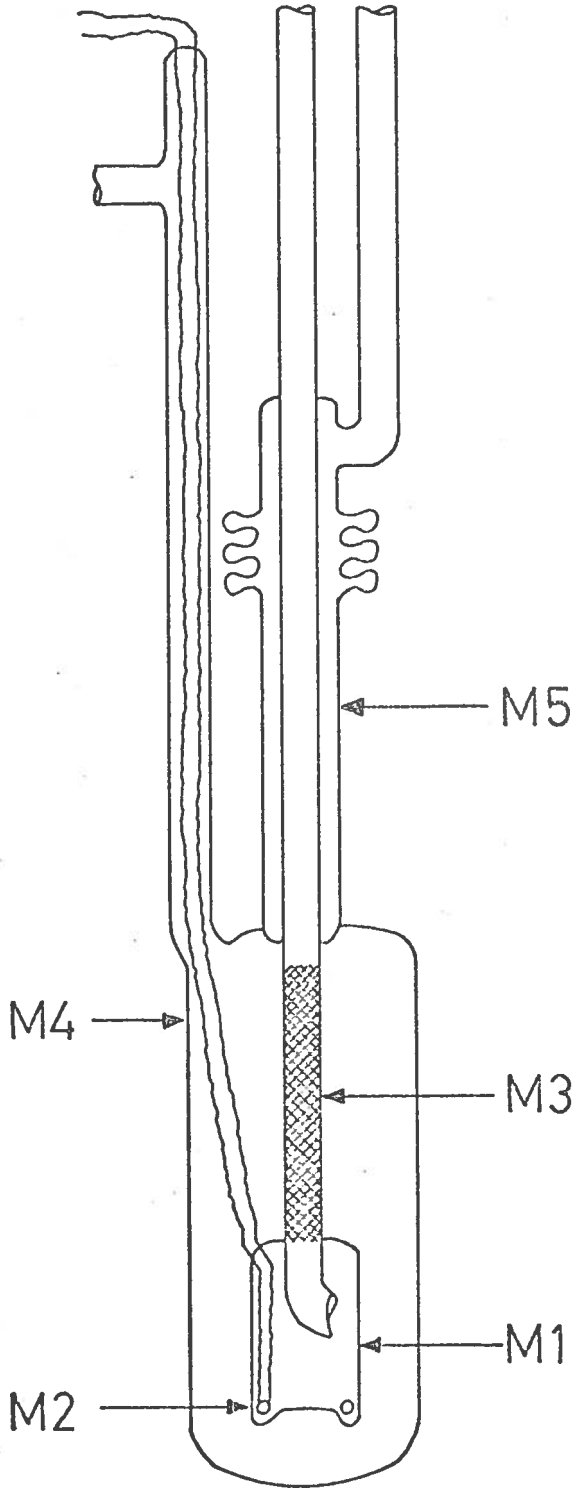

Fig. 2.2 - Distillation column

circuit, not shown in Fig. 2.2, incorporates an ammeter, a 240/6 V transformer, a rheostat, and a switch.

The boiler is joined to a glass tube (M3), approximately 15 cm long and 1 cm internal diameter, packed with 1/16" Dixon-Lessing gauze rings. The column and the boiler are enclosed in a vacuum jacket (M4) into which transfer gas (helium) can be introduced to cool the still. The upper part of the column is simply a non-packed glass tube, ~40 cm long, acting as a condenser. The heat transfer rate, and hence the rate of condensation of the liquid in the column, is controlled by the amount of helium introduced into the jacket (M5) through a tube connected to a 'gas-pipette' — the capillary by-pass between taps (29) and (30), in Fig. 2.3.

The exit of the column leads to a large U-tube mercury manometer (J, Fig. 2.3) capable of reading pressures up to about 200 kPa (~2 atm).

When in operation the column is immersed in a suitable refrigerant contained in a large dewar which has two unsilvered strips so that the interior may be illuminated from behind and the contents of the column easily observed.

The choice of the refrigerant is not a critical one. Liquid nitrogen is commonly used, but cases may arise when a careful selection of the cryogenic medium can facilitate the distillation. When the liquid to be purified has a high normal boiling point temperature, as is the case with xenon or with nitrous oxide, the rate of condensation along the column will be high, because of the large temperature gradient. Therefore, the pressure in the column will tend to be low, even if a very small amount of transfer gas is admitted in the upper jacket. On the other hand, the boiling rate cannot be indefinitely increased, as the column floods. A combination of these factors limits the effective range of the apparatus.

However, most of the disadvantages mentioned vanish if liquid nitrogen is replaced by a less cold refrigerant, such as a slurry of solid carbon dioxide in methanol.

Efficient control is exercised not only on the vaporization and condensation rates but also on that at which vapour is tapped off from the head of the column. A metallic needle valve (16, Fig. 2.3) is used to regulate the amount of vapour, D, withdrawn per unit of time. The amount of substance vaporized in the same time, V, is controlled by adjusting the current through the heater. The condensation rate depends on the height of refrigerant surrounding the column and on the pressure of the transfer gas in jacket (M5). The reflux rate – i.e., the amount of liquid, L, condensed per unit time – is related to D and V by the so-called (internal-)reflux ratio, r_i,

$$r_i = \frac{L}{V} = \frac{L}{L+D} \quad , \qquad \ldots (2.1)$$

which is a useful parameter in the treatment of the distillation problem, as it will be seen in the next paragraph.

It has been found empirically that r_i values ranging from 19:20 to 9:10 generally give good results.

2.2.4 *DISTILLATION PROCEDURE*

The apparatus, all in glass except for the brass valve (16), is shown in Fig. 2.3.

The procedure is, essentially, that described by DUNCAN[6] and also by CALADO[7].

Before starting a distillation the whole apparatus is thoroughly evacuated, and then a small amount of transfer gas is introduced into the lower jacket (M4) of the fractionation column from globe (N), via taps (26) and (27), at a pressure shown on manometer (O). The lower part of

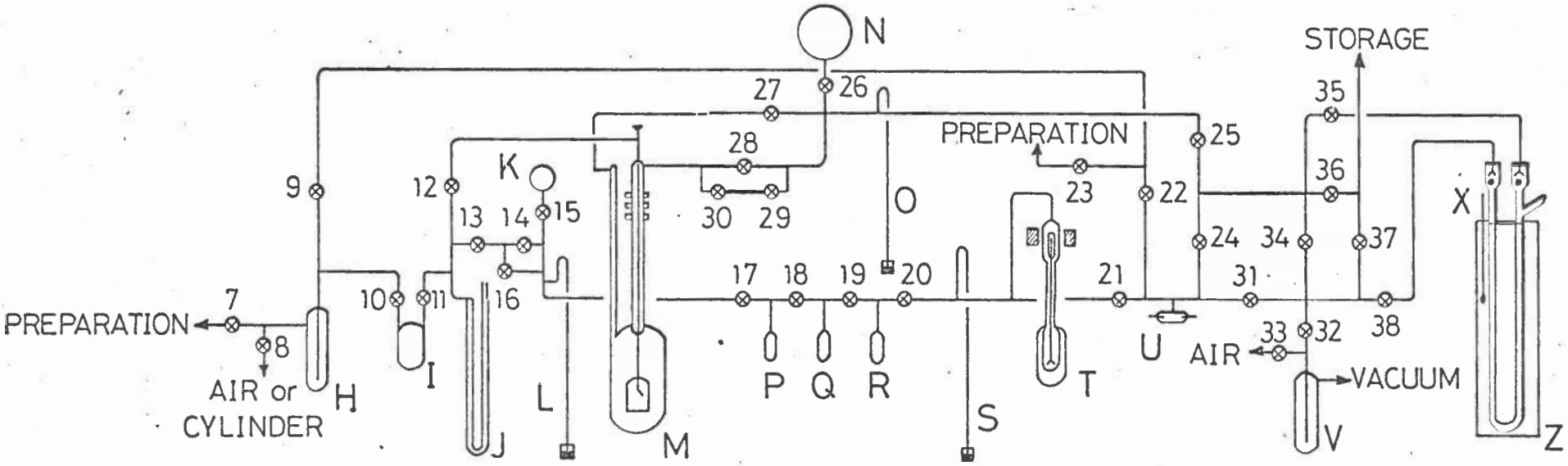

Fig. 2.3 - Distillation apparatus

the column is then immersed in the selected refrigerant, to a level slightly above the upper part of (M1), and the boiler is allowed to cool. Meanwhile, with taps (7) and (9) closed, the gas cylinder (i.e., the source of the gas to be purified) is connected to the apparatus via tap (8) and the line is repeatedly evacuated and flushed out with small portions of the crude gas. (Great care has to be taken in regulating the cylinder pressure reducer to avoid blowing off trap (H) or ejecting mercury from manometer (J) if, as an alternative, valves (12) and (13) are closed while (11) is left open to watch the pressure at which the gas is being admitted.)

Either for cylinder gases or for those from the storage line — the latter being admitted via taps (9), (22), (31) and (37) — a good practice consists of condensing them, as solids, in bulb (I) cooled with liquid nitrogen, while trap (H) is surrounded by carbon dioxide in methanol slurry, to condense any moisture or other high melting components. When enough material has been collected in bulb (I), tap (10) is closed and any volatile impurities are pumped off by opening taps (11), (13), and all other valves leading to the vacuum pumps, to (32). This process is repeated several times by letting the solid melt and re-freezing it, and then pumping out again any further volatile impurities which may have escaped from the solid.

The condensed gas in (I) is then transferred into the column as a liquid. This is a slow operation taking sometimes as long as two hours. Taps (10) to (14) are secured with strong rubber bands, as a precaution against being blown out. Tap (11) is opened, the refrigerant surrounding bulb (I) is lowered and the solid is allowed to melt. The pressure, shown on the open-tube manometer (J), is allowed to rise above the triple-point pressure of the substance to be distilled. Tap (12) is then carefully opened so that the condensate distils into the boiler of the column as a

liquid. During the transference the pressure is controlled by the level of the refrigerant below trap (I) in such a way that readings on (J) are kept between the triple-point pressure of the gas to be fractionated (to prevent the liquid in the column from freezing) and, say, ~150 kPa (~ 1.5 atm), for safety reasons. The heater (M 2) can be switched on at a low current (~ 0.2 A) to avoid freezing in the bottom of the column (M 1). When the boiler is about 2/3 full, tap (11) is closed and the contents of bulb (I) re-frozen. The helium in the lower jacket (M 4) is pumped away, via taps (24), (25), (27), (31) and (32), and the refrigerant level around the column is gradually raised to slightly above the three discoidal sections of the upper jacket (M 5). During the first stages of this process the pressure, read on (J), starts falling (as traces of helium remain in jacket (M 4) for a couple of minutes), but increasing the current through the heating coil may help to prevent freezing of the contents of the boiler. The liquid may eventually freeze in the column and in this case care must be taken to switch off the heater, since the expansion of liquid trapped below the solid in the boiler can crack the glass. Under these circumstances the large dewar with the refrigerant is lowered and the column warmed with the hair dryer up to the moment when all the solid in the boiler has melted. The heater is then switched on again, the dewar with the refrigerant replaced at the appropriate level, and the process continued. It is, however, usually possible to contrive that the pressure inside the column begins to rise before the formation of any solid in the boiler.

Transfer gas from globe (N) is then introduced into jacket (M 5) through the gas-pipette, after taps (25) and (27) have been shut. At this stage, the rate of condensation of the vapour inside the column is controlled by the amount of helium in the upper jacket since at low pressures

(below ~ 150 Pa) the thermal conductivity of the transfer gas is approximately proportional to its pressure. The judgement of the amount of transfer gas required largely depends on previous experience of handling the particular gases to be fractionated, and on the amount and nature of the impurities. In general, the lower the boiling-point temperature of the substance in the boiler the higher the number of helium gas-pipettes necessary to reach a steady-state in the column. For HCℓ and N_2O, for instance, 2 or 3 gas-pipettes at a pressure of 20-25 kPa (~ 150 - 200 torr) are usually enough, while for CF_4 and C_2H_4 four to seven doses may be required.

With tap (13) closed the column is operated under total reflux ($D = 0$, and therefore $r_i = 1$). Meanwhile, the level of liquid nitrogen surrounding the column and the current through the heater are adjusted, the latter being set at a value high enough to achieve the greatest possible rate of boiling without flooding the column. This is usually found to be somewhere between 0.7 and 1.0 A, the corresponding rate at which liquid drops from the column to the boiler being ~ 30 drops per minute. The pressure at which the liquid boils (observed on (J)) is, of course, also a function of the composition of the mixture to be distilled. This pressure should be kept constant, and well above the triple-point pressure of the main component of the mixture, by adjustment of the current and the rate of condensation of the liquid in the column as described. The actual values of the pressure inside the column when this reaches a steady state vary widely from case to case, ranging from as low as 20 kPa to slightly above 200 kPa (i.e., ~ 0.2 to ~ 2.0 atm).

When impurities more volatile than the major component are present, even if in small amounts, the pressure tends to rise to a relatively high value during the earlier stages of the total reflux period. These impurities

can be removed from the head of the column by carefully opening taps (13) and (14) with tap (17) closed. Tap (12) is then shut and the line evacuated via taps (17) - (21), (31) and (32), (opened in this order). This process is repeated, if necessary, until a constant pressure is obtained. At this stage the liquid is allowed to boil under conditions of total reflux for an additional period of about half an hour, so as to establish equilibrium in the column.

The first fraction of distilled material should be taken off at a high reflux ratio (e.g. 14:15 or 19:20), to eliminate impurities of boiling-point close to that of the major product. This is done by adjusting valve (16) with tap (13) opened and (14) closed. (The movement of the needle in valve (16) is controlled by a specially devised screw of very small pitch, to increase sensitivity.)

The actual reflux ratio, r_i, corresponding to a particular opening position of valve (16) can be assessed as follows. The number of moles, n, vaporized in t seconds is given by:

$$n = \frac{Q}{\Delta H_v} = \frac{i^2 r t}{\Delta H_v} , \qquad \ldots (2.2)$$

where Q is the energy supplied by the heating coil of resistance r when a current i flows through it during time t. ΔH_v, the enthalpy of vaporization of the liquid in the boiler, can be assumed, for the purpose of the present calculations, to be the enthalpy of vaporization at the normal boiling point of the pure main component of the liquid.

At a reflux ratio r_i, $Dt = (1 - r_i)\, Vt = (1 - r_i)\, n$ moles must leave the column in t seconds. Closing taps (14) and (17), with (13) and (15) open, traps this gas in the calibrated globe (K), and the pressure in this section of the line, as observed on manometer (L), increases (assuming the gas to be ideal) by

$$\Delta P = (1 - r_i)\, n \frac{RT}{V} , \qquad \ldots (2.3)$$

in t seconds. R is the gas constant, T is the room temperature in K and V_K is the volume of the dead space between taps (14) and (17), including globe (K). $V_K = 311\ cm^3$. Substituting n, as given by equation (2.2), into equation (2.3), one obtains

$$\Delta P = \frac{i^2 r t(1 - r_i) RT}{\Delta H_v V_K} . \qquad \ldots (2.4)$$

For this particular column, at a room temperature of $T = 295\,K$,

$$\Delta P/torr = \frac{12.10 \times 10^6 i^2 (1 - r_i)}{\Delta H_v} , \qquad \ldots (2.5)$$

for an interval $t = 30\,s$. (This is a convenient period for timing the take-off rate.) In this equation i is expressed in A and ΔH_v in $J\,mol^{-1}$.

For a given reflux ratio r_i the calculated value of the pressure increase ΔP that should be observed during time t (usually $t = 30\,s$), as calculated from equation (2.4) or (2.5), is compared with the actual ΔP value read on manometer (L) for the same interval (as measured with a stopwatch). Valve (16) is then adjusted as required, and the procedure repeated until manometer (L) falls at the appropriate rate to achieve the intended reflux ratio. This rate is checked at regular intervals throughout the distillation.

Values of the normal boiling-point temperatures and the corresponding enthalpies of vaporization for the substances used in this work are given in Table 2.1.

Trap (R) is immersed in liquid nitrogen, and taps (17) - (19) are opened allowing the first crude fraction to be collected in (R). Depending, however, upon the reflux ratio and on the amount of impurities in the initial crude sample, the time allotted to this first collection is usually less than an hour, after which time it is considered that most impurities are removed. The column is then isolated from the line by closing (13). In the case of expensive, corrosive or toxic substances this first fraction

TABLE 2.1

Normal Boiling Points T_b (K)[a] and Enthalpies of Vaporization ΔH_v ($J\,mol^{-1}$) at T_b for the Substances Involved in the Present Work,

Substance	Formula	T_b/K	Ref.	ΔH_v/$J\,mol^{-1}$	Ref.
Nitrogen	N_2	77.35	(21)	5577	(22)
Methane	CH_4	111.65	(8)	8222	(9)
Krypton	Kr	119.80	(8)	9046	(10)
Carbon Tetrafluoride	CF_4	145.16	(11)	11814	(12)
Xenon	Xe	165.06	(8)	12636	(4)
Ethylene	C_2H_4	169.39	(13)	13544	(14)
Boron Trifluoride	BF_3	172.9	(15)	19320	(15)
Nitrous Oxide	N_2O	184.65	(16)	16560	(16)
Hydrogen Chloride	$HC\ell$	188.20	(17)	16150	(2)
Hexafluoroethane	C_2F_6	194.85	(18)	16149	(18)
n-Butane	C_4H_{10}	272.65	(19)	22389	(19)
trans-2-Butene	C_4H_8	274.03	(20)	22757	(20)

a - Values of T_b in IPTS-68.

is quickly transferred from trap (R) to trap (H) or to a trap connected onto tap (8) (which can also serve to collect samples for mass spectrometric analysis). This trap is immersed in liquid nitrogen, and the fraction is transferred from (R) by opening taps (8), (9) and (20) - (22), while keeping (7), (10), (24) and (31) closed. The dewar surrounding (R) is removed and hot air is carefully blown onto the trap to speed the vaporization. Alternatively, the contents of (R) can be directly transferred to appropriate storage globes via tap (37). Immediately after the transference is over taps (8) and (12) are closed, taps (13), (14), (31) and (32) are opened and the line, including the left-hand limb of manometer (J), thoroughly evacuated. In this way, any impurities trapped over the mercury, in (J), are removed. If the material being distilled is inexpensive and harmless, it can be directly pumped away. The column is cautiously reopened

to the line by closing taps (14) and (20) and opening tap (12).

The second fraction is generally used to flush out the storage globes which have previously been evacuated, and is collected in trap (R). Only a small quantity of gas is needed for flushing out the globes and therefore, under usual conditions, the product of less than half an hour's distillation is enough for this purpose. The material is passed in the usual way, to the storage globes, via taps (20), (21), (31) and (37). The storage flasks are then evacuated again. Any residual gas left in the line is pumped away.

Meanwhile, having closed tap (19) and immersed trap (Q) in liquid nitrogen, the collection of the main fraction had been started. At this stage, the distillate should be very pure, and so the reflux ratio can be lowered to, say, 14:15 or 9:10 in order to speed up the distillation. When Q is about 2/3 full, tap (18) is closed, trap (P) is surrounded by liquid nitrogen in a small dewar and the last fraction is collected in exactly the same manner as the previous one.

The main fraction, in trap (Q), can then be tested for purity in the triple-point cell as described in the next section.

The distillation is halted when the level of the liquid in the boiler is about 2 mm above the heating coil. Tap (13) is closed and the heater is switched off. By lowering the large dewar surrounding the column the residue in the boiler can be transferred back to trap (H) or to the auxiliary trap attached to tap (8), acting as described previously for hazardous or expensive substances. Later, these traps (still immersed in liquid nitrogen) are removed from the line to a fume cupboard where the residues are allowed to vapourize.

2.3 TRIPLE-POINTS

The value of the triple-point pressure during melting is a function of the purity of the sample being tested. Constant readings at different stages of melting are indicative of high purity. This method of testing purity is particularly suited for the purposes of the present work since accurate values of the triple-point pressure of most of the substances used are subsequently needed in the calculations.

The measurement of the triple-point pressure of samples was carried out in an apparatus similar to that devised by CLUSIUS and STAVELEY[23] using a wide-bore U-tube mercury manometer of the type described by LAMBERT and PHILLIPS[24], with which pressures could be read to 0.01 torr (~ 1.3 Pa). Details of both the triple-point cell and the manometer are given in the next paragraphs, while the final purity of the samples used in this work is assessed in section 2.3.4.

2.3.1 *TRIPLE-POINT CELL*

The glass apparatus, indicated as (T) in Fig. 2.3 and shown in detail in Fig. 2.4, essentially consists of a vessel (T 3) of approximately 10 cm^3 capacity, joined to a tube (T 4) about 25 cm long. The vessel (T 3) is surrounded by a vacuum jacket (T 1). Inside the cell is a glass rod (T 5) terminating in small glass hooks (T 2). The rod may be raised or lowered by means of an electromagnet (T 7) acting upon a soft iron rod (T 6) contained in the upper end. This is to enable the crystal mass to be lifted to project above the liquid surface, so as to keep the three phases — solid, liquid and vapour — in equilibrium. This is essential, otherwise superheating of the liquid surface will occur and spuriously high readings will be obtained.

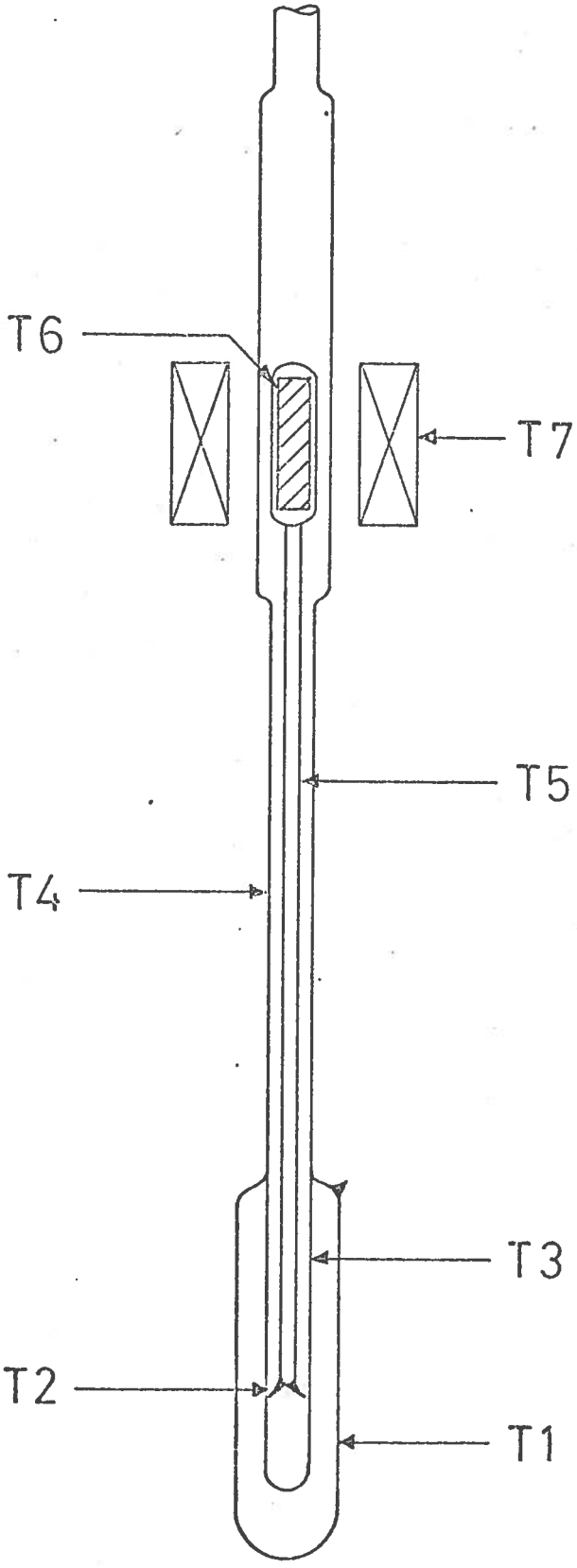

Fig. 2.4 - Triple point cell

2.3.2 *MERCURY MANOMETER*

The mercury manometer, indicated by (Z) in Fig. 2.3, is similar to that employed by LAMBERT and PHILLIPS[24]. It is constructed of calibrated glass tubing of 14 mm internal diameter and is filled by distilling mercury into it. The upper section of each limb of the manometer is fitted with a small ball-valve to prevent accidental passage of mercury into the line. The variation of the expansion coefficient of mercury with temperature cannot be neglected at room temperature and therefore the U-tube is encased in a glass-sided water jacket to avoid sudden changes of temperature.

The relative positions of the mercury levels and the heights of the menisci are read accurately by means of a travelling microscope. This is bolted to a carriage which can move vertically along a machined bar fixed to the side of the casing, and horizontally across the window of the manometer jacket. The focus can be adjusted onto the mercury menisci, or onto a vertical glass scale centrally mounted inside the water jacket, behind the manometer. The scale used is a high precision one, from Société Genevoise, Switzerland, which is assumed to be correct at 20°C and reliable to at least 0.01 mm. The magnification of the microscope is adjusted so that, when the eye-piece is focussed on either the menisci or on the scale mark, 25 divisions of the eye-piece graticule correspond to the distance between the centres of two adjacent scale marks, that is to 1 mm. The readings are taken to the nearest 1/4 division, corresponding to 0.01 mm. Illumination for the scale and the menisci is provided, from behind, by a parallel beam of diffused light from two 6 W light bulbs (connected to a 6 V transformer) enclosed in a metallic case provided with a narrow shaded window. This case is bolted to the carriage moving jointly with it. That the light beam is normal to the scale, the manometer and the window glass-

plate of the water jacket is checked by the absence of a 'ghost' meniscus.

As WHYTLAW-GRAY and TEICH[25] have pointed out, it is not enough to measure simply the difference between the top levels of the two mercury menisci in order to get the exact pressure; the heights of the menisci should also be taken into account if results of high accuracy are to be obtained. In fact, the height of the meniscus in contact with the gas is usually different from that on the vacuum side, and allowance should be made for the corresponding capillary depressions. KISTEMAKER[26] tabulated mercury capillary depressions for several diameters of glass tubing and different menisci heights. Extensive use of these tables is made in this type of work, and in view of this they have been reproduced, in part, in Appendix (A). To obtain pressure in 'international millimetres of mercury' the final values must be referred to temperature 0°C, latitude 45° and sea level, by multiplying those values by a further correction factor. This is tabulated in Appendix (B) for temperatures from 15.0 to 26.0°C. In the construction of these tables the different thermal expansions of mercury and glass have also been taken into account.

2.3.3 *TRIPLE-POINT PRESSURE DETERMINATION*

Before starting the measurements, the triple-point cell is thoroughly evacuated along with both arms of the manometer (Z), by opening taps (21), (24), (31), (32), (35) and (38), and the zero error of the manometer is recorded. This is never larger than 0.04 torr (~ 5 Pa). Taps (21) and (31) are closed again and the cell is cooled by surrounding it with liquid nitrogen to just below the junction neck of the vacuum jacket. The cell is then opened up to the appropriate trap (P), (Q) or (R) and the condensed gas is transferred into the cell as a liquid. This requires the same conditions as were used to fill the boiler; however, the vacuum jacket (T 1) reduces the rate of transfer considerably. The pressure at which the gas

is transferred can be watched on manometer (S) and should be kept below atmospheric pressure.

When the cell is about half full, tap (20) is shut, and trap (Q) (if this is the one in use) is immersed in liquid nitrogen. The liquid in the cell is allowed to solidify, forming a block around the bottom of the glass rod (T 5) . When the pressure, monitored on (S), is reduced to a few torr, the liquid nitrogen is removed and the outside of the cell is cleared of ice, using the hair dryer. For most substances, the liquid nitrogen is replaced, but at a level well below (usually 5 - 10 cm) the bottom of the cell. In other cases, nitrogen is too cold a refrigerant and the cell is simply surrounded by an empty cold dewar or, sometimes, by a less cold refrigerant. Meanwhile, tap (31) is closed, and tap (21) is carefully opened to the right-hand limb of the manometer. The material in the cell is slowly warmed by conduction down the walls of the tube (T 4) and down the glass rod (T 5) .

When the triple-point is reached, as indicated by the first signs of liquid, the pressure is measured on (Z), and further measurements made as many times as possible during melting. As melting proceeds, the rod is lifted up to keep the solid always partially above the liquid surface. The temperature of the water in the jacket, as read on thermometer (X), is registered and the correction factor, accounting for temperature, latitude and altitude effects, is calculated. For each of the pressure readings a rough visual estimate is also made of the fraction melted (of the contents of the cell), by observation through the unsilvered stripe of the dewar.

When sufficient readings at different stages of melting have been taken the glass rod is lowered, the level of the refrigerant around the cell is returned to its initial position, and the substance is allowed to

solidify. If the material is judged, from the constancy of its triple-point pressure during melting, to be of adequate purity, it can be transferred to the storage globes, by closing taps (24), (32) and (38), opening (37), and removing (or simply lowering the level of) the refrigerant surrounding the cell. The electromagnet is then switched off. Finally, the whole line is evacuated.

2.3.4 *TESTS OF PURITY*

On previous occasions[6,7] gaseous samples prepared by the fractional distillation procedure described have been found, by mass spectrometry, to contain no detectable impurity, that is, better than 99.99% pure. The purity of the final samples employed in this work, apart from those used in the heat of mixing determinations, was checked by measurement of the absolute values and constancy on melting of their triple-point pressures. For substances of low triple-point vapour pressure (less than, say, 1 kPa), such as carbon tetrafluoride and ethylene, this method has little significance and further tests had to be devised. These are dealt with later, in this section.

Table 2.2 summarizes the results of the triple-point pressure determinations for the substances used in the G^E and V^E experiments. Temperatures have been converted into a common scale — IPTS-68 — for reasons explained in Chapter 17 where details of the conversion procedures are also given. The references included in Table 2.2 were selected from an extensive literature search covering half a century (1928-1978)[27].

The agreement between the present results and literature values is excellent for all the substances studied. The small standard deviations obtained for the triple-point pressures of HCℓ, Xe and N_2O, denoting highly purified samples, deserve perhaps a brief comment. In the case of nitrous oxide the value reported is the result of nearly sixty readings

TABLE 2.2

Triple-Point Characterization of Molecularly Simple Substances

Substance	Ref.	T_t/K	Ref.	P_t/kPa
CF_4	(12),(28)	89.57	(30)	0.107 ± 0.004
	(29)	89.56	(29)	0.107 ± 0.001
	Selected	89.56	This work[a]	0.109 ± 0.013
C_2H_4	(14)	104.01	(31)	0.123
	Selected	104.01	This work[a]	0.125 ± 0.007
HCℓ	(2)	158.97	(33)	13.811 ± 0.004
	(32)	159.05	(34)	13.799 ± 0.004
	Selected	159.01	This work	13.807 ± 0.005
Xe	(8)	161.39	(33)	81.684 ± 0.003
			(34)	81.661 ± 0.003
	Selected	161.39	This work	81.667 ± 0.004
N_2O	(16)	182.32	(16),(36)	87.853
	(35)	182.34	(23)	87.882
			(37)	87.864
	Selected	182,32	This work	87.866 ± 0.001

[a] Readings with Texas Instruments gauge, using the general procedure described in the next Chapter.

involving six different samples, the corresponding standard deviation being even smaller than the experimental error of the readings (~ 3 Pa). (For this substance, at its triple-point, a change of ± 5 Pa in vapour pressure corresponds to a fluctuation of ± 1 mK in temperature.) For xenon only two series of measurements have been made, while the figure found for hydrogen chloride is the mean of three independent determinations amounting to more than thirty readings at different stages of the melting process.

To assess the effect of the chemical purification applied to nitrous oxide the triple-point vapour pressure of a sample was measured prior to fractionation. Comparison with the values obtained for a sample which was

submitted to the complete purification treatment is made in Table 2.3, as a function of the fraction melted of the two samples.

TABLE 2.3

Triple-point pressure (P_t/kPa) of two N_2O samples: A, chemically purified only; and B, chemically purified and distilled.

Fraction melted	P_t/kPa	
	Sample A	Sample B
0.1		87.867
0.2	87.865	87.866
0.3	87.863	87.870
0.4	87.863	87.866
0.5	87.862	87.869
0.6	87.861	
0.7	87.862	
0.8	87.858	
0.9	87.862	
Average	87.862 ± 0.003	87.867 ± 0.001

It is interesting to note that, within experimental error, the final result is the same for both samples, showing the effectiveness of the action of the alkali. The simplified purification process (i.e. omitting the fractionation) was therefore subsequently used for the samples for the calorimetric experiments.

For CF_4 and C_2H_4, the triple-point pressure is relatively small, and its constancy is therefore a much less sensitive criterion of purity. For these substances, measurement of the vapour pressure at the triple-point temperature of a suitably selected cryogenic material is an obvious alternative way of testing their purity, by comparison with existing vapour pressure data. Remeasuring the vapour pressure after evaporating about half the sample gives a further check on its purity, since the two results must coincide for a pure substance.

The vapour pressure of carbon tetrafluoride has been measured at

the triple-point temperatures of eight pure substances. There is no need to enlarge on this subject at this stage since the full discussion of the results is made in Chapter 17. For the present purposes it will suffice to note that the vapour pressure of CF_4 at the hydrogen chloride triple-point temperature is 244.500 ± 0.024 kPa as compared with 244.471 kPa from an indpendent set of measurements carried out in this laboratory on a different sample by Professor D.W. McCLURE[38]. (See also Chapter 11 of this thesis).

In the case of ethylene a vapour pressure of 205.216 kPa was measured at the triple-point temperature of nitrous oxide (182.32 K), the temperature selected for the test. Apparently there is no other value to compare with, apart from those derived from conventional vapour pressure studies. Among these the equation proposed by EGAN and KEMP[14] cannot reasonably be expected to extrapolate well to 182.32 K, and the more recent results presented by BIGELEISEN *et al.*[31], which extend up to 180.75 K, are also of little use for the present purposes of this work since no vapour pressure equation is given and also because there seem to be large uncertainties in the temperature scale used (near 180 K). The value of 204.681 kPa calculated from the work of MICHELS and WASSENAAR[39], which is not significantly different from that derived from the more elaborate equation of GARSIDE and SMITH[40], is lower than the present value by less than 0.3%. This difference has also been found by DOUSLIN and HARRISON[41] who ascribed it to the use by the Dutch workers of less pure ethylene samples. A difference of 0.05 K in the temperature scales could account for the discrepancy between the result of the present experiments and that derived from the work of MICHELS and WASSENAAR.

2.4 REFERENCES

(1) SWEENEY, O.R., J. Am. Chem. Soc., 1917, 39, 2186.

(2) GIAUQUE, W.F. and WIEBE, R., J. Am. Chem. Soc., 1928, 50, 101.

(3)(a) LEWIS, K.L., SAVILLE, G. and STAVELEY, L.A.K., J. Chem. Thermodynamics, 1975, 7, 389.

(b) KIDNAY, A.J., LEWIS, K.L., CALADO, J.C.G. and STAVELEY, L.A.K., J. Chem. Thermodynamics, 1975, 7, 847.

(c) McCLURE, D.W., LEWIS, K.L., MILLER, R.C. and STAVELEY, L.A.K., J. Chem. Thermodynamics, 1976, 8, 785.

(4) CLUSIUS, K. and RICCOBONI, L., Z. Physik. Chem., 1937, B38, 81.

(5)(a) PODBIELNIAK, W.J., Ind. Eng. Chem. (Anal. Ed.), 1931, 3, 177.

(b) PODBIELNIAK, W.J., Ind. Eng. Chem. (Anal. Ed.), 1933, 5, 119.

(c) PODBIELNIAK, W.J., Ind. Eng. Chem. (Anal. Ed.), 1941, 13, 639.

(6) DUNCAN, A.G., "The Thermodynamics of Mixing of Binary Condensed Gas Mixtures', Thesis, University of Oxford, (1966).

(7) CALADO, J.C.G., 'Thermodynamic Studies of Binary Condensed Gas Mixtures', Thesis, University of Oxford, (1969).

(8) LOVEJOY, D.R., Nature, 1963, 197, 353.

(9) CUTLER, A.J.B. and MORRISON, J.A., Trans. Faraday Soc., 1965, 61, 429.

(10) BEAUMONT, R.H., CHIHARA, H. and MORRISON, J.A., Proc. Phys. Soc. (London), 1961, 78, 1462.

(11) LOBO, L.Q. and STAVELEY, L.A.K., Cryogenics, 1979, 19, (in press).

(12) SMITH, J.H. and PACE, E.L., J. Phys. Chem., 1969, 73, 4232.

(13) DOUSLIN, D.R. and HARRISON, R.H., J. Chem. Thermodynamics, 1976, 8, 301.

(14) EGAN, C.J. and KEMP, J.D., J. Am. Chem. Soc., 1937, 59, 1264.

(15) Matheson Gas Data Book, 5th edition, Matheson Gas Products, Milwaukee, Wis., (1971), 43.

(16) BLUE, R.W. and GIAUQUE, W.F., J. Am. Chem. Soc., 1935, 57, 991.

(17) LEWIS, D.G., 'A Comparison of Some Thermodynamic Properties of Hydrogen Chloride and Deuterium Chloride', (Part II) Thesis, University of Oxford, (1973).

(18) PACE, E.L. and ASTON, J.G., J. Am. Chem. Soc., 1948, 70, 566.

(19) ASTON, J.G. and MESSERLY, G.H., J. Am. Chem. Soc., 1940, 62, 1917.

(20) GUTTMAN, L. and PITZER, K.S., J. Am. Chem. Soc., 1945, 67, 324.

(21) WAGNER, W., Cryogenics, 1973, 13, 470.

(22) GIAUQUE, W.F. and CLAYTON, J.O., J. Am. Chem. Soc., 1933, 55, 4875.

(23) CLUSIUS, K. and STAVELEY, L.A.K., Z. Physik. Chem., 1941, B 49, 1.

(24) LAMBERT, B. and PHILLIPS, C.S.G., Phil. Trans. Roy. Soc. London, 1949, 242A, 415.

(25) WHYTLAW-GRAY, R. and TEICH, N., Trans. Faraday Soc., 1948, 44, 774.

(26) KISTEMAKER, J., Physica, 1945, 11, 277.

(27) LOBO, L.Q., CALADO, J.C.G. and STAVELEY, L.A.K., 1978, (to be published).

(28) POOL, R.A.H., SAVILLE, G., HERRINGTON, T.M., SHIELDS, B.D.C. and STAVELEY, L.A.K., Trans. Faraday Soc., 1962, 58, 1692.

29) SIMON, M., KNOBLER, C.M. and DUNCAN, A.G., Cryogenics, 1967, 7, 138.

(30) ENOKIDO, H., SHINODA, T. and MASHICO, Y., Bull. Chem. Soc. Japan, 1969, 42, 3415.

(31) BIGELEISEN, J., FUKS, S., RIBNIKAR, S.V. and YATO, Y., J. Chem. Phys., 1977, 66, 1689.

(32) CHIHARA, H. and INABA, A., J. Chem. Thermodynamics, 1976, 8, 915.

(33) CALADO, J.C.G., KOZDON, A.F., MORRIS, P.J., PONTE, M.N. da, STAVELEY, L.A.K., and WOOLF, L.W., J. Chem. Soc. Faraday I, 1975, 71, 1372.

(34) CALADO, J.C.G., GRAY, C.G., GUBBINS, K.E., PALAVRA, A.M.F., SOARES, V.A.M., STAVELEY, L.A.K. and C.-H. TWU, J. Chem. Soc. Faraday I, 1978, 74, 893.

(35) HOGE, H.J., J. Res. Nat. Bur. Std., 1945, 34, 281.

(36) CLUSIUS, K., PIESBERGEN, U. and VARDE, E., Helv. Chim. Acta, 1960, 43, 1290.

(37) YATO, Y., LEE, M.W. and BIGELEISEN, J., J. Chem. Phys., 1975, 63, 1555.

(38) CLANCY, P., GUBBINS, K.E., LOBO, L.Q., McCLURE, D.W. and STAVELEY, L.A.K., 1975-79 (to be published).

(39) MICHELS, A. and WASSENAAR, T., Physica, 1950, 16, 221.

(40) GARSIDE, D.H. and SMITH, B.L., Physica, 1967, 37, 369.

(41) DOUSLIN, D.R. and HARRISON, R.H., J. Chem. Thermodynamics, 1976, 8. 301.

CHAPTER 3

VAPOUR PRESSURE AND MOLAR VOLUME MEASUREMENTS

For many of the molecularly simple species of interest in this type of work the temperature coefficient of the vapour pressure, expressed as $d\,\ell n\,P/dT$, is of the order of $0.1\ K^{-1}$ in the relevant temperature region. Consequently, if in the study of liquefied gases one is attempting to make pressure measurements which are reproducible to within a few parts in 10^4, the temperature fluctuations during the readings have to be kept within a narrow interval of a few mK (since $\delta T \sim 10 \times \delta P/P$).

STAVELEY and co-workers[1] (1956), introduced a technique capable of satisfying such a requirement. The vessel containing the sample whose vapour pressure is to be measured is immersed in a cryostatic bath which is, simply, a pure substance melting at its own triple-point. In this way, provided a sufficiently pure sample of the cryogenic material is used, the temperature at which a set of measurements is made is constant to at least one or two mK and, what is perhaps more important, the same temperature can be easily reproduced from one experiment to the next, as many times as is required.

The apparatus which makes use of this simple idea has been improved over the years[2-4]. The present version is described in the next section, and the experimental procedures for the vapour pressure and molar volume determinations are treated in sections 3.2 and 3.3 respectively.

3.1 THE APPARATUS AND ITS ACCESSORIES

The apparatus, shown in Fig. 3.1, is similar in principle to that previously described by DAVIES *et al.*[5]. The quartz-spiral pressure gauge was incorporated in it a few years later[3,6]. As originally constructed

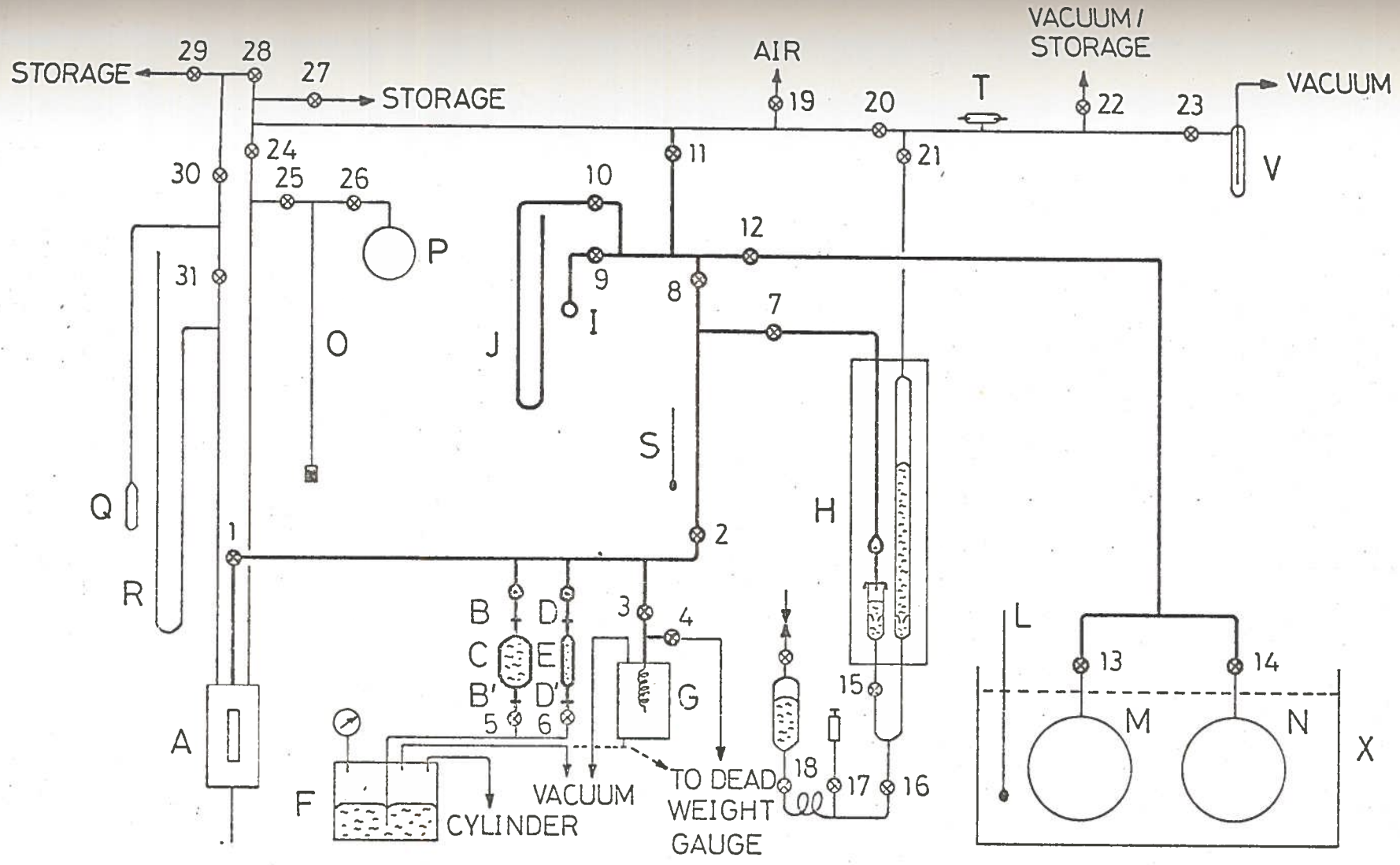

Fig. 3.1 - G^E and V^E apparatus

by DAVIES *et al.*, much of the line (i.e. tubing and valves) was made of metal. This occasionally led to troublesome leaks, and the metal was therefore replaced by glass, even though this meant a drop in the upper limit of the pressure at which one could operate from ~ 2.0 MPa to ~0.5 MPa.

The part of the apparatus at which the pressure is kept below ~0.1 MPa will be designated the 'low-pressure section' while that in which the pressure can reach ~0.5 MPa will be referred to throughout as the 'high-pressure section'. The latter is constructed of thick-walled glass and includes several spring-loaded capillary bore stopcocks. The capillary glass tubing, represented in the adjoining Fig. 3.1 by heavier-type lines, extends to those parts of the low-pressure section where the dead-space volume is to be minimized, except for the portion leading to the quartz-spiral gauge, which is made of capillary stainless steel.

3.1.1 *HIGH-PRESSURE SECTION*

The central component of the apparatus is the pyknomer assembly (A), which will be described in detail in subsection 3.1.2. It is connected to a mercury compressor vessel (C) of approximately 100 cm^3 capacity between the calibration marks (B) and (B′). The volume of vessel (E), which is made of calibrated glass tubing, is accurately known between marks (D) and (D′). Both (C) and (E) are constructed from thick glass, and both are connected to the mercury reservoir (F) through stainless steel tubing and valves (5) and (6) of the type described in Chapter 2. Two stainless steel ball-bearing safety valves located above the upper fiducial marks prevent the mercury in (C) and (E) from accidentally entering the calibrated dead-space volume above the pyknometer.

A very small internal diameter was chosen for the stainless steel tube leading to the quartz-spiral gauge (G) in order to keep the dead-space as small as possible. This tube is cemented with Araldite into the capillary glass line, below valves (3) and (4).

Another component of the high-pressure section, the Boyle's law manometer (J), is used to monitor the pressure at which liquid distils from the small bulb (I) into the pyknometer during the preparation of the mixtures.

In the present version of the apparatus the dead-weight gauge and mercury manometer (H) serve, simply, as primary standards for the calibration of (G) with which quicker, yet accurate, readings can be made.

3.1.2 *PYKNOMETER ASSEMBLY*

When in operation the assembly is surrounded by a large dewar containing the refrigerant, which in the author's work was always liquid nitrogen. This dewar has two unsilvered strips to permit observation of the inside. Illumination for this is provided from behind by a 60 W strip lamp.

The refrigerant must not be allowed to come into direct contact with the pyknometer assembly because its boiling point is too far below the triple-point temperature of the cryostat materials used throughout this work. The temperature is therefore controlled by means of a cylindrical copper shield which has attached to its base a copper rod to be immersed in the refrigerant thus providing cooling by conduction. After some practice, by controlling the level of the refrigerant, and hence the average temperature of the shield, it is possible to keep the cryostat substance at its triple-point for well over 2 or 3 hours, a time sufficient to make the necessary measurements. In addition, the shield has wound upon it a heater of resistance 80 Ω, although in practice this very seldom had to be used. All of the G^E and V^E measurements described in this thesis (with one exception) were in fact made with either HCℓ or N_2O in the cryostat, and for these substances, as soon as the desired triple-point conditions are established, these are thereafter maintained by having the copper rod not immersed in the liquid nitrogen, but about 1 cm above its surface.

The pyknometer system is shown in detail in Fig. 3.2. It consists of a small bulb of thickened glass (A 1) of about 2.2 cm^3 capacity. The inlet stem (A 2) is of accurately known capillary bore and has an etched calibration mark (A 3). The bulb was intentionally made small in order to carry out a considerable number of experiments with expensive gases, such as xenon and krypton, and also to facilitate thermal equilibrium. Inside the bulb there is a small iron-in-glass stirrer (A 4) (overall density $\sim 4\ g\ cm^{-3}$, to ensure that it sinks in dense liquids) operated by an electromagnet of approximately 10 cm internal diameter which surrounds the whole pyknometer assembly. The electromagnet is fitted with an oscillating mercury contact switch of frequency $\sim$ 1 Hz.

The pyknometer bulb and part of its stem are surrounded by a glass vessel (A 5) of about 6 cm^3 capacity into which the cryostat substance is condensed via tube (A 6). The cryostat feed-line is fitted with trap (Q) (Fig. 3.1) for initial condensation of the cryostat material from the appropriate storage globe. Also incorporated in this line is a U-tube manometer (R) (Fig.3.1), which is used to monitor the approach of the cryostat substance to its triple-point. The cryostat vessel (A 5) is itself surrounded by a glass jacket (A 7) about 20 cm long which provides thermal isolation when evacuated or thermal conduction when containing a small amount of helium admitted from globe (P) to a pressure given by manometer (O) (Fig.3.1).

The triple glass vessel (A 1) - (A 5) - (A 7) is enclosed in the cylindrical copper shield (A 8), which is 3 mm thick and fitted with observation slits. The shield is suspended by three metal struts (A 9), and has a base 2.5 cm thick (to even out any temperature fluctuations), to which is attached a copper rod about 15 cm long and 8 mm in diameter (A 10).

To prevent condensation of the gases in the inlet tubes in the event of their becoming too cold, a copper ring (A 11) wound with a heater

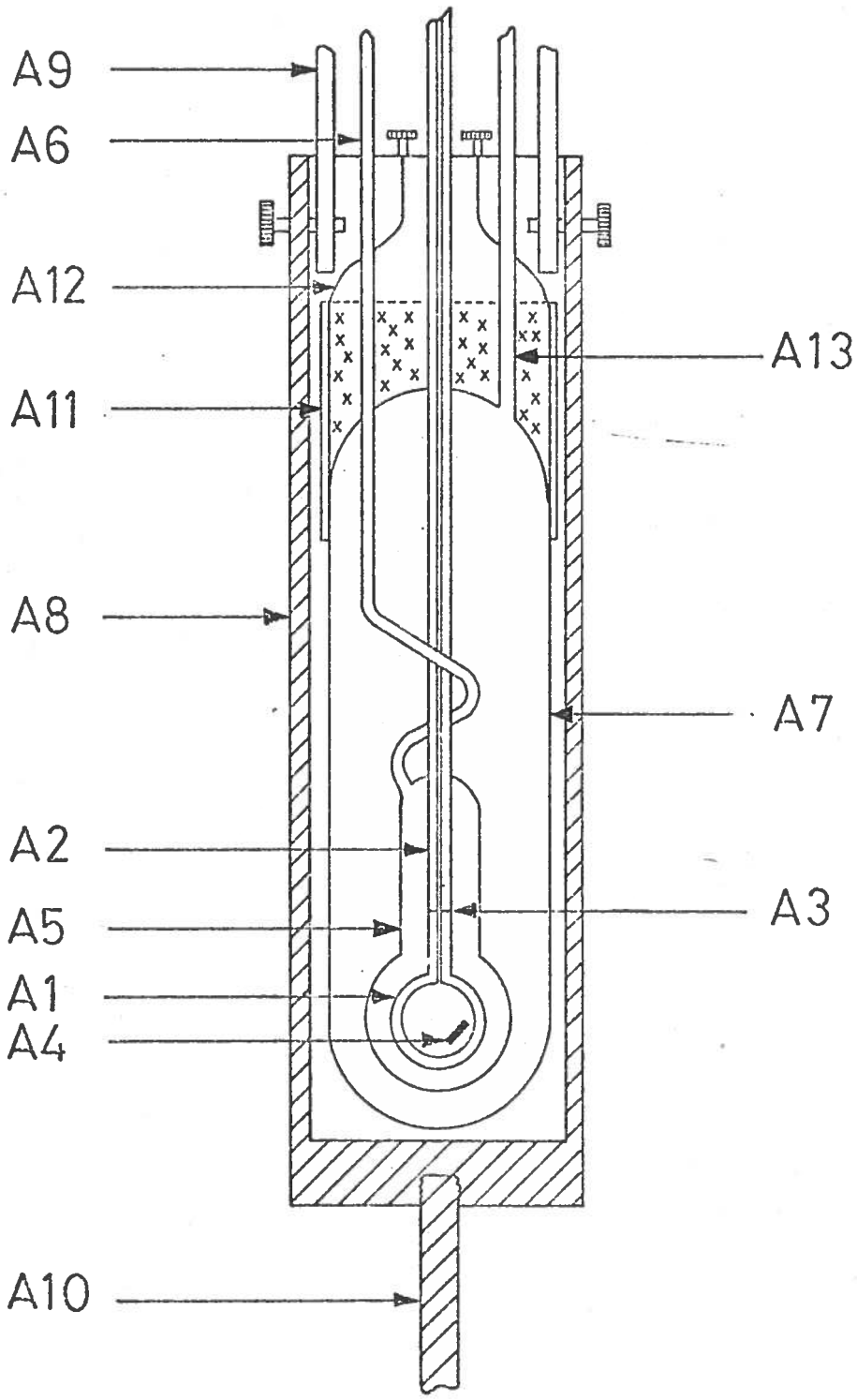

Fig. 3.2 - Pyknometer assembly

of resistance 25 Ω surrounds the upper part of jacket (A 7). Thermal contact between the shield, ring and jacket is achieved by four flexible copper strips (A 12), and also by filling the space inside the copper ring with a mixture of copper powder and paraffin wax (A 13). In practice, it was seldom necessary to use this device.

3.1.3 *PRESSURE INSTRUMENTATION*

All the pressure measurements, apart from the triple-point pressure determinations already described, were made using Texas Instruments quartz-spiral gauges. Three of these were, in fact, utilized (Models 145-01, 145-0 and 140 B). Which was selected for a set of measurements depended on the vapour pressure range to be studied. All three instruments were fitted with Type 1 capsules, the ranges being from zero to, respectively, 135, 710 and 1400 kPa.

Although calibration tables were provided by the manufacturers, it was decided to recalibrate the manometers in the laboratory. These calibrations were made against accurate primary standards: the mercury manometers (H) (Fig. 3.1) or (X) (Fig. 2.3), for pressures up to 85 kPa, and a Budenberg gas-operated dead-weight gauge, for pressures above 150 kPa. Between these two pressures, calibration was carried out by combining measurements of the atmospheric pressure (~ 100 kPa) made with a Fortin barometer with the readings of one of the quartz-spiral gauges.

The mercury manometer (H) (Fig. 3.1) is a modified, more sophisticated, version of that described in Chapter 2. The main difference relates to the left-hand limb, which in (H) was so constructed as to leave a very small dead-space volume. Moreover, this volume is kept constant while pressure measurements are being made. The mercury meniscus in contact with the gas is brought up to a sharp stainless steel point within the manometer, so closing an electrical circuit made through the mercury with a platinum

wire sealed through the glass at the bottom of the manometer. The level of mercury in the manometer can be varied by taking mercury from, or returning it to, an adjoining reservoir, the final adjustment being made with a stainless steel piston controlled by a screw of small pitch. The right-hand limb and the lower section of the left-hand limb are constructed from precision bore glass tubing of 13 mm internal diameter and they are both provided, at their lower ends, with devices for renewing and cleaning the mercury surface. The upper section of the left-hand limb is constructed from capillary glass tubing of 1 mm internal diameter. This section is also fitted with a small ball-valve to prevent the accidental passage of mercury into the calibrated dead-space, and is joined to the wide bore lower section through a stainless steel adaptor.

The Budenberg dead-weight gauge, schematically shown in Fig.3.3, consists of an accurately machined hollow steel piston and cylinder assembly (A) mounted vertically on a levelled base plate. It is connected to the quartz-spiral pressure gauge by a copper tube, via valve (D) and tap (4) (Fig. 3.1). The piston is approximately 11 cm long and has an effective area of $3.2261 \pm 0.0003\ cm^2$, as determined by the National Physical Laboratory[3]. Its upper end is attached to a circular light metal table 9.0 cm in diameter, which is designed to accommodate the circular loading weights. The pressure head is provided by the buffer vessel (F) (Fig.3.1) which is connected to an oxygen-free nitrogen cylinder. It is regulated by valves (F) and (G) (Fig. 3.3), and is shown, approximately, on gauge (C). In operation the weights on the freely rotating piston plus the atmospheric pressure should equal the pressure head. Because of this it is advisable to calibrate the quartz-spiral gauge with the space surrounding the spiral open to the atmosphere. In this manner, the digital counter readings will correspond to the loading weights only.

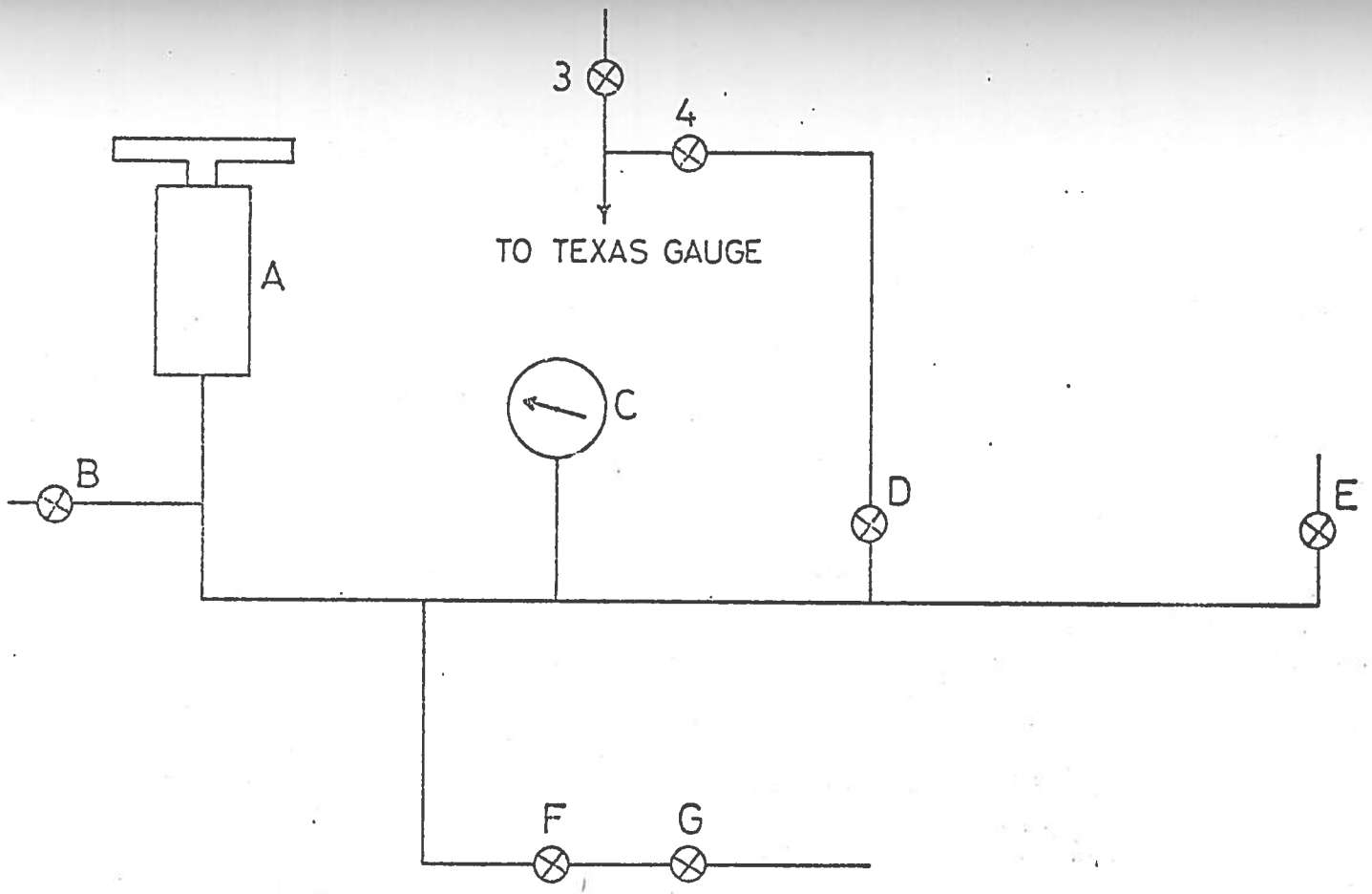

Fig. 3.3 - Dead-weight pressure gauge (schematic)

To calibrate a quartz-spiral gauge against the dead-weight gauge one operates in the following manner. With valve (3) (Fig. 3.1) closed, valve (4) is opened to inter-connect the two gauges. Valves (B), (E) and (F) on the dead-weight gauge are closed and valve (D) fully opened. The weights on the piston are chosen to produce a pressure of the desired magnitude. With valve (F) closed, valve (G) is opened and the pressure head regulated to a slightly higher value than is required to balance the piston, by careful control of a special valve attached to the nitrogen cylinder. Valve (F) is then carefully opened until the piston starts to rise. The piston is then spun manually at ~ 1 Hz and is kept at constant height, as shown by a reference mark, by adjusting the ballast pressure with valve (F). This is to ensure that the contact areas of the piston and cylinder are the same in every measurement. If the nitrogen flow is slightly excessive, the piston tends to bounce, and the flow of nitrogen is then reduced by slightly closing valve (F). Similarly, if the piston starts to fall due to an insufficient pressure head, valve (F) should be opened a little more. Under these conditions, the piston should spin for at least five minutes which provides sufficient time for a series of readings to be taken with the quartz-spiral gauge. When sufficient readings have been made, valve (F) is closed, the rotation of the piston and weights is stopped, and valve (B) is opened when the piston has fallen to its rest position. The procedure is repeated at various pressures.

3.1.4 *LOW-PRESSURE SECTION*

In its present form the low-pressure section of the apparatus is limited to the calibrated storage globes (M) and (N) (Fig. 3.1) of approximately 2.5 dm^3 capacity each, and the corresponding capillary lines to valve (12). The globes are housed in a thermostat (X), the temperature of which is kept at ~ 298.15 K by a toluene regulator with a Sunvic relay.

The water bath is also fitted with a stirrer and a 110 W heater connected to the relay system. The thermostat temperature is read to 0.01 K on thermometer (L) which was calibrated against a standard certificated by the National Physical Laboratory.

3.1.5 *CALIBRATIONS*

(i) *Pyknometer bulb*

To determine the molar volumes of the pure components and of the mixtures studied both the volume of the bulb and the cross-sectional area of its stem must be accurately known. The latter was determined[4] prior to assembly of the apparatus by the usual method of measuring the mass and length of mercury threads. The result of this calibration is given in Appendix (C).

The volume of the pyknometer bulb had originally been determined at room temperature by mercury filling, and the volume at lower temperatures deduced from the room temperature value by using the expansion data for pyrex glass of BUFFINGTON and LATIMER[7]. However, the repeated thermal cycling to which the bulb is inevitably subjected may cause the volume to change, and moreover as times goes on some mercury tends to condense in it. This makes frequent re-calibration highly desirable. Previous workers with this apparatus accomplished this by determining the number of moles of a selected pure liquid, usually methane or krypton, needed to fill the pyknometer to the etch mark. This result was used with the molar volume data of TERRY *et al.*[8] (who employed a much larger pyknometer, of $\sim 9\ cm^3$, hence increasing the accuracy) to find the final volume of the pyknometer.

It recently became apparent, however, from the work of McCLUNE[9] and that of HAYNES and HIZA[10] (who used a very precise buoyancy technique), that the molar volumes determined in this laboratory could be systematically too high, by 0.1 to 0.4%. This had, in fact, already been

noticed by STREETT *et al.*[11] on comparing their results for liquid xenon with those from THEEUWES and BEARMAN[12]. It was therefore decided to recalibrate the pyknometer whenever possible at the actual temperature at which measurements were to be made, to avoid the introduction of temperature corrections, and also to use as the calibrating fluid a substance such as ethane for which the recent density results of HAYNES and HIZA[10] were available. A measured amount of pure ethane was condensed (as explained in section 3.3) into the pyknometer, at the triple-point temperature of either hydrogen chloride (T_t = 159.01 K) or nitrous oxide (T_t = 182.32 K), and the distance between the level of the liquid meniscus in the stem and the etch mark was carefully measured with a cathetometer. As the cross-sectional area of the capillary was known, the exact volume of the pyknometer to the etch mark could be calculated. In this way the following values were obtained:

$$V_{pk}\ (159.01\ K) = 2.2015 \pm 0.0004\ cm^3$$
$$V_{pk}\ (182.32\ K) = 2.2026 \pm 0.0002\ cm^3 \quad ,$$

the standard deviations giving an indication of the precision of the measurements. The result at 159.01 K is the mean value of two sets of determinations, and that at 182.32 K corresponds to three independent experiments.

(ii) *Quartz-spiral gauges*

The calibration of the Texas Instruments gauges, as described in 3.1.3, gives pairs of values (P_g, P) which must be appropriately related so that the user can convert the values P_g of the readings on the digital counter into values of the true pressure P. The problem is thus to find a scale factor K_p such that

$$P = K_p\ P_g \ , \qquad \ldots (3.1)$$

K_p being itself, in general, a function of the pressure and hence of P_g.

The pairs (P_g, P) were therefore treated as follows. For each pair,

the quotient $K_p = P/P_g$ was calculated, and the set of K_p values so obtained was subsequently adjusted, by least squares, to a polynomial expression of the form

$$K_p = \sum_{i \leq 7} a_i P_g^i \quad . \qquad \ldots (3.2)$$

This was done by means of a standard computer routine which gave, in each case, the degree of the best polynomial and its coefficients.

The results for the three gauges employed in this work are recorded in Appendix (D).

In the final calculation of the pressure, account was also taken of a small correction recommended by the manufacturer. This correction is to be applied when the temperature of the capsule during the readings is different from that prevailing during the calibration runs. This factor has the form

$$K_t = \left[1 + 1.3 \times 10^{-4} (t - t_c)\right]$$

where t and t_c refer to the temperatures (°C) of the capsule during a particular reading and during the calibration run respectively.

Accordingly, the final values of the pressure are given by

$$P = K_t K_p P_g \quad . \qquad \ldots (3.3)$$

(iii) *Dead-space Volumes*

In the preparation of the liquid mixtures the amount of substance of each component condensed into the pykometer is determined from the difference beween the initial and final number of moles of that gas in the corresponding thermostatted globe, the numbers of moles being evaluated from appropriate pressure and temperature measurements.

From Fig. 3.1 it will be seen that during the pressure measurements the temperature of the gaseous mass is not uniform: the small qauntity of

gas filling the line will be at room temperature. It is therefore necessary to know the volume and temperature of this dead-space.

To calibrate the volume of the section of the line defined by valves (1), (4), (7), (10), (11), (13) and (14), and by the mercury surfaces at levels (B) and (D), a set of expansions was made taking as a reference the volume of vessel (E), between the fiducial marks (D) and (D′). The latter had been accurately determined prior to assembly by mercury weighing. Nitrogen was chosen as the working gas for the P-V-T determinations in view of the proximity of its Boyle temperature to room temperature.

It is also necessary to know the small volume between valve (10) and the mercury meniscus in the left-hand limb of the Boyle's law manometer (J). The calibration had recently been carried out and therefore it was not repeated. The result is given in Appendix (C).

The expansion method, using nitrogen at room temperature, was also used to determine the volume of the dead-space bounded by valves (1), (2) and (4), and by the mercury menisci at (B) and (D). This volume is important for the calculation of the composition of the vapour in equilibrium with the liquid mixture.

The volumes of the thermostatted globes had been calibrated by weighing (using distilled water), and their volumes were simply checked by making pressure measurements before and after expanding gaseous nitrogen contained in one of them, taken as a reference, into the volume of the line and the other globe.

The volume of the capillary stem of the pyknometer, hereafter designated by V_{gr}, was taken from MORRIS[4] who assembled this part of the apparatus.

A list of results of all the volume calibrations is presented in Appendic (C).

3.2 VAPOUR PRESSURES. EXPERIMENTAL PROCEDURE

The vapour pressures of the liquid mixtures and also of some of the pure components were measured in the apparatus just described (Fig. 3.1). In most cases the determinations were made at the lowest temperature at which both components are liquid, i.e. at the triple-point of the component of higher melting-point. (Operation below this point, at least over part of the phase diagram, is possible, although some technical difficulties may occur due to solidification of the component of higher melting-point in the pyknomecer.)

Before starting a run the apparatus is thoroughly evacuated and the two storage globes, (M) and (N), after being flushed out with a small amount of the gases to be stored, are filled to a pressure of ~ 100 kPa (~ 1 atm). The remainder of the apparatus is then evacuated again, and the thermostatted tank (X) is allowed to reach thermal equilibrium. Similarly, globe (P) must be filled to a pressure of ~ 30 kPa (~ 0.3 atm) with helium, used as a thermal exchange medium. The quartz-spiral gauge, which must have been switched on at least a couple of hours prior to operation, is set at zero.

An actual run consists of three more or less independent stages: the filling of the cryostat; the filling of the pyknometer; and the pressure measurements, including the preliminary homogenization of the vapour phase. These will be described in the next subsections.

3.2.1 *THE FILLING OF THE CRYOSTAT*

The pyknometer assembly is allowed to cool by surrounding it with liquid nitrogen contained in a large dewar, the refrigerant just touching the base of the copper shield. Tap (24) is closed and the small amount of helium trapped between taps (25) and (26) is allowed to expand into the jacket (A 7) (Fig.3.2), by opening (25).

The cryostat substance is then brought from the storage line and an appropriate amount of it is condensed into trap (Q) surrounded with liquid nitrogen, by opening tap (30), with (31) closed. When sufficient material is collected in (Q), tap (30) is closed, (31) opened, and the lines which have been used for the transference are evacuated. Taps (30) and (31) are then secured with strong rubber bands, the dewar surrounding trap (Q) is lowered, and the cryostat is allowed to warm. (The ring heater can be switched on at this stage, at a current of ~0.3 A). The pressure of the gas, monitored on manometer (R), should not be allowed to rise much beyond ~ 130 kPa (~ 1.3 atm), although it should be kept well above its triple-point pressure, so that the material can be condensed into the cryostat as a liquid. The surface of the liquid refrigerant is kept level with the bottom of the copper shield, either by adjusting the position of the large dewar, or adding more liquid nitrogen.

After a time (usually ~ 15-20 minutes, depending upon how long the pyknometer assembly has been cooling), the material will start to condense in vessel (A 5) (Fig. 3.2). The topping-up of the liquid nitrogen in the dewar is then stopped. During the condensation the pressure is conveniently maintained in the appropriate range by adjusting the level of the refrigerant surrounding trap (Q). When the liquid level in the cryostat is slightly below the etch mark on the pyknometer stem, thus ensuring that there will be a sufficient amount of substance to cover the bulb of the pyknometer when it is at its triple-point, the condensation is stopped by closing trap (31) and replacing the refrigerant round (Q).

The timing of the next set of operations depends on the previous experience of the operator in handling the particular cryostat substance. The aim is to allow the cryogenic material to approach its triple-point so as to avoid unnecessary cooling of the solid once it forms from the

liquid. This is achieved by appropriate choice of the moment to start pumping out the transfer gas in the jacket (A7), and to lower the large dewar containing the refrigerant to an appropriate level.

For substances like HCℓ and N_2O a convenient procedure is as follows. Immediately after closing tap (31), tap (11) is closed and tap (24) is opened to pump out all the helium in jacket (A7). When the pressure, read on (R), reaches a value slightly above that corresponding to the triple-point of the cryogenic substance, the large dewar surrounding the pyknometer assembly is lowered to a level at which the copper rod just touches the surface of the refrigerant. The temperature of the cryostat will continue to drop, as indicated by the readings on (R). Provided the cryostat liquid is sufficiently pure it will eventually supercool (pure nitrous oxide, for instance, showed a tendency to supercool by up to 12 K before freezing, as estimated from the fall in pressure on (R)), until the solid suddenly forms from the liquid and the vapour pressure, on (R), jumps back to a value slightly below that of the triple-point. The dewar is further lowered to a position in which its top is level with the upper part of the copper shield, and the assembly is allowed to warm until the solid in the cryostat starts to melt. (To speed up this process the shield heater can be switched on at a current of ~ 0.15 A). The dewar is then raised to its final position at which the lower end of the copper rod is ~ 1 cm above the surface of the liquid nitrogen in the dewar. The cryostat substance should then continue to melt, but only very slowly, allowing ample time for all subsequent operations. If the melting rate of the material is faster than expected, the triple-point can be easily restored by careful evaporation of a little of liquid into trap (Q) (by slightly opening (31)), and by adjusting the level of the refrigerant. That the cryostat substance is at its triple-point can be checked by watching the pressure on manometer (R), and also by visual observation.

3.2.2 *THE FILLING OF THE PYKNOMETER*

Since the less volatile component is often the same substance as that used in the cryostat, it is good practice not to start introducing this component until the cryostat material is already melting, to avoid freezing of that component in the pyknometer stem.

To introduce the first, less volatile, component into the pyknometer, tap (1) is closed, and by opening either tap (13) or (14) the gaseous component is admitted into the calibrated volume V_{R2} (Appendix (C)) of the line. The levels of the mercury in vessels (C) and (E) are restored to the fiducial marks (B) and (D), and the initial pressure of the gas is then read on the Texas Instruments gauge whose operating temperature is also recorded. These readings are taken at 60 s intervals during five minutes, as well as the room temperature and that of the thermostat tank (X). The distance (mm) between the zero reference mark and the mercury meniscus in the left-hand limb of manometer (J) is also recorded. Valve (9) is closed, and bulb (I) immersed in liquid nitrogen. The approximate amount of gas required for the experiment is then condensed into (I) by carefully opening tap (9), watching the pressure drop on the digital counter of the gauge (G). Taps (12) and (13) are closed, the refrigerant around bulb (I) is lowered, valve (9) is opened, and the pressure is allowed to increase to about 150 kPa (~ 1.5 atm). At this point valve (1) is opened to condense the gas into the pyknometer. When all the component has been transferred, tap (1) is closed, (12) and (13) are opened, and the residual pressure of the gas in the globe is recorded, as are the relevant temperatures and the mercury level in the left-hand arm of manometer (J), as described above. Tap (13), or (14), is then closed, tap (11) is opened and the line is evacuated for half an hour. Meanwhile, the cryostat is adjusted to the triple-point conditions once more.

From the knowledge of the initial and final pressures, the calibrated volumes and the respective temperatures, the number of moles of the less volatile component condensed in the pyknometer can be calculated, as it will be shown in Chapter 5.

The second component is introduced into the pyknometer in the same way. Care must be taken not to allow the first component, already in the pyknometer, to diffuse back into the line, and for this reason, during the condensation, it is necessary to have the second, more volatile, component at a relatively higher pressure, well above the triple-point pressure of the first component. A pressure of 0.2 - 0.3 MPa ($\sim$ 2-3 atm) is usually sufficient.

At the end of this stage the pyknometer should be about half to two-thirds full of a liquid mixture whose composition can be calculated to within a few parts in 10^4, as shown in Appendix (E). The amount of each component will be about 10^{-2} moles.

As a move towards making the mixture homogeneous the stirrer is switched on for 5-10 minutes, and the line is evacuated up to tap (1) for another half an hour. The conditions prevailing in the cryostat are, meanwhile, checked once again, and the triple-point restored if necessary.

3.2.3 *THE MEASUREMENT OF THE VAPOUR PRESSURE*

Before starting the measurements of the vapour pressure of the mixture it is necessary to ensure that both phases are homogeneous and as close to equilibrium as possible. The homogeneity of the liquid phase initially contained in the pyknometer is achieved by switching on the magnetic stirrer for about 15 minutes. To perform the pressure measurements the dead-space bounded by taps (1), (2) and (4) and the quartz-spiral — whose volume is designated by V_{R1} (Appendix C) — must be full of

vapour, this being achieved by opening tap (1). However, opening up the pyknometer to the dead-space will draw off vapour richer in the more volatile component, and the long, narrow pyknometer capillary will hinder rapid equilibration by diffusion. Moreover, the composition of the liquid also changes during the withdrawal. An appropriate technique has, therefore, been developed to establish the required conditions of homogeneity and equilibrium. This consists of evaporating part of the liquid into a volume twice that of the final dead-space (that is, into 2 V_{R1}), making this vapour homogeneous and condensing half back into the pyknometer bulb. Calculations[2] have shown that the vapour pressure obtained by this technique does not significantly differ from the true equilibrium vapour pressure, and this is confirmed by the observed constancy of the vapour pressure measured after following the procedure just outlined.

In detail, the experimental procedure for establisning the equilibrium vapour pressure is then as follows. After thorough evacuation of the line up to tap (1), valve (2) is closed. The magnetic stirrer, which at this stage should have been working for ~ 15 minutes, is left switched on. Tap (1) is then carefully opened, and the vapour allowed to pass into the line. The level of mercury in vessel (E) is very slowly lowered, by withdrawing mercury through valve (6), to a previously defined position corresponding to leave a space of volume ~ V_{R1} between the mercury surface and the upper mark (D). This expansion of the dead-space to a total volume ~ 2 V_{R1} should take ~ 10 minutes. Tap (1) is now fully opened and then closed, and the stirrer is switched off allowing the electromagnet to cool. The level of mercury in vessel (C) is lowered to mark (B′) (by opening valve (5), having the ballast vessel (F) connected to the vacuum source), and then raised to the upper mark (B), by applying pressure to vessel (F). This is repeated twice more, to thoroughly mix up the vapour. On the last compression the mercury is returned to mark (B). The level of mercury

in vessel (E) is raised a little to increase slightly the pressure in the dead-space volume above that in the pyknometer, and thus prevent further vapour from diffusing into the line. The stirrer is switched on, tap (1) is re-opened, and the level in vessel (E) is slowly raised to the calibration mark (D). The conditions in the cryostat are checked, and adjusted to the triple-point if necessary. (The heaters are also checked to ensure that both are switched off). The stirrer is left working, and the vapour pressure of the mixture watched on (G). After a few minutes steady pressure readings can be obtained. The light behind the cryostat is switched off. (Otherwise, heating of the sample by absorption of radiation can cause slight but significant vapour pressure increases.) The vapour pressure of the mixture is then recorded over a period of 30-60 minutes, readings being taken every minute. The room temperature is also recorded over the same period. The stirrer is usually switched off after the first 15-20 minutes.

The pressure should remain constant within a few parts in 10^4 until a large amount of the cryostat material has melted. If too much melts before the readings are complete, it can be refrozen by controlled evaporation (into trap (Q)), having closed tap (1). When the triple-point conditions are restored tap (1) is re-opened, and the readings are continued.

After the determination is complete, the mercury in vessels (C) and (E) is lowered slightly to avoid it getting into the calibrated space as a result of decompression. Taps (2) and (11) are carefully opened, the large dewar is lowered, helium is admitted to the glass jacket, both heaters are switched on, and the mixture is either pumped away or collected in a storage globe. Tap (31) is also opened and the cryostat material condensed back into trap (Q) to be transferred to its storage globe.

3.2.4 *VAPOUR PRESSURE OF A PURE COMPONENT*

The measurement of the vapour pressure of a pure substance at the triple-point of a particular material presents no special difficulties. The filling of the cryostat and the pyknometer are performed as described above. The amount of substance does not, of course, have to be measured, although it is important to see that there is sufficient liquid in the pyknometer to ensure that it will not all evaporate into the dead-space when tap (1) is opened. There is no need to mix the vapour, as it is a single component. However, it is advisable to stir the liquid in the pyknometer when the cryostat substance is at its triple-point, in order to help the liquid to reach thermal equilibrium. The measurement of the vapour pressure is then carried out as described previously.

The triple-point pressure of a pure substance is usually measured in the so-called triple-point cell, as described in Chapter 2.

3.3 MOLAR VOLUMES. EXPERIMENTAL PROCEDURE

The principle involved is very simple and consists in determining the number of moles required to fill the pyknometer to the calibration mark on its stem.

The two first stages – the filling of the cryostat and the pyknometer – are conducted much in the same way as for the vapour pressure measurements. On filling the cryostat, care must be taken to ensure that the bulb of the pyknometer is completely covered, but the calibration mark on its stem is left uncovered. This means filling up the cryostat to within 2-3 mm below the etch mark. On bringing the cryostat material to its triple-point by the evaporation technique, crystals may form around the stem obscuring the mark (and possibly the liquid meniscus). But experience has shown that these crystals melt relatively more quickly than the main body of the cryostat material, so that readings can be taken as soon

as the etch mark and the meniscus are visible, well in the early stages of melting of the bulk material.

In so far as the filling of the pyknometer is concerned, the differences are again only slight. It is preferable to introduce the second component into two stages. This is because the liquid mixture must finally fill the pkynometer stem to a level within ± 1-2 mm from the etch mark when the cryostat reaches its triple-point. The first portion of the second, more volatile component should fill the pyknometer just to the neck. Then, the stirrer is switched on for a few minutes, the cryostat material is adjusted to its triple-point, and when it starts melting the rest of the component is carefully allowed to condense, filling the pyknometer capillary. When the liquid meniscus reaches the region of the stem near the etch mark, as shown by visual observation, tap (1) is closed, preventing any further condensation.

As the liquid meniscus must be above the level of the substance in the cryostat (so that it can be seen), it is obvious that the small portion of liquid not surrounded by the cryogenic bulk material may well be at a temperature slightly higher than the rest of the mixture. By measuring the vapour pressure of a pure liquid filling the pyknometer to a level near the etch mark (as if it was intended for a molar volume determination), and from the knowledge of a vapour pressure equation for that substance, it is easy to find the actual temperature of the surface of the liquid. This result can be used, with the temperature coefficient of the molar volume of the liquid in the pyknometer, to show that the effect of this slight overheating of the liquid in the capillary on the value of the molar volume is usually less than one part in 10^4.

When the filling of the pyknometer is over, the third stage of the experiment begins. The dead-space, from the etch mark to tap (1), has been made deliberately small (V_{gr} = 1.425 cm^3), and therefore there is no need to mix the vapour. To homogeneize the liquid mixture one can cool the cryostat, by repeated evaporation or other suitable method, until a temperature has been reached at which all the liquid contained in the capillary has contracted back into the bulb. The contents of the pyknometer are then stirred for about 20 minutes, while the assembly is allowed to warm to the triple-point. The stirrer is switched off, and measurements of the heights of the liquid meniscus and etch mark are made with a cathetometer. Readings are taken until a series of values of the meniscus height constant to better than 0.1 mm for half an hour has been obtained. The room temperature is also recorded at one minute intervals.

The shut-down is performed as described previously.

A final remark should be made on the molar volume determinations of mixtures involving one component whose triple-point temperature is higher than that of the cryostat substance. This is the case of the xenon + carbon tetrafluoride system, the molar volumes of whose mixtures where determined at the hydrogen chloride triple-point temperature (Chapter 11). At this temperature, xenon is a solid, and as it is the less volatile component it has to be the first to be condensed into the pyknometer.

To avoid it freezing in the capillary, tap (1) is opened only after the cryostat substance has melted completely and has a vapour pressure ~ 3 kPa above that of its triple-point. After the xenon has condensed, the assembly is cooled to the HCℓ triple-point by slightly raising the level of the refrigerant. (When all the cryostat material is in the liquid state, even at temperatures just above that of its triple-point, cooling by evaporation will consume too much of the cryostat contents, and there-

fore should be avoided.) For the introduction of the second component — carbon tetrafluoride — the two steps technique described above is used with a slight modification. After condensation of the main quantity of CF_4, to a level slightly below the neck of the pyknometer, the assembly is allowed to warm (by lowering the large dewar with the refrigerant). When all the HCℓ in the cryostat has melted, the stirrer is switched on. Usually at this stage xenon has already started to melt too, mixing with the carbon tetrafluoride, and it is possible to free the stirrer from the remaining solid xenon in the pyknometer. The contents of the bulb are then stirred for a period, until xenon has completely melted and mixed with CF_4. The assembly is cooled to the hydrogen chloride triple-point temperature, the stirrer switched off, and the final portion of the second component allowed to condense into the pyknometer up to the vicinity of the etch mark. The experiment is then continued as described for the general case.

3.4 REFERENCES

(1) MATHOT, V., STAVELEY, L.A.K., YOUNG, J.A. and PARSONAGE, N.G., Trans. Faraday Soc., 1956, 52, 1488.

(2) DUNCAN, A.G., 'The Thermodynamics of Mixing of Binary Condensed Gas Mixtures', Thesis, University of Oxford, (1966).

(3) CALADO, J.C.G., 'Thermodynamic Studies of Binary Condensed Gas Mixtures', Thesis, University of Oxford, (1969).

(4) MORRIS, P.J., 'A Study of the Thermodynamic Properties of Binary Mixtures of Liquified Gases', (Part II) Thesis, University of Oxford (1972).

(5) DAVIES, R.H., DUNCAN, A.G., SAVILLE, G. and STAVELEY, L.A.K. Trans. Faraday Soc., 1967, 63, 855.

(6) CALADO, J.C.G. and STAVELEY, L.A.K., Trans. Faraday Soc., 1971, 67, 289.

(7) BUFFINGTON, R.M. and LATIMER, W.T., J. Am. Chem. Soc., 1928, 48. 2305.

(8)(a) TERRY, M.J., 'An Experimental Study of Equations of State for Liquefied Gases', (Part II) Thesis, University of Oxford (1966).

(b) TERRY, M.J., LYNCH, J.T., BUNCLARK, M., MANSELL, K.R. and STAVELEY, L.A.K., J. Chem. Thermodynamics, 1969, 1, 413.

(9) McCLUNE, C.R., Cryogenics, 1976, 16 , 289.

(10) HAYNES, W.M. and HIZA, M.J., J. Chem. Thermodynamics, 1977, 9, 179.

(11) STREETT, W.B., SAGAN, L.S. and STAVELEY, L.A.K., J. Chem. Thermodynamics, 1973, 5, 633.

(12) THEEUWES, F. and BEARMAN, R.J., J. Chem. Thermodynamics, 1970, 2, 507.

CHAPTER 4

ENTHALPY OF MIXING MEASUREMENTS

A good indication of the technical difficulties involved in low-temperature heat of mixing calorimetry is how seldom these measurements have been successfully attempted. Heats of mixing are known for only about two dozen binary systems involving liquefied gases, as opposed to the large number of studies carried out at or near room temperature. In fact, direct experimental results from only four or five laboratories have been reported over the last twenty years or so, and some of these[1] are not currently available. Moreover, since the Leiden[2] and the Brussels[3] calorimeters do not seem to have been in use in recent years, only the Oxford group appears to be active in this field at the present time. WORMALD and his co-workers[4] have developed several flow calorimeters with which heats of mixing of liquefied gases have sometimes been measured. Their measurements in the liquid region generally correspond to high pressure conditions and, therefore, the excess enthalpy H^E at the saturation vapour pressure is obtained by extrapolation. Flow calorimeters require relatively large quantities of liquid, and at the present time the cost of experiments with expensive gases may be prohibitive. In due course, no doubt, semi-micro apparatus using this technique will be devised.

Measurements on such systems have been made in Oxford by STAVELEY and his collaborators[5-7], who designed and developed a static low-temperature isoperibol calorimeter with a sample vessel which was made deliberately small to permit the study of mixtures involving costly components. A brief description of this technique will be given before commenting on its advantages and limitations.

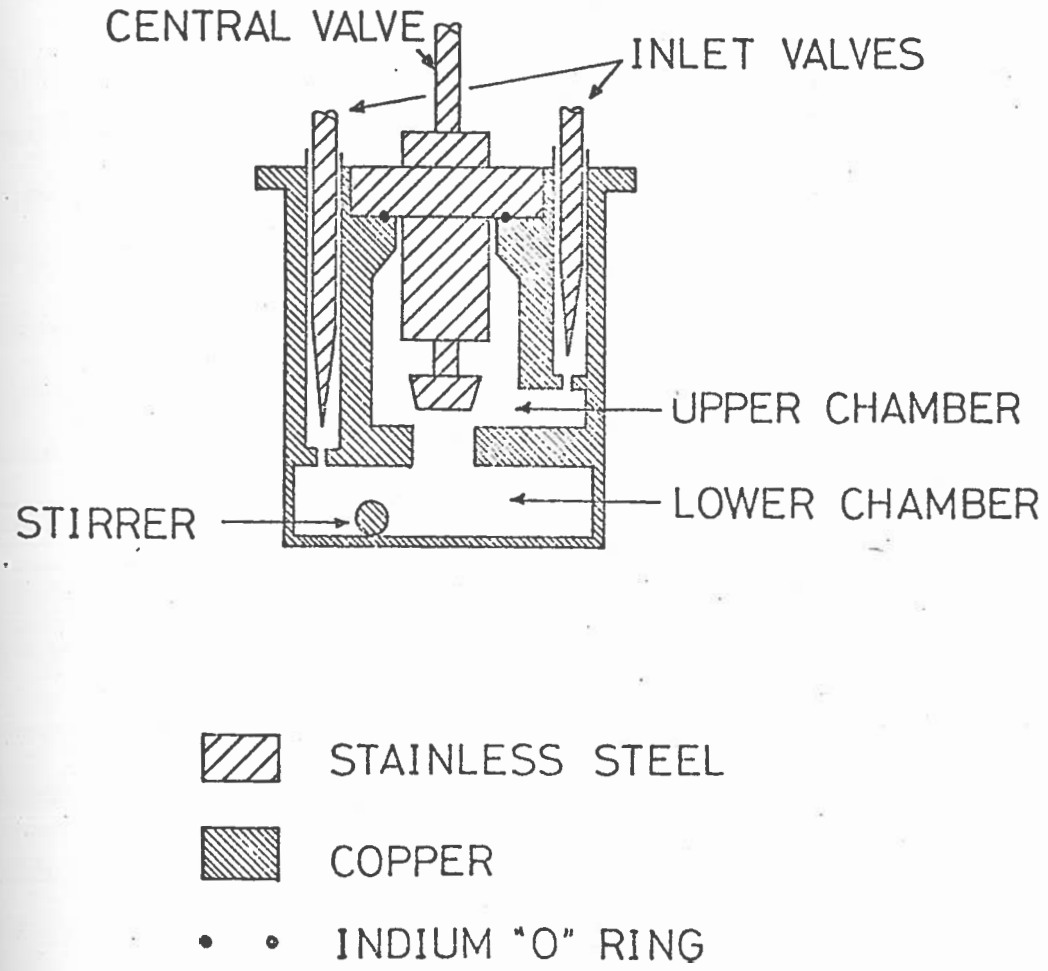

Fig. 4.1 - Calorimeter vessel

Essentially the apparatus, diagramatically shown in Fig. 4.1, consists of two chambers of known volume separated by a partition, which in the latter models takes the form of a metallic valve. Initially this valve is closed and the gases are condensed in each of the two compartments. The calorimeter is then brought to the working temperature, the central valve is opened to allow the liquids to mix, and the energy change is determined. Since before mixing the vapour pressures of the two liquids are not equal, being also different from that of the resulting mixture, some transference of each component between liquid and vapour phases is inevitable. Corrections have therefore to be applied for the energy associated with such vaporization and/or condensation. The importance of these corrections increases as the relative magnitude of the pressures involved goes up, and this effectively limits the working range of the apparatus to below ~ 1.3 MPa. An additional restriction is that only those mixtures can be studied for which sufficient is known about the vapour-liquid equilibrium, thus enabling the necessary corrections to be made with acceptable accuracy. Within its working range this type of calorimeter is, however, capable of giving results of high reproducibility.

More than one third of the available H^E values of low-temperature binary liquid mixtures have been obtained during the last two years with the present version of the calorimeter. This was in existence when the present author commenced his investigations, but parts of it had to be re-made, thereby, it is believed, resulting in some improvement in performance. In the next sections the apparatus and its accessories are described as well as the experimental procedure used in the measurements.

4.1 THE HEAT OF MIXING LOW-TEMPERATURE CALORIMETER

4.1.1 *GLASS APPARATUS*

The low-pressure part of the apparatus is schematically shown in Fig. 4.2, together with the metallic calorimeter assembly (C) and the Texas Instruments pressure gauge (A). With the exception of the stainless steel capillary tubing leading to the calorimeter and to the quartz-spiral gauge, all the low-pressure section is made of glass. In the glass-to-metal junctions, (L 1) - (L 4), common Araldite cement was used. The calibrated globes (G 1) and (G 2) provide the storage space for the pure gases while (G 3) is a large flask used to store the mixtures at the end of the experiments. The helium transfer gas is stored in the globe (G 4). The feed lines are of capillary tubing to keep the dead-space volumes as small as possible. These volumes were measured by a simple gas expansion method using the wide-bore lower section of the right-hand limb of the constant volume mercury manometer (U) to provide the reference volume. The latter was calibrated prior to assembly by weighing the mercury between the levels defined by two sharp metal needles connected to an electrical circuit. Although this mercury manometer can be used for the pressure measurements, these were usually made with the quartz-spiral gauge. An efficient evacuation system, which is essential for the success of the experiments, is provided by a rotary vacuum pump backing a series of two mercury diffusion pumps. With this system pressures of $\sim 10^{-3} - 10^{-4}$ Pa ($\sim 10^{-5} - 10^{-6}$ torr) can usually be obtained, as read on the Penning gauge (P).

4.1.2 *CALORIMETER*

The calorimeter assembly is shown in Fig, 4.3, and an exploded diagram of its innermost copper vessel, which was re-made for the present study, is given in Fig. 4.4.

The actual mixing vessel (C 1) is approximately 50 mm height, and

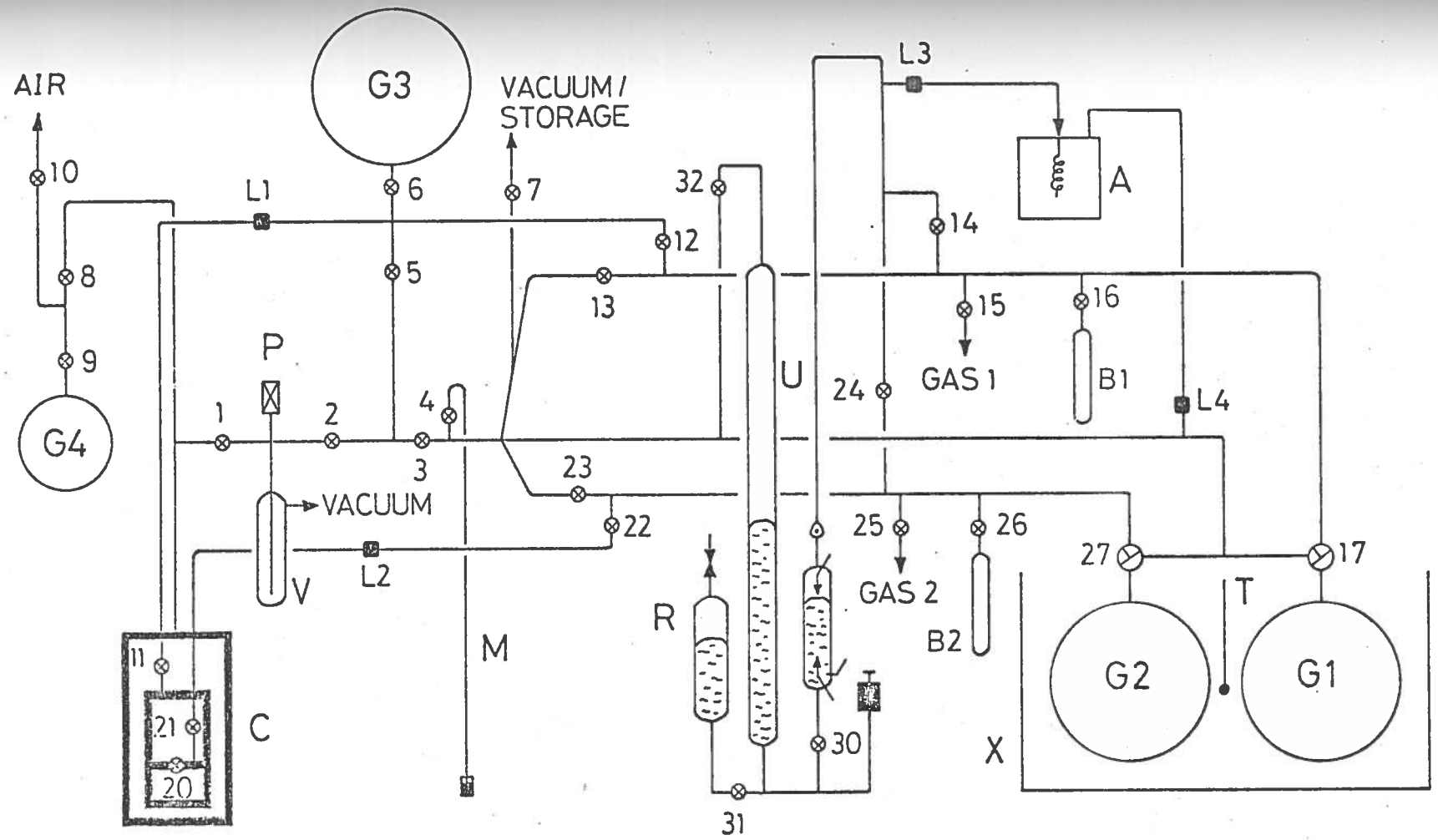

Fig. 4.2 - H^E apparatus

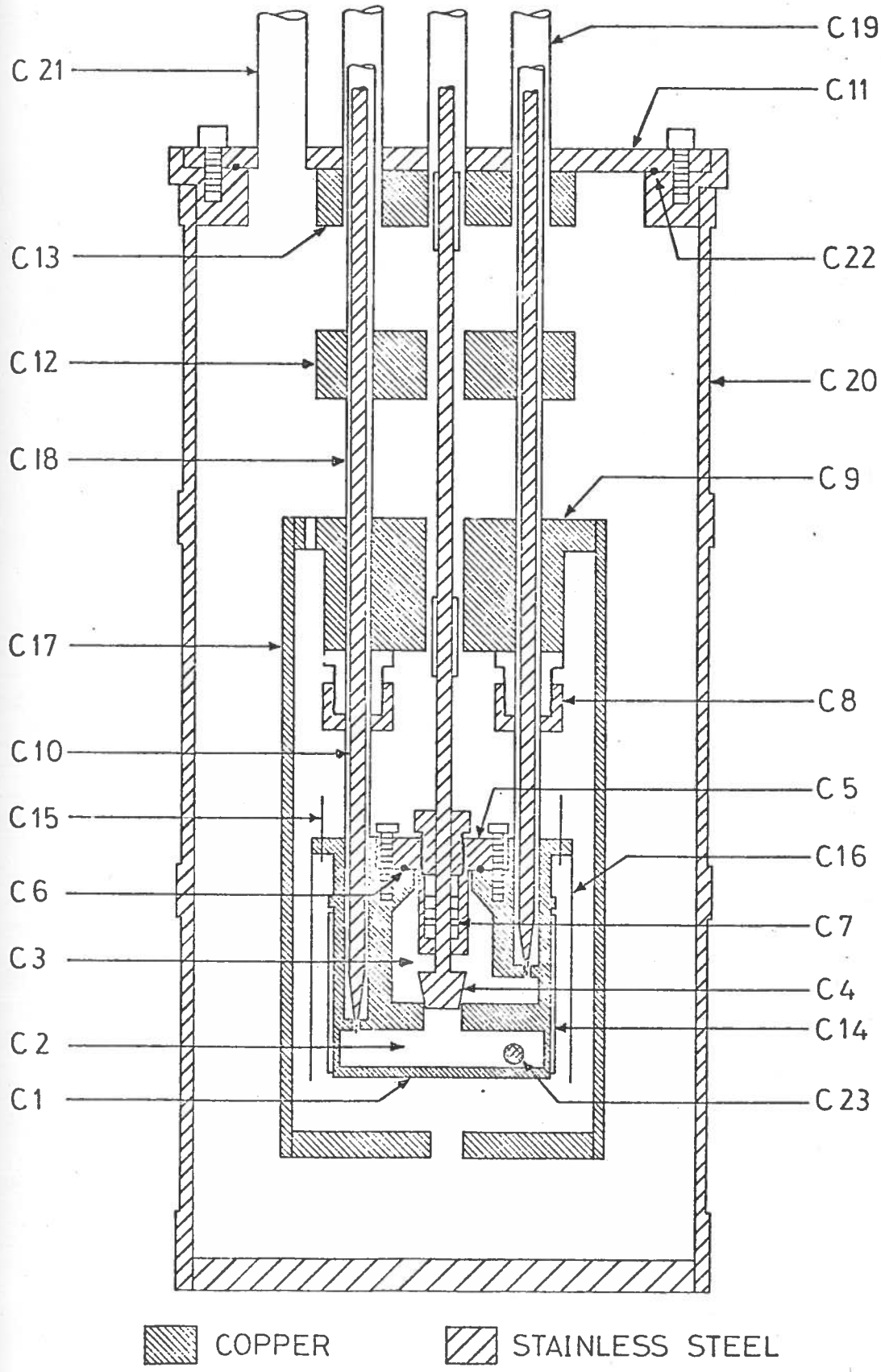

Fig. 4.3 - Calorimeter assembly

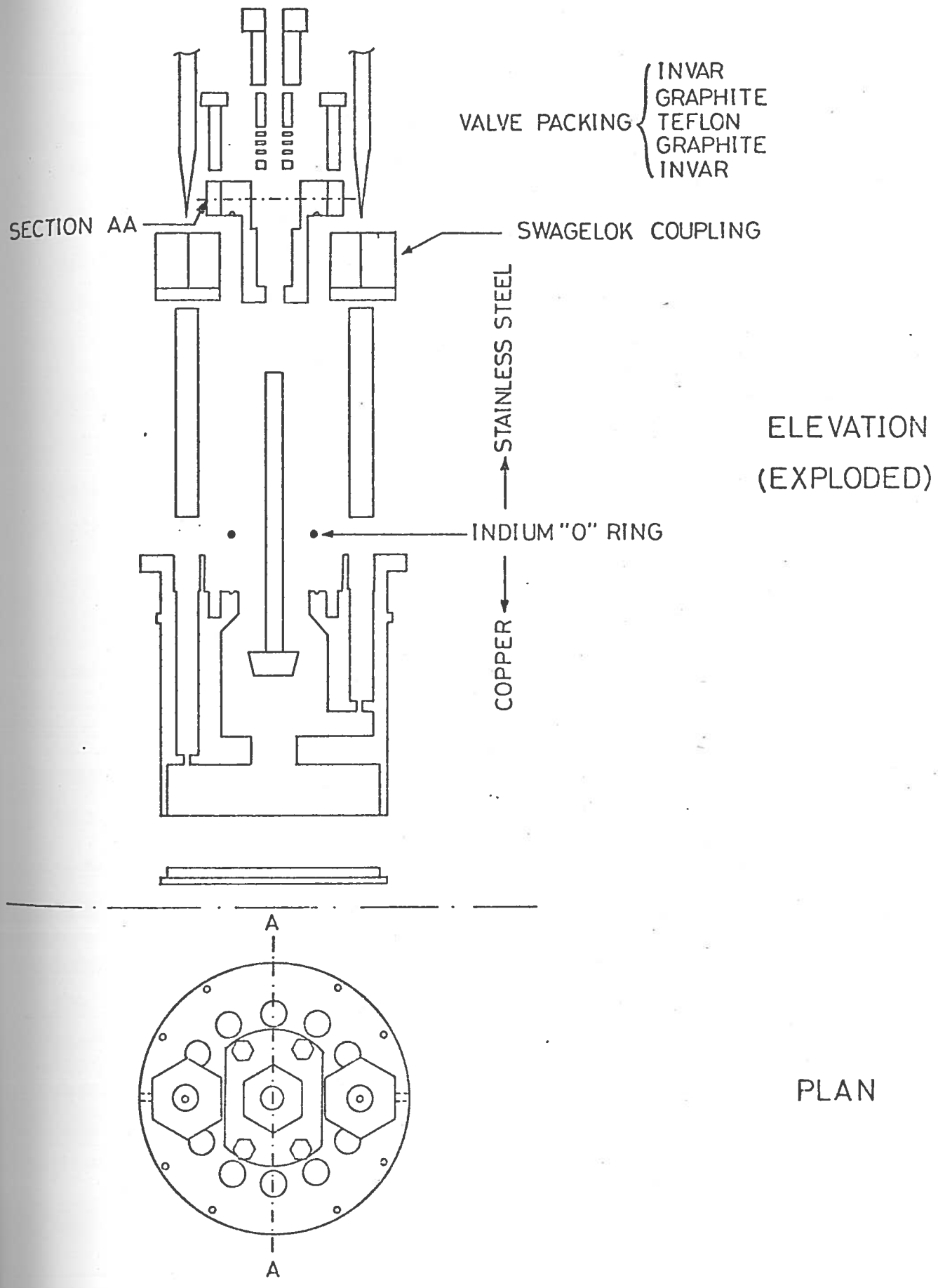

Fig. 4.4 - Calorimeter vessel (exploded)

about 42 mm in diameter. Two cavities (C 2) and (C 3) were machined in the copper block, leaving volumes of ~8 and ~ 3 cm^3 for the lower and upper chambers, respectively. An orifice 8 mm in diameter, which serves as the seat for a metal valve (C 4), separates the two compartments. The valve (C 4) is a 316 SS stainless steel cone, accurately machined and mirror polished. The angle of the cone is 14°. The component (C 5) is also made of stainless steel and is screwed onto the mixing vessel. Sealing is achieved by an 'O'-ring (C 6) held in a groove and made from extruded indium wire of 1 mm diameter. The use of an indium 'O'-ring permits the valve to be easily disassembled when the cone needs to be re-polished. The packing of the valve (C 7) was kept in the form previously described[7]. It includes a Teflon washer 0.635 mm thick as the active seal, the contraction of which with reduction in temperature is compensated by a pair of graphite washers (0.790 mm thick) and two Invar spacers (7.900 and 1.600 mm height, respectively).

Ten holes ~ 5 mm in diameter were drilled in the top of the copper vessel. Eight of them serve to lighten the vessel, the inlet tubes being soft soldered onto the remaining two. These tubes carry "Swagelok' fittings (C 8) to allow the vessel to be easily dismantled from the shield support (C 9). The pure liquids are kept in their respective compartments by two stainless steel needle valves (C 10), which pass through the inlet tubes and terminate in seal assemblies about 56 cm above the level of the vacuum-can lid (C 11). With these valves, the cavities in the mixing vessel are sharply defined. The two inlet tubes also serve to fix the shield support (C 9), and the copper ring (C 12). (C 9) is further secured to the latter by two supporting tubes (not shown in Fig. 4.3) soldered into the three copper blocks (C 13), (C 12) and (C 9).

A heater coil of manganin wire (~ 400 Ω) is wound non-inductively

on a copper sleeve (C 14), and is interspaced with a copper resistance thermometer of resistance ~ 25 Ω at room temperature. The sleeve is a close fit on the outside of the mixing vessel, and thermal contact is assisted by smearing the mating surfaces with Apiezon N grease, which is frozen at the usual working temperatures. The leads from the heater and thermometer are connected to gold-plated contacts which protrude from eight insulated lead-throughs (C 15) in the upper flange of the mixing vessel. A gold-plated radiation shield (C 16) is firmly secured onto the upper flange. It serves to return any heat which is radiated from the mixing vessel during the brief heating periods.

The mixing vessel is surrounded by a copper shield (C 17) on which is wound (non-inductively, as before) a heater coil of resistance ~ 450 Ω interspaced with a second copper resistance thermometer (~ 25 Ω). This shield provides the isoperibol conditions, by being maintained at a constant temperature throughout the mixing process and the subsequent compensation of the heat of mixing.

The copper ring (C 12) is also fitted with a heater coil (~ 240 Ω) and thermometer (~ 30 Ω) assembly so that its temperature can be controlled. It was intended to serve the same purpose as the 'floating-ring' which is sometimes incorporated in low-temperature heat-capacity calorimeters (that is to reduce heat transfer through the leads to the outside colder nitrogen refrigerant). In practice, it is only used when it is necessary to raise the working temperature of the calorimeter.

The electrical leads to the heaters and resistance thermometers are wound around the equilibration copper blocks — (C 9), (C 12) and (C 13) — at each level in the apparatus so as to reduce heat leakage to the liquid nitrogen cryostat in which the whole assembly is placed. Heat leakage is also reduced by using stainless steel in the construction of the inlet

tubes (C 18) and valve stems. To reduce the risk of the two liquids freezing in the inlet tubes as they are introduced into the mixing vessel, those tubes are surrounded by vacuum jackets (C 19) above the vacuum-can lid. During the experiments the vacuum-can (C 20) is evacuated to $\sim 10^{-3}$ - 10^{-4} Pa by pumping out through tube (C 21), which also serves to carry the electrical leads to the outside of the apparatus. An efficient seal between the can and its lid — both of which are made of stainless steel — is achieved by using an indium 'O'-ring (C 22) made from 1 mm gauge wire carried on a groove 0.5 mm deep on the top of the can.

The whole assembly is suspended from its stand by a metallic ball joint situated ~ 6 cm above the can lid. This joint makes it possible to shake the entire calorimeter assembly (at approximately 2 Hz through an amplitude of ~ 1 cm), so that the small phosphor-bronze ball (C 23), moving in the lower chamber, stirs the liquid in the vessel.

4.1.3 *MEASURING CIRCUITS* †

Most of the measuring equipment is housed in a compact console.

Both the resistance of the calorimeter copper thermometer and the power input to the corresponding heater coil are measured on a Tinsley type 4363 D -Auto precision (d.c.) vernier potentiometer.

The current to the potentiometer (~ 20 mA) is supplied by a Tinsley type 5750 (d.c.) current controller. This is fed from the mains, through a 12 V (a.c.) Advance Voltstat transformer, and is designed in such a way that any changes in the resistance of the external circuit do not affect the current to the potentiometer. The standard cell used by this current

---

† Some of the detail in this and later sections may at first sight appear excessive. It has been included since it is essential information for anyone wishing to continue this work, and has not appeared in any previous thesis. Before details such as the precise nature of the batteries used, voltage applied to photocell circuits, and so on had been finally settled it was not at all uncommon for an experiment to prove abortive, in spite of careful preparation, owing to failure of a component or some other relatively trivial mishap.

controller is one half of a Tinsley double Weston standard cell type 1149, the other half of which is connected to the standardizing circuit of the potentiometer.

The output signal from the potentiometer is passed to a Tinsley type 5214 photocell galvanometer amplifier (fitted with adjustable parallel feedback), and from this to a Servoscribe 1S (multi-range) potentiometric recorder (accuracy better than ± 5 μV). Sufficient freedom from vibrations is provided by a piece of polymer foam on which the amplifier rests on a rigid bench.

During the mixing experiments the potentiometer is operated continuously thus giving a continuous trace of the temperature changes occuring in the calorimeter, as explained below.

(i) *Calorimeter Thermometer Circuit*

The circuit of the calorimeter thermometer is diagramatically shown in Fig.4.5. The current passing through the copper resistance thermometer (R_T) is supplied by a Tinsley type 5388 automatic current controller (C). The actual current is supplied by an internal 6 V 'deac' Ni - Cd accumulator, and the power for the light beam for the photocells in the amplifier circuit comes from a 6 V Advance Voltstat transformer. The output from this transformer may be switched to an internal battery-charging circuit when the voltage of the accumulator drops to below 5.5 V. (This state of affairs is shown by the failure of a light spot to appear on a small window in the front of the apparatus.) A 4.2 V mercury Mallory cell is used to supply a reference voltage to the d.c. amplifier in the current controller.

The feedback is provided by a standard resistor (R_s) which determines the current I from the current controller. (W) is the Weston standard cell.

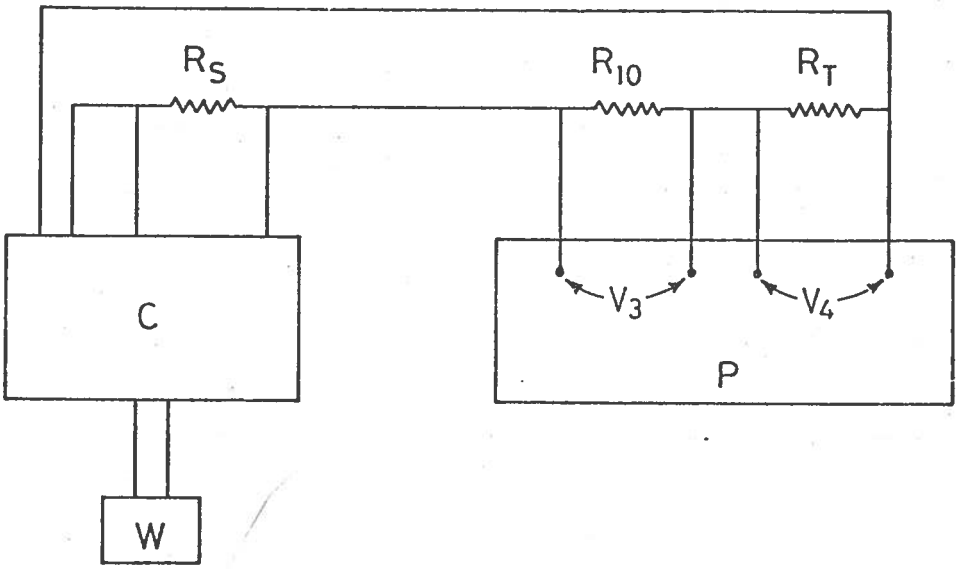

Fig. 4.5 - Calorimeter thermometer circuit

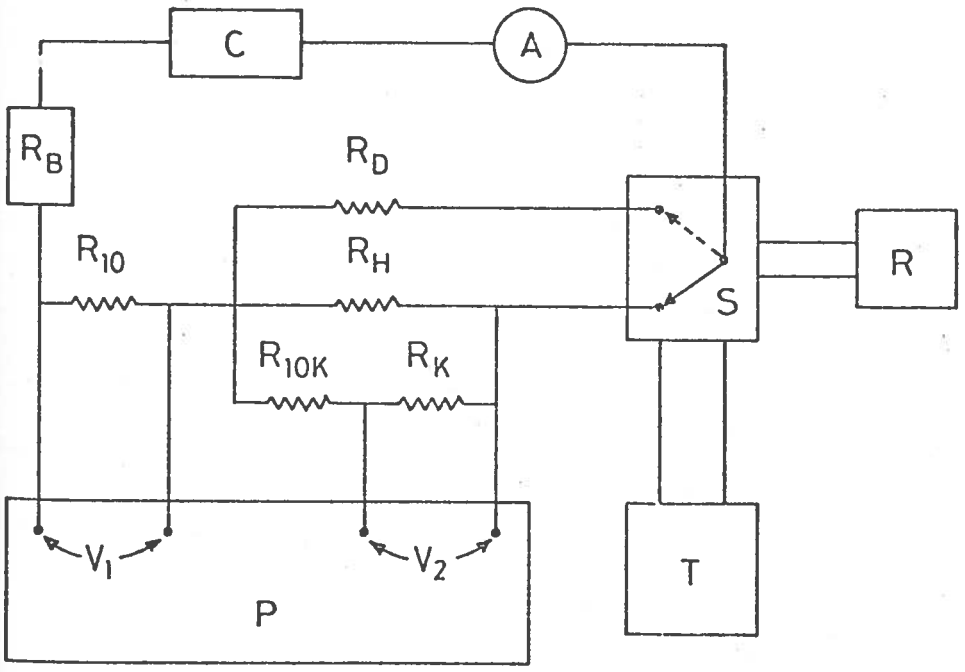

Fig. 4.6 - Calorimeter heater circuit

At 20° C, V_w = 1.01859 V and R_s = 336.2 Ω. In the usual conditions the current through the thermometer is $I \simeq 3$ mA.

The potential across the terminals of the copper resistance thermometer, V_4, is read directly on channel 4 of the potentiometer (P), while the current through the thermometer is determined by measuring, on channel 3, the potential drop V_3 across a standard resistor (R_{10}) of 10.0000 Ω resistance at 20° C. The resistance of the thermometer is then given by

$$R_T = V_4/(V_3/R_{10}) \quad . \qquad \ldots (4.1)$$

The thermometer is calibrated in situ, as described in the next section.

(ii) *Calorimeter Heater Circuit*

Current and voltage measurements for the calorimeter heater are made using channels 1 and 2 of the potentiometer, (Fig. 4.6). This current is supplied by a transistorised variable power supply (C), built in the laboratory's electronic workshop. (R_B) is a Pye resistance box which is adjusted in such a way as to cause the current (mA), read on the ammeter (A), to be approximately numerically equal to the voltage setting of (C). (In the present arrangement R_B = 610 Ω).

The current through the heater resistance (R_H) is determined by measuring, on channel 1, the potential V_1 across a Tinsley type 1659 standard resistor, R_{10} = 10.0006 Ω. The circuit is fitted with a stabilizing resistance (R_D) through which the current is diverted when no heating is required from (R_H). The Tinsley resistance box (R_D) is adjusted to give no change in the readings made on the ammeter (A) when the current is switched to the calorimeter heater coil. (Under the usual conditions $R_D \simeq 380$ Ω). Changeover from (R_D) to (R_H) is effected by means of a double-pole relay (S) with gold-plated contacts. The second pole simultaneously activates an incremental timer (T), Labgear type D 4108 (resolution 10^{-4} s).

The relay is energised by a 24 V, 1 A power supply (R).

The potential V_2 read on channel 2 of the potentiometer, is measured at the terminals of a standard resistor (R_K), of 999.98 Ω resistance, via a potential divider. The second resistance in this device (R_{10K}) was calibrated against a standardized Tinsley resistor of the same nominal characteristics. (R_{10K}), which is a Pye model, was found to have a resistance of 9992.3 ± 0.1 Ω. (All the resistance values quoted so far refer to 20° C).

When the heater (R_H) is switched on, the current I_{10} through (R_{10}) is the sum of the currents I_H and I_K through the heater and the divider, respectively. Therefore,

$$I_H = I_{10} - I_K$$

or

$$I_H = (V_1/R_{10}) - I_K .$$

On the other hand, the potential drop V_H across the heater is given by

$$V_H = R_H I_H$$

and also by

$$V_H = (R_K + R_{10K}) I_K .$$

Since

$$I_K = V_2/R_K ,$$

by appropriate substitutions the value of the resistance of the heater R_H is found to be

$$R_H = \frac{V_H}{I_H} = \frac{V_2 (R_K + R_{10K})}{V_1 (R_K/R_{10}) - V_2} . \qquad \ldots (4.2)$$

Finally, the energy Q_H dissipated in the calorimeter heater during t seconds is given by

$$Q_H = R_H I_H^2 t = \frac{(R_K + R_{10K})}{R_K^2} \left(\frac{R_K}{R_{10}} V_1 - V_2 \right) V_2 t \qquad \ldots (4.3)$$

which, inserting the numerical values of the various resistances, reduces to

$$Q_H/J = 0.010993\ (99.992\ V_1 - V_2)\ V_2\ t\ . \qquad \ldots\ (4.4)$$

(iii) *Shield Circuit*

The isoperibol principle requires that the temperature of the shield is kept constant during an experiment. This temperature is sensed by a copper resistance thermometer (R_t), as shown in Fig. 4.7. The small resistances (R_ℓ) represent the thermometer leads, while ($2\,R_\ell$) stands for the compensating dummy thermometer leads. These resistances are incorporated in a Wheatstone bridge, together with two equal resistors 25 Ω each ($R_{a,c}$) and a Muirhead resistance box (R_b). The latter is graduated in 0.1 Ω steps. The power supply arm of the bridge comprises a switch (S), a 1.25 V mercury Mallory cell (E) and a 470 Ω resistor (R_d). Apart from (R_t), (R_ℓ) and (R_b) the bridge assembly is enclosed in an insulated metallic box on the calorimeter stand.

The resistances (R_b) are selected in order to compensate R_t at the chosen temperature. When this temperature is reached, R_t will tend to decrease further since, due to heat leakage to the cryostat fluid, the temperature of the shield will tend to fall. The signal produced by the unbalanced bridge is fed to a Pye assembly (PY) of a d.c. amplifier indicator and a galvanometer modulator. The amplified signal is passed to a Leeds and Northrup three-term controller (LN) which generates an output signal of appropriate sign and magnitude. This signal is fed to a 50 V stabilized d.c. power supply (CR) from which the current finally passes to the shield heater (R_h). The heat dissipated by the latter causes the shield temperature to rise, so as to bring the bridge circuit back to balance (that is, to bring the pen of the (LN)-recorder (R) to its zero central position (full scale ± 5 mV)).

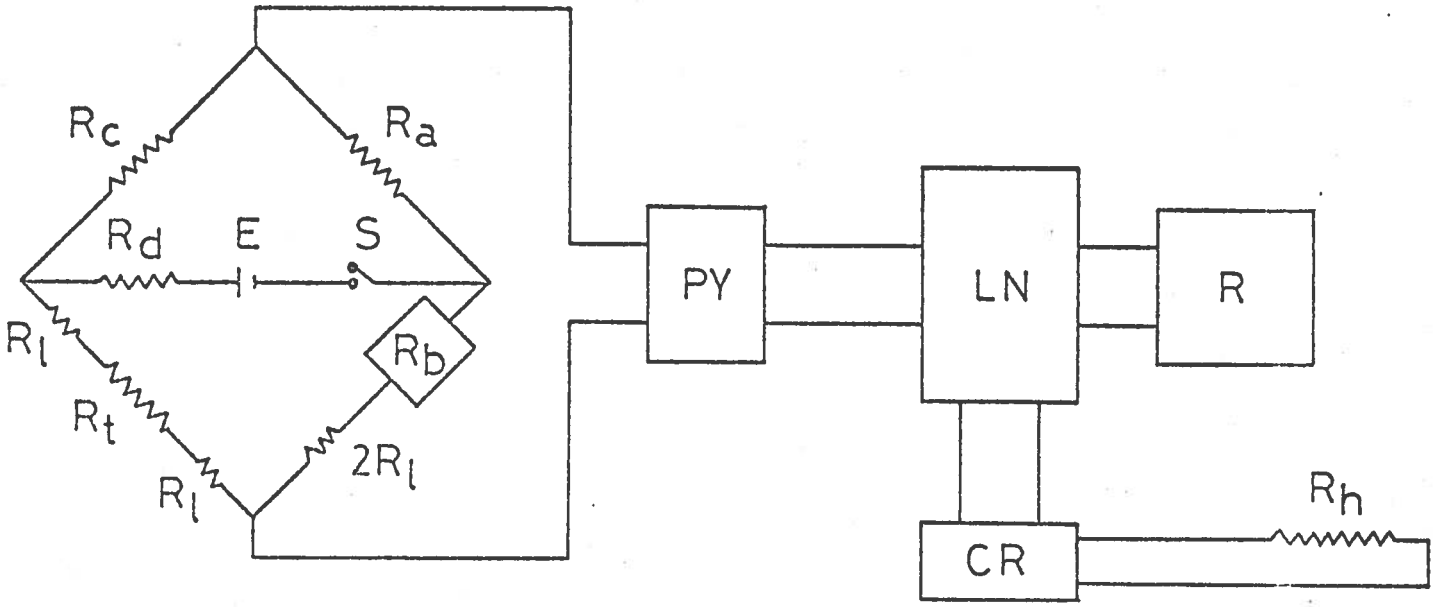

Fig. 4.7 - Shield circuit

(iv) *Ring Circuit*

The 'floating-ring' circuit works on the same principle as that of the shield. Its stability is, however, lower than in the previous case since the control system is less sophisticated. The resistance box, analogous to (R_b) in Fig. 4.7, is graduated in 1 Ω steps, and the ratio R_a/R_c is 10 in the present arrangement. The signal from the bridge is fed to an SCR unit in which it is transformed, rectified and smoothed, and then passed to the ring heater.

4.1.4 *CALIBRATIONS*

(i) *Volumes*

The results of the volumes calibrations are summarized in Appendix (F).

Prior to assembling the glass apparatus K.L. LEWIS determined the volumes of the storage globes (G 1) and (G 2) by weighting with water.

The dead-space volumes and also those of the two compartments of the calorimeter were determined, at room temperature, by a simple gas (helium) expansion method, taking the volume of the lower section of the right-hand limb of the mercury manometer (U), Fig. 4.2, as the reference. Helium was chosen because its second virial coefficient is both small and practically constant at temperatures near that of the room[8]. The volumes of the chambers in the sample vessel of the calorimeter at the working low-temperatures were obtained by extrapolation using copper thermal expansion data from RUBIN *et al*[9].

(ii) *Copper Resistance Thermometers*

The three resistance thermometers — ring, shield and calorimeter — are calibrated in situ by measuring their resistances in the temperature region of interest and simultaneously determining the vapour pressure of suitable liquefied gases condensed in the lower chamber of the calorimeter.

To minimize the relative error in the pressure readings on the one hand, and, on the other, to avoid blowing out the taps in the glass line, the vapour pressure of the working liquid should be as high as possible but never exceed 0.2 MPa .

Since for the 'floating-ring' thermometer only a very crude calibration is needed, a temperature-resistance curve from previous work was adopted, after checking a few points.

The shield thermometer is calibrated in the same run as that of the calorimeter. The former does not need, of course, to be calibrated as accurately as the calorimeter one, for which the operation can usually be carried out to ~ 0.01 K .

The experimental procedure for carrying out these calibrations is as follows. The electrical circuits are switched on and the complete apparatus, including the vacuum-can, is thoroughly evacuated down to taps (17) and (27) - Fig. 4.2 - at the entrance of the storage globes. This is done at room temperature, and although a pressure of $\sim 10^{-3}$ Pa ($\sim 10^{-5}$ torr) or better can usually be reached in the sample vessel and its line at this stage of the process, the readings on the Penning gauge normally stabilize around 5×10^{-2} Pa due to the large internal volume of the can. The can is then isolated from the vacuum line by closing tap (1) and a small quantity of helium is let into it. The needle valve of the upper compartment (11) is closed (moderately tightly) but the central valve of the calorimeter (20) is left open as well as (21). The shield controller is set (through the resistance box (R_b), Fig. 4.7) at a point corresponding to the lower limit of the temperature range in which the calibration is to be made, the cryostat is filled with liquid nitrogen, and the calorimeter assembly allowed to cool. Meanwhile, the potentiometer is standardized, channel 4 is selected, and the fall in the temperature is followed on the

chart recorder. (This corresponds to the pen moving from left to right across the chart paper). When the shield passes the pre-selected temperature (shown by the indicator on (PY) crossing its null position) the current to the shield circuit is set, through (CR), at an appropriate value in order to prevent the shield from reaching too low a temperature. Under these conditions the shield will eventually further cool although at a lower rate. After a time the calorimeter will have nearly reached the required temperature. All the taps in the glass line are then closed and secured with strong rubber bands. The transfer gas in the vacuum-can is pumped out, and the potentiometer is switched to a higher sensitivity (series resistance = $10^3\ \Omega$). In general, as a good vacuum in the can is achieved at this stage, the shield circuit quickly comes back to its in-balance position at which it can easily be maintained by adjusting the current from the corresponding power supply. The temperature of the calorimeter is then very slowly approaching that of the shield, due to the small gradient between the two, and this is shown by the almost vertical linear trace of the pen on the chart recorder.

The next step is to condense the gas in the calorimeter. To prevent it from freezing in the inlet tubing it is advisable to switch on the ring heater (by setting the resistance box in the corresponding circuit at a high value), and to warm the tubes above the can lid with the hair dryer. Tap (24) is opened to permit the pressure in the line to be monitored on the quartz gauge, an adequate amount of gas is condensed ($\sim$ 2 cm^3 of liquid) from the storage globe (G 2) into trap (B 2), and the globe is isolated from the line by closing (27). The dewar around the trap is lowered to enable the solid to melt completely, the pressure being watched on (A). When a value about 0.1 MPa ($\sim$ 1 atm) is reached tap (22) is opened and the liquid is allowed to distill into the mixing vessel. The pressure in

the line should never exceed 2 MPa (~ 2 atm), this being achieved in the usual way be adjusting the level of the refrigerant below the trap. The condensation is followed on the chart recorder which shows the increase in the temperature of the calorimeter due to the heat given out by the fluid. When the condensation is complete valve (21) is closed and the line thoroughly pumped out for several minutes. Taps (22) to (26) are then shut, and (12) and (14) are opened. After zeroing the Texas Instruments gauge valve (11) is also opened.

At this stage the temperature of the mixing vessel, and possibly of the shield as well, is usually a little above the intended value. The ring heater is switched off, and a small amount of transfer gas is admitted to the outer can to allow the calorimeter and the shield to cool. Usually the working temperature is reached in a few minutes. The helium is pumped away, the stirrer is switched on, and the temperature of the shield is adjusted as described above (this time using the maximum sensitivity in the amplifier (PY)). One must always ensure that the shield (and the ring, if necessary) are slightly hotter than the mixing vessel at this stage of the process in order to be certain that the vapour pressures which are subsequently measured are those of the liquid in the mixing vessel.

The potentiometer, still on channel 4, is switched to its maximum sensitivity by setting the series resistance at 0 Ω. The temperature drift, as indicated by the movement from right to left (warming) of the pen on the chart recorder, should be linear and very small (< 5 mK per minute). The vapour pressure of the liquid, read on (A), should also be changing very slowly. When the pen is approaching the central division of the chart (that is, its standardization position) the following quantities are measured: the vapour pressure of the liquid, the temperature of the Texas Instruments gauge, the potential difference across the terminals of the

calorimeter thermometer (V_4), and the potential on channel 3 (V_3) (which will give the current passing through the thermometer). The set of readings is repeated over a period of several minutes, the value of the resistance introduced by the box (R_b) being also recorded. (If an accurate calibration of the shield thermometer is intended, one should wait for the moment at which the slope of the temperature-time straight line on the chart changes sign to make one more set of readings, since at that point the temperatures of the shield and the vessel are equal).

The setting of the shield heater circuit is then increased by 0.1 - 0.2 Ω, and the mixing vessel is heated to enable the next vapour pressure measurement to be made (after allowing the system to reach a new steady state). The process is repeated until the desired temperature range is covered.

When the experiment is over the values of the potentials V_3 and V_4 are transformed, through equation (4.1), into the corresponding resistances R_T of the calorimeter thermometer.

Since the vapour pressure equations are usually of the form $\ln P = f(T)$, f being a nonlinear and sometimes non-rational function, the measured vapour pressure values are converted into the corresponding temperatures using the Newton-Raphson method.

The resulting pairs (T, R_T), where T is the temperature of the thermometer and R_T is its resistance, are adjusted to a convenient polynomial of the form

$$R_T = \sum_{i=0}^{7} a_i T^i \quad , \qquad \ldots (4.5)$$

as before. Frequently the calibrations refer to a short temperature interval (5 to 10 K) so that it is seldom necessary to consider $i > 2$.

For the shield thermometer a graph of the best straight line through

the (T,R_t) experimental points is adequate. Such a graph is presented in Appendix (G), where the calibration line of the 'floating-ring' thermometer is also shown. (Points at the temperatures of the normal boiling point of nitrogen, the ice point and room are also included.)

Three substances were employed in the calibrations, according to the temperature range to be covered: krypton (for the interval 116-120 K) carbon tetrafluoride (for 135 K < T < 149 K), and ethane (for 155 K < T < 165 K and 180 K ≲ T < 188 K). In the case of ethane the vapour pressure equation of GOODWIN *et al.*[10] was used and therefore IPTS-68 temperatures were directly obtained. For krypton the vapour pressure equation was taken from the work of MICHELS *et al.*[11] and therefore the resulting temperatures had to be converted into IPTS-68 values, using the method described in Chapter 17. The situation was similar for carbon tetrafluoride, for which case the vapour pressure expression of SMITH and PACE[12] was adopted. This was the only non-Antoine-type equation available for CF_4 at the time the calibration was made and was selected for that reason.

The results of these calibrations are indicated in Appendix (H).

4.2 EXPERIMENTAL PROCEDURE

In this section we shall concentrate on the experimental procedure for an enthalpy of mixing determination. This can be divided into two more or less independent stages: the first concerns the condensation of the two liquids into the calorimeter, and the second the mixing process and the subsequent measurement of the energy change associated with it.

First, one has to decide in which compartment of the calorimeter each of the component gases is to be condensed. Whenever the more volatile of these has a moderately high vapour pressure (> 0.3 MPa or so) at the final working temperature, it is convenient to condense it in the

lower chamber, to reduce the risk of leakage through the valve packing. This criterion was by no means strictly adhered to, however, and on some occasions the reverse order was adopted.

Each component is condensed at a temperature a little below its normal boiling point. Usually the more volatile one is condensed first and then the apparatus is warmed to the temperature at which the second component is to be introduced. However, if one of the liquids is almost involatile at the working temperature (as with C_2H_4 and CF_4) the above procedure may have to be reversed, this component being introduced first. The apparatus is then allowed to cool to below the normal boiling point of the more volatile component, and after the admission of the latter the calorimeter is warmed to the temperature at which the two liquids are to be mixed. The first of the two cases is the one considered in this section since it is by far the more frequent one.

To carry out a heat of mixing experiment, after thorough evacuation of the whole system, the central valve and the needle valve (11) are closed, (a better seal between the central valve and its seat is obtained at room temperature, as opposed to closing it at lower temperatures), the resistance (R_b) in the shield circuit is set at a value corresponding to the temperature selected for the admission of the first component, the potentiometer is standardized and switched to its channel 4, and the apparatus is cooled as described in the last section. A continuous record of the change of the temperature of the calorimeter and its contents is obtained by running the potentiometer in channel 4 (output V_4) throughout the experiment (except when otherwise indicated).

While the system is attaining the chosen temperature, taps (14), (22) and (23) are closed, tap (27) is opened, and the pressure and temperature of the gas in globe (G 2) and its line are read on (A) and (T), respectively, at one minute intervals over a five minute period. The temperature

in the quartz gauge is also recorded. The required amount of the more volatile component is then condensed in the cold finger (B 2), (as shown by the pressure decrease in the line), tap (27) is closed, and the liquid transferred into the lower chamber of the calorimeter by opening (22) and (26), as previously described. The rise in temperature of the calorimeter vessel due to the condensation of the first component, is watched on the chart recorder (with the series resistance of the potentiometer set at $10^3\,\Omega$). The time is noted. When trap (B 2) is empty, valve (21) is closed, and as much as possible of the gas remaining in the line is condensed back into (B 2). The refrigerant around this is removed, tap (27) is opened, and (B 2) warmed to room temperature. The pressure in the line and the temperature of the gas in the globe (G 2) are read again, as before.

At this stage the heating of the cell to the desired temperature for condensation of the second component can be started. This is done by switching on the calorimeter heater, having set the resistance (R_b) in the shield circuit at the appropriate value.

Meanwhile, tap (27) is closed, the line is evacuated to a vacuum of 10^{-2} Pa or better, and tap (22) is opened, thus allowing the residual gas trapped between (21) and (22) to expand into the line. The pressure and temperature of this gas are measured in the usual manner, and the entire line (down to (21)) is thoroughly evacuated. When a satisfactory vacuum (10^{-3} Pa or better) is achieved, all the stopcocks in the lower line are closed, including (24).

In preparation for the admission of the second component, tap (14) is opened and the upper line is pumped out down to valve (11). When the assembly reaches the desired temperature, the central valve is checked for leakage in the following manner.

After closing (13) and zeroing the pressure gauge, valve (11) is opened, the time is noted, and the pressure in the line is read on (A).

If there is no leakage through the central valve, the pressure gauge stays at its zero and the experiment can be continued; if not, after a time of $\sim$ 5 minutes has elapsed, the pressure in the line is read again. The knowledge of the build-up in pressure and of the time elapsed, allows the leak rate to be determined. If this is less than $\sim 7.5 \times 10^{-9}$ mol s^{-1} ($\hat{\equiv}$ $\Delta P \simeq$ 500 Pa h^{-1}), it is considered acceptable[7] and the run is continued, but it should be stressed that in none of the experiments relevant to this thesis was there any detectable leakage between the two chambers.

The second component is now admitted in exactly the same manner as the first, more volatile, liquid. The time is noted at the beginning of the condensation period, in case any corrections for leakage through the central valve have later to be made.

To start the second phase of the experiment, the cryostat dewar is filled with liquid nitrogen to the top of the vacuum-can, and the shaker is turned on. The resistance (R_b) in the shield circuit is set at a value corresponding to a temperature very slightly below that at which mixing will take place, while the mixing vessel is brought to the immediate upper vicinity of that temperature. Depending on the relative magnitude of the latter temperature and that prevailing at the end of the condensation of the second component, the apparatus must be either heated, by using the cell heater, or cooled, by admitting helium in the can and pumping it out slightly before the desired temperature is reached. (If faster cooling of the mixing vessel is wanted, the shield heater can be switched off for a while, since the shield can usually be restored rapidly to the temperature required.)

A steady-state is usually obtained in a short time, after which the (PY) amplifier in the shield circuit can be switched to its maximum sensitivity (position '1'). At this stage of the process — the shield (and the ring, if in use) being slightly cooler than the cell — the mixing vessel

cools at a very slow rate, provided a good vacuum (5×10^{-2} Pa or better) is maintained in the outer can. With the potentiometer at its maximum sensitivity (series resistance = 0 Ω), and a chart speed of ~ 600 cm h^{-1} on the recorder (set at the '1 mV' position) a straight line of slope ~ 45° is obtained on the chart. This corresponds to a cooling rate of the mixing vessel of ~ 2 - 5 mK per minute.

The potentiometer is then standardized, and V_3 is measured. (The current through the calorimeter thermometer, and hence V_3, does not significantly change during one experiment, or from this to the next, so that the potential drop V_4 can be taken for all practical purposes as a sufficiently good measure of the temperature of the mixing vessel). To calibrate the chart against thermometer voltage increment, V_4 is shifted by a certain amount (usually - 10 μV) and the deflection of the pen (~ 50-80 chart divisions) is noted. This enables one to determine, at a later stage, the actual temperature at which the central valve is opened. After some practice it is possible to operate so that the pen is set at the left hand edge of the chart paper when V_4 is shifted to the value corresponding to the desired temperature of the experiment.

While the pen is tracing the linear temperature-time fore-drift (Fig. 4.8), the timer is checked to ensure that it is set at 0.0000 s and is in the 'ready' position. The potentiometer series resistance is then switched to the 10^3 Ω position (this corresponds, in Fig. 4.8, to the large step following the 'fore-drift' line), the shaker is turned off, and the central valve is opened (counting the number of turns needed; usually 3-5). The time is noted. The shaker is switched on again to help the two liquids mix. All the experiments in a series will be carried out virtually at the same temperature if, for the same value of V_4, the distance between the null point of the pen on the chart (i.e., division '50' — the potentiometer standardization position) and the terminal point of the fore-drift is

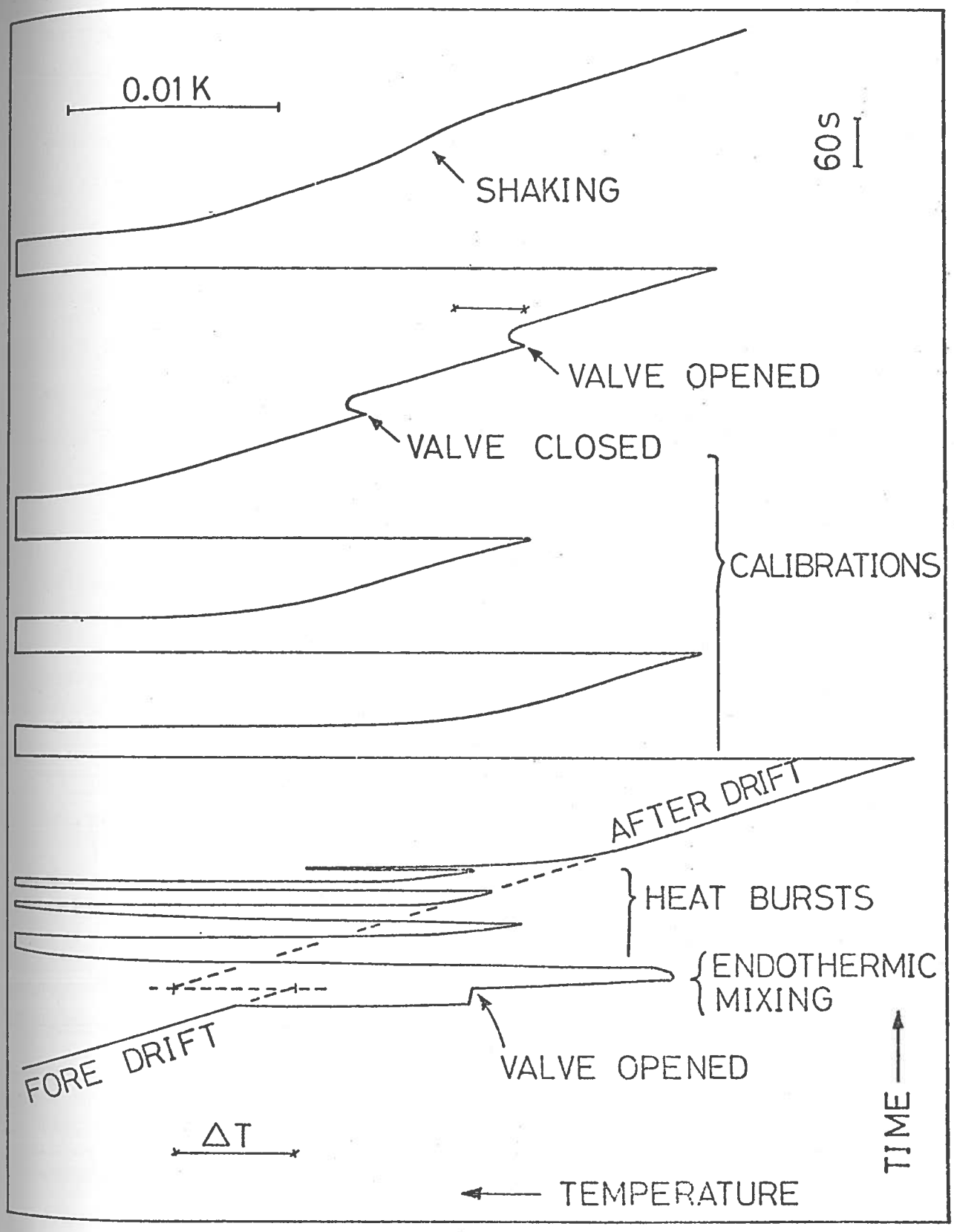

Fig. 4.8
Calorimetric experiment: temperature vs. time diagram

maintained nearly constant from one experiment to the following ones.

The mixing process is practically instantaneous and, in general, endothermic, as shown by the steep temperature (V_4) decrease immediately after the valve opening.

Energy is then supplied to the system by switching on the calorimeter heater in bursts until exact compensation is virtually accomplished. This is achieved by allowing the pen, after a heat burst, to return to its new equilibrium point (at which a linear after-drift would start); when this point is sufficiently close to the central division of the chart (division '50'), say, within ± 1 chart divisions, the compensation process is considered to be completed, and the potentiometer is switched to its initial high sensitivity (series resistance = 0 Ω). This corresponds, in Fig. 4.8, to the last, small peak after the three heat bursts, following which, as will be seen from the figure, the after-drift has been traced on full sensitivity. (Further compensation may be made if necessary provided the 10^3 Ω series resistance is switched in again). Typical values of the heater current fall between 16 and 36 mA, the higher values being used for the more endothermic processes.

After a short while the after-drift becomes linear and parallel to the fore-drift. The total heating time is then noted. The distance between the fore-drift and after-drift lines determines the uncompensated energy in the process. This energy corresponds to the difference (ΔT, Fig. 4.8) between the initial temperature of the system (pure components in separate chambers) and that of its final state (liquid mixture) if the mixing process and the subsequent compensation are assumed to be carried out instantaneously, and ideally at the moment the central valve is opened. The compensation can usually be carried out to within 0.01 K, i.e. so that ΔT does not exceed this figure. (In the case illustrated by Fig. 4.8, ΔT

represents an over-compensation, since the 'final' temperature is larger than the 'initial' one.)

To calibrate the chart recorder deflection against the thermal energy supplied to the calorimeter — in order to convert the distance between the two linear drifts into energy, or into its equivalent time — a series of 3 - 6 heat capacity calibrations are made immediately after the mixing experiment is over. Short heat bursts (10 - 20 s each) are supplied, allowing the drift to become linear after each one. Care must be taken to re-set the timer at its zero before the beginning of each burst, and to note the exact time at the end of each one.

After the last calibration the central valve is closed. A positive deflection is observed on the chart but soon the temperature drift becomes linear again. The valve is then re-opened (counting the number of turns) and the same effect is observed. The after-drift is allowed to become linear. This last observation provides the information needed to allow for the heat of friction on opening the valve and also for the correction for the thermal effect associated with the simultaneous slight change of the internal volume of the calorimeter. (This change causes some of the liquid to evaporate.) The combined effect of these corrections is, however, small ($\sim$ 1 J) in every case. An investigation of the 'heat of shaking' showed that this was always negligible.

There remains the measurement of the current supplied to the calorimeter heater and the associated potential drop. This is done by switching the electrical supply back to the heater from the dummy resistance, and by determining on the potentiometer the potential differences V_1 and V_2. The first gives the current through the calorimeter heater and the second gives the potential difference across its terminals. Due to the stability of the power supply unit (C), Fig. 4.6, the values obtained in these

measurements are considered to be equal to those applicable during the compensation of the mixing process. The two values are measured three times each, the mean values being adopted in the subsequent calculations (of the resistance R_H, and energy Q_H, using equations (4.2) and (4.4) respectively).

Provided the heat of mixing is relatively small numerically ($H^E_{\frac{1}{2}} \geqslant -100\,J\,mol^{-1}$), the calorimeter can be used if the mixing is exothermic. There is, of course, no need for compensation, but all other operations are carried out exactly as described.

From the previous section it will be apparent that the apparatus can also be used to measure the vapour pressure of liquid mixtures (provided this does not exceed $\sim 0.2\,MPa$), and hence to determine the respective excess Gibbs energy G^E (7). Since this method is, however, less precise than that described in Chapter 3, it was not used in the present work, and therefore only a brief reference will be made to it.

If it is required to measure the vapour pressure of the mixture in the calorimeter, the liquid nitrogen in the cryostat is adjusted to surround the lower part of the vacuum-can, and the shield (and ring, if necessary) are adjusted so as to cause the calorimeter to heat up, but at as low a rate as possible. The needle valve to the upper compartment is opened slightly and the vapour phase above the mixture is allowed to bleed slowly into the line connected to the pressure gauge. It is necessary to supply energy to the calorimeter during this process in order to compensate for the cooling due to the evaporation of the liquid. The vapour pressure is then measured, as before, at the appropriate value of the thermometer voltage.

This ends the mixing experiment, and all that remains is to extract the mixture from the calorimeter. For efficient removal of the mixture it

is necessary that the calorimeter is at a temperature sufficiently high for there to be a significant vapour pressure (> 30-40 kPa) of both components. It is extremely important to ensure that all the mixture has been removed from the calorimeter before commencing the next run, particularly to avoid damage to the central valve by closing it on solid mixture that have been inadvertently left in the mixing vessel.

4.3 REFERENCES

(1) KÖHLER, W., 'Dissertation', University of Göttingen, (1964).

(2) KNOBLER, C.M., van HEIJNINGEN, R.J.J. and BEENAKKER, J.J.M., Physica, 1961, 27, 296.

(3)(a) JEENER, J., Rv. Scient. Instrum., 1957, 28, 263.

(b) LAMBERT, M. and SIMON, M., Physica, 1962, 28, 1191.

(4)(a) WORMALD, C.J., LEWIS, K.L. and MOSEDALE, S.E., J. Chem. Thermodynamics, 1977, 9, 27.

(b) LEWIS, K.L., MOSEDALE, S.E. and WORMALD, C.J., J. Chem. Thermodynamics, 1977, 9, 221.

(c) MOSEDALE, S.E. and WORMALD, C.J., J. Chem. Thermodynamics, 1977, 9, 483.

(5)(a) POOL, R.A.H. and STAVELEY, L.A.K., Trans. Faraday Soc., 1957, 53, 1186.

(b) POOL, R.A.H., SAVILLE, G., HERRINGTON, T.M., SHIELDS, B.D.C. and STAVELEY, L.A.K., Trans. Faraday Soc., 1962, 58, 1692.

(6) LEWIS, K.L., SAVILLE, G. and STAVELEY, L.A.K., J. Chem. Thermodynamics, 1975, 7, 389.

(7)(a) LEWIS, K.L. and STAVELEY, L.A.K., J. Chem. Thermodynamics, 1975, 7, 855.

(b) LEWIS, K.L. and STAVELEY, L.A.K., J. Physics E, 1975, 8, 811.

(8) BREWER, J., 'Determination of Mixed Virial Coefficients', AFOSR No. 67-2795, (1967).

(9) RUBIN, T., ALTMAN, H.W. and JOHNSTON, H.L., J. Am. Chem. Soc., 1954, 76, 5289.

(10) GOODWIN, R.D., RODER, H.M. and STRATY, G.S., 'Thermophysical Properties of Ethane, from 90 to 600 K at Pressures to 700 bar', N.B.S. Tech. Note 684, (1976).

(11) MICHELS, A., WASSENAAR, T. and ZWIETERING, T.N., Physica, 1952, 18, 63.

(12) SMITH, J.H. and PACE, E.L., J. Phys. Chem., 1969, 73, 4232.

PART 3

CALCULATIONS

CHAPTER 5 - CALCULATION OF THE EXCESS MOLAR GIBBS ENERGY G^E

CHAPTER 6 - CALCULATION OF THE EXCESS MOLAR VOLUME V^E

CHAPTER 7 - CALCULATION OF THE EXCESS MOLAR ENTHALPY H^E

CHAPTER 5

CALCULATION OF THE EXCESS MOLAR GIBBS ENERGY G^E

5.1 G^E FROM TOTAL VAPOUR PRESSURE MEASUREMENTS

This section is concerned with the calculation of the excess molar Gibbs energy G^E from experimental values of the vapour pressure of liquid mixtures of known composition.

G^E can be written in terms of the excess chemical potentials of the components, μ_i^E, as

$$G^E = \sum_i x_i \mu_i^E , \qquad \ldots (5.1)$$

where x_i is the mole fraction of component i and

$$\mu_i^E = \mu_i - \mu_i^{id} . \qquad \ldots (5.2)$$

The superscript 'id' indicates the ideal mixture. The chemical potentials μ_i^{id} and μ_i are given, respectively, by

$$\mu_i^{id}(P,T,x_i) = \mu_i^0(P,T) + RT \ln x_i \qquad \ldots (5.3)$$

for a component of an ideal mixture, and by

$$\mu_i(P,T,x_i) = \mu_i^0(P,T) + RT \ln(\gamma_i x_i) \qquad \ldots (5.4)$$

when i is a component of a non-ideal solution. In both expressions $\mu_i^0(P,T)$ is the chemical potential of pure i at the same temperature T and pressure P as the mixture under discussion. γ_i is the activity coefficient of i in the actual mixture. By combining (5.1) to (5.4) one obtains for the excess molar Gibbs energy:

$$G^E = RT \sum_i x_i \ln \gamma_i . \qquad \ldots (5.5)$$

The calculation of G^E is thus transformed into the equivalent problem of finding the values of the activity coefficients, which can be obtained as follows.

The general conditions for thermodynamic equilibrium between a liquid (L) and a vapour (G) are

$$\begin{aligned} T^G &= T^L \\ P^G &= P^L \\ \mu_i^G &= \mu_i^L \end{aligned} \qquad \ldots (5.6)$$

where the latter equality can conveniently be expressed in terms of the fugacities[1]:

$$f_i^G = f_i^L \ . \qquad \ldots (5.7)$$

The fugacity of a component of a gaseous mixture f_i^G is simply given by [1]

$$f_i^G = \varphi_i \, y_i \, P \ , \qquad \ldots (5.8)$$

where φ_i is the vapour-phase fugacity coefficient of component i at the temperature T and pressure P and y_i is the mole fraction of i in the vapour. For the liquid phase, however, it is convenient to write the fugacity f_i^L in terms of the activity coefficient γ_i [1]:

$$f_i^L = \gamma_i \, x_i \, f_i^0 \ , \qquad \ldots (5.9)$$

f_i^0 being the fugacity of component i in some adequately chosen standard state. This standard state must be specified to make γ_i a (numerically) meaningful quantity. For our purposes, the pure liquid at the temperature T and pressure P of the mixture is an appropriate choice for the standard state of each component. This clearly corresponds to the so-called 'symmetrical normalization' of the activity coefficients, since $\gamma_i = 1$ when component i is a pure liquid ($x_i = 1$).

Therefore, at equilibrium:

$$\gamma_i = \frac{\varphi_i \, y_i \, P}{x_i \, f_i^0} \ . \qquad \ldots (5.10)$$

Both φ_i and f_i^0 are directly related to certain physical properties of the system, and consequently equation (5.10) makes it possible to use these properties to obtain G^E. Methods for the calculation of φ_i and f_i^0 are presented in textbooks of Thermodynamics, especially those oriented towards Chemical Engineering[1,2]. SOOD and HASELDEN[3] have also reviewed this subject. Accordingly, it will only be treated briefly here.

The general expression for the fugacity coefficient φ_i of component $\underline{i}$ in the vapour, at the temperature T and pressure P, is

$$RT \ln \varphi_i = \int_0^P \left(V_i^G - \frac{RT}{P} \right) dP \qquad \ldots (5.11)$$

where

$$V_i^G = \left(\frac{\partial V^G}{\partial n_i} \right)_{P,T,n_j} \qquad \ldots (5.12)$$

is the partial molar volume of component $\underline{i}$ in the vapour phase, and n_i is the number of moles of $\underline{i}$. $V^G = \sum_i n_i V$ is the total volume of the gaseous mixture. Therefore, V_i^G can be calculated from an equation of state. As the integration in equation (5.11) is to be carried out with respect to the pressure P, a convenient choice is the virial equation of state in its pressure expansion form:

$$\frac{PV}{RT} = 1 + B'P + C'P^2 + \ldots \qquad \ldots (5.13)$$

where B', C', ... are the second, third, ... virial coefficients. For our present purposes the expansion truncated after the third term is adequate. The coefficients B and C in the density expansion form of the virial equation of state,

$$\frac{PV}{RT} = 1 + \frac{B}{V} + \frac{C}{V^2} + \ldots , \qquad \ldots (5.14)$$

are more commonly tabulated than B' and C', which are related to B and C by the equations

and

$$B' = B/RT \qquad \ldots (5.15)$$

$$C' = (C - B^2)/(RT)^2 \ . \qquad \ldots (5.16)$$

For a mixture with $\underline{m}$ components B and C are given by

$$B = \sum_{i=1}^{m} \sum_{j=1}^{m} y_i y_j B_{ij} \qquad \ldots (5.17)$$

and

$$C = \sum_{i=1}^{m} \sum_{j=1}^{m} \sum_{k=1}^{m} y_i y_j y_k C_{ijk} \ . \qquad \ldots (5.18)$$

B_{ij} and C_{ijk} are functions only of the temperature, being independent of density (or pressure) and composition.

Since all the work described in this thesis refers to two-component systems, we shall limit our formal treatment from now on to binary mixtures.

By combining (5.13) with equations (5.15) to (5.18), V_i^C can be calculated from (5.12), and the fugacity coefficient φ_i subsequently obtained from equation (5.11). For component 1 the result is

$$\begin{aligned} RT \ln \varphi_1 = {} & B_{11} P + y_2^2 \delta_{12} P \\ & + (C_{111} - B_{11}^2) P^2/2RT \\ & - y_2^2 \phi_1 (C_{ijk}, B_{ij}, y_2) P^2/2RT \end{aligned} \qquad \ldots (5.19)$$

where

$$\delta_{12} = 2B_{12} - B_{11} - B_{22} , \qquad \ldots (5.20)$$

and the function $\phi_1(C_{ijk}, B_{ij}, y_2)$ is given by

$$\phi_1 = \varepsilon_1 + 2\zeta_1 y_2 + 3\theta y_2^2 \qquad \ldots (5.21)$$

with

$$\begin{aligned} \varepsilon_1 = \Big[& 3(C_{111} - 2C_{112} + C_{122}) \\ & - 2(3B_{11}^2 + 6B_{11}B_{12} - B_{11}B_{22} - 2B_{12}^2) \Big] \end{aligned} \qquad \ldots (5.22)$$

$$\zeta_1 = \Big[(-C_{111} + 3C_{112} - 3C_{122} + C_{222}) - 4(-B_{11}^2 + 3B_{11}B_{12} - B_{11}B_{22} - 2B_{12}^2 + B_{12}B_{22})\Big] \quad \ldots (5.23)$$

and

$$\theta = -\left(B_{11}^2 - 4B_{11}B_{12} + 2B_{11}B_{22} + 4B_{12}^2 - 4B_{12}B_{22} + B_{22}^2\right) . \quad \ldots (5.24)$$

An expression similar to equation (5.19) holds for $RT \ln \varphi_2$.

As a consequence of the choice of the standard state, f_i^0 is obtained from the general expression for the fugacity of a pure liquid $\underline{i}$ at (the) temperature T and pressure P (of the system)[2]:

$$\begin{aligned} RT \ln f_i^0 &= RT \ln f_i^* \\ &= RT \ln P_i^* \\ &+ \int_0^{P_i^*} \left(V_i^{*G} - \frac{RT}{P}\right) dP \\ &+ \int_{P_i^*}^{P} V_i^{*L}\, dP \end{aligned} \quad \ldots (5.25)$$

where the superscript $*$ indicates a pure species. To evaluate the first integral in the right-hand side of equation (5.25) the virial equation of state can be used, as before. The calculation of the second integral is more involved if the usual assumption of considering the molar volume of the liquid V_i^{*L} as constant between the saturation pressure P_i^* and P is to be avoided. The difficulty is removed by expanding V_i^{*L} in powers of P around $P = 0$ and neglecting all terms beyond, say, the third:

$$V_i^{*L} = \left(V_i^{*L}\right)_{P=0} + \left(\frac{\partial V_i^{*L}}{\partial P}\right)_{P=0} P + \frac{1}{2}\left(\frac{\partial^2 V_i^{*L}}{\partial P^2}\right)_{P=0} P^2 . \quad \ldots (5.26)$$

This is equivalent to assuming that the isothermal compressibility of the liquid,

$$\kappa^{*}_{T,i} = -\frac{1}{V^{*L}_{i}}\left(\frac{\partial V^{*L}_{i}}{\partial P}\right) , \qquad \ldots (5.27)$$

is a linear function of the pressure.

On this basis, we obtain:

$$\left.\begin{aligned} RT \ln f^{0}_{i} = {} & RT \ln P^{*}_{i} + B_{ii} P^{*}_{i} \\ & + (C_{iii} - B^{2}_{ii})\, P^{*2}_{i} / 2RT \\ & + \left(V^{*L}_{i}\right)_{P=0} (P - P^{*}_{i}) \\ & - \tfrac{1}{2}\left(\frac{\partial V^{*L}_{i}}{\partial P}\right)_{P=0} (P^{2} - P^{*2}_{i}) \\ & + \tfrac{1}{6}\left\{V^{*L}_{i}\left[\kappa^{*2}_{T,i} - \left(\frac{\partial \kappa^{*}_{T,i}}{\partial P}\right)\right]\right\}_{P=0} (P^{3} - P^{*3}_{i}) \end{aligned}\right\} \qquad \ldots (5.28)$$

By replacing φ_i and f^{0}_{i} as given by (5.19) and (5.28), respectively, in equation (5.10) the activity coefficient γ_i can now be calculated, from the vapour pressure and other measurable physical properties of the mixture and its components.

In theoretical studies[4] the excess functions are usually estimated at zero pressure. Since the activity coefficients resulting from equation (5.10) refer to the pressure P (and temperature T) of the system, these must be converted into values for $P = 0$ to enable the experimental G^{E} to be compared with that derived from the theory. The transformation is carried out through the well known equation for the dependence of γ_i on pressure[1]:

$$\left(\frac{\partial \ln \gamma_i}{\partial P}\right)_{T,x} = (V^{L}_{i} - V^{*L}_{i})/RT \qquad \ldots (5.29)$$

thus giving:

$$(\ln \gamma_i)_{P=0} = (\ln \gamma_i)_{P} + \frac{1}{RT}\int_{P}^{0} (V^{L}_{i} - V^{*L}_{i})\, dP . \qquad \ldots (5.30)$$

In the calculation of the integral the partial molar volume of component i, V_i^L, can be assumed to be expanded in powers of the pressure in a manner similar to that used for the molar volume of the pure component, i.e. as in equation (5.26).

The activity coefficient of component 1, γ_1, is then obtained from the following equation:

$$
\begin{aligned}
RT \ln \gamma_1 = {} & RT \ln (y_1 P / x_1 P_1^*) && \tau_{1,0} \\
& + \left[B_{11} - (V_1^{*L})_{P=0} \right] (P - P_1^*) && \tau_{1,1} \\
& + y_2^2 \delta_{12} P && \tau_{1,2} \\
& + (C_{111} - B_{11}^2)(P^2 - P_1^{*2})/2RT && \tau_{1,3} \\
& - y_2^2 \phi_1 (C_{ijk}, B_{ij}, y_2) P^2/2RT && \tau_{1,4} \\
& + (V_1^{*L} - V_1^L)_{P=0} P && \tau_{1,5} \\
& + \tfrac{1}{2} \left(\frac{\partial V_1^{*L}}{\partial P} \right)_{P=0} P_1^{*2} && \tau_{1,6} \\
& - \tfrac{1}{2} \left(\frac{\partial V_1^L}{\partial P} \right)_{P=0} P^2 && \tau_{1,7} \\
& + \tfrac{1}{6} \left\{ V_1^{*L} \left[\kappa_{T,1}^{*2} - \left(\frac{\partial \kappa_{T,1}^*}{\partial P} \right) \right] \right\}_{P=0} P_1^{*3} && \tau_{1,8} \\
& - \tfrac{1}{6} \left\{ V_1^L \left[\kappa_{T,1}^2 - \left(\frac{\partial \kappa_{T,1}}{\partial P} \right) \right] \right\}_{P=0} P^3 . && \tau_{1,9}
\end{aligned}
\qquad \ldots (5.31)
$$

γ_2 is calculated from an analogous expression for component 2.

Finally, the excess molar Gibbs energy at zero pressure G^E is given by

$$G^E = \sum_{i=1}^{2} \sum_{n=0}^{9} x_i \tau_{i,n} . \qquad \ldots (5.32)$$

Terms $\tau_{i,n}$ are not, of course, equally important. CALADO[5] examined the magnitude of terms $\tau_{i,0}$ to $\tau_{i,7}$, and this subject will be fully discussed in one of the following chapters of this thesis. Meanwhile, a few general remarks can be made.

The total contribution of the two terms $\tau_{i,5}$ is

$$\tau_{1,5} + \tau_{2,5} = -P\left(V^L - \sum_i x_i V_i^{*L}\right)_{P=0}$$
$$= -P\,(V^E)_{P=0} \qquad \ldots (5.33)$$

and therefore this contribution can be neglected when the excess molar volume V^E is small and the system is under low or moderate pressure. Moreover, if the vapour pressure of the mixture P is relatively small, all terms involving P^2 or higher powers of the pressure are also small.

For these conditions equation (5.31) reduces to that first obtained by SCATCHARD and RAYMOND[6]:

$$\mu_1^E = RT\ \ell n\ \gamma_1 = RT\ \ell n\,(y_1 P/x_1 P_1^*)$$
$$+ \left[B_{11} - (V_1^{*L})_{P=0}\right](P - P_1^*)$$
$$+\ y_2^2\ \delta_{12}\ P\ . \qquad \ldots (5.34)$$

The absence of experimentally determined values of the cross-second virial coefficient B_{12} for most of the mixtures studied requires the introduction of a further assumption: that B_{12} is simply the mean of the B values for the pure components,

$$B_{12} = (B_{11} + B_{22})/2\ , \qquad \ldots (5.35)$$

(the so-called[7] 'naive formula'). (Even the more recent methods for estimating cross-virial coefficients[8] are of doubtful reliability when polar components like HCℓ are involved.)

5.2 G^E AS A FUNCTION OF COMPOSITION

Having obtained the values of G^E, at constant temperature T, for liquid mixtures covering the whole composition range, the next step is to represent these values by an adequate equation. In a recent paper MARSH[9] examined this problem in great detail and showed that the various equations proposed to fit G^E can be reduced to the general expression

$$G^E/RT = x_1 x_2 \left[\sum_{m=0}^{m'} A_m Z^m \Big/ \sum_{n=0}^{n'} B_n Z^n \right] \qquad \ldots (5.36)$$

where $Z = (2x_1 - 1)$ and $B_0 = 1$. However, the improvement obtained by the introduction of parameters beyond the second, B_1, in the denominator is not significant. This case corresponds to the equation first proposed by MYERS and SCOTT[10], in which B_1 is the 'skewing parameter'.

For binary mixtures of molecularly simple substances G^E is always a fairly symmetrical function of the composition, so that we found no need to use anything more complicated than a Redlich-Kister-type expression

$$G^E/RT = x_1(1-x_1)\left[A_G + B_G(2x_1 - 1) + C_G(2x_1 - 1)^2\right] \qquad \ldots (5.37)$$

as first suggested by GUGGENHEIM[11a] and later recommended by SCATCHARD[11c]. This is equivalent to taking $B_n = 0$ for $n \neq 0$ in equation (5.36). In some cases even two parameters, A_G and B_G, were found to be sufficient to represent the experimental data obtained in the present work.

The activity coefficients are readily obtained from (5.37), as indicated in Appendix (I) where further comments on this equation are made.

5.3 CALCULATION OF THE COMPOSITIONS OF THE LIQUID AND VAPOUR PHASES

To calculate G^E using equation (5.32) it is necessary to know the compositions of the vapour and liquid phases, y_i and x_i. However, the experimental measurements described in Chapter 3 only give the total (liquid + vapour) number of moles of each component admitted into the pyknometer,

and hence the gross mole fractions X_i in the system. A procedure for converting these overall compositions into the actual compositions of the two phases is therefore required.

The number of moles of component $\underline{i}$ condensed into the pyknometer, n_i, is obtained from the difference between two terms representing, respectively, the initial and final amounts of gas in the thermostated storage globe (and its line). These terms are both of the form

$$n_i = \frac{P}{R} f_i\left(\frac{V}{T}\right) \qquad \ldots (5.38)$$

where $f_i(V/T)$ is a function which allows for the fact that different parts of the apparatus are at different temperatures:

$$f_i\left(\frac{V}{T}\right) = \frac{V_{Gi}}{T_w}\left[1 - \frac{B_i(T_w)P}{RT_w}\right] + \frac{V_{R2}}{T_r}\left[1 - \frac{B_i(T_r)P}{RT_r}\right] . \qquad \ldots (5.39)$$

In this expression V_{Gi} is the volume of the storage globe, which is maintained at the temperature of the water bath T_w; and V_{R2} is the volume of the dead-space in the supply line, at room temperature T_r (Appendix (C)).

The compositions of the liquid and vapour phases can be related to the gross mole fractions X_i through the simple material balance of the system:

- the total number of moles in the system, n, and those in the vapour and liquid phases, n^G and n^L, must satisfy

$$n = n^G + n^L ;$$

- and the balance for component 1, for instance, is

$$X_1 n = y_1 n^G + x_1 n^L .$$

By combining the two equations the so-called 'lever rule' is obtained:

$$\frac{n^G}{n - n^G} = \frac{X_1 - x_1}{y_1 - X_1} . \qquad \ldots (5.40)$$

In assessing the amount of gas mixture in the vapour phase, n^G, the volume of the vapour in the system is again divided into regions according

to the different temperatures prevailing in each one, namely: the temperature of the pyknometer bulb T_{pk}, the room temperature T_r, and the temperature gradient between T_{pk} and T_r corresponding to the gas mixture in the pyknometer stem from the etch mark to tap (1), Fig. (3.1). The volume of this last region V_{gr} was made deliberately small, so that the gas in that section can be treated as ideal. Considering that the distribution of temperature is linear (constant gradient), the number of moles of gas in this section is then given by

$$n_{gr} = \frac{P}{R} \frac{V_{gr}}{T_{pk} - T_r} \ln \frac{T_r}{T_{pk}} \quad . \qquad \ldots (5.41)$$

Therefore, the total number of moles of mixture in the vapour phase is obtained from an expression similar to (5.38),

$$n^G = \frac{P}{R} f\left(\frac{V}{T}\right), \qquad \ldots (5.42)$$

where the function $f(V/T)$ is now that introduced by MATHOT *et al.*[12]

$$f\left(\frac{V}{T}\right) = \frac{V_{pk} - V^L}{T_{pk}} \left[1 - \frac{B(T_{pk})P}{RT_{pk}}\right] + \frac{V_{Rl}}{T_r}\left[1 - \frac{B(T_r)P}{RT_r}\right] + \frac{V_{gr}}{T_{pk} - T_r} \ln \frac{T_r}{T_{pk}} \quad , \qquad \ldots (5.43)$$

the second virial coefficient of the gas mixture B being calculated through equation (5.17). The volume of the liquid mixture in the pyknometer V^L is considered to be simply the sum of the volumes of the two pure liquids, an assumption which cannot give rise to a serious error since the excess volumes and the amounts of liquids in the pyknometer are always small.

With the relations above, the compositions y_1 and x_1 can be evaluated by successive approximations. A further assumption is made to initiate the iteration: the liquid mixture is considered to be a regular solution,

so that

$$\ell n\ \gamma_1 = \alpha x_2^2 . \qquad \ldots (5.44)$$

From equation (5.31) it follows that

$$y_1 = \frac{x_1 P_1^* \gamma_1}{P} \exp\left[\left(\sum_{n=1}^{9} \tau_{1,n}\right)\Big/ RT\right] \qquad \ldots (5.45)$$

and, therefore, by using (5.44),

$$y_1 = \frac{x_1 P_1^*}{P} \beta_1 \qquad \ldots (5.46)$$

where

$$\beta_1 = \exp\left[\alpha x_2^2 + \left(\sum_{n=1}^{9} \tau_{1,n}\right)\Big/ RT\right] . \qquad \ldots (5.47)$$

A first approximation for the value of α is obtained by considering only the first term $\tau_{1,0}$ in equation (5.31),

$$\ell n\ \gamma_1 = \ell n \frac{y_1 P}{x_1 P_1^*} = \alpha x_2^2 , \qquad \ldots (5.48)$$

and noting that in this case the Gibbs-Duhem relationship,

$$x_1 \left(\frac{\partial \ell n\ \gamma_1}{\partial x_1}\right)_{P,T} + x_2 \left(\frac{\partial \ell n\ \gamma_2}{\partial x_1}\right)_{P,T} = 0 , \qquad \ldots (5.49)$$

requires that

$$\ell n\ \gamma_2 = \ell n \frac{y_2 P}{x_2 P_2^*} = \alpha x_1^2 . \qquad \ldots (5.50)$$

Then, for the equimolar mixture ($x_1 = x_2 = 0.5$)

$$y_1 = \frac{P_1^*}{P_1^* + P_2^*} , \qquad \ldots (5.51)$$

and therefore the combination of (5.48) and (5.51) gives

$$\alpha = 4\ \ell n \left(\frac{2 P_{\frac{1}{2}}}{P_1^* + P_2^*}\right) . \qquad \ldots (5.52)$$

In this equation $P_{\frac{1}{2}}$ is the vapour pressure of the equimolar mixture, which can be estimated from a plot of the experimental values.

An improved estimate of the composition of the liquid is then obtained by substituting the values of n^G and y_1, as given by (5.42) and (5.46) respectively, into equation (5.40) and solving for x_1:

$$x_1 = \frac{X_1 n}{n + f(V/T)(P_1^* \beta_1 - P)/R} \quad . \qquad \ldots (5.53)$$

Accordingly, the actual numerical calculation in any particular case starts by assuming as a first approximation that $x_1 = y_1 = X_1$, thus giving a value for β_1. This is used in (5.46) and (5.53) to obtain better approximations for y_1 and x_1. The process is then recycled until a consistent pair of values for y_1 and x_1 is obtained.

This is not, of course, the end of the calculation since this was carried out on the assumption of a first approximation value, α, for the parameter A_G and assuming that the two other parameters in the G^E equation were zero ($B_G = C_G = 0$).

The estimated compositions y_1 and x_1 are then used to calculate G^E from equation (5.32), with which a better value A_G of α can be obtained by applying a numerical method due to BARKER[13], as is described in Appendix (J). Essentially this method was devised to find a self-consistent set of compositions (y_1 and x_1) and G^E values, by adjusting through an iterative procedure the parameters A_G, B_G and C_G which minimize the sum of the squares of the pressure residuals

$$R_p = P_{exp} - P_{calc} \qquad \ldots (5.54)$$

(the exact meaning of P_{calc} being also given in the appendix).

The errors affecting the final value of G^E are discussed in Appendix (K).

5.4 REFERENCES

(1) PRAUSNITZ, J.M., 'Molecular Thermodynamics of Fluid-Phase Equilibria', Prentice-Hall, Englewood Cliffs (1969).

(2) SMITH, B.D., 'Design of Equilibrium Stage Processes', McGraw-Hill, New York (1963).

(3) SOOD, S.K. and HASELDEN, G.G., Cryogenics, 1970, 10, 199.

(4)(a) LEONARD, P.J., HENDERSON, D. and BARKER, J.A., Trans. Faraday Soc., 1970, 66, 2439.

(b) CHAMBERS, M.V. and McDONALD, I.R., Mol. Phys., 1975, 29, 1053.

(c) TWU, C.-H., GUBBINS, K.E. and GRAY, C.G., Mol. Phys., 1975, 29. 713.

(5) CALADO, J.C.G., Técnica, 1972, 34, 237.

(6) SCATCHARD, G. and RAYMOND, C.L., J. Am. Chem. Soc., 1938, 60, 1278.

(7) GUGGENHEIM, E.A. and McGLASHAN, M.L., Proc. Roy. Soc. (London), 1951, A206, 448.

(8)(a) TSONOPOULOS, C., A.I. Ch. E. Journal, 1974, 20, 263.

(b) TSONOPOULOS, C., A.I. Ch. E. Journal, 1975, 21, 827.

(c) TARAKAD, R.R. and DANNER, R.P., A.I. Ch. E. Journal, 1977, 23, 685.

(9) MARSH, K.N., J. Chem. Thermodynamics, 1977, 9, 719.

(10) MYERS, D.B. and SCOTT, R.L., Ind. Eng. Chem., 1963, 55, 43.

(11)(a) GUGGEMHEIM, E.A., Trans. Faraday Soc., 1937, 33, 151.

(b) REDLICH, O. and KISTER, A.T., Ind. Eng. Chem., 1948, 40, 341.

(c) SCATCHARD, G., Chem. Rev., 1949, 44, 7.

(12) MATHOT, V., STAVELEY, L.A.K., YOUNG, J.A. and PARSONAGE, N.G., Trans. Faraday Soc., 1956, 52. 1488.

(13) BARKER, J.A., Austral. J. Chem., 1953, 6, 207.

CHAPTER 6

CALCULATION OF THE EXCESS MOLAR VOLUME V^E

6.1 V^E FROM DENSITY MEASUREMENTS

The amount of each component admitted into the pyknometer is found as before (section 5.3). Therefore, the total number of moles of component i in the pyknometer is given by the difference of the two terms obtained from equations (5.38) and (5.39). Once the overall mole fractions X_i have been obtained, the calculation of the distribution of the two components between the liquid and vapour phases can be made. This calculation is now easier than in the previous case, partly because of the small volume occupied by the vapour, and partly because of the knowledge of the P,x relationship derived from the vapour pressure measurements which have lead to G^E.

The volume occupied by the vapour in the pyknometer stem is

$$V^G = V_{gr} - \phi (h_m - h_r) \qquad \ldots (6.1)$$

where h_m and h_r are the heights of the liquid meniscus and the reference mark in the capillary, respectively. The second term in the right-hand side of this expression is very small, so that V^G is of the order of magnitude of V_{gr} itself.

The number of moles of mixture in the vapour phase n^G is then given by an expression similar to equation (5.41)

$$n^G = \frac{P}{R} \frac{V^G}{T_{pk} - T_r} \ell n \frac{T_r}{T_{pk}} \quad , \qquad \ldots (6.2)$$

where P is the vapour pressure of the liquid mixture. As a first approximation P can be calculated assuming that the composition of the liquid mixture is given by the gross mole fractions, i.e. $x_i \simeq X_i$.

Since $n^G \ll n^L$, the composition of the vapour phase can be obtained from the approximate relationship

$$y_i = \frac{\gamma_i x_i P_i^*}{P} \simeq \frac{x_i P_i^*}{P} \exp(A_G x_j^2) \qquad \ldots (6.3)$$

taking again $x_i \simeq X_i$ as a first approximation.

A better value for x_i is then obtained from the lever rule, equation (5.40), and the process is recycled until self-consistency is achieved. Usually 2-3 cycles are sufficient.

The molar volume of the liquid mixture V (or the density) is then easily calculated from

$$V = V^L / (n - n^G) \qquad \ldots (6.4)$$

where

$$V^L = V_{pk} + \phi (h_m - h_r) \qquad \ldots (6.5)$$

is the volume of the liquid in the pyknometer.

The excess molar volume of the mixture is defined by the equation

$$\begin{aligned} V^E &= V - V^{id} \\ &= V - \sum_i x_i V_i^* \end{aligned} \qquad \ldots (6.6)$$

where the V_i^* are the molar volumes of the pure components.

All the molar volumes in equation (6.6) relate of course to the respective saturation vapour pressures. For comparative purposes it is convenient to refer all the measurements to a constant value of the pressure, usually taken to be zero. This correction requires a knowledge of the isothermal compressibilities of the pure liquids and of the mixture as well. Experimental values for the latter are not usually available, so that it is usually assumed to be a linear function of the mole fraction. This correction is only significant at pressures well above those involved in the present experiments, for which the corrections to zero pressure were found to be less

than the uncertainty in V^E (which is discussed in Appendix (L)), and therefore were not considered.

6.2 V^E AS A FUNCTION OF COMPOSITION

The excess molar volumes can usually be fitted to an equation of the type

$$V^E = x_1 (1 - x_1) \left[A_V + B_V (2x_1 - 1) + C_V (2x_1 - 1)^2 \right] \quad \ldots (6.7)$$

with parameters A_V, B_V and C_V adjusted to minimize the volume residuals

$$R_V = V^E_{exp} - V^E_{calc} \quad \ldots (6.8)$$

where V^E_{calc} is the value obtained from equation (6.7).

For sharply skewed curves MYERS and SCOTT[1] suggested the introduction of an expression involving a fourth parameter in the denominator of the right-hand side of equation (6.7). SOARES[2] found, however, no significant improvement on using such an expression to fit the V^E values of the systems $C_2H_4 + CH_4$ and $C_2H_4 + Kr$, which are assymmetric (but not strongly so). In the case of $N_2O + C_2H_4$ we reached the same conclusion, as discussed later in this work.

6.3 PARTIAL MOLAR VOLUMES

A brief reference is made here to the calculation of the partial molar volumes of the components of binary liquid mixtures, V_i, from the knowledge of the excess molar volume V^E, since those values appear in some of the terms in equation (5.31).

It can easily be shown, by applying the definition (5.12) to a liquid mixture, that

$$V_1 = V - x_2 \left(\frac{\partial V}{\partial x_2} \right)_{P,T} \quad \ldots (6.9)$$

and

$$V_2 = V - x_1 \left(\frac{\partial V}{\partial x_1} \right)_{P,T} . \quad \ldots (6.10)$$

Using the molar volume of the mixture, V, as given by equation (6.6) with V^E replaced by the right-hand side of equation (6.7), the following expressions are obtained:

$$V_1 = V_1^* + x_2^2 \left[A_V + B_V (3 - 4x_2) + C_V (1 - 2x_2)(5 - 6x_2) \right] \quad \ldots \quad (6.11)$$

$$V_2 = V_2^* + x_1^2 \left[A_V + B_V (4x_1 - 3) + C_V (2x_1 - 1)(6x_1 - 5) \right] \quad \ldots \quad (6.12)$$

6.4 REFERENCES

(1) MYERS, D.B. and SCOTT, R.L., Ind. Eng. Chem., 1963, 55, 43

(2) SOARES, V.A.M., 'Estudo Termodinâmico de Misturas Líquidas Binárias Contendo Etileno', Tese de Doutoramento, Inst. Sup. Técnico, Lisboa (1976).

CHAPTER 7

CALCULATION OF THE EXCESS MOLAR ENTHALPY H^E

7.1 H^E FROM CALORIMETRIC MEASUREMENTS

In a heat of mixing experiment carried out as described in Chapter 4, no work is done on or by the surroundings, $W = 0$, and therefore the energy supplied to the system, Q_H, must exactly compensate the change in the internal energy of the system ΔU:

$$\Delta U = Q_H \ . \qquad \ldots (7.1)$$

To relate ΔU to the excess enthalpy H^E the treatment presented by LEWIS *et al.*[1] can be adapted as follows. The energy change ΔU can be expressed in terms of the partial molar internal energies of the components in the liquid mixture and in the vapour phase in equilibrium with it, and of the internal energies of the pure components. Designating by (L) and (G) the liquid and vapour phases, respectively, ΔU is then written as

$$\begin{aligned}\Delta U = &\Big[n_1^F(L)\, U_1(L, P_m) + n_2^F(L)\, U_2(L, P_m) \\ &\quad + n_1^F(G)\, U_1(G, P_m) + n_2^F(G)\, U_2(G, P_m) \Big] \\ - &\Big[n_1^I(L)\, U_1^*(L, P_1^*) + n_2^I(L)\, U_2^*(L, P_2^*) \\ &\quad + n_1^I(G)\, U_1^*(G, P_1^*) + n_2^I(G)\, U_2^*(G, P_2^*) \Big] \qquad \ldots (7.2)\end{aligned}$$

where the superscripts I and F refer to the initial (pure components) and final (mixture) states of the system, respectively, and the asterisk * indicates a pure species, as before.

On the other hand, the change in the internal energy due to the mixing process is, for the liquid phase,

$$\begin{aligned}\Delta U(L) &= n^F(L)\, U^E(L, P_m) \\ &= n^F(L) \left[H^E(L, P_m) - P_m V^E(L, P_m) \right] \qquad \ldots (7.3)\end{aligned}$$

where $n^F(L) = n_1^F(L) + n_2^F(L)$; or, if it is assumed that mixing takes place at the final pressure P_m,

$$\Delta U(L) = \left[n_1^F(L)\, U_1(L, P_m) + n_2^F(L)\, U_2(L, P_m)\right] - \left[n_1^F(L)\, U_1^*(L, P_m) + n_2^F(L)\, U_2^*(L, P_m)\right] . \quad \ldots (7.4)$$

Equations similar to (7.3) and (7.4) hold for the vapour phase. Therefore, from (7.2) and (7.4),

$$\begin{aligned}\Delta U = &\left[\Delta U(L) + n_1^F(L)\, U_1^*(L, P_m) + n_2^F(L)\, U_2^*(L, P_m)\right] \\ &+ \left[\Delta U(G) + n_1^F(G)\, U_1^*(G, P_m) + n_2^F(G)\, U_2^*(G, P_m)\right] \\ &- \left[n_1^I(L)\, U_1^*(L, P_1^*) + n_2^I(L)\, U_2^*(L, P_2^*) + n_1^I(G)\, U_1^*(G, P_1^*) + n_2^I(G)\, U_2^*(G, P_2^*)\right] \quad \ldots (7.5)\end{aligned}$$

Designating by δn_i the number of moles of i transferred from one phase to the other (i.e., condensed or evaporated),

$$\left.\begin{aligned} n_i^I(L) &= n_i^F(L) - \delta n_i \\ n_i^I(G) &= n_i^F(G) + \delta n_i \end{aligned}\right\} , \quad \ldots (7.6)$$

and substituting (7.3) and the analogous expression for the vapour phase into eqn (7.5), the following expression is obtained for ΔU:

$$\begin{aligned}\Delta U = &\, n^F(L)\left[H^E(L, P_m) - P_m V^E(L, P_m)\right] + n^F(G)\left[H^E(G, P_m) - P_m V^E(G, P_m)\right] \\ &+ n_1^F(L)\left[U_1^*(L, P_m) - U_1^*(L, P_1^*)\right] + n_2^F(L)\left[U_2^*(L, P_m) - U_2^*(L, P_2^*)\right] \\ &+ n_1^F(G)\left[U_1^*(G, P_m) - U_1^*(G, P_1^*)\right] + n_2^F(G)\left[U_2^*(G, P_m) - U_2^*(G, P_2^*)\right] \\ &- \delta n_1 \left[U_1^*(G, P_1^*) - U_1^*(L, P_1^*)\right] + \delta n_2 \left[U_2^*(G, P_2^*) - U_2^*(L, P_2^*)\right] \quad \ldots (7.7)\end{aligned}$$

This expression can be simplified as follows. The general thermodynamic relationships

$$U = H - PV \quad \ldots (7.8)$$

and

$$\left(\frac{\partial H}{\partial P}\right)_T = V - T\left(\frac{\partial V}{\partial T}\right)_P \quad \ldots (7.9)$$

give

$$\left(\frac{\partial U}{\partial P}\right)_T = -T\left(\frac{\partial V}{\partial T}\right)_P - P\left(\frac{\partial V}{\partial P}\right)_T \qquad \ldots (7.10)$$

By applying eqn (7.10) to the pure liquids one obtains:

$$U_i^*(L, P_m) - U_i^*(L, P_i^*) = -\alpha_{P,i}^* V_i^*(P_m - P_i^*)\, T + \tfrac{1}{2}\kappa_{T,i}^* V_i^*(P_m^2 - P_i^{*2}) \qquad \ldots (7.11)$$

where $\alpha_{P,i}^*$ is the expansion coefficient, $\kappa_{T,i}^*$ the isothermal compressibility, and V_i^* the molar volume of the pure liquid. In the conditions under which the calorimeter is usually operated the last term in (7.11) is negligible.

Assuming, further, that the virial equation of state truncated after the second term is adequate for the pure gases at the pressures involved (which are never high) eqn (7.10) gives

$$U_i^*(G, P_m) - U_i^*(G, P_i^*) = -T\,\frac{dB_{ii}}{dT}\,(P_m - P_i^*)\,. \qquad \ldots (7.12)$$

Moreover, in the two last terms in the right-hand side of eqn (7.7),

$$U_i^*(G, P_i^*) - U_i^*(L, P_i^*) = \Delta U_{v,i} = \Delta H_{v,i} - P_i^* \Delta V_{v,i} \qquad \ldots (7.13)$$

where the subscript v stands for vaporization. Thus, by substituting the results (7.11) to (7.13) into eqn (7.7), the final expression for H^E is obtained:

$$
\left.
\begin{aligned}
H^E(L) = {} & \frac{Q_H}{n(L)} && \psi_1 \\
& + P_m V^E(L) && \psi_2 \\
& - \frac{n(G)}{n(L)} \left[H^E(G) - P_m V^E(G) \right] && \psi_3 \\
& + T \left[x_1 \alpha^*_{P,1} V^*_1 (P_m - P^*_1) + x_2 \alpha^*_{P,2} V^*_2 (P_m - P^*_2) \right] && \psi_4 \\
& + T \left[\frac{n_1(G)}{n(L)} \frac{dB_{11}}{dT} (P_m - P^*_1) + \frac{n_2(G)}{n(L)} \frac{dB_{22}}{dT} (P_m - P^*_2) \right] && \psi_5 \\
& + \frac{\delta n_1}{n(L)} \left[\Delta H_{v,1} + P^*_1 \Delta V_{v,1} \right] && \psi_6 \\
& + \frac{\delta n_2}{n(L)} \left[\Delta H_{v,2} + P^*_2 \Delta V_{v,2} \right] && \psi_7
\end{aligned}
\right\} \qquad (7.14)
$$

or, in condensed form,

$$
H^E = \sum_{m=1}^{7} \psi_m \, . \qquad \ldots (7.15)
$$

In this equation Q_H is the only quantity directly determined from experiment, terms ψ_2 to ψ_7 being corrections. Among the latter, ψ_2 to ψ_5 are usually very small but ψ_6 and ψ_7 — the 'vaporization corrections' — which rise rapidly with increasing vapour pressures, are never negligible. For the equimolar mixture the combined effect of these two terms (which, in general, have opposite signs) is responsible for ~ 10% of the value of H^E at low pressures (0.2 - 0.3 MPa), and up to ~ 50% for the experiments carried out at moderate pressures (of ~ 1.2 MPa, which are for practical purposes the limiting working pressures that can be used in the apparatus). For mixtures containing less than, say, 20% of one component these corrections can reach higher values and therefore the apparatus is not well suited to study dilute solutions.

The uncertainty in the H^E determinations is discussed in Appendix (M).

The H^E values evaluated from eqn (7.14) refer to the vapour pressure

of the mixture P_m. For reasons already indicated in previous chapters it is desirable to convert these values into results at zero pressure. In principle, this can be easily done through the general relationship (7.9) written in terms of the excess functions. In practice, however, $(\partial V^E/\partial T)_P$ is seldom known†, so that an approximate method has to be used. Equation (7.9) can be written as

$$\left(\frac{\partial H}{\partial P}\right)_T = V(1 - \alpha_P T) \qquad \ldots (7.15)$$

and consequently, assuming the isothermal compressibilities of the liquids to be constant in the interval $P = 0$ to P_m,

$$\begin{aligned} H^E(P=0) = H^E(P_m) - P_m \Big[& (x_1 V_1^* + x_2 V_2^* + V^E) \\ & (1 - \alpha_{P,m} T)(1 + \tfrac{1}{2} \kappa_{T,m} P_m) \\ & - V_1^*(1 - \alpha_{P,1}^* T)(1 + \tfrac{1}{2} \kappa_{T,1}^* P_m) \\ & - V_2^*(1 - \alpha_{P,2}^* T)(1 + \tfrac{1}{2} \kappa_{T,2}^* P_m) \Big] \end{aligned} \qquad \ldots (7.16)$$

where

$$\alpha_{P,m} = x_1 \alpha_{P,1}^* + x_2 \alpha_{P,2}^* + \alpha_P^E \qquad \ldots (7.17)$$

$$\kappa_{T,m} = x_1 \kappa_{T,1}^* + x_2 \kappa_{T,2}^* + \kappa_T^E \qquad \ldots (7.18)$$

In most cases the excess coefficients α_P^E and κ_T^E are, again, not known but no serious error is introduced by assuming that both are zero. Values of the expansion coefficient for the pure liquids,

$$\alpha_{P,i}^* = \frac{1}{V_i^*}\left(\frac{\partial V_i^*}{\partial T}\right)_P , \qquad \ldots (7.19)$$

---

† In the last three years or so, investigations have been made of the equation of state over a temperature range of binary liquified gas mixtures, from which information about $(\partial V^E/\partial T)_P$ can be derived, but so far none of the systems involved in this thesis have been studied in this way.

can be assumed, when not available, to be those at saturation pressure, $\alpha^*_{\sigma,i}$, which can be obtained from results for the density as a function of temperature. To assess the values of the isothermal compressibilities one can use the approximate relationship

$$\frac{(\Delta H_{v,i} - RT)}{V^*_i} \simeq \frac{T\alpha^*_{P,i}}{\kappa^*_{T,i}} \qquad \ldots (7.20)$$

since both sides of this equation are a measure of the square of the solubility parameter[2].

Better estimates of $\alpha^*_{P,i}$ and $\kappa^*_{T,i}$ can, of course, be obtained from exact relations involving the velocity of sound in the liquid[3], but such data are usually not available for most of the substances studied in this work.

7.2 H^E AS A FUNCTION OF COMPOSITION

As for G^E, the excess molar enthalpy can be adequately represented by an expression of the type

$$H^E/RT = x_1(1-x_1)\left[A_H + B_H(2x_1 - 1) + C_H(2x_1 - 1)^2\right]. \qquad \ldots (7.21)$$

For a given system, H^E is usually measured at a temperature slightly above (or approximately equal to) that of the triple-point at which the determination of G^E is carried out. (In this work the difference between the two temperatures was less than 2K on all occasions but one). Therefore, without serious error H^E can be considered to be constant over this small temperature range, so that S^E, the excess molar entropy, can be estimated from the general relationship

$$TS^E = H^E - G^E . \qquad \ldots (7.22)$$

S^E can then be represented by

$$S^E/R = x_1(1-x_1)\left[A_S + B_S(2x_1 - 1) + C_S(2x_1 - 1)^2\right] \qquad \ldots (7.23)$$

with parameters

$$A_S = A_H - A_G$$
$$B_S = B_H - B_G \qquad \ldots (7.24)$$
$$C_S = C_H - C_G$$

7.3 CALCULATION OF THE COMPOSITIONS

The amount of each component admitted to the calorimeter is given by the difference

$$n_i = n_i(I) - n_i(II) - n_i(III) \ , \qquad \ldots (7.25)$$

where (I) and (II) refer to, respectively, the initial and final numbers of moles of gas in the calibrated storage globe and its supply line to tap (12) [or (22), Fig. 4.2], and (III) denotes the residual amount of gaseous component trapped between taps (11) and (12), [or (21) and (22)], as described before. At room temperature only the second virial coefficients need be invoked for an acceptable calculation of all three quantities:

$$n_i(Z) = \left[-1 + (1 + 4B_{ii} P/RT)^{\frac{1}{2}} \right] B_{ii}/2V \qquad \ldots (7.26)$$

where $V = V_{I,i}$ for $Z \equiv I$ or $\equiv II$, and $V = V_{r,i}$ in the case of $Z \equiv III$. (Values of the volumes $V_{I,i}$ and $V_{r,i}$ are given in Appendix (F).)

Before mixing (superscript I) each component is present in its compartment partly as a liquid (L) and partly as a vapour (G). A simple material balance gives the amount of substance in each phase expressed in terms of known quantities:

$$n_i^I(G) = n_i - n_i^I(L) \qquad \ldots (7.27)$$

$$n_i^I(L) = [n_i - v_i/V_i(G)]/[1 - V_i(L)/V_i(G)] \qquad \ldots (7.28)$$

where v_i ($= v_I$ or $= v_{II}$, Appendix (F)) is the volume of the chamber of the calorimeter in which component i is initially contained. The total number of moles in the system (L + G),

$$n = n_1 + n_2 \qquad \ldots (7.29)$$

remains constant throughout the experiment, as well as n_1 and n_2 themselves. On mixing the two components, however, transference of material between the liquid and the vapour inevitably occurs. After mixing — superscript F — the volume available for the gas mixture is

$$V(G) = V - V(L) \qquad \ldots (7.30)$$

where

$$V = v_I + v_{II} \qquad \ldots (7.31)$$

is the total volume of the system, so that eqn (7.30) can be written as

$$n^F(G)\, V(G, P_m) = V - \Big[n_1^F(L)\, V_1^*(L, P_m) + n_2^F(L)\, V_2^*(L, P_m) + n^F(L)\, V^E(L, P_m) \Big] \qquad \ldots (7.32)$$

where the molar volumes of the components of the liquid mixture, $V_i^*(L,P_m)$, are obtained from those at the respective saturation pressures through

$$V_i^*(L, P_m) = V_i^*(L, P_i^*)\Big[1 + \kappa_{T,i}^*(P_i^* - P_m) \Big] . \qquad \ldots (7.33)$$

Since the pressures in the apparatus are never very high, and moreover $n(G) \ll n(L)$, it can be assumed that the molar volume of the vapour is given by

$$V(G, P_m) = \Big[1 + (1 + 4BP_m/RT)^{\frac{1}{2}} \Big] RT/2P_m . \qquad \ldots (7.34)$$

Therefore, after rearrangement of (7.32), an expression is obtained,

$$n_1^F(G) = \Big\{ V - n_2^F(G)\, V(G, P_m) - n_1 V_1^*(L, P_m) - \Big[n_2 - n_2^F(G) \Big] V_2^*(L, P_m) - \Big[n - n_2^F(G) \Big] V^E(L, P_m) \Big\} \Big/ \Big[V(G, P_m) - V_1^*(L, P_m) - V^E(L, P_m) \Big] , \qquad \ldots (7.35)$$

from which the amount of component 1 in the vapour mixture can be evaluated.

Since in investigating a particular system, the vapour pressure and density determinations are generally carried out prior to the heat of mixing experiments, expressions of the forms $P = P(x_i)$, for the vapour pressure, and $V^E = V^E(x_i)$, for the excess molar volume of the liquid mixture, are already available at this stage of the calculation, so that an iterative procedure can be used to obtain the compositions and the amounts of substances in the two phases at equilibrium.

By applying eqn (5.7) one has

$$\varphi_i \, y_i \, P_m = \gamma_i \, x_i \, f_i^0 \, , \qquad (5.10)$$

the standard state fugacity f_i^0 being obtained from eqn (5.25) by assuming (with no significant error) that the pure liquids are incompressible between the saturation pressures P_i^* and the vapour pressure of the mixture P_m:

$$f_i^0 = P_i^* \varphi_i^* \exp\left\{V_i^*(L)\left[P_m - P_i^*\right]\Big/RT\right\} \, , \qquad \ldots (7.36)$$

where the fugacity coefficient of the pure component i at its own saturation pressure, φ_i^*, is given by

$$\varphi_i^* = \exp\left\{(1/RT)\int_0^{P_i^*}\left[V_i^*(G) - RT/P\right]dP\right\} \, . \qquad \ldots (7.37)$$

In eqn (5.10) the activity coefficient γ_i is calculated from the excess molar Gibbs energy, G^E, through eqns (AI.2) and (AI.3). The fugacity coefficient φ_i of component i in the vapour mixture is given by eqn (5.11). Assuming that the pure gases and the vapour mixture are described by the virial equation of state, then[4]

$$\varphi_i^* = \frac{RT}{P_i^* V_i^*(G)} \exp\left[2\,B_{ii}/V_i^*(G)\right] \qquad \ldots (7.38)$$

and

$$\varphi_i = \frac{RT}{P_m V(G, P_m)} \exp\left[2\left(y_i B_{ii} + y_j B_{ij}\right)/V(G, P_m)\right] . \qquad \ldots (7.39)$$

The iteration starts by assuming

$$n_i^F(L) = n_i^I(L)$$

so that a first approximation value can be worked out for the composition of the liquid:

$$x_1 = 1 - x_2 = \frac{n_1^F(L)}{n_1^F(L) + n_2^F(L)} . \qquad \ldots (7.40)$$

This value is used in the calculation of the vapour pressure of the mixture, P_m, from the experimental curve, after which $V(G, P_m)$ is obtained from eqn (7.34).

The next step is to estimate the approximate composition of the vapour. To do this it is assumed that

$$n_2^F(G) = n_2^I(G) ,$$

and a first value for the amount of component 1 in the gas mixture $n_1^F(G)$ is calculated from eqn (7.35), thus enabling the composition

$$y_1 = 1 - y_2 = \frac{n_1^F(G)}{n_1^F(G) + n_2^F(G)} \qquad \ldots (7.41)$$

to be obtained, to a first approximation. With this, a better value for the vapour pressure of the mixture P_m is given by the expression

$$P_m = \frac{\gamma_1 x_1 P_1^* \varphi_1^*}{y_1 \varphi_1} \exp \left\{ V_1^*(L) \left[P_m - P_1^* \right] \Big/ RT \right\} \qquad \ldots (7.42)$$

which is derived by substituting (7.36) into (5.10). In the right-hand side of this expression one can use for P_m the value taken from the experimental curve, as before. The improved vapour pressure P_m is now used in the counterpart of eqn (7.42) for component 2,

$$y_2 = \frac{\gamma_2 x_2 P_2^* \varphi_2^*}{P_m \varphi_2} \exp \left\{ V_2^*(L) \left[P_m - P_2^* \right] \Big/ RT \right\} , \qquad \ldots (7.43)$$

so as to obtain a better estimate of the mole fraction y_2. The ratio

between this new value of y_2 and that from the previous approximation is then applied as a correction factor to give a second, better approximate value for the number of moles of component 2 in the vapour phase:

$$[\text{new}]\, n_2^F(G) = [\text{previous}]\, n_2^F(G)\, \frac{[\text{new}]\, y_2}{[\text{previous}]\, y_2} . \qquad \ldots (7.44)$$

With this new value of $n_2^F(G)$ the amount of component 2 in the liquid phase can be corrected,

$$n_2^F(L) = n_2 - n_2^F(G) , \qquad \ldots (7.45)$$

and a second value for $n_1^F(G)$ obtained from eqn (7.35). An improved figure for the number of moles of component 1 in the liquid is then given by

$$n_1^F(L) = n_1 - n_1^F(G) , \qquad \ldots (7.46)$$

and the whole process is recycled until two consecutive values of y_2 do not differ significantly. The final values obtained for the compositions of the two phases, as well as those of the required amounts of substances, are used in eqn (7.14) to calculate H^E.

7.4 H^E FOR TWO PARTIALLY MISCIBLE LIQUIDS

This section has been inserted in connection with the calorimetric experiments carried out with liquid HCℓ and CF_4, which are only partially miscible. In such a case the excess molar enthalpies of the two liquid layers in equilibrium, $H^E(L^I)$ and $H^E(L^{II})$, can still be calculated from at least two (and preferably several) measurements of the energy Q_H supplied to the calorimeter to compensate the energy of mixing of both liquid phases (which form simultaneously).

The derivation of the expression relating $H^E(L^I)$ and $H^E(L^{II})$ to the experimentally determined quantity Q_H is carried out exactly as before, (section 7.1), with only minor formal differences. The final result is

$$
\begin{aligned}
H^E(L^I) + \frac{1-F}{F} H^E(L^{II}) = & \\
= \frac{1}{K} \Big\{ & Q_H && \xi_1 \\
& + \left[F\, V^E(L^I) + (1-F)\, V^E(L^{II}) \right] P_m && \xi_2 \\
& - n(G) \left[H^E(G) - P_m V^E(G) \right] && \xi_3 \\
& + T \left[x_1(L)\, \alpha^*_{P,1}\, V^*_1 (P_m - P^*_1) + x_2(L)\, \alpha^*_{P,2}\, V^*_2 (P_m - P^*_2) \right] && \xi_4 \\
& + T \left[n_1(G)\, \frac{dB_{11}}{dT} (P_m - P^*_1) + n_2(G)\, \frac{dB_{22}}{dT} (P_m - P^*_2) \right] && \xi_5 \\
& + \delta n_1 \left[\Delta H_{v,1} - P^*_1 \Delta V_{v,1} \right] && \xi_6 \\
& + \delta n_2 \left[\Delta H_{v,2} - P^*_2 \Delta V_{v,2} \right] \Big\} && \xi_7
\end{aligned}
\qquad \ldots (7.47)
$$

where

$$
F = \frac{x_1(L^{II}) - x_1(L)}{x_1(L^{II}) - x_1(L^I)} \qquad \ldots (7.48)
$$

is the fraction of the total liquid $(L^I + L^{II})$ existing in the system as liquid phase (L^I), and

$$
K = Fn(L) , \qquad \ldots (7.49)
$$

the symbol (L) indicating the total liquid in the system.

Equation (7.47) clearly reduces to (7.14) when $F = 1$, i.e. when only one liquid phase, (L^I), is present.

After rearrangement (7.47) can be written as

$$
X + Y/F = Z \qquad \ldots (7.50)
$$

where

$$
X = H^E(L^I) - H^E(L^{II}) \qquad \ldots (7.51)
$$

$$
Y = H^E(L^{II}) \qquad \ldots (7.52)
$$

$$
Z = \sum_{m=1}^{7} \xi_m / K , \qquad \ldots (7.53)
$$

so that by plotting Z as a function of 1/F a straight line must be obtained. The slope of this line is $H^E(L^{II})$, $H^E(L^I)$ being obtained from the intercept given by extrapolation to F = 1.

The amounts of substance in the three phases in equilibrium (L^I, L^{II} and G), as well as their respective compositions (which remain constant for all the H^E experiments carried out in the two phase region), are calculated as shown in Chapter 14.

7.5 REFERENCES

(1) LEWIS, K.L., SAVILLE, G. and STAVELEY, L.A.K., J. Chem. Thermodynamics, 1975, 7, 389.

(2) HILDEBRAND, J.H. and SCOTT, R.L., 'The Solubility of Non-Electrolytes', Reinhold, New York, 3rd ed., 1950, p.424.

(3) ROWLINSON, J.S., 'Liquids and Liquid Mixtures', Butterworth, London, 2nd ed., 1969, p.16.

(4) PRAUSNITZ, J.M., 'Molecular Thermodynamics of Fluid-Phase Equilibria', Prentice-Hall, Englewood Cliffs, 1969, p.101.

PART 4

RESULTS AND DISCUSSION

CHAPTER 8 - THE SYSTEM ARGON + KRYPTON

CHAPTER 9 - THE SYSTEM XENON + HYDROGEN CHLORIDE

CHAPTER 10 - THE SYSTEM XENON + NITROUS OXIDE

CHAPTER 11 - THE SYSTEM XENON + CARBON TETRAFLUORIDE

CHAPTER 12 - THE SYSTEM XENON + HEXAFLUOROETHANE

CHAPTER 13 - THE SYSTEM HYDROGEN CHLORIDE + NITROUS OXIDE

CHAPTER 14 - THE SYSTEM HYDROGEN CHLORIDE + CARBON TETRAFLUORIDE

CHAPTER 15 - THE SYSTEM NITROUS OXIDE + ETHYLENE

CHAPTER 16 - THE SYSTEM ETHYLENE + METHANE

CHAPTER 17 - THE VAPOUR PRESSURE OF CARBON TETRAFLUORIDE

CHAPTER 8

THE SYSTEM ARGON + KRYPTON

8.1 INTRODUCTION

Argon + krypton and krypton + xenon are the only two-component rare-gas systems that can be studied as liquids over the whole composition range. Being constituted of monatomic, spherically symmetrical molecules, these two systems are of fundamental importance in testing theories of mixtures of non-electrolytes. In fact, the experimental results hitherto available on the thermodynamic properties of these two mixtures have frequently been compared with the predictions of various theories, making it desirable to have reliable information on these two systems over as wide a range of conditions as possible. Moreover, argon + krypton has sometimes been used as the reference system in perturbation theory calculations[1].

DAVIES *et al.*[2] determined G^E and V^E for Ar + Kr at 115.77 K. This is the triple-point temperature of krypton, and hence the lowest temperature at which the whole liquid range can be covered. They also measured G^E at 103.94 K, when the coverage was limited by the separation of crystalline krypton from mixtures with $x(Ar) < 0.4$. Prior to this, two sets of vapour pressure measurements at ~88 K, and hence confined to a still smaller composition range, had been made[3,4]. These gave very discordant values of G^E from those of DAVIES *et al.*[2]. CHUI and CANFIELD[5] also measured G^E and V^E at 115.77 K obtaining results in fair agreement with those reported by DAVIES *et al.* These studies showed that whereas G^E is an almost symmetrical function of composition (mole fraction), the corresponding V^E curve is markedly asymmetric.

The excess molar enthalpy H^E has only recently been measured by LEWIS[6], at 116.9 K, in this laboratory, using the previous version[7] of

the calorimeter described in Chapter 4 of this thesis. These measurements showed that H^E is asymmetric in relation to composition, being skewed towards the less volatile component (Kr). By combining the results for H^E with those of DAVIES *et al.* for G^E one concludes that the excess molar entropy, S^E, is negative over the entire composition range. The S^E curve, which also has an asymmetric dependence on composition, is skewed in the same direction as the curve of V^E against mole fraction, i.e. showing its minimum in the argon-rich half of the diagram, at $x(Ar) \simeq 0.65$.

Recent publications have made it possible to estimate G^E at temperatures far above that of the triple-point of krypton. Some of the usual assumptions (e.g. neglect of third virial coefficients) have to be dropped in such conditions. Moreover, the relative contribution of terms $\tau_{i,n}$ in equation (5.32) to the final values of G^E can then be estimated at pressures much higher than those commonly encountered in our work. Such calculations were made by the author, and are described in the following sections. The correlation of the calculated values of $G^E_{\frac{1}{2}}$, at 138 and 143 K, with those previously reported in the literature for lower temperatures and with the experimental results for H^E is then examined.

8.2 CALCULATION OF G^E AT 138 AND 143 K

SCHOUTEN, DEERENBERG and TRAPPENIERS[8] measured the vapour-liquid equilibrium compositions and the corresponding vapour pressures of Ar + Kr at eight temperatures between 138 and 193 K. We used their results to calculate the excess molar Gibbs energy for the equimolar mixture, $G^E_{\frac{1}{2}}$, at the two lowest temperatures at which they investigated this system. Since at the high pressures involved terms $\tau_{i,3}$ and $\tau_{i,4}$ in (5.32) cannot be expected to be negligible, the availability of reliable information on third virial coefficients is fundamental for the present calculations. Fortunately, by the time the results of SCHOUTEN *et al.* appeared, CALIGARIS and HENDERSON[9] published values of third virial coefficients

for argon and krypton (and xenon), and also for the corresponding cross-coefficients. These had been calculated on the basis of an accurate intermolecular potential energy function, so that they are probably of high quality.

Second virial coefficients were taken from the work of BYRNE, JONES and STAVELEY[10], and the molar volumes and isothermal compressibilities of the pure liquids were obtained by extrapolating to zero pressure data from STREETT and STAVELEY[11,12].

The differentials $(\partial V_i/\partial P)_{P=0}$ needed to evaluate terms $\tau_{i,7}$ and $\tau_{i,9}$ were calculated from estimates of $(\partial V^E/\partial P)_{P=0}$ made from the results of BLAGOI and SOROKIN[13]. The limited information available here forced us to assume that the curve of V^E against $\underline{x}$ is symmetrical, so that

$$V^E = A_V x_1 x_2 ,$$

and for the equimolar mixture

$$V_1^* - V_1 = V_2^* - V_2 = -V^E . \qquad \ldots (8.1)$$

Therefore, we assumed that

$$\left(\frac{\partial V_i}{\partial P}\right)_{P=0} = \left(\frac{\partial V_i^*}{\partial P}\right)_{P=0} + \left(\frac{\partial V^E}{\partial P}\right)_{P=0} . \qquad \ldots (8.2)$$

Table 8.1 summarizes the data used in the calculation of $G_{\frac{1}{2}}^E$ at 138 and 143 K. The results of this calculation are given in Table 8.2, and are represented in Fig. 8.1 in which values from DAVIES *et al.*[2] are also shown.

TABLE 8.1

NUMERICAL DATA USED IN CALCULATING $G^E_{\frac{1}{2}}$ AT 138 AND 143 K AND AT ZERO PRESSURE. COMPONENT 1 ≡ Ar; COMPONENT 2 ≡ Kr

Property	138 K	143 K	Source (Ref)
p/kPa	1564	1905	(8)
p_1^*/kPa	2928	3610	(8)
p_2^*/kPa	350	462	(8)
y_1	0.841	0.821	(8)
V_1^*/cm^3 mol^{-1} ($P = 0$)	46.3	60.6	(11)
V_2^*/cm^3 mol^{-1} ($P = 0$)	37.0	37.7	(12)
B_{11}/cm^3 mol^{-1}	−101.7	−95.0	(10)
B_{22}/cm^3 mol^{-1}	−234.6	−219.0	(10)
B_{12}/cm^3 mol^{-1}	−153.8	−143.9	(10)
C_{111}/cm^6 mol^{-2}	2235	2242	(9)
C_{112}/cm^6 mol^{-2}	2464	2603	(9)
C_{122}/cm^6 mol^{-2}	1997	2550	(9)
C_{222}/cm^6 mol^{-2}	−1398	439	(9)
$\kappa_{T,1}^*$/kPa^{-1} ($P = 0$)	41×10^{-6}	49×10^{-6}	(11)
$(\partial\kappa_{T,1}^*/\partial P)$/kPa^{-2} ($P = 0$)	58×10^{-10}	68×10^{-10}	(11)
$\kappa_{T,2}^*$/kPa^{-1} ($P = 0$)	2.8×10^{-6}	3.2×10^{-6}	(12)
$(\partial\kappa_{T,2}^*/\partial P)$/kPa^{-2} ($P = 0$)	0.7×10^{-10}	1.0×10^{-10}	(12)
V^E/cm^3 mol^{-1} ($P = 0$)	−6	−8	(13)
$(\partial V^E/\partial P)_T$/cm^3 mol^{-1} kPa^{-1} ($P = 0$)	58×10^{-5}	84×10^{-5}	(13)

TABLE 8.2

ESTIMATION OF $G^E_{\frac{1}{2}}$ FOR Ar + Kr AT 138 AND 143 K, USING EQUATION (5.32)

Term	$\tau_{i,n}$	
	138 K	143 K
$\tau_{i,0}$	+141.3	+143.2
$\tau_{i,1}$	- 64.1	- 52.5
$\tau_{i,2}$	+ 17.0	+ 17.7
$\tau_{i,3}$	- 17.9	- 20.7
$\tau_{i,4}$	+ 11.4	+ 13.8
$\tau_{i,5}$	+ 9.4	+ 15.2
$\tau_{i,6}$	- 4.0	- 9.6
$\tau_{i,7}$	+ 0.5	+ 1.3
$\tau_{i,8}$	- 0.4	- 1.0
$\tau_{i,9}$	+ 0.7	+ 1.9
$G^E_{\frac{1}{2}} = \frac{1}{2} \sum \tau_{i,n}$	93.9	108.3

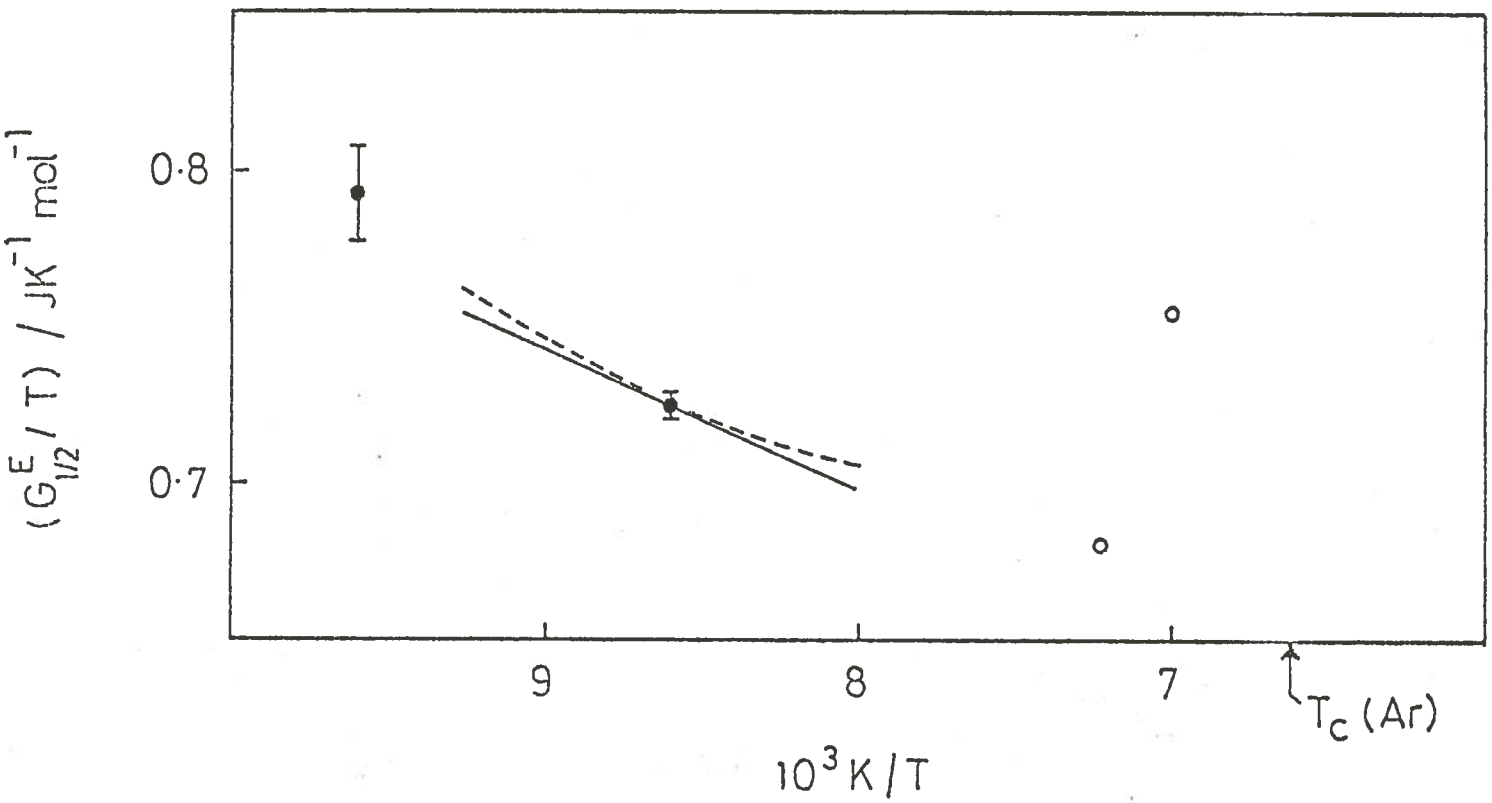

Fig. 8.1 - Ar + Kr: Plot of $G^E_{\frac{1}{2}}/T$ against 1/T

8.3 DISCUSSION

It would be helpful if estimates could be presented of the uncertainty associated with the two calculated values of $G^E_{\frac{1}{2}}$, but we shall not attempt this since for some of the contributing terms such estimates cannot be made reliably. The largest contribution to G^E comes from the $\tau_{i,0}$ terms. The values of these depend on the compositions of coexisting liquid and vapour phases given by SCHOUTEN *et al.*[8], whose results appear to be of high quality. The terms most vulnerable to error are probably $\tau_{i,5}$ to $\tau_{i,9}$ and while the last three of these make relatively small contributions to $G^E_{\frac{1}{2}}$, this is not so for the $\tau_{i,5}$ and $\tau_{i,6}$ terms. The results of BLAGOI and SOROKIN[13] from which $\tau_{i,5}$ has been assessed are limited to one mixture with $x \simeq 0.5$ at 120.0, 129.3, and 141.6 K. Thus, to obtain $(V^E)_{P=0}$ and $(\partial V^E/\partial P)_{P=0}$, we have had to interpolate and extrapolate with respect to temperature, and then extrapolate to $P = 0$. Therefore it must be conceded that at present there is considerable uncertainty in the estimates of V^E and its pressure coefficient at zero pressure, especially at 143 K. Consequently our estimate for V^E at $P = 0$ at this temperature of $-8\ \mathrm{cm^3\,mol^{-1}}$ may perhaps be in error by as much as $2\ \mathrm{cm^3\,mol^{-1}}$, which could affect the value of $G^E_{\frac{1}{2}}$ by $\pm 4\ \mathrm{J\,mol^{-1}}$. The uncertainty in V^E at zero pressure may seem to be rather high. However, as the P, V^E isotherms are steep at low pressures, the more so the higher the temperature, more precise estimates cannot be made from the information hitherto available. Unpublished results of Dr M.N. da PONTE[14] seem to give slightly (numerically) lower values for $(V^E)_{P=0}$. Similar comments may apply to the pressure coefficient of the molar volume of argon, $(\partial V_1^*/\partial P)_{P=0}$, which is necessary for the calculation of $\tau_{i,6}$. At least at the upper temperature, neglect of virial coefficients higher than the third may begin to be also a significant source of error. This is why, although SCHOUTEN *et al.* gave vapour pressure results at several still higher temperatures, it was clearly pointless to attempt to use these to calculate G^E.

From the relation

$$\left[\frac{\partial(G^E/T)}{\partial(1/T)}\right]_{P,x} = H^E \qquad \ldots (8.3)$$

the slope of the curve representing $G^E_{\frac{1}{2}}/T$ as a function of 1/T, Fig. 8.1, is at any point $H^E_{\frac{1}{2}}$. The full line in the figure has been drawn through the experimental point at 115.77 K (the value of $G^E_{\frac{1}{2}}$ which we regard as the most reliable of those available) with a slope equal to the experimental value of $H^E_{\frac{1}{2}}$ at 116.9 K. It is probable, however, that H^E decreases with rising temperature, as we shall see. The values of $H^E_{\frac{1}{2}}$ calculated by LEE, HENDERSON and BARKER[15] at 103.94 and 115.77 K differ by about 27% of the calculated value for the higher of these two temperatures. The proportionate $dH^E_{\frac{1}{2}}/dT$ for our experimental value of $H^E_{\frac{1}{2}}$ at 115.77 K is $-0.9\,JK^{-1}\,mol^{-1}$. If this value of $dH^E_{\frac{1}{2}}/dT$ is assumed to remain constant, the dependence of $G^E_{\frac{1}{2}}$ on T will then be given by the dashed line in Fig. 8.1. However, the fall in H^E with rising temperature probably becomes increasingly rapid. To illustrate this we have combined our calculated values of $G^E_{\frac{1}{2}}$ with the experimental ones reported by DAVIES *et al.*[2] in order to make a rough estimate of the change in $H^E_{\frac{1}{2}}$ with temperature. This calculation is summarized in Table 8.3, and the corresponding results are represented in Fig. 8.2 (where the experimental value of $H^E_{\frac{1}{2}}$ at 116.9 K is also shown). In this figure the dashed curve would represent the change in (the mean values of) $H^E_{\frac{1}{2}}$ with temperature if our calculated $G^E_{\frac{1}{2}}$ were free of uncertainty. Both Figs. 8.1 and 8.2, suggest that our estimate of $G^E_{\frac{1}{2}}$ at the upper temperature (143 K) is somewhat high. However, according to Fig. 8.2, $H^E_{\frac{1}{2}}$ becomes zero at $T \simeq 133$ K. This can perhaps be compared with the corresponding behaviour of the argon + methane system since the critical temperatures and volumes of methane and krypton do not differ very much. For $Ar + CH_4$, H^E has been measured at lower temperatures, in this laboratory, by LEWIS *et al.*[16] and by KIDNAY *et al.*[17], and at higher

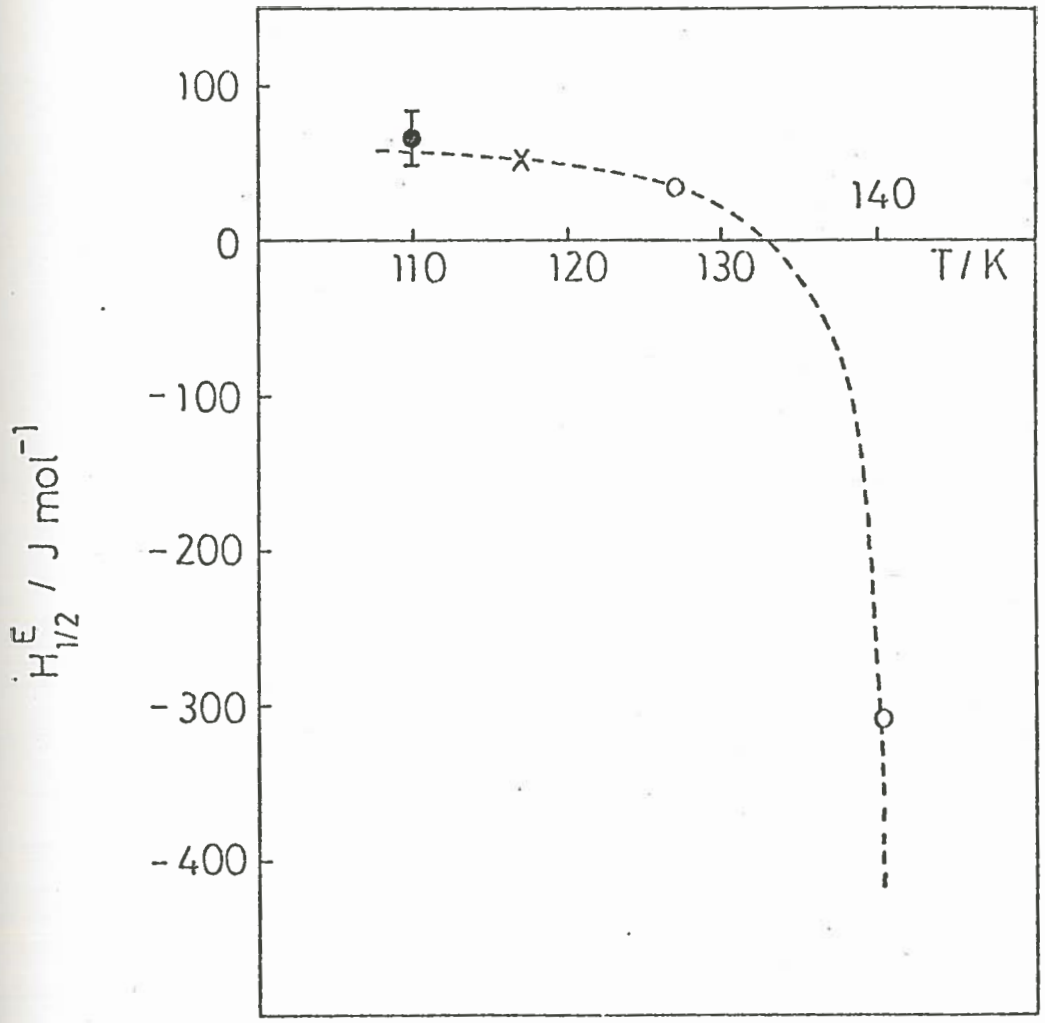

Fig. 8.2

Ar + Kr: $H^E_{\frac{1}{2}}$ (calculated) as a function of temperature. The cross (X) is the experimental value from Ref. (6).

TABLE 8.3

CALCULATION OF $H_{\frac{1}{2}}^E$ USING EQUATION (8.3)

$\frac{T}{K}$	$\frac{(10^3/T)}{K^{-1}}$	$\frac{\Delta(10^3/T)}{K^{-1}}$	$\frac{G_{\frac{1}{2}}^E}{J\,mol^{-1}}$	$\frac{(G_{\frac{1}{2}}^E/T)}{J\,K^{-1}\,mol^{-1}}$	$\frac{\Delta(G_{\frac{1}{2}}^E/T)}{J\,K^{-1}\,mol^{-1}}$	$\frac{(T)}{K}$	$\frac{\langle H_{\frac{1}{2}}^E \rangle}{J\,mol^{-1}}$	Reference
103.94	9.62		82.5 ± 1.6	0.793 ± 0.015				(2)
		- 0.98			- 0.068 ± 0.018	109.9	+ 69 ± 18	
115.77	8.64		83.9 ± 0.4	0.725 ± 0.003				(2)
		- 1.39			- 0.045	127.0	+ 32	
138	7.25		93.9	0.680				This work
		- 0.26			+ 0.076	140.5	- 292	
143	6.99		108.4	0.756				This work

temperatures by MOSEDALE and WORMALD[18]. H^E falls rapidly as the critical temperature (150.8 K) of argon is approached, and in fact changes sign at about 136 K. This is consistent with our estimate value of ~ 133 K for Ar + Kr. Therefore, it appears that for these two systems, $H_{\frac{1}{2}}^E$ becomes zero a few degrees (~ 14 - 18 K) below the critical temperature of the more volatile component (argon). As we shall see in a future chapter of this thesis, a similar situation is encountered for $C_2H_4 + CH_4$.

8.4 REFERENCES

(1) FLYTZANI-STEPHANOPOULOS, M., GUBBINS, K.E. and GRAY, C.G., Mol. Phys., 1975, 30. 1649.

(2) DAVIES, R.H., DUNCAN, A.G., SAVILLE, G. and STAVELEY, L.A.K., Trans. Faraday Soc., 1967, 63, 855.

(3) SCHMIDT, H., Z. physik. Chem., 1960, 24, 265.

(4) WILHELM, G. and SCHNEIDER, G., Z. physik. Chem., 1962, 32, 62.

(5) CHUI, C.-H. and CANFIELD, F.B., Trans. Faraday Soc., 1971, 67. 2933.

(6) LEWIS, K.L., LOBO, L.Q. and STAVELEY, L.A.K., J. Chem. Thermodynamics, 1978, 10, 351.

(7)(a) LEWIS, K.L. and STAVELEY, L.A.K., J. Chem. Thermodynamics, 1975, 7, 855.

(b) LEWIS, K.L. and STAVELEY, L.A.K., J. Phys. E , 1975, 8, 811.

(8) SCHOUTEN, J.A., DEERENBERG, A. and TRAPPENIERS, N.J., Physica, 1975, 81A, 151.

(9) CALIGARIS, R.E. and HENDERSON, D., Mol. Phys., 1975, 30, 1853.

(10) BYRNE, M.A., JONES, M.R. and STAVELEY, L.A.K., Trans. Faraday Soc., 1968, 64, 1747.

(11) STREETT, W.B. and STAVELEY, L.A.K., J. Chem. Phys., 1969, 50. 2302.

(12) STREETT, W.B. and STAVELEY, L.A.K., J. Chem. Phys., 1971, 55, 2495.

(13)(a) BLAGOI, Y.P. and SOROKIN, V.A., Trans. Phys. Tech. Inst. Low. Temp. Acad. Sci. Ukrainian SSR, Physics Condensed State, 1969, Part U, 5.

(b) BLAGOI, Y.P., BUTKO, A.E., MICHAILENKO, S.A. and SOROKIN, V.A., Acad. Sci. Ukrainian SSR, Phys.-Tech. Inst. Low. Temps., Kharkov, 1975.

(14)(a) da PONTE, M.N., (Private communication), 1978.

(b) CALADO, J.C.G. and da PONTE, M.N., Communication to the 8th E.T.C., Guildford, U.K., 1978.

(15) LEE, J.K., HENDERSON, D. and BARKER, J.A., Mol. Phys., 1975, 29, 429.

(16) LEWIS, K.L., SAVILLE, G. and STAVELEY, L.A.K., J. Chem. Thermodynamics, 1975, 7, 389.

(17) KIDNAY, A.J., LEWIS, K.L., CALADO, J.C.G. and STAVELEY, L.A.K., J. Chem. Thermodynamics, 1975, 7, 847.

(18) MOSEDALE, S.E. and WORMALD, C.J., J. Chem. Thermodynamics, 1977, 9, 483.

CHAPTER 9

THE SYSTEM XENON + HYDROGEN CHLORIDE

9.1 INTRODUCTION

The system xenon + hydrogen chloride is a suitable model on which to test theories of mixtures which take account of polarity. On the one hand xenon has a relatively high polarizability ($\alpha = 41.5 \times 10^{-25}$ cm^3) [1], and on the other the small dimensions of the HCℓ molecule enhance the importance to its otherwise only moderate dipole, $\mu = 1.07\,\mathrm{D} = 3.6 \times 10^{-30}\,\mathrm{C\,m}$ [2]. In fact, it is known[3] that in the quantitative treatment of interactions involving dipoles the reduced dipole moment,

$$\mu_R = \mu/(\varepsilon\sigma^3)^{\frac{1}{2}} \quad , \qquad \ldots (9.1)$$

where ε and σ are the intermolecular potential parameters, is a more relevant property than μ itself.

Every dipolar molecule also has, of course, a quadrupole moment which derives from the charge distribution. This is not a serious setback since it is possible for theory to take account of the separate effects of both kinds of multipoles. CALADO *et al.*[4] measured G^E and V^E for this particular system, and although the threoretical treatment of CHAMBERS and McDONALD[5] (who used a Stockmayer intermolecular potential) failed to reproduce the experimental results it has recently been shown[6] that the perturbation theory developed by GUBBINS, GRAY and co-workers[7] leads to almost perfect agreement with experiment as far as G^E and V^E are concerned, not only for Xe + HCℓ but also for Xe + HBr and HCℓ + HBr.

However, it is now recognized that successful prediction of the excess enthalpy H^E is a more exacting test of a theory than the prediction of G^E [8]. Accordingly we have made a direct calorimetric determination of H^E for several mixtures of Xe and HCℓ covering most of the composition

range, to provide theoreticians with the experimental data needed to take the test of theory a step further. These measurements were carried out at a temperature of 182.26 ± 0.05 K, making it also possible to calculate the excess molar entropy S^E by combining the H^E results with the previously reported[4] experimental values of G^E at the triple-point temperature of nitrous oxide.

9.2 DETERMINATION OF H^E AT 182.26 K

The measurements of H^E were made using the calorimeter previously described in this thesis. Hydrogen chloride — component 1 — was admitted into the upper compartment, and xenon — component 2 — into the lower one.

Values of some of the physical properties of the pure components and of the mixture are needed to perform the calculation of H^E. The vapour pressures and molar volumes of the pure substances were taken from this work (Chapters 10 and 13). To account for deviations from ideality in the liquid mixture activity coefficients at 182.26 K, derived from a Redlich-Kister equation for G^E, were taken from CALADO *et al.*[4].

For xenon, accurate values of the second virial coefficient have been interpolated from the experimental work of BREWER[9], namely

$$B_{22}(182.26\ \mathrm{K}) = -334\ \mathrm{cm^3\ mol^{-1}}\ .$$

A reasonable self-consistent set of experimental values of B for hydrogen chloride is provided by the recent results of Dr U. LEUCHS[10], from 190 to 480 K, and the two values (at 328.7 and 368.7 K) due to GLOCKLER *et al.*[11], the latter being the sole published work on the subject. By extrapolation we have estimated

$$B_{11}(182.26\ \mathrm{K}) = -500\ \mathrm{cm^3\ mol^{-1}}\ .$$

We may mention here that the experimental low-temperature values of B_{11} are considerably larger (in absolute value) than those calculated by CALADO

et al.[4,6]. Use of such values in the processing of our raw calorimetric results would give slightly higher values for H^E, but for no mixture would this increase exceed $4\ J\,mol^{-1}$.

Values of V^E, the excess molar volume of the liquid, were available at the higher temperature of 195.48 K [4]. No attempt has been made to estimate V^E at 182.26 K, at which temperature higher values might be expected, as no reliable method for doing this exists. Fortunately the corresponding correction term in eqn (7.14), ψ_2, is never larger than $0.2\ J\,mol^{-1}$ for this system, and consequently even a 100% increase in V^E would not affect H^E to a significant extent.

In the calculation of the vaporization corrections, values for xenon,

$$\Delta H_{v,2}\ (182.26\ K) = 12000\ J\,mol^{-1}$$

and

$$\Delta V_{v,2}\ (182.26\ K) = 5700\ cm^3\,mol^{-1}$$

the molar enthalpy of vaporization and the molar volume change on vaporization, respectively, were taken from STREETT, SAGAN and STAVELEY[12]. In the case of hydrogen chloride, i.e. to calculate term ψ_6 in eqn (7.14), $\Delta H_{v,1}$ at the normal boiling-point (T = 188.13 K) was selected from the early, but accurate, work of GIAUQUE and WIEBE[13], and converted into a value at the actual working temperature of our experiments (182.26 K) by using the general thermodynamic relationship

$$\left[\frac{\partial\,(\Delta H_v)}{\partial T}\right]_p = \Delta C_p\ , \qquad \ldots\ (9.2)$$

where

$$\Delta C_p = C_p^G - C_p^L\ , \qquad \ldots\ (9.3)$$

superscripts G and L identifying the vapour and liquid phases. The mean value,

$$C_{p,1}^L = 58.87\ J\,mol^{-1}\,K^{-1}\ ,$$

in the relevant interval was taken from reference (13). The molar heat capacity of the gas had to be estimated. It was assumed that at the low pressures involved HCℓ could be treated as a perfect gas. Therefore,

$$C_P^G = R + C_V^G \qquad \ldots (9.4)$$

and

$$C_V^G = C_V(\text{trans}) + C_V(\text{vib}) + C_V(\text{rot}). \qquad \ldots (9.5)$$

At the low temperatures considered here the vibrational contribution $C_v(\text{vib})$ is almost zero, so that

$$C_{P,1}^G \simeq (7/2)\,R = 29.10\,\text{J mol}^{-1}\,\text{K}^{-1}$$

as the molecule is diatomic. The resultant value

$$\Delta H_{v,1}\,(182.26\,\text{K}) = 16320\,\text{J mol}^{-1}$$

was used in the calculation. The volume change on vaporization

$$\Delta V_v = V^G - V^L$$

was estimated assuming a virial expansion truncated after the second term, this approach giving

$$\Delta V_{v,1}\,(182.26\,\text{K}) = 20690\,\text{cm}^3\,\text{mol}^{-1}\ .$$

For the expansion coefficient and the isothermal compressibility of pure xenon values of

$$\alpha_{P,2}^* = 2.5 \times 10^{-3}\,\text{K}^{-1}$$

and

$$\kappa_{T,2}^* = 2.2 \times 10^{-3}\,\text{MPa}^{-1}\ ,$$

respectively, were interpolated from reference (12). Again, there are no reported direct determinations of these quantities for pure liquid HCℓ. Fortunately, in 1968, PRICHARD[14], in this laboratory, measured the molar volumes of hydrogen chloride at the saturation vapour pressure as a function of temperature, between 162.44 and 236.50 K, using a pyknometer of about 10 cm^3 capacity. These results are certainly very accurate, making

it possible to estimate α_σ, the expansion coefficient at the saturation vapour pressure. As this pressure is low, a negligible error is introduced by considering the above mentioned value to hold good for the expansion coefficient at constant (zero) pressure, so that

$$\alpha^*_{P,1} \simeq \alpha^*_{\sigma,1} = 2.1 \times 10^{-3}\,K^{-1} .$$

The isothermal compressibility, $\kappa^*_{T,1}$, was estimated from eqn (7.20):

$$\kappa^*_{T,1} \simeq 0.8 \times 10^{-3}\,MPa^{-1} .$$

The experimental results are presented in Table 9.1 in a form which shows *inter alia* the relative importance of the vaporization corrections ($\psi_{6,7}$), and which makes possible the re-calculation of H^E from the experimental measurements if better values later become available for the relevant physical properties of the pure components and the mixture, e.g., the second virial coefficients of the pure and mixed gases at the working temperature. The total (liquid + gas) amount of substance of each component used in the experiments, n_1 and n_2, and the energy required to compensate for the mixing process, Q_H, are also shown in the table, as well as the mole fractions of HCℓ in the liquid and vapour phases, x_1 and y_1, respectively. Since in this case the values of H^E at the saturation pressure of the mixture and at zero pressure are close to each other, calculation indicating that the difference between them is not larger than $0.2\,J\,mol^{-1}$, only the latter, $H^E(0)$, are included in the table. R_H is the enthalpy residual,

$$R_H = H^E_{exp} - H^E_{calc} , \qquad \ldots (9.6)$$

where H^E_{calc} is the excess molar enthalpy calculated from eqn (9.7) below.

The experimental values of $H^E(0)$ fit eqn (9.7), [eqn (7.21)],

$$H^E/RT = x_1(1-x_1)[A_H + B_H(2x_1 - 1) + C_H(2x_1 - 1)^2] \qquad \ldots (9.7)$$

with

TABLE 9.1

EXCESS MOLAR ENTHALPY H^E OF HCℓ + Xe AT 182.26 ± 0.05 K

n_1/mol	n_2/mol	x_1	y_1	Q/J	$\psi_{6,7}$/J	$H^E(0)$/J mol^{-1}	R_H/J mol^{-1}
0.02135	0.04597	0.3201	0.2050	53.397	- 5.943	728.3	- 0.5
0.03672	0.04846	0.4351	0.2192	72.264	- 4.932	808.6	- 2.6
0.03106	0.03237	0.4971	0.2271	55.328	- 5.303	820.4	+ 7.9
0.03393	0.03378	0.5081	0.2286	58.241	- 5.085	809.9	+ 0.2
0.04661	0.03330	0.5902	0.2412	62.758	- 4.099	752.5	- 7.5
0.04122	0.01913	0.6948	0.2634	40.579	- 3.639	633.7	+ 2.6

$$A_H = 2.1430$$

$$B_H = - 0.3178$$

$$C_H = - 0.3654 \ ,$$

the standard deviation being

$$\sigma(H^E) = \pm 6.6 \text{ J mol}^{-1} \ .$$

This represents 0.8% of the estimated value of $H^E(0)$ for the equimolar mixture

$$H^E_{\frac{1}{2}}(0) = 811.9 \text{ J mol}^{-1} \ .$$

By combining the G^E results at 182.26 K of CALADO *et al.*[4] with our calculated curve for H^E at zero pressure, as described in section 7.2, S^E/R is obtained:

$$S^E/R = x_1(1 - x_1)[A_S + B_S(2x_1 - 1) + C_S(2x_1 - 1)^2] \qquad \ldots (9.8)$$

where

$$A_S = 0.3333$$

$$B_S = - 0.2085$$

$$C_S = - 0.5639 \ .$$

The three curves H^E, G^E and TS^E are represented in Fig. 9.1 with the experimental points for $H^E(0)$.

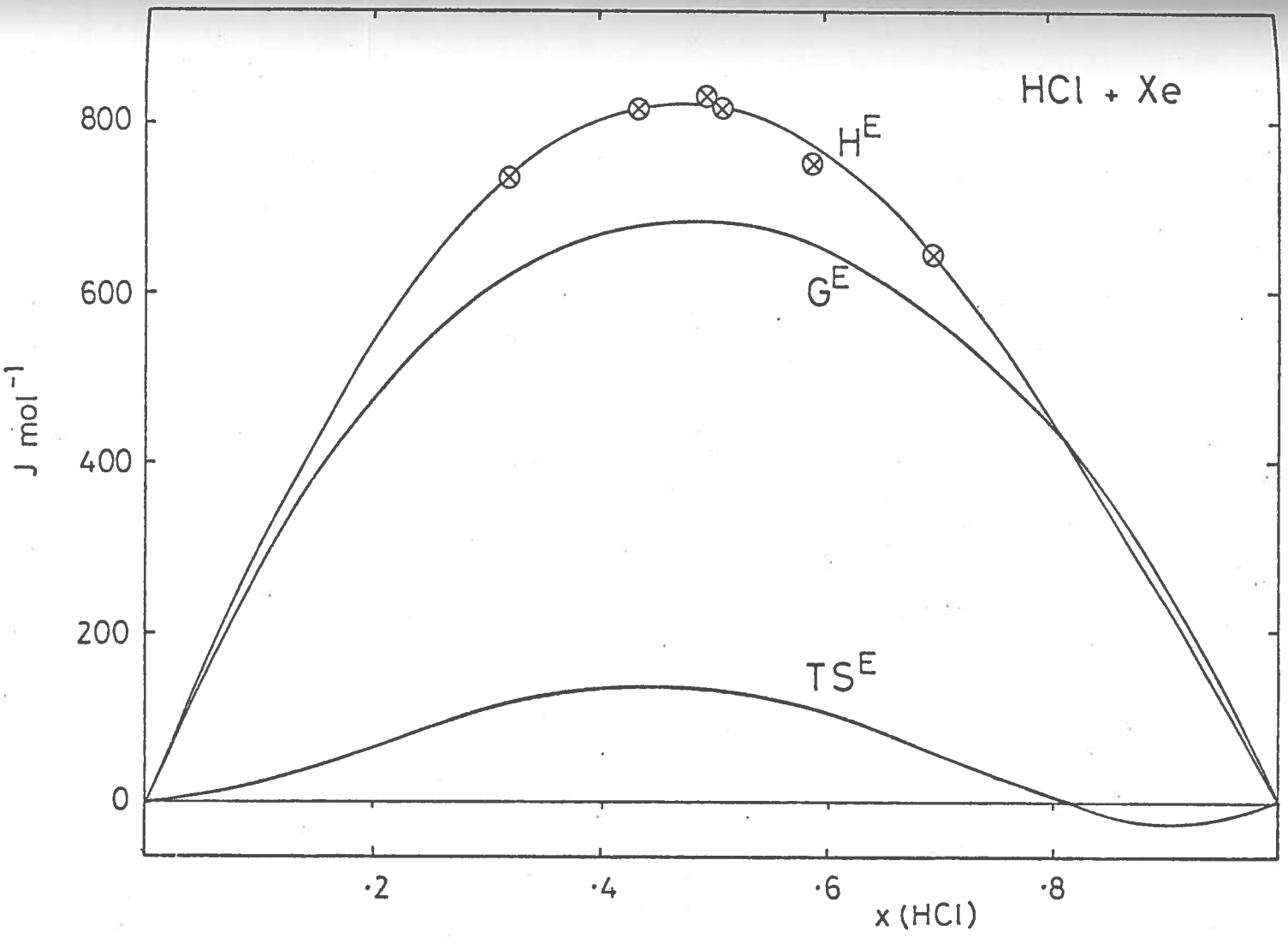

Fig. 9.1

HCℓ + Xe: G^E, H^E and TS^E as functions of composition, at 182.26 K. G^E from Ref. (4).

9.3 DISCUSSION

As already pointed out, too much reliance should not be placed on the shape of the TS^E curve at low and high mole fractions of HCℓ, since this curve is sensitive to the precise shape of the H^E and G^E curves in these regions. Nevertheless there is no doubt that for this system TS^E is relatively small in comparison with H^E and G^E, and over most of the composition range, at least, it is positive. The small S^E suggests that most of the non-ideality of the liquid mixture is due to energy of interaction effects between the molecules rather than to structural factors in the solution.

There are no previous experimental determinations of H^E to compare with the present results for this system. CALADO *et al.*[4], however, having measured G^E at three temperatures — 159.07, 182.26 and 195.42 K — estimated a mean value of $H^E_{\frac{1}{2}}$ over this temperature range. Their figure of $880 \pm 80\ J\ mol^{-1}$ is consistent with the more accurate calorimetric measurement reported here.

GUBBINS and his co-workers studied this system from the theoretical point of view by using perturbation theory. In their first attempt[6] the following model potential was used:

MODEL 'A'

$$\text{Xe} - \text{Xe} \ : \ u = u^{(12,6)}$$
$$\text{HC}\ell - \text{HC}\ell \ : \ u = u^{(12,6)} + u^{\text{mult}}$$
$$\text{Xe} - \text{HC}\ell \ : \ u = u^{(12,6)} + u^{0\ \text{ind}}$$

where $u^{(12,6)}$ is the common (12,6) intermolecular potential. The leading multipole terms in u^{mult} are the dipole-dipole ($u^{\mu\mu}$), dipole-quadrupole ($u^{\mu Q}$), quadrupole-dipole ($u^{Q\mu}$), and quadrupole-quadrupole (u^{QQ}). $u^{0\ \text{ind}}$ is the isotropic part of the potential arising from induction effects (dipole-induced dipole and quadrupole-induced dipole two-body terms).

This approach reproduces almost exactly the experimental values of G^E (and hence the P-x-y curves) at the three temperatures for which results are available. This is remarkable agreement. It should be noted here that a negative correction factor ($k_{12} = -0.0114$) to the geometric-mean Berthelot rule,

$$\varepsilon_{12} = (1 - k_{12})(\varepsilon_{11}\,\varepsilon_{22})^{\frac{1}{2}} , \qquad \ldots (9.9)$$

had to be used, in contrast with the large, positive k_{12} value obtained by CALADO *et al.*[4] on applying the theory of LELAND, ROWLINSON and SATHER[15] to estimate $G^E_{\frac{1}{2}}$. Values of the second virial coefficient of pure HCℓ calculated by using the above mentioned pair potential model[16] do not agree, however, with the recent experimental results of LEUCHS[10].

Since model 'A' was less good, although still reasonable, when applied to estimate the excess volume of the liquid mixture V^E, CLANCY, GUBBINS and GRAY[17] tried to improve the model potential by introducing the leading anisotropic dispersion (u^{dis}) and anisotropic overlap (u^{ov}) potential terms; whence,

MODEL 'B'

$$\text{Xe - Xe} \;:\; u = u^{(12,6)}$$
$$\text{HCℓ - HCℓ} \;:\; u = u^{(12,6)} + u^{mult} + u^{dis} + u^{ov}$$
$$\text{Xe - HCℓ} \;:\; u = u^{(12,6)} + u^{0\,ind} + u^{ov} .$$

This yielded only marginal improvement in the predicted V^E, while agreement for G^E remained excellent. Correction factors $k_{12} = 0.014$ to the Berthelot rule, and $j_{12} = -0.011$ to the Lorentz arithmetic-mean rule,

$$\sigma_{12} = \tfrac{1}{2}(1 + j_{12})(\sigma_{11} + \sigma_{22}) , \qquad \ldots (9.10)$$

were used.

In a still more recent study[18] CLANCY and GUBBINS applied both potential models, 'A' and 'B', to estimate H^E for the HCℓ + Xe system. Their results are shown in Fig. 9.2 in which the experimental points are

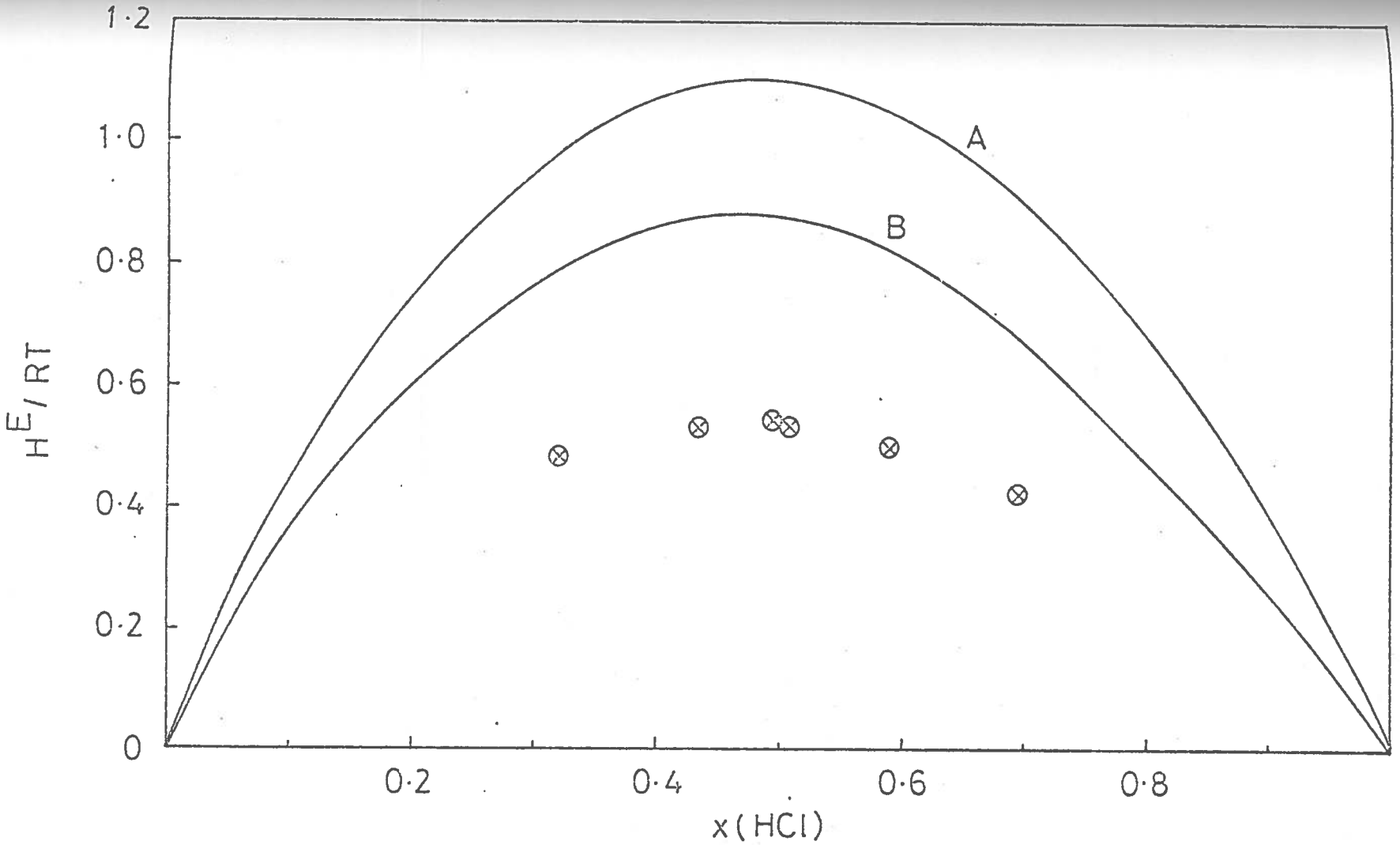

Fig. 9.2

HCℓ + Xe: H^E (182.26 K) as a function of composition. Comparison between theory (A and B) and experiment (circles)

also included. The two models 'A' and 'B' give H^E values that are substantially higher than experiment, model 'A' being high by a factor of about two and model 'B' by about 63%. This illustrates the sensitivity of H^E to the intermolecular potential. The small potential terms u^{dis} and u^{ov}, which have little effect upon V^E, cause now a significant change in H^E.

The discrepancies between theoretical and experimental values of the excess enthalpy can be due to a variety of reasons. The most important of these may be related to the potential model used for the HCℓ-HCℓ interaction, and for Xe-HCℓ as well. In the first case the present lack of thermodynamic data for HCℓ, namely P-V-T results for the pure liquid in the high-pressure region, is certainly a limiting factor which hinders improvement. Both theoretical[19] and computer simulation[20] results have shown recently that multibody induction terms are important in liquids. These were not taken into consideration in models 'A' and 'B'. However, CLANCY and GUBBINS used WERTHEIM's theory[19] to obtain a first estimate of the importance of such multibody induction effects. Following WERTHEIM, these may be estimated by replacing the true (gas-phase) dipole moment μ by a re-normalized (liquid phase) value μ' that takes into account these multibody terms. For pure HCℓ at the conditions of our H^E experiments a ratio of $\mu'/\mu \simeq 1.28$ was obtained neglecting the effect of the HCℓ quadrupole. Using this re-normalized dipole moment in model 'B' (the other parameters being readjusted to fit the properties of pure liquid HCℓ, and G^E and V^E for the mixture) the predicted value of $H^E_{\frac{1}{2}}$ is lowered by about six percent.

Hydrogen bonding in pure liquid HCℓ has not been considered so far and this may also be an important cause for the lack of agreement between theory and experiment.

We may recall here that for the Ar + Kr system the perturbation theory of BARKER and HENDERSON also give values of H^E which are higher than experiment (~ 33% higher for the equimolar mixture), as mentioned in Chapter 8. Since perturbation theories are, at present, the most powerful tool for the treatment of liquid mixtures, these results show how far current theories still are from predicting reliable values of all the excess properties, especially when dipolar liquids are involved.

9.4 REFERENCES

(1) HILL, N., VAUGHAN, W.E., PRICE, A.H. and DAVIES, M. 'Dielectric Properties and Molecular Behaviour', Van Nostrand, London, 1969, p.236.

(2) STOGRYN, D.E. and STOGRYN, A.P., Mol. Phys., 1966, 11, 371.

(3) GUBBINS, K.E. and TWU, C.-H., Communication to the Engineering Foundation Conference on the Estimation and Correlation of Phase Equilibria and Fluid Properties in the Chemical Industry, Pacific Grove, California, U.S.A., 1977.

(4) CALADO, J.C.G., KOZDON, A.F., MORRIS, P.J., da PONTE, M.N., STAVELEY, L.A.K. and WOOLF, L.A., J. Chem. Soc. Faraday I, 1975, 71, 1372.

(5) CHAMBERS, M.V. and McDONALD, I.R., Mol. Phys., 1975, 29, 1053.

(6) CALADO, J.C.G., GRAY, C.G., GUBBINS, K.E., PALAVRA, A.M.F., SOARES, V.A.M., STAVELEY, L.A.K. and TWU, C.-H., J. Chem. Soc. Faraday I, 1978, 74, 893.

(7)(a) TWU, C.-H., GUBBINS, K.E. and GRAY, C.G., Mol. Phys., 1975, 29, 713.

(b) FLYTZANI-STEPHANOPOULOS, M., GUBBINS, K.E. and GRAY, C.G., Mol. Phys., 1975, 30, 1649.

(c) TWU, C.-H., GUBBINS, K.E. and GRAY, C.G., J. Chem. Phys., 1976, 64, 5186.

(8)(a) LEONARD, P.J., HENDERSON, D. and BARKER, J.A., Trans. Faraday Soc., 1970, 66, 2439.

(b) SINGER, J.V.L. and SINGER, K., Mol. Phys., 1970, 19, 279.

(9) BREWER, J., 'Determination of Mixed Virial Coefficients', AFOSR No. 67-2795 (1967).

(10) LEUCHS, U., private communication (1978).

(11) GLOCKLER, G., ROE, C.P. and FULLER, D.L., J. Chem. Phys., 1933, 1, 703.

(12) STREETT, W.B., SAGAN, L.S. and STAVELEY, L.A.K., J. Chem. Thermodynamics, 1973, 5, 633.

(13) GIAUQUE, W.F. and WIEBE, R., J. Am. Chem. Soc., 1928, 50, 101.

(14) PRICHARD, P.C., 'A Comparison of Some Thermodynamic Properties of Some Simple Isotopic Compounds', (Part II) Thesis, University of Oxford (1968).

(15) LELAND, T.W., ROWLINSON, J.S. and SATHER, G.A., Trans. Faraday Soc., 1968, 64, 1447.

(16) GUBBINS, K.E., private communication (1977).

(17) CLANCY, P., GUBBINS, K.E. and GRAY, C.G., Faraday Disc., 1979, 66, in press.

(18) LOBO, L.Q., STAVELEY, L.A.K., CLANCY, P. and GUBBINS, K.E., J. Chem. Soc. Faraday II, 1979, submitted for publication.

(19)(a) WERTHEIM, M.P., Mol. Phys., 1973, 26, 1425.

(b) WERTHEIM, M.P., Mol. Phys., 1977, 34, 1109.

(20) PATEY, G.N. and VALLEAU, J.P., Chem. Phys. Lett., 1976, 42, 407.

CHAPTER 10

THE SYSTEM XENON + NITROUS OXIDE

10.1 INTRODUCTION

The previous Chapter dealt with the system xenon + hydrogen chloride and hence was largely concerned with the influence of a dipole in the polar species. Here we present the results of an experimental study of the system xenon + nitrous oxide (dinitrogen oxide, N_2O), selected to serve as a model for mixtures of the type non-polar molecules + quadrupolar molecules.

Other systems of this type have already been investigated. In most of these the quadrupole moment Q in the polar molecule is very small as in the case of mixtures involving one of the rare gases and a homonuclear diatomic species (usually O_2 or N_2) or in those for which the latter is replaced by ethane. The only systems in this class for which Q may be significantly larger are those involving ethylene as one component, namely $Kr + C_2H_4$ [1] and $Xe + C_2H_4$ [2]. However, H^E has not yet been measured for xenon + ethylene, and there is still some uncertainty about the true value of the quadrupole moment of ethylene [3,4].

It was therefore clearly desirable to choose as the polar component in our model system a compound with a relatively large quadrupole moment. A suitable choice might seem to be carbon dioxide, but the relatively high triple-point temperature [5,6] (T_t = 216.58 K) and pressure [7,8] (P_t = 517.98 kPa) of this substance rule it out on practical grounds, at least as far as studies of a mixture with a rare gas are concerned. The molecule of nitrous oxide has a quadrupole moment [3] ($Q = -3.0 \times 10^{-26}$ esu cm^2 $= -10.0 \times 10^{-40}$ C m^2) which is not much smaller than that of carbon dioxide [3] ($Q = -4.3 \times 10^{-26}$ esu cm^2 $= -14.3 \times 10^{-40}$ C m^2), and though it has a dipole moment, this is so small [3] (μ = 0.166 D = 0.55×10^{-30} C m) that

one would expect from what is known of the relation between the magnitude of a dipole moment and its effect on the bulk properties of a mixture that the influence of the *dipole* moment of N_2O on the properties of the $Xe + N_2O$ system would be negligible.

10.2 DETERMINATION OF G^E, V^E and H^E

G^E and V^E were determined at the triple-point temperature of nitrous oxide (T_t = 182.32 K) and H^E at a slightly higher temperature (184.05 K), since attempts to measure H^E at the triple-point of one of the two components might present experimental difficulties owing to the partial solidification of that component.

As mentioned before, in the evaluation of G^E, V^E and H^E from the actual experimental measurements, values of certain physical properties must be adopted, and it will be convenient to summarize these here and to indicate their source. Nitrous oxide will be referred to as component 1 throughout this Chapter, and xenon as component 2.

The value of 182.26 K reported by BLUE and GIAUQUE[9] for the triple-point of N_2O was estimated[6,10] to be equivalent to 182.32 K on IPTS - 68, using the method described in Chapter 17.

The molar volumes and vapour pressures of the pure liquids were measured using the apparatus and techniques described earlier in this thesis. The value

$$V_1^*(182.32\,K) = 35.487 \pm 0.002\,cm^3\,mol^{-1}$$

obtained for N_2O at its own triple-point temperature is the average of six independent determinations. There are no values of similar accuracy to compare with. (Cf. 35.80 $cm^3\,mol^{-1}$, reference (11); and 35.46 $cm^3\,mol^{-1}$, as extrapolated from density results in reference (12).) Three determinations of the molar volume of xenon at the same temperature gave

$$V_2^*\,(182.32\,K) = 46.453 \pm 0.010\,cm^3\,mol^{-1}\ .$$

This can be compared with $46.409\,cm^3\,mol^{-1}$ from the work of THEEUWES and BEARMAN[13], and $46.534\,cm^3\,mol^{-1}$ as obtained by TERRY *et al.*[14].

The triple-point pressure of N_2O has already been discussed, in section 2.3.4. For xenon, our measured value of the pressure is

$$P_2^*\,(182.32\,K) = 247.742\,kPa\ .$$

The corresponding values interpolated from the results of MICHELS and WASSENAAR[15], and THEEUWES and BEARMAN[13] are 247.434 and 247.306 kPa, respectively. The differences between these figures and ours are covered by a difference of $\sim 0.03\,K$ in the temperature scales.

The second virial coefficient B for N_2O at room temperature was taken from the work of COUCH *et al.*[16] and SCHAMP *et al.*[17], namely

$$B_{11}\,(298.15\,K) = -133.2\,cm^3\,mol^{-1}\ .$$

B_{11} at low-temperature was calculated to be

$$B_{11}\,(182.32\,K) = -400\,cm^3\,mol^{-1}$$

from the equation of PITZER and CURL[18]:

$$B = \left[0.1445 - 0.330/T_R - 0.1385/T_R^2 - 0.0121/T_R^3 + \omega\,(0.073 + 0.46/T_R - 0.50/T_R^2 - 0.097/T_R^3 - 0.0073/T_R^8)\right](RT_c/P_c). \qquad \ldots\ (10.1)$$

The acentric factor ω,

$$\omega = -\log\,(P_R)_{T_R = 0.7} - 1.000\ , \qquad \ldots\ (10.2)$$

was estimated as

$$\omega_1 = 0.160$$

from the vapour pressure data of HOGE[19] and the critical constants listed by MATHEWS[20]. For xenon, the necessary B_{22} values were taken from BREWER's report[21] (cf. Chapter 9).

Interpolation from the results of STREETT, SAGAN AND STAVELEY[22] gave

$$\Delta H_{v,2}\ (184.05\ K) = 11930\ J\ mol^{-1}$$

and

$$\Delta V_{v,2}\ (184.05\ K) = 5300\ cm^3\ mol^{-1}\ ,$$

which were used to evaluate the correction term ψ_7 in eqn (7.14). The corresponding values for nitrous oxide,

$$\Delta H_{v,1}\ (184.05\ K) = 16590\ J\ mol^{-1}$$

$$\Delta V_{v,1}\ (184.05\ K) = 16800\ cm^3\ mol^{-1}\ ,$$

were calculated by the method described (for HCℓ) in Chapter 9. The data needed to evaluate $\Delta H_{v,1}$ were taken from reference (9).

Finally, the expansion coefficient and the isothermal compressibility of xenon were interpolated from reference (21), cf. Chapter 9, while for N_2O we used

$$\alpha^*_{P,1} \simeq \alpha^*_{\sigma,1} = 2.1 \times 10^{-3}\ K^{-1}\ ,$$

derived from the density data of LEADBETTER *et al.*[12], and

$$\kappa^*_{T,1} \simeq 0.9 \times 10^{-3}\ MPa^{-1}\ ,$$

estimated from the approximate relationship (7.20).

Nitrous oxide was condensed into the upper chamber of the calorimeter.

10.2.1 *G^E AT 182.32 K*

Table 10.1 gives our results for the excess molar Gibbs energy, G^E, and for the total vapour pressure of the mixture, P, as a function of x_1, the liquid mole fraction of N_2O. R_p are the pressure residuals defined through eqn (5.54). The values in Table 10.1 of y_1, the mole fraction of nitrous oxide in the vapour in equilibrium with the liquid mixture, are calculated.

TABLE 10.1

VAPOUR PRESSURE P AND EXCESS MOLAR GIBBS ENERGY G^E OF N_2O + Xe AT 182.32 K.

x_1	y_1	P/kPa	R_P/Pa	G^E/J mol^{-1}
0.0000	0.0000	247.742	-	0
0.0928	0.0906	249.539	+ 84	149.6
0.1914	0.1546	246.745	+ 1	274.3
0.3099	0.2080	240.267	- 56	378.7
0.4384	0.2521	231.168	+ 172	436.3
0.5662	0.2950	218.731	- 284	433.2
0.7516	0.3813	191.942	+ 223	335.9
0.8557	0.4805	163.939	- 92	226.4
0.9227	0.6071	136.379	- 17	113.7
1.0000	1.0000	87.866	-	0

The system is markedly non-ideal, forming a positive azeotrope which is not far from being a tangent azeotrope. The P - x - y curve is represented in Fig. 10.1.

A three-term Redlich-Kister equation was found to be adequate for G^E, namely

$$G^E/RT = x_1(1-x_1)\left[A_G + B_G(2x_1 - 1) + C(2x_1 - 1)^2\right] \quad \ldots (10.3)$$

with

$$A_G = 1.1829 \qquad (\sigma_A = 0.0015)$$

$$B_G = 0.0532 \qquad (\sigma_B = 0.0028)$$

$$C_G = 0.0425 \qquad (\sigma_C = 0.0056) ,$$

the σ_I being the standard deviations of the parameters. For the equimolar mixture,

$$G^E_{\frac{1}{2}} = 448.2 \pm 0.6 \text{ J mol}^{-1} .$$

The experimental points and the G^E curve calculated from eqn (10.3) are represented in Fig. 10.2 as a function of composition. The meaning of the remaining curves in this figure is given in section 10.2.3.

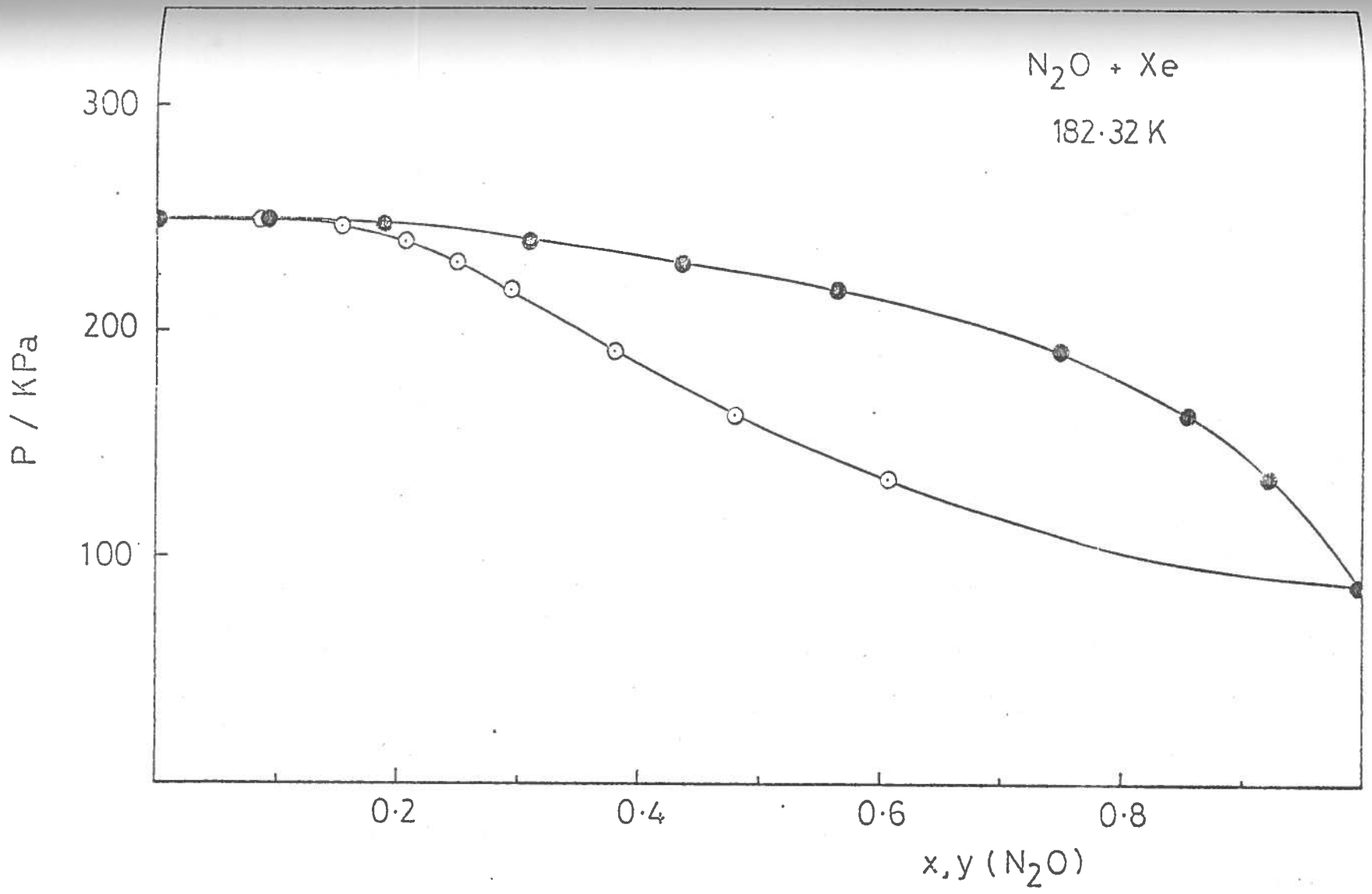

Fig. 10.1 - N_2O + Xe: P - x - y diagram at 182.32 K

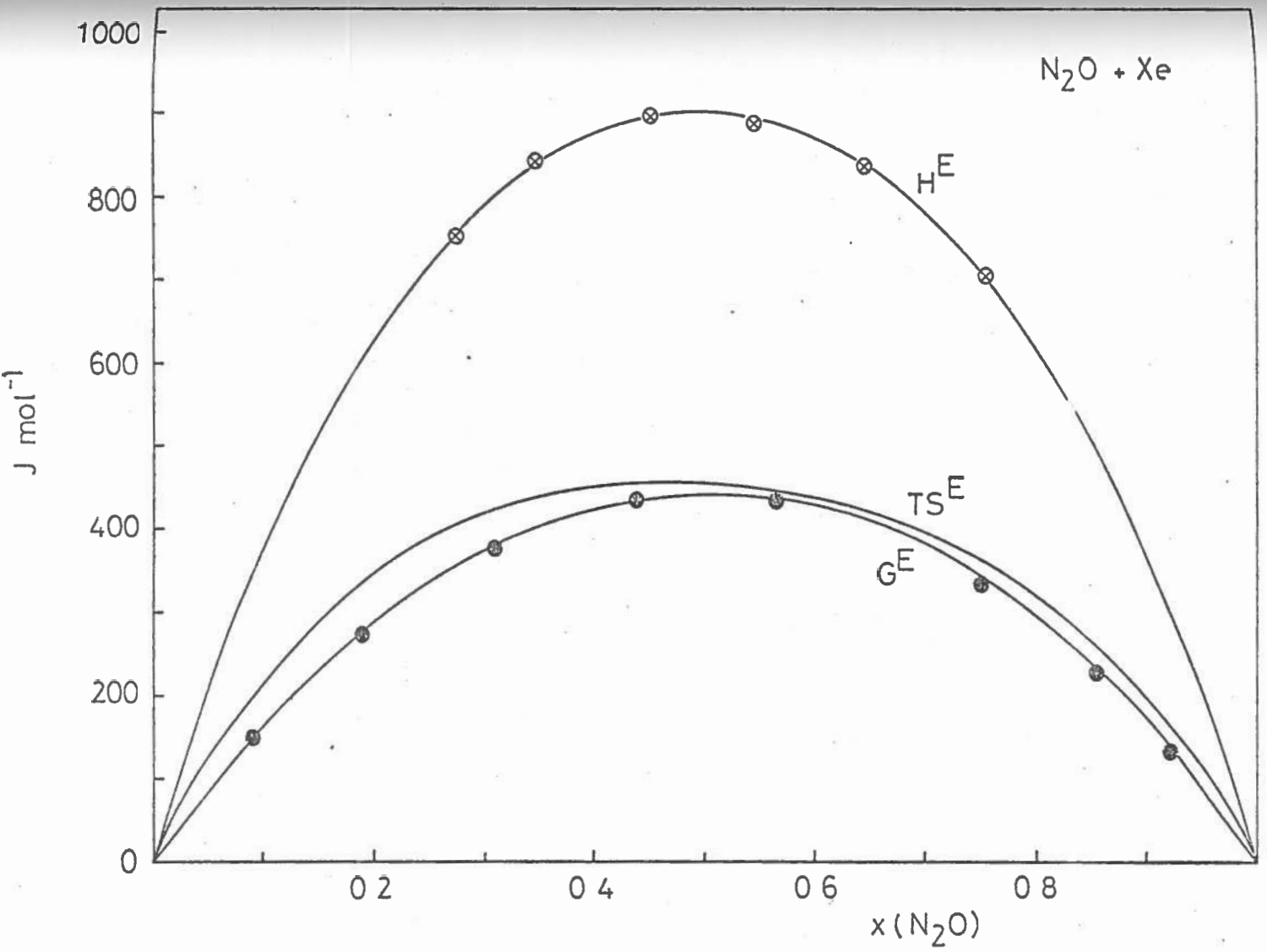

Fig. 10.2

$N_2O + Xe$: G^E (182.32 K), H^E (184.05 K) and $TS^E = H^E - G^E$ as functions of composition .

10.2.2 *V^E AT 182.32 K*

The molar volumes of mixtures of known composition and the derived values of V^E are recorded in Table 10.2. These values of V^E refer to mixing at the saturation vapour pressure. (The difference from the values at zero pressure is negligible.) They fit the equation, [eqn (6.7)],

$$V^E = x_1 (1 - x_1) \left[A_V + B_V (2 x_1 - 1) + C_V (2 x_1 - 1)^2 \right] \qquad \ldots (10.4)$$

with

$$A_V = 2.617 \text{ cm}^3 \text{ mol}^{-1}$$

$$B_V = -0.878 \text{ cm}^3 \text{ mol}^{-1}$$

$$C_V = 0.100 \text{ cm}^3 \text{ mol}^{-1} \ ,$$

the standard deviation of this fitting being

$$\sigma(V^E) = \pm 0.006 \text{ cm}^3 \text{ mol}^{-1} \ .$$

For the equimolar mixture,

$$V^E_{\frac{1}{2}} = 0.654 \text{ cm}^3 \text{ mol}^{-1}$$

R_V in Table 10.2 is defined by eqn (6.8).

TABLE 10.2

MOLAR VOLUME V AND EXCESS MOLAR VOLUME V^E OF $N_2O + Xe$ AT 182.32 K

x_1	$V/\text{cm}^3 \text{ mol}^{-1}$	$V^E/\text{cm}^3 \text{ mol}^{-1}$	$R_V/\text{cm}^3 \text{ mol}^{-1}$
0.0000	46.453	0	-
0.1528	45.206	0.428	+ 0.004
0.2848	43.942	0.611	- 0.003
0.3922	42.821	0.669	- 0.001
0.5032	41.589	0.653	+ 0.000
0.6394	39.988	0.547	- 0.002
0.7725	38.371	0.390	+ 0.009
0.8927	36.853	0.190	- 0.000
0.9101	36.624	0.151	- 0.010
1.0000	35.487	0	-

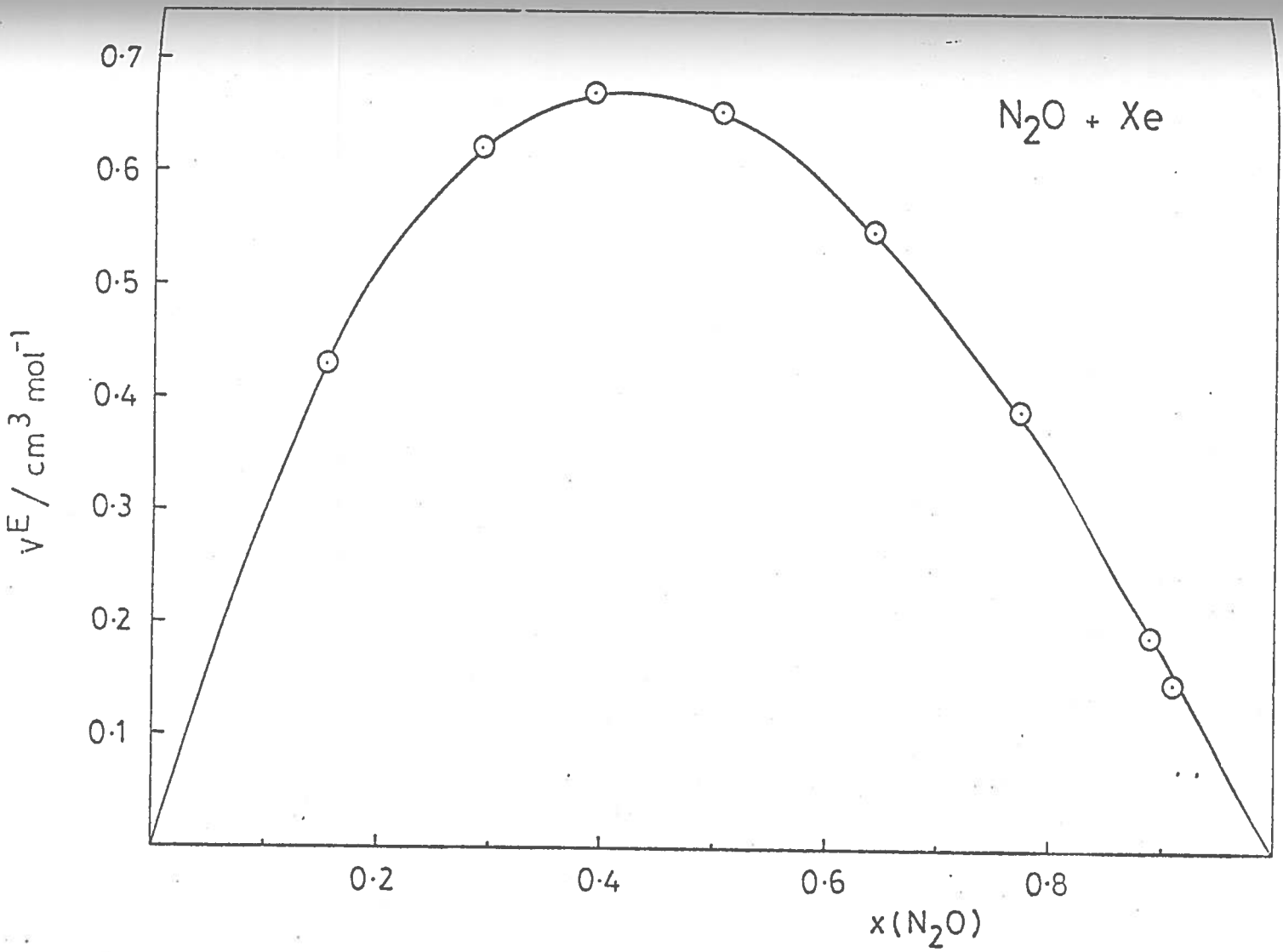

Fig. 10.3

N_2O + Xe: V^E (182.32 K) as a function of composition

The experimental V^E points are represented in Fig. 10.3 together with the curve calculated from eqn (10.4).

10.2.3 *H^E AT 184.05 K*

The experimental results for H^E at 184.05 ± 0.01 K are represented in Table 10.3 in the form adopted in Chapter 9. The values of H^E have been calculated both for mixing at the saturation vapour pressure of the mixture, $H^E(P_m)$, and at zero pressure, $H^E(0)$. As the vapour pressures under the prevailing experimental conditions were comparatively low, the differences $H^E(P_m) - H^E(0)$ are very small, in no case exceeding 0.2 J mol^{-1}.

The $H^E(0)$ values fit the equation

$$H^E/RT = x_1 (1 - x_1)\left[A_H + B_H (2 x_1 - 1) + C_H (2 x_1 - 1)^2\right] \quad \ldots (10.5)$$

with

$$A_H = 2.3574$$

$$B_H = -0.0273$$

$$C_H = 0.5827 \ ,$$

the standard deviation being

$$\sigma(H^E) = \pm 5.5 \text{ J mol}^{-1} \ .$$

For the equimolar mixture

$$H^E_{\frac{1}{2}}(0) = 901.8 \text{ J mol}^{-1} \ .$$

Finally, the values of S^E at 182.32 K, derived on the assumption that H^E at this temperature is not significantly different from that at 184.05 K, conform to the equation

$$S^E/R = x_1 (1 - x_1)\left[A_S + B_S (2 x_1 - 1) + C_S (2 x_1 - 1)^2\right] , \quad \ldots (10.6)$$

with

$$A_S = 1.1747$$

$$B_S = -0.0805$$

$$C_S = 0.5402 \ .$$

For the equimolar mixture,

$$TS^E_{\frac{1}{2}} = 453.6 \text{ J mol}^{-1} \ .$$

TABLE 10.3

EXCESS MOLAR ENTHALPY H^E OF N_2O + Xe AT 184.05 ± 0.01 K

n_1/mol	n_2/mol	x_1	y_1	Q/J	$\psi_{6,7}$/J	$H^E(0)$/J mol^{-1}	R_H/J mol^{-1}
0.02052	0.05347	0.2750	0.1925	58.533	- 3.114	753.9	- 5.0
0.02347	0.04439	0.3442	0.2206	59.847	- 2.903	842.7	+ 6.0
0.04012	0.04836	0.4513	0.2591	81.273	- 1.910	898.8	+ 2.4
0.04753	0.03909	0.5455	0.2920	78.297	- 1.239	890.7	- 4.6
0.04301	0.02287	0.6469	0.3317	55.889	- 0.693	838.1	- 0.7
0.04734	0.01451	0.7562	0.3906	43.114	+ 0.658	706.1	+ 1.8

In Fig. 10.2 H^E and TS^E are plotted against the mole fraction of N_2O. The curves are calculated from eqns (10.5) and (10.6) respectively.

10.3 DISCUSSION

Since Xe + N_2O and Xe + C_2H_4 are mixtures for which the interaction between non-polar and quadrupolar molecules may be relevant, it is interesting to compare the experimental values of the excess thermodynamic functions of the two systems. CALADO and SOARES[2] reported values of $G^E_{\frac{1}{2}}$ and $V^E_{\frac{1}{2}}$ for Xe + C_2H_4 at 161.38 K of 145.4 J mol^{-1} and 0.346 cm^3 mol^{-1}, respectively. A value of $H^E_{\frac{1}{2}} \simeq 220$ J mol^{-1} was also predicted[1] for this system. The corresponding experimental results obtained for Xe + N_2O at 182.32 K show that all three excess functions are higher than for Xe + C_2H_4. Even taking into account the different temperatures at which the determinations for the two systems were made, the smaller G^E and H^E values found in the first case suggest that the true quadrupole moment of ethylene may be lower than that of nitrous oxide, so that the value $Q(C_2H_4) = 1.5 \times 10^{-26}$ esu cm^2 = 5.0×10^{-40} C m^2, experimentally obtained by induced birefringence[3], may perhaps be preferred to the higher value of $Q(C_2H_4) = 3.85 \times 10^{-26}$ esu cm^2 = 12.8×10^{-40} C m^2 proposed by SPURLING and MASON[4]. Use of this last

figure in perturbation theory calculations[23,24] gives, however, good estimates for both G^E and V^E of $Xe + C_2H_4$ and other systems. Such simple comparisons may, of course, be questionable since other factors may play an important role. Thus, for example, from the work of GUBBINS, GRAY and their collaborators[25], one might expect quadrupole moments to determine the leading interaction terms, but the shape of the quadrupolar molecules may be very different, as is the case with ethylene and nitrous oxide, and this may also be an important factor.

From simple molecular considerations, one might expect the smaller N_2O molecules to accommodate more easily in the Xe matrix than those of C_2H_4 which are effectively of about the same size as the xenon atoms. However, the order of magnitude of the experimental V^E for the two binary systems is the reverse of this, V^E for $Xe + N_2O$ being large and positive.

Turning now to the comparison between $Xe + N_2O$ and $Xe + HC\ell$, from the qualitative point of view it seems reasonable to expect the first of these two systems to be less non-ideal than the second, since in addition to the quadrupole moment in the polar species (which is higher, in absolute value, for hydrogen chloride than for nitrous oxide[3]), allowance has to be made for the much stronger dipole moment of $HC\ell$. In fact, at the triple-point temperature of N_2O the values of $G^E_{\frac{1}{2}}$ are, respectively, 448.2 and 685.6 $J\,mol^{-1}$ for the two systems. Contrasting with this, however, it is not at all clear why $H^E_{\frac{1}{2}}$ for $Xe + N_2O$ should be still higher than that of $Xe + HC\ell$. Moreover, in the case of $Xe + N_2O$, TS^E is remarkably large, being of the order of magnitude of G^E itself over the entire composition range (Fig. 10.2). As the experiments were carried out at (or near) the triple-point temperature of nitrous oxide, this large S^E suggests that perhaps a considerable amount of local order prevails in pure liquid N_2O at its own triple-point, which is destroyed on the addition of xenon.

(Application of a technique such as inelastic neutron scattering might throw light on this possibility.) Even taking into account that TS^E for Xe + HCℓ will probably become larger at the triple-point temperature of HCℓ (159.01 K) than it is at 182.26 K (cf. Chapter 9), the relatively low absolute values of this function suggest that a comparable degree of order or structure does not exist in liquid HCℓ or, if it does, it is not readily destroyed by the xenon molecules. This may imply that the nature of the intermolecular forces in liquid HCℓ is markedly different from that in N_2O. [There seems to be, in fact, evidence from slow inelastic neutron scattering[26] that zig-zag (90°) association between HCℓ molecules, due to hydrogen bonding, may persist to some extent in the liquid state.]

MACHADO and GUBBINS[27] have recently studied this system by using perturbation theory. [A slightly higher value of $Q(N_2O)$ was adopted[28]: -3.5×10^{-26} esu cm^2 = -11.7×10^{-40} C m^2.] The model potential employed in this case is:

$$\text{Xe} - \text{Xe} \quad : \quad u = u^{(n_2,6)}$$

$$N_2O - N_2O \quad : \quad u = u^{(n_1,6)} + u^{\text{mult}}$$

$$\text{Xe} - N_2O \quad : \quad u = u^{(n_{1,2},6)}$$

where

$$u^{\text{mult}} = u^{\mu\mu} + u^{\mu Q} + u^{QQ}$$

and

$$n_2 = 12 \qquad n_1 = 15 \qquad n_{1,2} = (n_1 n_2)^{\frac{1}{2}} \quad ,$$

the potential parameters for the pure species being

$$N_2O: \quad \varepsilon_1/k = 265.5\ \text{K} \qquad \sigma_1 = 0.3762\ \text{nm}$$

$$\text{Xe} : \quad \varepsilon_2/k = 231.52\ \text{K} \qquad \sigma_2 = 0.3960\ \text{nm} .$$

As usual, n_i, ε_i and σ_i for the two components were obtained by fitting to experimental data on the pure fluids. The subsequent calculation based on this model reproduces our experimental values of V^E and G^E once

deviation parameters to the Lorentz-Berthelot rules of

$$j_{12} = 0.0040$$

$$k_{12} = 0.0133$$

are used. The estimated H^E are then only $\sim 5\%$ in excess of the experimental values. This satisfactory agreement between theory and experiment is interesting. Too few systems have so far been examined to enable us to generalize, but the comparison we have just made raises the possibility that it may be easier to treat with quantitative success systems where the molecules have quadrupoles (or higher multipoles, as we shall see) than those with strongly dipolar molecules.

10.4 REFERENCES

(1) CALADO, J.C.G., da PONTE, M.N., SOARES, V.A.M. and STAVELEY, L.A.K., J. Chem. Thermodynamics, 1978, 10, 35.

(2) CALADO, J.C.G. and SOARES, V.A.M., J. Chem. Thermodynamics, 1977, 9, 911.

(3) STOGRYN, D.E. and STOGRYN, A.P., Mol. Phys., 1966, 11, 371.

(4) SPURLING, T.H. and MASON, E.A., J. Chem. Phys., 1967, 46, 322.

(5) LOVEJOY, D.R., Nature, 1963, 197, 353.

(6) DOUGLAS, T.B., J. Res. Nat. Bur. Std., 1969, 73A, 451.

(7) MEYERS, C.H. and van DUSEN, M.S., J. Res. Nat. Bur. Std., 1933, 10, 381.

(8) MICHELS, A., BLAISSE, B. and HOOGSCHAGEN, J., Physica, 1942, 9, 565.

(9) BLUE, R.W. and GIAUQUE, W.F., J. Am. Chem. Soc., 1935, 57, 991.

(10) HUST, J.G., Cryogenics, 1969, 9, 443.

(11) CLUSIUS, K., PIESBERGEN, U. and VARDE, E., Helv. Chim. Acta, 1960, 43, 1290.

(12) LEADBETTER, A.J., TAYLOR, D.J. and VINCENT, B., Can. J. Chem., 1964, 42, 2930.

(13) THEEUWES, F. and BEARMAN, R.J., J. Chem. Thermodynamics, 1970, 2, 507.

(14) TERRY, M.J., LYNCH, J.T., BUNCLARK, M., MANSELL, K.R. and STAVELEY, L.A.K., J. Chem. Thermodynamics, 1969, 1, 413.

(15) MICHELS, A. and WASSENAAR, T., Physica, 1950, 16, 253.

(16) COUCH, E.J., HIRTH, L.J. and KOBE, A., J. Chem. Eng. Data, 1961, 6, 229.

(17) SCHAMP, W.H., MASON, E.A. and SU, K., Physics Fluids, 1962, 5, 769.

(18) PITZER, K.S. and CURL, R.F., Jr., J. Am. Chem. Soc., 1957, 79, 2369.

(19) HOGE, H.J., J. Res. Nat. Bur. Std., 1945, 34, 281.

(20) MATHEWS, J.F., Chem. Rev., 1972, 72, 71.

(21) BREWER, J., 'Determination of Mixed Virial Coefficients', AFOSR No. 67-2795 (1967).

(22) STREETT, W.B., SAGAN, L.S. and STAVELEY, L.A.K., J. Chem. Thermodynamics, 1973, 5, 633.

(23) CLANCY, P., GUBBINS, K.E. and GRAY, C.G., Faraday Disc., 1979, 66, (in the press).

(24) TWU, C.-H. and GUBBINS, K.E., Chem. Eng. Sci., 1978, 33, 879.

(25)(a) TWU, C.-H., GUBBINS, K.E. and GRAY, C.G., Mol. Phys., 1975, 29, 713.

(b) FLYTZANI-STEPHANOPOULOS, M., GUBBINS, K.E. and GRAY, C.G., Mol. Phys., 1975, 30, 1649

(26) BOUTIN, H. and SAFFORD, G.J., 'Inelastic Scattering of Neutrons, Proc. 4th Symposium', Bombay, 1964, 2, 393.

(27)(a) CLANCY, P. and GUBBINS, K.E., private communication (1979).

(b) MACHADO, J., GUBBINS, K.E., LOBO, L.Q. and STAVELEY, L.A.K., 1976/79, (to be published).

(28) BOULET, C., LACOME, N. and ISNARD, P., Can. J. Phys., 1973, 51. 605.

CHAPTER 11

THE SYSTEM XENON + CARBON TETRAFLUORIDE

11.1 INTRODUCTION

The system which concerns us in this Chapter is one in which the molecules of one component (xenon) are non-polar, while those of the other (carbon tetrafluoride) possess an octupole. Experimental results are already avaialble for systems of this kind, such as $Ar + CH_4$ [1] and $Kr + CH_4$ [2]. However, it is to be expected from the work of TWU, GUBBINS and GRAY[3,4] that the effect of the octupole on the excess thermodynamic functions should rise rapidly with increasing magnitude of the moment. Carbon tetrafluoride, with an octupole moment[5,6] $\Omega(CF_4) = 3.1 \times 10^{-34}$ esu cm^3 = 10.5×10^{-50} C m^3, is therefore a better choice for a model system than methane[6] [$\Omega(CH_4) = 2.1 \times 10^{-34}$ esu cm^3 = 7.0×10^{-50} C m^3], while xenon, having the most polarizable molecule of the stable rare gases, is a better choice for the non-polar component of the mixture than argon or krypton.

We report in this chapter experimental measurements of V^E and H^E for the system $Xe + CF_4$. G^E had recently been measured in this laboratory by Professor D.W. McCLURE[7].

11.2 DETERMINATION OF V^E AND H^E

As mentioned before, it is desirable that when the excess functions are determined the vapour pressures should not be too high, otherwise the corrections which must be made assume greater relative importance and it may not be possible to make them with the desired reliability if, as is so often the case, accurate values of some of the auxiliary properties, namely low-temperature virial coefficients, are not available. Because of this McCLURE measured G^E at the triple-point of HCℓ, at which temperature the vapour pressure of the more volatile component, CF_4, is 244.500 kPa. We

have chosen to determine V^E at the same temperature. One minor disadvantage of this choice of temperature is that it is a little below the triple-point of xenon, and consequently the molar volume of supercooled liquid xenon has had to be obtained by extrapolation. It was, however, possible to make measurements of liquid mixtures up to a xenon mole fraction of $\simeq 0.91$. The slightly different technique that had to be used in these measurements (section 3.3) proved to be adequate. It may be added that particular attention had to be paid to thorough mixing of the two components owing to their considerable difference in density.

The H^E measurements could not, of course, be carried out below the triple-point temperature of xenon, and in fact were made at 163.01 ± 0.02 K.

Throughout this Chapter xenon will be designated as component 1, and carbon tetrafluoride as component 2.

11.2.1 *V^E AT 159.01 K*

The average of three independent determinations of the molar volume of pure CF_4 was

$$V_2^* (159.01\ \mathrm{K}) = 57.362 \pm 0.002\ \mathrm{cm^3\ mol^{-1}} .$$

To estimate V^E, the experimental values of the molar volume of eight mixtures covering most of the composition range were calculated from the actual measurements and, together with the molar volume of pure liquid CF_4, adjusted by least squares to polynomials of the form

$$V = \sum_{i=0}^{i \leqslant 7} a_i x_1^i . \qquad \ldots (11.1)$$

The best fitting was obtained for $i = 3$, so that V^E could be adequately represented by the expression

$$V^E = x_1 (1 - x_1) \left[A_V + B_V (2 x_1 - 1) \right] . \qquad \ldots (11.2)$$

Since

$$V^E = V - x_1 V_1^* - (1 - x_1) V_2^* \quad , \qquad \ldots (11.3)$$

the three unknowns, A_V, B_V and V_1^* could be evaluated, the results being

$$A_V = 7.747 \text{ cm}^3 \text{ mol}^{-1}$$

$$B_V = -2.027 \text{ cm}^3 \text{ mol}^{-1}$$

and

$$V_1^* (159.01 \text{ K}) = 44.017 \text{ cm}^3 \text{ mol}^{-1} \quad .$$

The standard deviation of the fitting was

$$\sigma(V^E) = \pm 0.063 \text{ cm}^3 \text{ mol}^{-1} \quad ,$$

V^E for the equimolar mixture being

$$V_{\frac{1}{2}}^E = 1.937 \text{ cm}^3 \text{ mol}^{-1}.$$

The results for the molar volumes of the two pure components can be compared with those derived from the expressions presented by TERRY *et al.*[8]. From this source one obtains for supercooled xenon at 159.01 K a value of 44.082 $\text{cm}^3 \text{ mol}^{-1}$ which is 0.15% higher than our result mentioned above. This difference agrees closely with the comparable figure of 0.17% obtained for liquid xenon at 182.32 K (cf. section 10.2). In the case of CF_4 the value interpolated from the same work is 57.600 $\text{cm}^3 \text{ mol}^{-1}$. However, if, as has been suggested[9,10], the results of TERRY *et al.* are systematically too high by up to 0.4%, and if the value of V_2^* obtained from that source is reduced by 0.4%, the resulting figure of 57.370 $\text{cm}^3 \text{ mol}^{-1}$ is in close agreement with our measured value reported above.

The standard deviation assigned to V^E is somewhat larger than in the other systems reported in this thesis, which may perhaps reflect the difficulty in completely mixing these two particular liquids.

Table 11.1 summarises the results of the volume measurements, while Fig. 11.1 shows the experimental V^E points and the curve calculated from eqn (11.2).

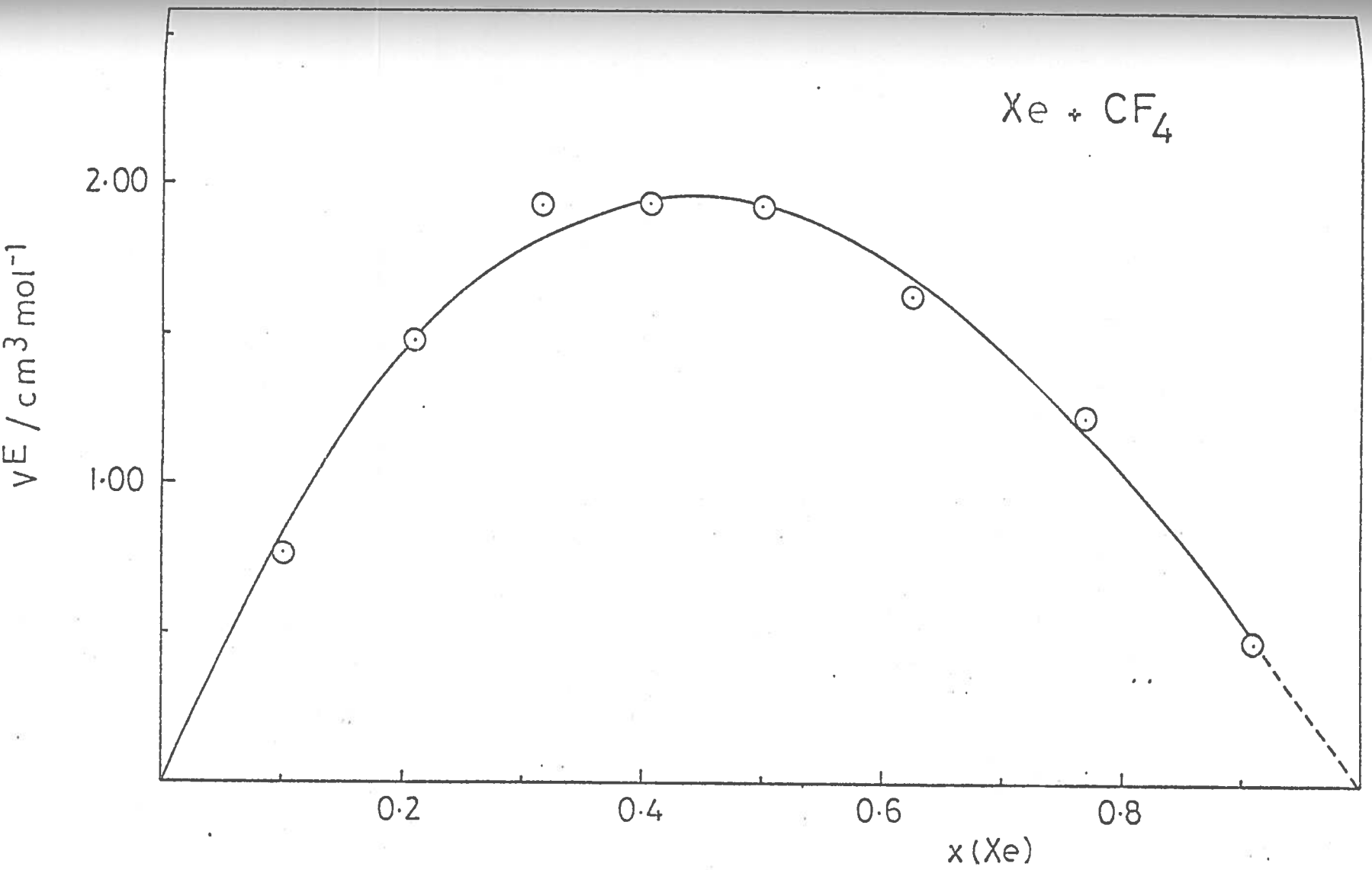

Fig. 11.1

$Xe + CF_4$: V^E (159.01 K) as a function of composition

TABLE 11.1

MOLAR VOLUME V AND EXCESS MOLAR VOLUME V^E OF $Xe + CF_4$ AT 159.01 K

x_1	$V/cm^3\,mol^{-1}$	$V^E/cm^3\,mol^{-1}$	$R_V/cm^3\,mol^{-1}$
0.0000	57.362	0	-
0.1001	56.792	0.765	- 0.078
0.2092	56.048	1.478	+ 0.002
0.3172	55.061	1.932	+ 0.094
0.4077	53.868	1.936	- 0.025
0.5044	52.557	1.926	- 0.006
0.6250	50.652	1.630	- 0.067
0.7716	48.296	1.232	+ 0.061
0.9117	45.670	0.474	- 0.015
(1.0000)	(44.017)[a]	0	-

a - supercooled

11.2.2 *H^E AT 163.01 K*

With regard to the necessary auxiliary data, the second virial coefficient for xenon was taken from BREWER's report[11], wnile for CF_4 we used the results of LANGE and STEIN[12] and of DOUSLIN *et al.*[13]. Since none of these extend to sufficiently low temperatures (the data for xenon stopping at 173.15 K and those for carbon tetrafluoride at 203.15 K), values of B_{11} and B_{22} at our working temperature had to be obtained by extrapolation. Polynomials of the form

$$B/V_c = f(T/T_c) \qquad \ldots (11.4)$$

adjusted to the literature values were used for that purpose, the critical constants being taken from MATHEWS[14] for Xe, and from KUDCHADKER *et al.*[15] for CF_4. Our estimates for the second virial coefficients of the two substances are

$$B_{11}\,(163.01\,K) = -413\,cm^3\,mol^{-1}$$

and

$$B_{22}\,(163.01\,K) = -329\,cm^3\,mol^{-1}\ .$$

We used, again, reference (9) to obtain most of the information needed for Xe :

$$\Delta H_{v,1}\,(163.01\,K) = 12670\ J\ mol^{-1}$$

$$\Delta V_{v,1}\,(163.01\,K) = 14700\ cm^3\ mol^{-1}$$

and

$$\alpha^*_{P,1} = 2.3 \times 10^{-3}\ K^{-1}$$

$$\kappa^*_{T,1} = 1.7 \times 10^{-3}\ MPa^{-1}\ .$$

The enthalpy of vaporization of CF_4 was estimated to be

$$\Delta H_{v,2}\,(163.01\,K) = 10980\ J\ mol^{-1}$$

from the work of SMITH and PACE[16], while a figure of

$$\Delta V_{v,2}\,(163.01\,K) = 4020\ cm^3\ mol^{-1}$$

was obtained in the usual way. The molar volume and expansion coefficient of liquid carbon tetrafluoride were taken from reference (8) corrected as indicated above:

$$V^*_2\,(163.01\,K) = 58.259\ cm^3\ mol^{-1}$$

$$\alpha^*_{P,2} \simeq \alpha^*_{\sigma,2} = 3.9 \times 10^{-3}\ K^{-1}\ .$$

The isothermal compressibility was estimated from eqn (7.20)

$$\kappa^*_{T,2} \simeq 3.8\ \ 10^{-3}\ MPa^{-1}\ .$$

The vapour pressure equation presented in Chapter 17 [see also reference (17)] was used to calculate

$$P^*_2\,(163.01\,K) = 305.058\ kPa\ .$$

The G^E results of McCLURE[7] provided the activity coefficients needed to calculate H^E from the raw calorimetric data.

Xenon was admitted into the upper compartment of the calorimeter.

The results of the determination of H^E are presented in Table 11.2 in the usual way. The differences $H^E(P_m) - H^E(0)$ vary from $0.6\ J\,mol^{-1}$, for the central points, to $0.3\ J\,mol^{-1}$ for the points near the extremes of the diagram.

TABLE 11.2

EXCESS MOLAR ENTHALPY H^E OF $Xe + CF_4$ AT 163.01 ± 0.02 K

n_1/mol	n_2/mol	x_1	y_1	Q/J	$\psi_{6,7}$/J	$H^E(0)$/J mol^{-1}	R_H/J mol^{-1}
0.01649	0.07939	0.1719	0.1789	53.195	- 5.584	507.9	- 18.0
0.02647	0.06768	0.2823	0.2221	77.167	- 4.786	786.1	+ 27.9
0.03544	0.05994	0.3740	0.2446	84.895	- 3.905	867.8	- 17.8
0.03270	0.04784	0.4099	0.2515	77.489	- 4.283	934.6	+ 15.9
0.03500	0.03656	0.4959	0.2643	70.032	- 4.017	953.6	- 5.2
0.04251	0.01845	0.7129	0.2830	48.605	- 2.968	780.8	- 23.6
0.05737	0.00994	0.8680	0.3205	31.346	+ 0.288	487.3	+ 29.3

A two-term Redlish-Kister equation,

$$H^E/RT = x_1 (1 - x_1) \left[A_H + B_H (2 x_1 - 1) \right] , \qquad \ldots (11.5)$$

was found to be adequate for the representation of the concentration dependence of $H^E(0)$, with

$$A_H = 2.8310$$

$$B_H = 0.1597 ,$$

the standard deviation of the fitting being

$$\sigma(H^E) = \pm 25.0 \text{ J mol}^{-1} .$$

For the equimolar mixture,

$$H^E_{\frac{1}{2}}(0) = 959.3 \text{ J mol}^{-1} .$$

Here too the standard deviation is somewhat larger than that in the rest of our calorimetric work, which may again be a consequence of somewhat slower mixing. There was in fact evidence of difficulty in mixing in the temeperature-time traces for all the calorimetric experiments involving this system, even though the cryostat was agitated as vigorously as possible. We may add that this was one of the most endothermic mixing processes

we have encountered in binary liquefied gas systems, and relatively high heating currents, of ~ 40 mA, had to be used.

Finally, assuming that H^E at 159.01 K has the same value as at 163.01 K, a combination of eqn (11.5) with the expression for G^E [7],

$$G^E/RT = x_1 (1 - x_1) \left[A_G + B_G (2 x_1 - 1) + C_G (2 x_1 - 1)^2 \right] \quad \ldots \quad (11.6)$$

where

$$A_G = 1.9504 \pm 0.0040$$

$$B_G = 0.2504 \pm 0.0102$$

$$C_G = 0.2226 \pm 0.0197$$

gives for the excess molar entropy of mixing at 159.01 K the following equation:

$$S^E/R = x_1 (1 - x_1) \left[A_S + B_S (2 x_1 - 1) + C_S (2 x_1 - 1)^2 \right] \quad \ldots \quad (11.7)$$

with

$$A_S = 0.8806$$

$$B_S = -0.0907$$

$$C_S = -0.2226 \ .$$

For the equimolar mixture

$$TS^E_{\frac{1}{2}} = 314.9 \text{ J mol}^{-1} \ .$$

H^E, G^E and TS^E are plotted against the mole fraction of xenon in Fig. 11.2.

11.3 DISCUSSION

CLANCY and GUBBINS, in a yet unpublished study[18], applied perturbation theory to the treatment of the $Xe + CF_4$ system. The potential model is, as before, defined by the following set of expressions:

$$Xe - Xe : \quad u = u^{(n_1,6)}$$

$$CF_4 - CF_4 : \quad u = u^{(n_2,6)} + u^{mult}$$

$$Xe - CF_4 : \quad u = u^{(n_{1,2},6)}$$

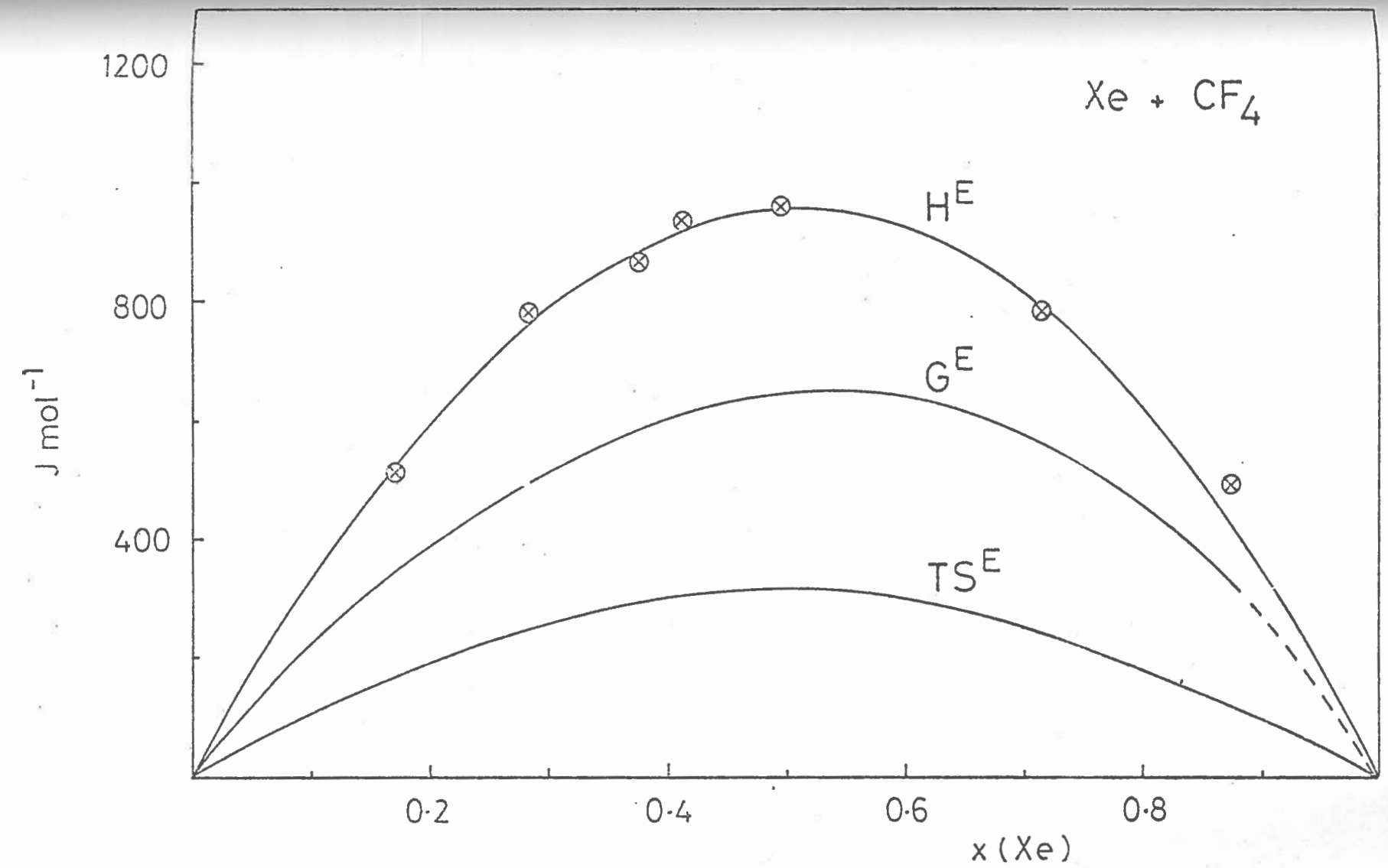

Fig. 11.2

$Xe + CF_4$: G^E (159.01 K), H^E (163.01 K) and $TS^E = H^E - G^E$ as functions of composition. G^E from Ref. (7).

but where now u^{mult} stands for the anisotropic octupole-octupole interaction,

$$u^{mult} = u^{\Omega\Omega} \quad ,$$

and the exponents n_i of the repulsive part of the isotropic pair potential are respectively

$$n_1 = 12 \qquad n_2 = 14 \qquad n_{1,2} = (n_1 n_2)^{\frac{1}{2}} \quad .$$

The potential parameters for the intermolecular potential of the two pure species are

$$\text{Xe} : \quad \varepsilon_1/k = 231.52\,\text{K} \qquad \sigma_1 = 0.3960\ \text{nm}$$

$$CF_4 : \quad \varepsilon_2/k = 206.72\,\text{K} \qquad \sigma_2 = 0.4196\ \text{nm} \quad .$$

The deviation parameters were adjusted so as to reproduce the experimental values of $V^E_{\frac{1}{2}}$ and $G^E_{\frac{1}{2}}$, this giving

$$j_{12} = 0.0105$$

$$k_{12} = 0.1180 \quad .$$

The estimated excess molar enthalpy $H^E_{\frac{1}{2}}$ is, then, $\sim 8\%$ higher than our experimental value, which may be regarded as an encouraging result if one considers the simple form of the potential model used.

It should be noted that the theoretical treatment of systems involving CF_4 is somewhat handicapped by the inadequacy of the information at present available on the density of the pure liquid (no measurements appear to have been made above ~ 185 K), which is required if one is to get the 'best' value of the set of parameters (n, ε, σ) of the pair potential. [The availability of vapour pressure data may help to some extent to overcome this difficulty (Chapter 17).]

Another factor that also has caused some uncertainty in the theoretical studies of systems of which CF_4 is one component, concerns the actual value of its octupole moment. In fact, several values lying in the range 3.1 to 7.9×10^{-34} esu cm^3 have been reported[3,5,6]. This seems to

be mainly a consequence of the lack of suitable direct methods for the experimental determination of Ω. [Some of the discrepancies are due to the different definitions adopted by the authors for this quantity, but it is, of course, possible to convert values from different conventions into each other[19,20].] In the above mentioned theoretical treatment of $Xe + CF_4$ the value of $\Omega\ (CF_4)$ recently proposed by BIRNBAUM and COHEN[5,6] was adopted, since it gave the best agreement with the properties of liquid carbon tetrafluoride.

11.4 REFERENCES

(1) KIDNAY, A.J., LEWIS, K.L., CALADO, J.C.G. and STAVELEY, L.A.K. J. Chem. Thermodynamics, 1975, 7, 847.

(2) CALADO, J.C.G. and STAVELEY, L.A.K., Trans. Faraday Soc., 1971, 67, 1261.

(3) TWU, C.-H., GUBBINS, K.E. and GRAY, C.G., Mol. Phys., 1975, 29, 713.

(4) TWU, C.-H., 'Perturbation Theory for High Pressure Behaviour of Liquid Mixtures', (PH.D.) Thesis, University of Florida, 1976.

(5) BIRNBAUM, G. and COHEN, E.R., Mol. Phys., 1976, 32, 161.

(6) COHEN, E.R. and BIRNBAUM, G., J. Chem. Phys., 1977, 66, 2443.

(7) CLANCY, P., GUBBINS, K.E., LOBO, L.Q., McCLURE, D.W. and STAVELEY, L.A.K., 1975/79 (to be published).

(8) TERRY, M.J., LYNCH, J.T., BUNCLARK, M., MANSELL, K.R. and STAVELEY, L.A.K., J. Chem. Thermodynamics, 1969, 1, 413.

(9) STREETT, W.B., SAGAN, L.S., and STAVELEY, L.A.K., J. Chem. Thermodynamics, 1973, 5, 633.

(10) da PONTE, M.N., STREETT, W.B. and STAVELEY, L.A.K., J. Chem. Thermodynamics, 1978, 10, 151.

(11) BREWER, J., 'Determination of Mixed Virial Coefficients', AFOSR No. 67-2795 (1967).

(12) LANGE, H.B., Jr. and STEIN, F.P., J. Chem. Eng. Data, 1970, 15, 56.

(13) DOUSLIN, D.R., HARRISON, R.H., MOORE, R.T. and McCULLOUGH, J.P., J. Chem. Phys., 1961, 35, 1357.

(14) MATHEWS, J.F., Chem. Rev., 1972, 72, 71.

(15) KUDCHADKER, A.P., ALANI, G.H. and ZWOLINSKI, B.J., Chem. Rev., 1968, 68, 659.

(16) SMITH, J.H. and PACE, E.L., J. Phys. Chem., 1969, 73. 4232.

(17) LOBO, L.Q. and STAVELEY, L.A.K., Cryogenics, 1979, 19, (in the press).

(18) CLANCY, P. and GUBBINS, K.E., private communication (1979).

(19) STOGRYN, D.E. and STOGRYN, A.P., Mol. Phys., 1966, 11, 371.

(20) GRAY, C.G., Can. J. Phys., 1968, 46, 135.

CHAPTER 12

THE SYSTEM XENON + HEXAFLUOROETHANE

12.1 INTRODUCTION

CALADO and AZEVEDO[1] have recently investigated the thermodynamic properties of binary liquid mixtures of ethane with argon, krypton and xenon. The excess Gibbs energy G^E and the excess enthalpy H^E for the $Ar + C_2H_6$ system had already been measured[2] at 90.2 K, both quantities proving to be large and positive. Indeed, at 90 K this last system is probably not far from an upper critical solution temperature. For $Kr + C_2H_6$ at 115.77 K, CALADO and AZEVEDO found that G^E and H^E, while still positive, are much smaller than for $Ar + C_2H_6$ at 90.2 K. For $Xe + C_2H_6$ at 161.38 K, however, G^E is negative over the whole range of composition. The volume change on mixing, V^E, was also found to be negative for this system. But perhaps their most surprising observations was that H^E, measured by AZEVEDO in the calorimeter described in Chapter 4 of this thesis, is also negative, and in fact of such a magnitude that S^E, the excess molar entropy, is negative as well. Thus, for the mixing of liquid xenon and liquid ethane, all four excess functions are negative. Such behaviour has often been regarded as evidence of 'association'. It can be encountered, for example, on mixing two liquids between the molecules of which hydrogen-bonding occurs. While there is no very obvious reason why the xenon and ethane molecules should associate with each other, the ethane molecule has a quadrupole moment[3], $Q(C_2H_6) = -0.65 \times 10^{-26}$ esu cm^2 $= -2.2 \times 10^{-40}$ C m^2, and the xenon molecule has a relatively high polarizability, so that the intermolecular attraction due to dispersion forces must be augmented by quadrupole-induced dipole interaction. The same, of course, can be said of some other liquefied mixtures already studied, for which there is no evidence of 'association'. However, it is possible that the relative dimensions of

the Xe and C_2H_6 molecules and the shape of the latter permit relatively close approach of the rare gas atom to the effective charge sites in an ethane molecule. Since for practical purposes it is not possible to replace xenon by a still more polarizable monatomic substance, it seemed worthwhile to exchange the ethane for a compound with a non-polar molecule of similar shape but with a larger quadrupole moment than C_2H_6. The obvious choice seemed to be hexafluoroethane. The quadrupole moment of the C_2F_6 molecule does not appear to have been measured, but as the C-F bond is more polar than the C-H bond, $Q(C_2F_6)$ should be larger than $Q(C_2H_6)$. Of course, the replacement of C_2H_6 by C_2F_6 necessarily means a change in other factors as well. For instance, the average distance between a xenon atom and a hexafluorethane molecule must be larger than that between a xenon molecule and one of ethane. Nevertheless, the comparison of the thermodynamic properties of the two systems seemed worth making, and we report in this chapter the results of the measurements of H^E at 175.00 ± 0.05 K for this system. The experiments were carried out in collaboration with S.C. ALDERSLEY who also measured[4] G^E and V^E for this mixture at the triple-point temperature of C_2F_6 (173.08 K).

12.2 DETERMINATION OF H^E AT 175.00 K

Throughout this chapter, hexafluoroethane will be designated by component 1, and xenon by component 2. C_2F_6 was admitted into the upper compartment of the calorimeter.

In the evaluation of H^E from the actual calorimetric measurements, values of the second virial coefficient B_{22} for xenon were derived from Brewer's report[5], and those for hexafluoroethane, B_{11}, were obtained by a short extrapolation from the work of PACE and ASTON[6]:

$$B_{11}\ (175.00\ K) = -900\ cm^3\ mol^{-1}$$

$$B_{22}\ (175.00\ K) = -361\ cm^3\ mol^{-1}$$

As regards the remaining auxiliary data, those for xenon were interpolated from reference (7), while the values of the required properties of C_2F_6 were taken (or estimated in the usual way) from reference (6); namely:

$$\Delta H_{v,1}\,(175.00\,K) = 17150\,J\,mol^{-1}$$
$$\Delta H_{v,2}\,(175.00\,K) = 12260\,J\,mol^{-1}\ .$$

The necessary activity coefficients were derived from the G^E curve obtained by ALDERSLEY[4], the excess molar volume V^E being taken from the same reference.

The values of the excess molar enthalpy H^E are recorded, in the usual form, in Table 12.1. For no mixture did the difference between $H^E(P_m)$, for mixing at the saturation vapour pressure of the mixture, and for mixing at zero pressure, $H^E(0)$, exceed $0.3\,J\,mol^{-1}$, which is well within the experimental error.

TABLE 12.1

EXCESS MOLAR ENTHALPY H^E OF $C_2F_6 + Xe$ AT $175.00 \pm 0.05\,K$

n_1/mol	n_2/mol	x_1	y_1	Q/J	$\psi_{6,7}$/J	$H^E(0)$/J mol^{-1}	R_H/J mol^{-1}
0.02549	0.09178	0.2167	0.1060	55.007	- 2.394	449	- 9
0.02021	0.04076	0.3326	0.1132	53.367	- 4.514	810	+ 12
0.03674	0.04644	0.4407	0.1196	85.554	- 0.075	1030	+ 10
0.04501	0.04708	0.4867	0.1233	94.793	+ 2.028	1052	- 18
0.04221	0.02993	0.5841	0.1345	75.793	+ 1.085	1071	- 3
0.03425	0.01665	0.6752	0.1513	48.784	- 0.699	957	+ 5

The $H^E(0)$ values fit the equation

$$H^E/RT = x_1(1-x_1)\left[A_H + B_H(2x_1 - 1) + C_H(2x_1 - 1)^2\right] \qquad \ldots (12.1)$$

with

$$A_H = 2.9654$$
$$B_H = 0.7798$$
$$C_H = -2.0862$$

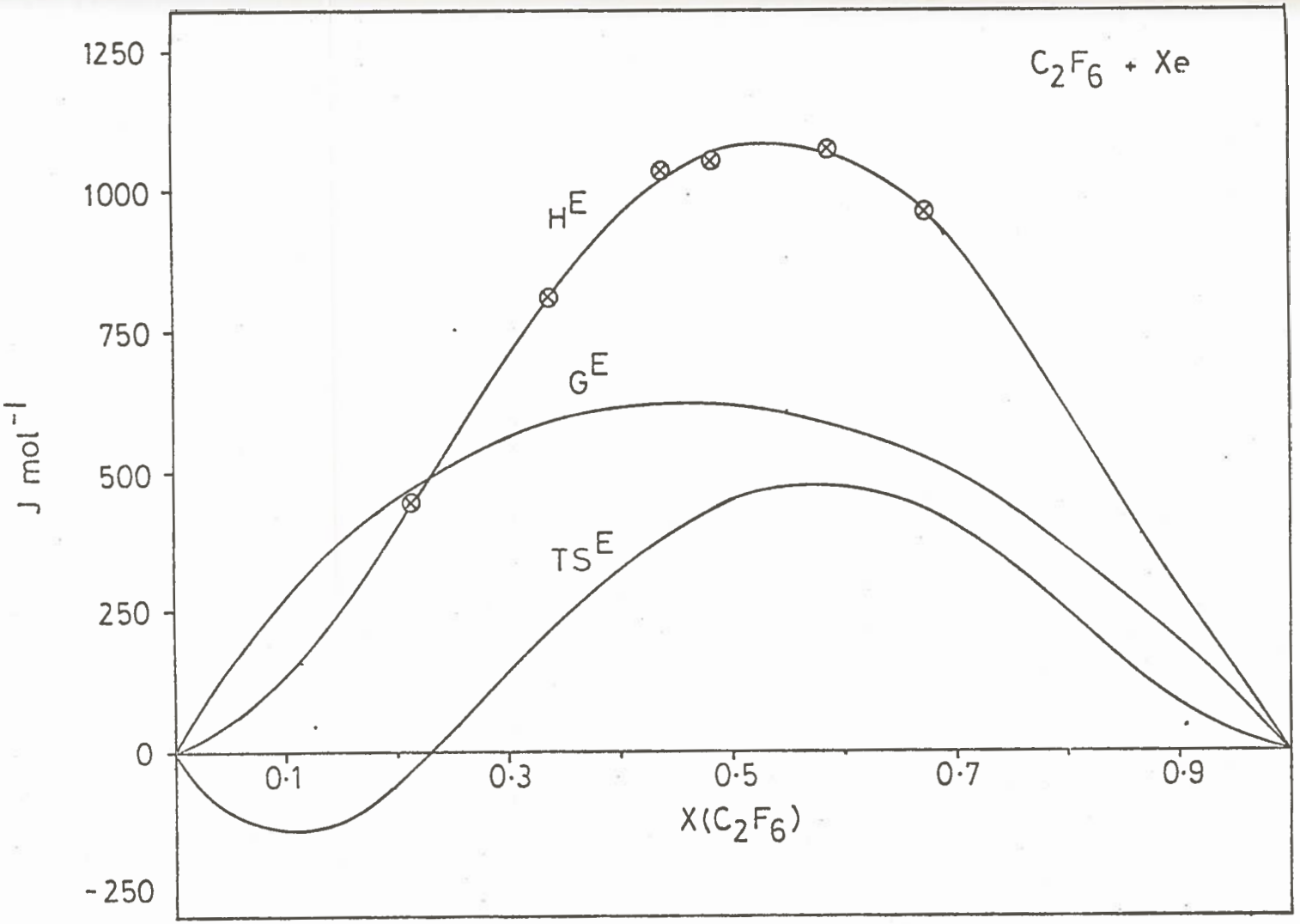

Fig. 12.1

C_2F_6 + Xe : G^E (173.08 K), H^E (175.00 K) and $TS^E = H^E - G^E$ as functions of composition. G^E from Ref. (4).

the standard deviation being

$$\sigma(H^E) = \pm 15\,J\,mol^{-1} .$$

For the equimolar mixture

$$H^E_{\frac{1}{2}}(0) = 1079\,J\,mol^{-1} .$$

If the equation for H^E based on the results at 175.00 K is assumed to be valid at 173.08 K and is combined with ALDERSLEY's equation for G^E (4),

$$G^E/RT = x_1(1-x_1)\left[A_G + B_G(2x_1-1) + C_G(2x_1-1)^2\right] \quad \ldots (12.2)$$

where

$$A_G = 1.7268 \pm 0.0060$$

$$B_G = -0.3259 \pm 0.0115$$

$$C_G = 0.1813 \pm 0.0246 ,$$

the following equation is obtained for S^E :

$$S^E/R = x_1(1-x_1)\left[A_S + B_S(2x_1-1) + C_S(2x_1-1)^2\right] \quad \ldots (12.3)$$

with

$$A_S = 1.2386$$

$$B_S = 1.1057$$

$$C_S = -2.2675 ,$$

giving for the equimolar mixture

$$TS^E_{\frac{1}{2}} = 443.9\ J\ mol^{-1} .$$

The three curves, H^E, G^E and TS^E are plotted against the mole fraction of C_2F_6 in Fig. 12.1.

12.3 DISCUSSION

In contrast to the xenon + ethane system, for $Xe + C_2F_6$ all four excess functions, G^E, H^E, S^E and V^E are throughout large and positive, except for S^E at low mole fractions of hexafluoroethane. Therefore $Xe + C_2F_6$ is very different thermodynamically from $Xe + C_2H_6$.

It is possible to see on a simple molecular basis that two liquids which differ sufficiently in the size (σ) and energy (ε) parameters which determine the pair intermolecular potential energy function could mix with negative G^E, H^E and V^E values. If one liquid consists of relatively large molecules which exert strong attractive forces on one another, and the other of much smaller molecules held together by weaker forces, then if the size difference is sufficiently large one can imagine that on mixing the two liquids the smaller molecules enter the 'cavities' between the larger molecules of the other fluid, so that V^E is negative. The smaller molecules would then come under the influence of the stronger attraction of the larger molecules, which would reduce both the energy of the system and 'escaping tendency' of the smaller molecules, thus making possible a negative H^E and negative departures from Raoult's Law, i.e. a negative G^E. This matter has been considered quantitatively by FLYTZANI-STEPHANOPOULOS[8] for a mixture of Lennard-Jones molecules (i.e. molecules conforming to a 12-6 potential). These calculations showed that for $\sigma_{11}/\sigma_{22} = 2$ and $\varepsilon_{11}/\varepsilon_{22} = 1.92$, H^E, G^E and V^E are all negative. For $\sigma_{11}/\sigma_{22} = 2$ and $\varepsilon_{11}/\varepsilon_{22} = 1$, V^E is negative, G^E just so, and H^E virtually zero. As expected from our crude qualitative argument above, the tendency towards negative excess functions increases with increasing σ_{11}/σ_{22} and $\varepsilon_{11}/\varepsilon_{22}$ ratios. The potential parameters of Xe and C_2H_6 are[9], respectively,

$$\text{Xe}: \quad \varepsilon/k = 231.5\,\text{K} \qquad \sigma = 0.396\,\text{nm}$$

$$C_2H_6: \quad \varepsilon/k = 251.8\,\text{K} \qquad \sigma = 0.435\,\text{nm}$$

while those for C_2F_6 can be roughly estimated from the critical properties[10] of this substance and those of CF_4, on a corresponding states basis. Since for

$$CF_4: \quad \varepsilon/k = 206.5\,\text{K} \qquad \sigma = 0.426\,\text{nm} \quad , \quad \text{Ref. (9)}$$

$$T_c = 227.6\,\text{K} \qquad V_c = 140\,\text{cm}^3\,\text{mol}^{-1} \quad , \quad \text{Ref. (10)}$$

and for

C_2F_6: $T_c = 292.9\,K$ $V_c = 224\ cm^3\ mol^{-1}$, Ref. (10)

one obtains

C_2F_6: $\varepsilon/k = 265.7\,K$ $\sigma \simeq 0.498\ nm$.

Therefore the ratio $\varepsilon_{11}/\varepsilon_{22}$ for $C_2H_6 + Xe$ and $C_2F_6 + Xe$ is about the same ($\simeq 1.1$) for the two systems, while the ratios of the σ parameters are, respectively,

$$\sigma(C_2H_6)/\sigma(Xe) \simeq 1.1$$

and

$$\sigma(C_2F_6)/\sigma(Xe) \simeq 1.3\,,$$

so that one might expect the excess thermodynamic properties of $C_2F_6 + Xe$ to be lower than those of $C_2H_6 + Xe$. The relative behaviour of the two systems is, however, the reverse of this.

We cannot therefore see any hope of an interpretation of the negative excess functions of the $C_2H_6 + Xe$ system simply on the basis of the relatively small difference in size of the two kinds of molecules.

GUBBINS and his co-workers[11] have considered a binary mixture of molecules which are spherically symmetrical, but polarizable, with molecules which have a quadrupole acting at their centre. They applied a perturbation treatment to examine the effect of increasing magnitude of the quadrupole moment, and showed that this would give rise to increasing, positive values of all three excess functions G^E, H^E and V^E. In this respect, therefore, the $C_2F_6 + Xe$ system might be said to behave predictably. This suggests that it will not be possible to interpret the 'abnormal' behaviour of the ethane + xenon system unless a more refined model is adopted, which, instead of simply assigning a centrally-acting quadrupole moment to the ethane molecule, takes account of the shape of this molecule, and adopts a more realistic view of the charge distribution within it.

12.4 REFERENCES

(1) CALADO, J.C.G. and AZEVEDO, E.J.S.G., Communication to the 8th Experimental Thermodynamics Conference, Guildford, U.K., (1978).

(2) LEWIS, K.L. and STAVELEY, L.A.K., J. Chem. Thermodynamics, 1975, 7, 855.

(3) STOGRYN, D.E. and STOGRYN, A.P., Mol. Phys., 1966, 11, 371.

(4)(a) ALDERSLEY, S.C., 'Thermodynamic Studies of Binary Condensed Gas Mixtures', (Part II) Thesis, University of Oxford, 1978.

(b) ALDERSLEY, S.C., LOBO, L.Q. and STAVELEY, L.A.K., J. Chem. Thermodynamics, 1979, 11 (in the press).

(5) BREWER, J., 'Determination of Mixed Virial Coefficients', AFOSR No. 67-2795 (1967).

(6) PACE, E.L. and ASTON, J.G., J. Am. Chem. Soc., 1948, 70, 566.

(7) STREETT, W.B., SAGAN, L.S. and STAVELEY, L.A.K., J. Chem. Thermodynamics, 1973, 5, 633.

(8) FLYTZANI-STEPHANOPOULOS, M., (M.Sc.) Thesis, University of Florida, 1975.

(9) TWU, C.-H. and GUBBINS, K.E., Chem. Eng. Sci., 1978, 33, 879.

(10) AMBROSE, D. and TOWNSEND, R., 'Vapour-liquid Critical Properties', N P L, Teddington, U.K., 1977.

(11)(a) TWU, C.-H., GUBBINS, K.E. and GRAY, C.G., Mol. Phys., 1975, 29, 713.

(b) FLYTZANI-STEPHANOPOULOS, M., GUBBINS, K.E. and GRAY, C.G., Mol. Phys., 1975, 30, 1649.

(c) TWU, C.-H., GUBBINS, K.E. and GRAY, C.G., J. Chem. Phys., 1976, 64, 5186.

CHAPTER 13

THE SYSTEM HYDROGEN CHLORIDE + NITROUS OXIDE

13.1 INTRODUCTION

The first chapters in this Part of the present work were concerned with binary systems in which the molecules of one component were non-polar. Having studied examples from each of the possible combinations giving such mixtures, the next stage in this systematic research appeared to be the experimental investigation of binary systems involving at least one dipolar component. For reasons already mentioned, hydrogen chloride seemed to be an adequate choice for that component. Among the systems in this particular group, one case of possible strong dipole + dipole interaction — HCℓ + HBr — had already been studied by CALADO *et al.*[1], who, however, did not measure H^E. Owing to the possibility of corrosion of the calorimeter by liquid hydrogen bromide we have not used this substance in our own H^E experiments. Therefore, in the absence of any other suitable small, simple dipolar molecule, we passed to the experimental examination of the remaining two combinations: dipole + quadrupole and dipole + octupole. The system hydrogen chloride + nitrous oxide, on which we report in this chapter, seemed to be a convenient choice as a model for the first of these combinations. Actually, the HCℓ molecule is not in fact a pure dipole nor is N_2O an example of pure quadrupolar molecule. But, as already pointed out, the dipole moment of nitrous oxide is small (Chapter 10) and can hardly be responsible for any detectable effect in the excess thermodynamic functions. On the other hand, the quadrupole moment of HCℓ has been estimated[2] as $Q = +3.8 \times 10^{-26}$ esu cm^2 = $+12.7 \times 10^{-40}$ C m^2 and this is a value sufficiently high to influence the excess functions to a considerable extent. It may be added that the quadrupoles of HCℓ and N_2O have opposite signs.

The total vapour pressure as a function of composition, from which G^E is derived, was measured for $HC\ell + N_2O$ at 182.32 K, the triple point of nitrous oxide. V^E was measured at the same temperature, but the enthalpy of mixing H^E, for reasons of experimental convenience, at a slightly higher temperature (184.03 K).

13.2 DETERMINATION OF G^E, V^E AND H^E

The values and the sources of the ancillary data needed in the evaluation of G^E, V^E and H^E from the actual experimental results have already been stated: in Chapter 9 for $HC\ell$, and in Chapter 10 for N_2O. In the present chapter, hydrogen chloride (which for the H^E experiments was condensed into the lower compartment of the calorimeter) will be designated by component 1, and nitrous oxide by component 2.

13.2.1 *G^E AT 182.32 K*

The total vapour pressure is given in Table 13.1 as a function of the liquid mole fraction of $HC\ell$ (x_1). The system forms a positive azeotrope at $x_1 \simeq 0.25$ (Fig. 13.1). However, G^E is an almost symmetrical function of the mole fraction, as is so often the case for binary liquefied gas mixtures. The vapour pressure of liquid $HC\ell$ at the N_2O triple-point was found to be 72.134 kPa, in satisfactory agreement with 72.147 kPa as reported by CALADO *et al.*[3].

The G^E values fit a Redlich-Kister equation,

$$G^E/RT = x_1(1-x_1)\left[A_G + B_G(2x_1 - 1) + C_G(2x_1 - 1)^2\right], \quad \ldots (13.1)$$

with parameters

$$A_G = 0.3875 \quad (\sigma_A = 0.0022)$$
$$B_G = -0.0171 \quad (\sigma_B = 0.0045)$$
$$C_G = 0.0209 \quad (\sigma_C = 0.0108)$$

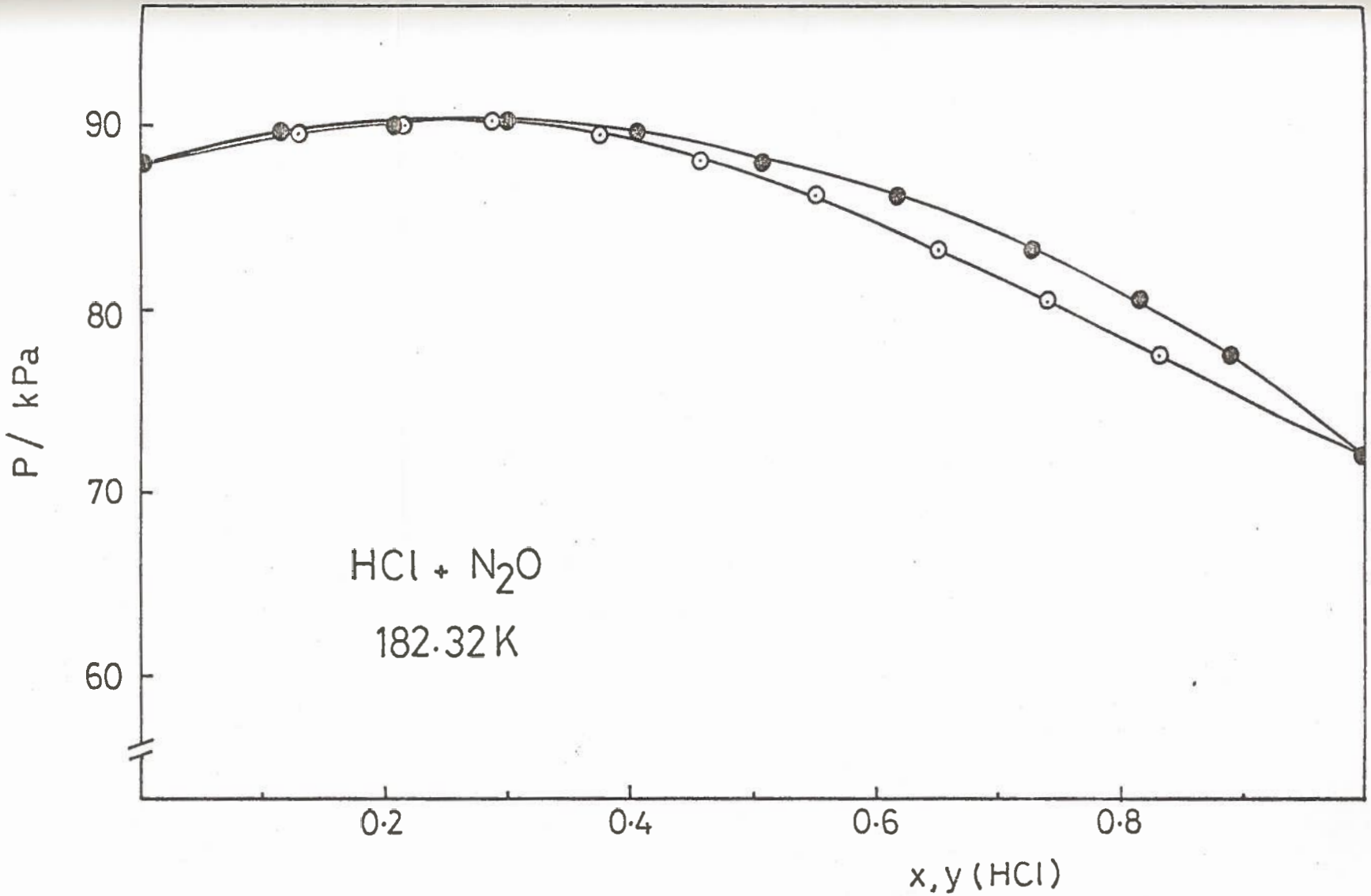

Fig. 13.1 - HCℓ + N_2O: P - x - y diagram at 182.32 K

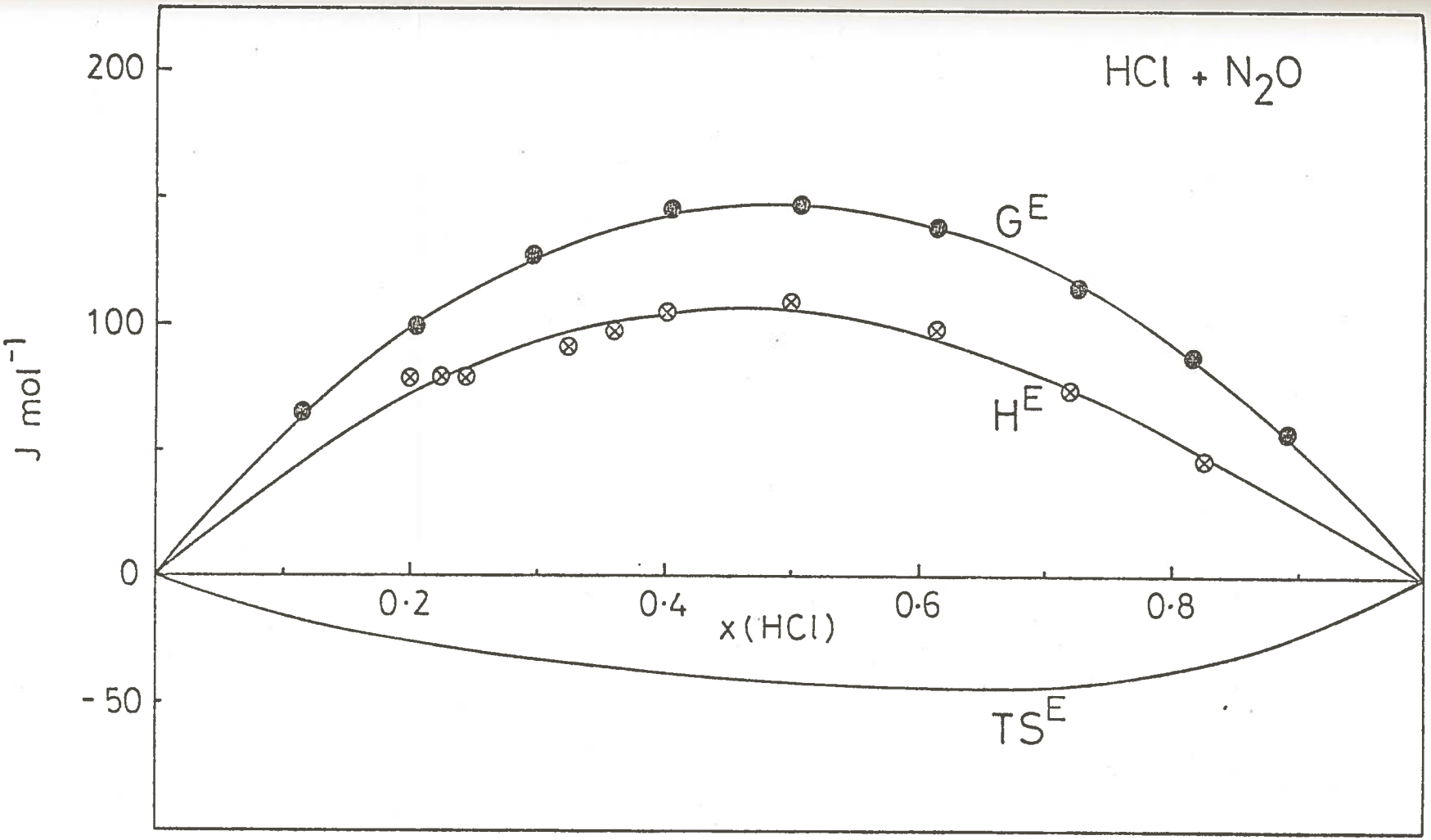

Fig. 13.2

$HC\ell + N_2O$: G^E (182.32 K), H^E (184.03 K) and $TS^E = H^E - G^E$ as functions of composition.

TABLE 13.1

VAPOUR PRESSURE AND EXCESS MOLAR GIBBS ENERGY OF $HC\ell + N_2O$ AT 182.32 K

x_1	y_1	P/kPa	R_p/Pa	G^E/J mol^{-1}
0.0000	0.0000	87.866	-	0
0.1166	0.1275	89.789	+ 20	65.0
0.2070	0.2126	90.185	- 132	98.5
0.2970	0.2890	90.357	+ 79	127.3
0.4051	0.3761	89.657	+ 85	144.8
0.5082	0.4589	88.242	- 41	146.6
0.6179	0.5493	86.292	+ 23	138.4
0.7288	0.6514	83.364	- 105	113.6
0.8152	0.7406	80.707	+ 35	88.2
0.8915	0.8332	77.684	+ 41	57.1
1.0000	1.0000	72.134	-	0

For the equimolar mixture

$$G^E_{\frac{1}{2}} = 146.9 \pm 0.8 \text{ J mol}^{-1} .$$

The experimental points and the G^E curve given by eqn (13.1) are represented in Fig. 13.2.

13.2.2 *V^E AT 182.32 K*

The molar volumes of the pure components and of mixtures of known composition are recorded in Table 13.2 where the derived values of V^E are also indicated. The excess molar volumes refer to mixing at the saturation vapour pressure, and fit the equation

$$V^E = x_1(1 - x_1)\left[A_V + B_V(2x_1 - 1) + C_V(2x_1 - 1)^2\right] , \qquad \ldots (13.2)$$

with

$$A_V = 0.583 \text{ cm}^3 \text{ mol}^{-1}$$

$$B_V = 0.083 \text{ cm}^3 \text{ mol}^{-1}$$

$$C_V = 0.129 \text{ cm}^3 \text{ mol}^{-1} ,$$

the standard deviation of this fitting being

$$\sigma(V^E) = \pm 0.007 \text{ cm}^3 \text{ mol}^{-1} \ .$$

For the equimolar mixture

$$V^E_{\frac{1}{2}} = 0.146 \text{ cm}^3 \text{ mol}^{-1} \ .$$

The value of the molar volume of pure HCℓ, (Table 13.2),

$$V_1^* (182.32 \text{ K}) = 30.413 \pm 0.005 \text{ cm}^3 \text{ mol}^{-1}$$

is the mean of two independent determinations. When compared with the result interpolated from PRICHARD's work[4], $30.477 \text{ cm}^3 \text{ mol}^{-1}$, a difference of -0.2%, in the usual direction, is observed.

The curve calculated from eqn (13.2) and the V^E experimental points are shown in Fig. 13.3.

TABLE 13.2

MOLAR VOLUMES V AND EXCESS MOLAR VOLUMES V^E OF HCℓ + N_2O AT 182.32 K

x_1	$V/\text{cm}^3 \text{ mol}^{-1}$	$V^E/\text{cm}^3 \text{ mol}^{-1}$	$R_V/\text{cm}^3 \text{ mol}^{-1}$
0.0000	35.487	0	-
0.0994	35.044	0.061	+ 0.007
0.1956	34.592	0.097	+ 0.006
0.3056	34.052	0.115	- 0.006
0.3159	34.002	0.118	- 0.005
0.4018	33.579	0.131	- 0.007
0.4121	33.535	0.139	+ 0.000
0.5244	32.982	0.156	+ 0.009
0.6247	32.464	0.147	+ 0.004
0.7162	31.981	0.128	- 0.003
0.7961	31.562	0.114	+ 0.004
0.8890	31.039	0.063	- 0.009
1.0000	30.413	0	-

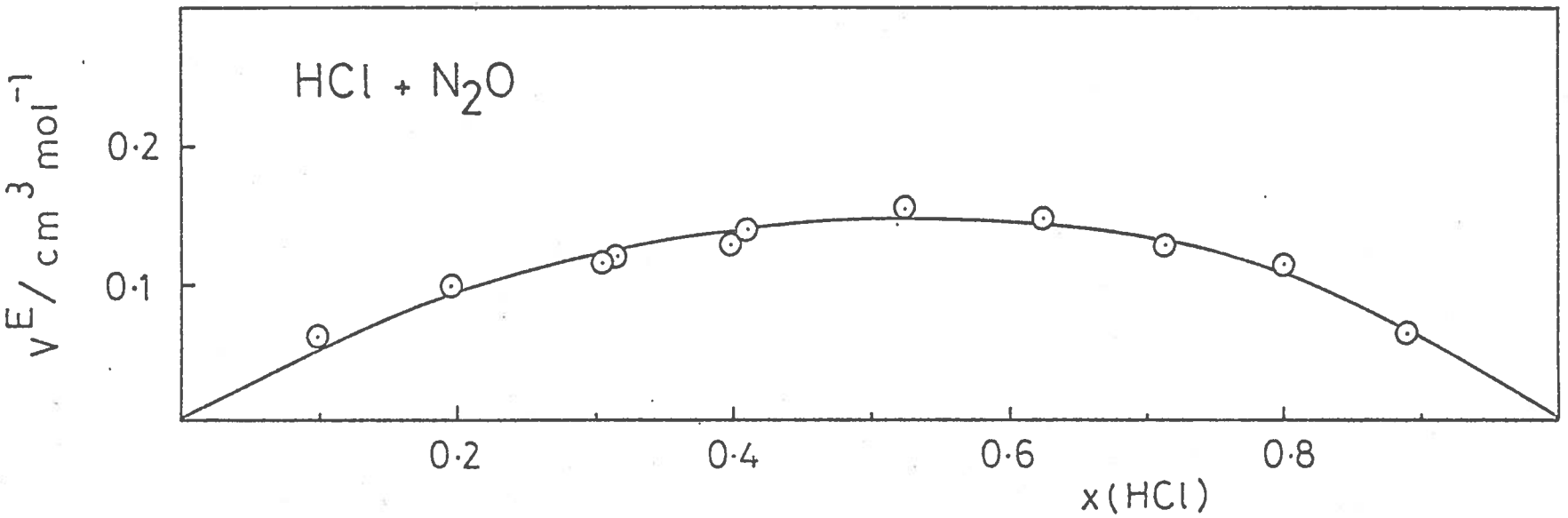

Fig. 13.3

HCℓ + N_2O: V^E (182.32 K) as a function of composition

13.2.3 *H^E AT 184.03 K*

The experimental results for H^E are presented in Table 13.3 in the form used in previous chapters. H^E is listed as $H^E(0)$, its value at zero pressure, but in fact for the relatively low pressures involved the difference $H^E(P_m) - H^E(0)$ is negligible ($\leqslant 0.1$ J mol^{-1} in every case).

The $H^E(0)$ values can be represented by the equation

$$H^E/RT = x_1(1-x_1)\left[A_H + B_H(2x_1 - 1) + C_H(2x_1 - 1)^2\right] \quad \ldots (13.3)$$

with

$$A_H = 0.2757$$

$$B_H = -0.0547$$

$$C_H = -0.0461 \ ,$$

the standard deviation being

$$\sigma(H^E) = \pm 4.6 \text{ J mol}^{-1} \ .$$

For the equimolar mixture eqn (13.3) gives

$$H^E_{\frac{1}{2}} = 105.4 \text{ J mol}^{-1} \ .$$

TABLE 13.3

EXCESS MOLAR ENTHALPY OF HCℓ + N_2O AT 184.03 ± 0.02 K

n_1/mol	n_2/mol	x_1	y_1	Q/J	$\psi_{6,7}$/J	H^E/J mol^{-1}	R_H/J mol^{-1}
0.01240	0.04938	0.2007	0.2064	6.474	- 1.659	78.8	+ 7.2
0.02021	0.06975	0.2246	0.2272	8.679	- 1.601	79.3	+ 1.5
0.01922	0.05996	0.2427	0.2426	7.831	- 1.612	79.3	- 2.7
0.02439	0.05021	0.3270	0.3119	8.267	- 1.555	90.9	- 6.4
0.03223	0.05740	0.3597	0.3381	10.204	- 1.479	98.1	- 3.2
0.03419	0.05063	0.4033	0.3727	10.247	- 1.433	104.8	+ 0.0
0.04387	0.04392	0.5000	0.4501	10.784	- 1.265	109.3	+ 3.9
0.05619	0.03483	0.6177	0.5486	9.806	- 0.987	97.6	+ 3.6
0.06163	0.02382	0.7217	0.6440	6.888	- 0.697	73.0	- 1.5
0.05490	0.01162	0.8259	0.7538	3.414	- 0.350	46.5	- 2.0

By making the usual assumption, S^E as obtained from the equations for G^E and H^E is given by

$$S^E/R = x_1(1-x_1)\left[A_S + B_S(2x_1 - 1) + C_S(2x_1 - 1)^2\right] \quad \ldots (13.4)$$

with

$$A_S = -0.118$$

$$B_S = -0.0376$$

$$C_S = -0.0670 \ .$$

For the equimolar mixture,

$$TS^E_{\frac{1}{2}} = -41.4 \text{ J mol}^{-1} \ .$$

H^E and TS^E are plotted against the mole fraction of HCℓ, in Fig. 13.2.

13.3 DISCUSSION

Some early vapour pressure-composition results for this system obtained by KLEMENC and KHOL at temperatures given as -100, -95 and -90°C are quoted in the International Critical Tables as a 'personal communication'[5]. These data lead to the following values of $G^E_{\frac{1}{2}}$: 162 J mol^{-1} at 173 K, 148 J mol^{-1} at 178 K, and 156 J mol^{-1} at 183 K. The trend of these values suggests a rather large uncertainty, but they are roughly the same as our own figure of 146.9 J mol^{-1}.

The dominant characteristic of HCℓ + N_2O, when compared with the systems studied so far (with the exception of Ar + Kr, which can be regarded as a reference system), is the low relative values of all its primary excess thermodynamic functions: G^E, H^E and V^E. The derived excess entropy S^E is also small in absolute value, being negative over the entire composition range. This behaviour may suggest some kind of partly ordered relation between the two sorts of molecule in the mixture, the development of which would partially compensate the breakdown of any structural organisation of the pure liquids (especially N_2O).

From simple molecular considerations one might expect the excess properties of $HC\ell + N_2O$, especially G^E and H^E, to be lower than those of its two complementary binary systems: $HC\ell + Xe$ and $N_2O + Xe$. In fact, the forces between the $HC\ell$ and N_2O molecules might reasonably be expected to be less dissimilar than the corresponding ones between the xenon molecules and those of either polar species. Therefore, from this point of view, $HC\ell + N_2O$ might be a less non-ideal system than the remaining two binary systems in this set.

From the qualitative point of view, the experimental results support the conclusions of the generalized perturbation theory treatment of GUBBINS, GRAY and co-workers[6,7]. In fact, TWU *et al.*[6] taking Ar + Kr as the reference system examined the changes caused in the values of the main thermodynamic functions of this system by successfully assigning a dipole, a quadrupole, or an octupole to one or both of its components. While the introduction of any one of the multipoles considered in one (only) of the components produced an increase in the G^E, H^E, S^E and (in the numerical value of) V^E functions, the simultaneous assignment of a multipole to both components caused only minor changes in the same properties (in relation to those of the reference). Moreoever, as FLYTZANI-STEPHANOPOULOS *et al.*[7] pointed out, if the quadrupole moments in the two components have opposite signs (as in $HC\ell + N_2O$) the tendency to lower values of G^E is even greater, leading to negative azeotropy for sufficiently high values of the moments. Comparing the properties of $HC\ell + N_2O$ with those of $HC\ell + Xe$ and $N_2O + Xe$ one can therefore say that the changes in the experimental values of the excess thermodynamic functions are not inconsistent with the predictions of the theory. Therefore, it is believed that the theoretical calculations on this system — which are now in progress at Cornell University — will reproduce reasonably well the experimental results, if not for H^E (see Chapter 9), at least for G^E and V^E.

13.4 REFERENCES

(1) CALADO, J.C.G., GRAY, C.G., GUBBINS, K.E., PALAVRA, A.M.F., SOARES, V.A.M., STAVELEY, L.A.K. and TWU, C.-H., J. Chem. Soc. Faraday I, 1978, 74, 893.

(2) STOGRYN, D.E. and STOGRYN, A.P., Mol. Phys., 1966, 11, 371.

(3) CALADO, J.C.G., KOZDON, A.F., MORRIS, P.J., PONTE, M.N.da, STAVELEY, L.A.K. and WOOLF, L.A., J. Chem. Soc. Faraday I, 1975, 71, 1372.

(4) PRICHARD, P.C., 'A Comparison of Some Thermodynamic Properties of Some Simple Isotopic Compounds', (Part II) Thesis, University of Oxford, (1968).

(5) International Critical Tables, McGraw-Hill, vol. III, 285 (1928).

(6) TWU, C.-H., GUBBINS, K.E. and GRAY, C.G., Mol. Phys., 1975, 29, 713.

(7) FLYTZANI-STEPHANOPOULOS, M., GUBBINS, K.E. and GRAY, C.G., Mol. Phys., 1975, 30, 1649.

CHAPTER 14

THE SYSTEM HYDROGEN CHLORIDE + CARBON TETRAFLUORIDE

14.1 INTRODUCTION

In selecting a suitable system for the purposes of our work, a number of factors have to be considered. From the practical point of view, the two substances should be available, or preparable, in a state of high purity, and be chemically stable and non-corrosive. Furthermore, they must have suitably overlapping liquid ranges, in which the vapour pressure of neither component is too high, otherwise uncertainty in the corrections for non-ideality of the vapour phase may present a problem, and technical difficulties may also arise. On the other hand, since reliable potential energy functions will be needed in the theoretical treatment, the molecules should be as small as possible.

The particular system dealt with in this chapter is $HC\ell + CF_4$, chosen to serve as a model of a solution in which the molecules of one component have dipoles, and those of the other octupoles. For the component whose molecules have an octupole, but no dipole or quadrupole, a substance with tetrahedral molecules was the obvious choice. Methane would have been acceptable in principle as the octupolar component, but its octupole moment is lower than that of carbon tetrafluoride and, moreover, there is no substance with an overlapping liquid range with a small molecule and a reasonably large dipole. According to the literature liquid $HC\ell$ can attack copper, but laboratory tests carried out by PRICHARD[1] showed that, in practice, the reaction rate is too slow for any measurable corrosion effect to be observed in the course of a day or so. The system $HC\ell + CF_4$ therefore seemed on balance to be perhaps the best choice, especially as the systems $HC\ell + Xe$ and $CF_4 + Xe$ had already been studied (Chapters 9 and 11).

In making the vapour pressure measurements at 159.01 K on mixtures of $HC\ell + CF_4$ of known composition needed to give G^E, it soon became apparent however from the constancy of the vapour pressure over a wide composition range that the liquids are only partially miscible at this temperature, and indeed that the mutual solubilities are quite low. Further experiments at a higher temperature (173.08 K, the triple-point of C_2F_6) showed the expected increase in solubility, but it was clear that this temperature is still well below the consolute temperature. Nevertheless, it was considered worthwhile to estimate G^E for the limited composition range over which the two liquids form a solution. We have also attempted to determine H^E for the formation of the two saturated solutions, having regard to the known sensitivity of this excess function to the values of the parameters entering into the theoretical calculations. These are to be carried out by Professor K.E. GUBBINS and his group, at Cornell, and are in progress at present.

The following sections are therefore concerned with the determination of G^E from total vapour pressure measurements for the limited homogeneous solutions found at 159.01 K and 173.08 K, with constructing the liquid-vapour phase diagram at these temperatures, and with the determination of H^E for the two liquid mixtures in equilibrium at 162.97 K.

14.2 DETERMINATION OF G^E AT 159.01 K AND 173.08 K

Throughout this chapter $HC\ell$ will be designated as component 1, and CF_4 as component 2.

As already explained, to calculate the true composition of the liquid mixture in the vapour pressure experiments, it is necessary to have values of the vapour pressures, liquid molar volumes and second virial coefficients of the two components at the working temperature. The vapour pressures and the molar volumes were measured in the usual way, with the

following results (literature values in brackets)

at T = 159.01 K

P_1^* = 13.807 ± 0.005 kPa $\qquad$ P_2^* = 244.500 ± 0.024 kPa

(V_1^* = 29.070 $cm^3\ mol^{-1}$) [1] $\qquad$ V_2^* = 57.363 ± 0.002 $cm^3\ mol^{-1}$

(57.600 $cm^3\ mol^{-1}$) [4]

at T = 173.08 K

P_1^* = 39.707 ± 0.012 kPa $\qquad$ P_2^* = 508.613 ± 0.033 kPa

(39.623 kPa [2]; 39.842 kPa [3])

V_1^* = 29.884 ± 0.006 $cm^3\ mol^{-1}$ $\qquad$ V_2^* = 60.760 ± 0.015 $cm^3\ mol^{-1}$

(29.916 $cm^3\ mol^{-1}$) [1] $\qquad$ (60.998 $cm^3\ mol^{-1}$) [4]

The value V_1^* (159.01 K) = 29.070 $cm^3\ mol^{-1}$ used in the calculations is a short extrapolation from the work of PRICHARD[1], after a correction of -0.15% was applied (based on the ratios between PRICHARD's figures and ours for HCℓ at 173.08 and 182.32 K). The triple-point pressure of HCℓ is compared with literature values in Table 2.2 of this work. Comments on P_2^* at both temperatures are made in Chapter 17.

As regards second virial coefficients, their sources have already been indicated in Chapters 9 and 11 for HCℓ and CF_4 respectively. The actual figures used in the present calculation were:

B_{11} (159.01 K) = − 680 $cm^3\ mol^{-1}$ $\qquad$ B_{22} (159.01 K) = − 343 $cm^3\ mol^{-1}$

B_{11} (173.08 K) = − 595 $cm^3\ mol^{-1}$ $\qquad$ B_{22} (173.08 K) = − 296 $cm^3\ mol^{-1}$.

The vapour pressure experimental results are recorded in Table 14.1. In this table, X_1 is the overall mole fraction of HCℓ in the system (phases $L^I + L^{II} + G$). The existence of two liquid layers at both temperatures is clearly shown by the constancy of the vapour pressure P over much of the composition (X_1) range.

TABLE 14.1

VAPOUR PRESSURE P AND EXCESS MOLAR GIBBS ENERGY G^E OF $HC\ell + CF_4$ AT 159.01 K AND 173.08 K

T/K	X_1	x_1	y_1	P/kPa	G^E/J mol^{-1}	R_G/J mol^{-1}
159.01	0.0000	0.0000	0.0000	244.500	0	-
	0.1166			253.942		
	0.2924			254.018		
	0.4309			254.183		
	0.5557			254.100		
		0.9482	0.0616	241.555	205	- 2
		0.9569	0.0787	184.526	163	- 10
		0.9782	0.0964	150.978	96	+ 8
		0.9800	0.1162	123.547	84	+ 3
	1.0000	1.0000	1.0000	13.807	0	-
173.08	0.0000	0.0000	0.0000	508.613	0	-
	0.1292			533.167		
	0.1446			532.988		
	0.2949			533.235		
	0.6173			533.317		
		0.9195	0.1097	384.556	252	+ 2
		0.9355	0.1334	312.092	202	+ 2
		0.9549	0.2032	199.438	131	- 9
		0.9704	0.2330	174.926	97	+ 5
	1.0000	1.0000	1.0000	39.707	0	-

In attempting to evaluate G^E for the limited region over which the two components are mutually soluble, it was thought inadvisable to use Barker's method, since in the range in question, not only is the composition of the liquid very unbalanced, but also, owing to the considerable difference in volatility of the two liquids, the vapour pressure is changing very rapidly with mole fraction (and therefore large pressure residuals would result as a consequence of relatively small deviations in composition). Instead, we proceeded by minimizing G^E itself, following the general method described in section 5.3.

We started by using a first approximation value $A_G \neq 0$ and making $B_G = C_G = 0$ [in eqn (5.37)]. The A_G value was then optimized so as to give the minimum sum of the resulting G^E residuals,

$$R_G = G^E \text{ [eqn (5.5)]} - G^E \text{ [eqn (5.37)]} , \qquad \ldots (14.1)$$

and a consistent set of the compositions x_1 and y_1 (to better than 0.0001). However, as this first approximation showed, and indeed as was only to be expected, for such a non-ideal system one could scarcely take G^E to be a symmetrical (parabolic) function of mole fraction. To allow for some assymetry while keeping the adjustable number of parameters as low as possible we did not take the calculation beyond the term in B_G. A first trial value for this parameter was found by calculating the quotient

$$(R_G/RT) / [x_1 (1 - x_1)(2 x_1 - 1)]$$

for each experimental point, and taking for B_G the average value of such quotients. The whole procedure was then recycled to work out the optimum B_G. In this way the following values for the parameters in the equation

$$G^E/RT = x_1 (1 - x_1)\left[A_G + B_G (2 x_1 - 1)\right] \qquad \ldots (14.2)$$

(and the respective G^E standard deviations) were obtained:

at T = 159.01 K

$$A_G = 3.90$$

$$B_G = -0.80 ,$$

giving

$$\sigma(G^E) = \pm 9 \text{ J mol}^{-1} ;$$

at T = 173.08 K

$$A_G = 3.35$$

$$B_G = -1.20$$

giving

$$\sigma(G^E) = \pm 8 \text{ J mol}^{-1} .$$

The final values of the G^E residuals, R_G, are included in Table 14.1 with the experimental vapour pressures, the calculated compositions

of the liquid and vapour phases, and the excess molar Gibbs energies.

For the (hypothetical) equimolar mixture :

$$G^E_{\frac{1}{2}} \simeq 1.3 \text{ kJ mol}^{-1} \quad \text{at} \quad 159.01 \text{ K}$$

and

$$G^E_{\frac{1}{2}} \simeq 1.2 \text{ kJ mol}^{-1} \quad \text{at} \quad 173.08 \text{ K} .$$

14.3 COMPOSITION OF THE VAPOUR AND THE TWO LIQUID PHASES IN EQUILIBRIUM

Since at both temperatures at which vapour pressures were measured the liquid separates into two layers (except in the extreme regions of the diagram), there are three phases at equilibrium — the two liquids and the vapour. We now consider the calculation of the compositions of these phases, starting with the two liquid phases, L^I and L^{II}.

From the general conditions for phase equilibrium, eqns (5.6), and by using (5.7) and (5.9) the equality between the fugacities of component i in the two liquid mixtures can be written as

$$\gamma_i(L^I)\, x_i(L^I)\, f_i^0(L^I) = \gamma_i(L^{II})\, x_i(L^{II})\, f_i^0(L^{II}) ,$$

so that, choosing the same standard state for component i in both phases,

$$f_i^0(L^I) = f_i^0(L^{II}) ,$$

one obtains for the two components in the system

$$\gamma_1(L^I)\, x_1(L^I) = \gamma_1(L^{II})\, x_1(L^{II}) \qquad \ldots (14.3)$$

$$\gamma_2(L^I)\, x_2(L^I) = \gamma_2(L^{II})\, x_2(L^{II}) . \qquad \ldots (14.4)$$

The activity coefficients γ_i are given by eqns (AI.2) and (AI.3), Appendix (I), C_G being zero in the present case. Therefore, by substituting these results in eqns. (14.3) and (14.4), one has

$$x_1(L^I)\ \exp\left\{(A_G + 3B_G)\left[x_2(L^I)\right]^2 - 4B_G\left[x_2(L^I)\right]^3\right\}$$

$$= x_1(L^{II})\ \exp\left\{(A_G + 3B_G)\left[x_2(L^{II})\right]^2 - 4B_G\left[x_2(L^{II})\right]^3\right\} \quad (14.5)$$

and

$$x_2(L^I)\ \exp\left\{(A_G - 3B_G)\left[x_1(L^I)\right]^2 + 4B_G\left[x_1(L^I)\right]^3\right\}$$

$$= x_2(L^{II})\ \exp\left\{(A_G - 3B_G)\left[x_1(L^{II})\right]^2 + 4B_G\left[x_1(L^{II})\right]^3\right\}. \quad (14.6)$$

Since these two equations and the two general relationships

$$x_1(L^I) + x_2(L^I) = 1 \quad \ldots (14.7)$$

$$x_1(L^{II}) + x_2(L^{II}) = 1 \quad \ldots (14.8)$$

must be simultaneously satisfied, the four values of x_i can be obtained. This was done by applying the Newton-Raphson numerical method[5], which gave the following values for the composition of the two liquid phases in equilibrium

at T = 159.01 K

$x_1(L^I) = 0.947$ $\qquad$ $x_1(L^{II}) = 0.010$

at T = 173.08 K

$x_1(L^I) = 0.881$ $\qquad$ $x_1(L^{II}) = 0.013$.

The composition of the vapour phase in equilibrium with the two liquid layers was obtained by applying the general conditions leading to eqn (5.45) (and its analogue for component 2), in which any one of the two layers, L^I or L^{II}, can be taken as the liquid phase. In this way, it was found that

at T = 159.01 K

$$y_1 = 0.05 \pm 0.01$$

while

at T = 173.08 K

$$y_1 = 0.07 \pm 0.02 .$$

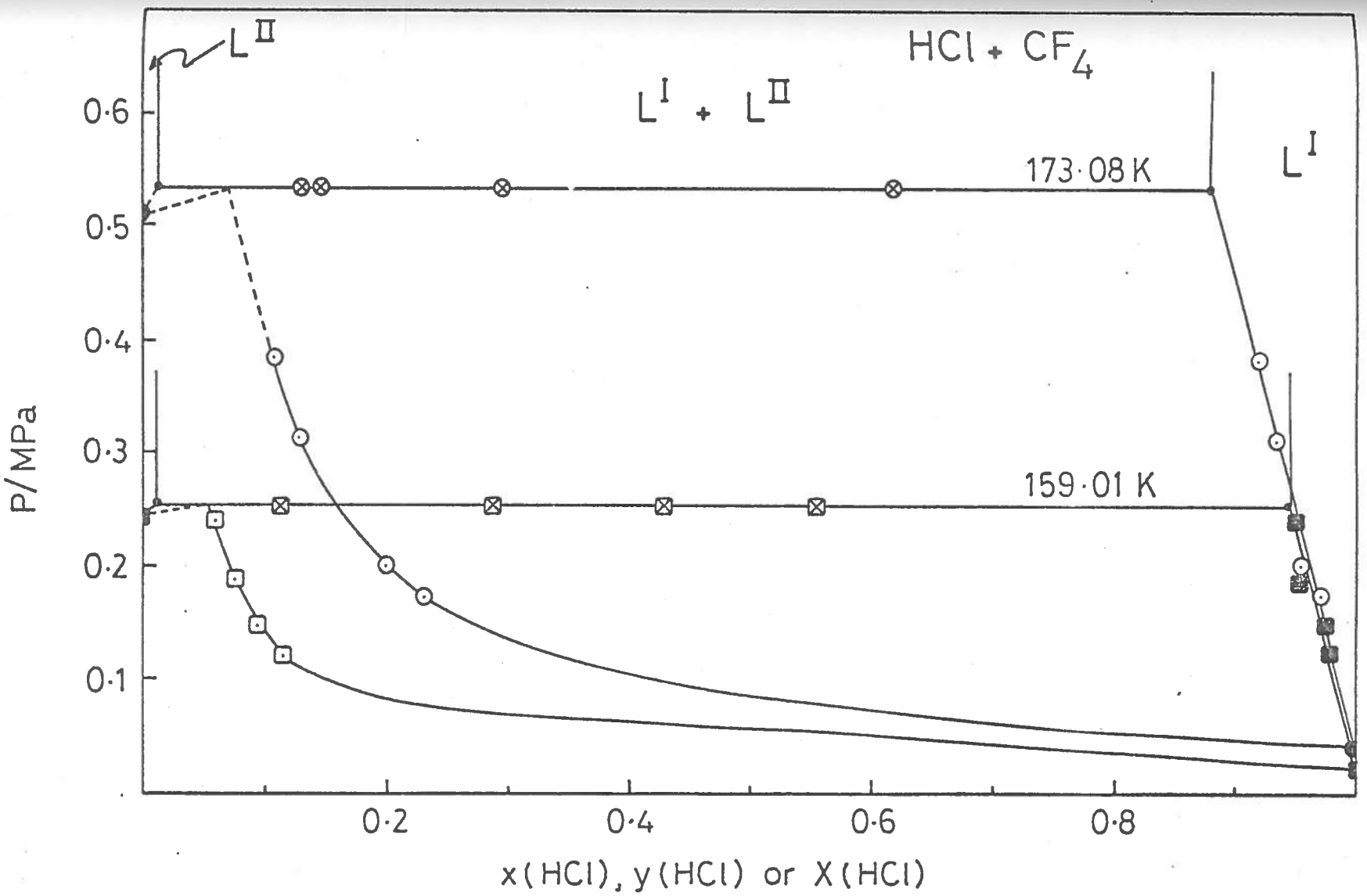

Fig. 14.1

$HCl + CF_4$: Pressure vs composition diagram at two temperatures (159.01 and 173.08 K). The crossed circles and crossed squares correspond to P vs X_1 in the two liquid phase region.

Using the results so obtained for the composition of the liquid phases L^I and L^{II} and the co-existing vapour phase, together with the x_i and y_i recorded in Table 14.1, it is possible to plot the liquid-vapour phase diagram for the system. This is shown in Fig. 14.1 for both temperatures. The experimental points obtained in the constant pressure region are also represented in this figure (crossed circles and crossed squares) as a function of the overall mole fraction of HCℓ, (X_1), in the pyknometer.

14.4 DETERMINATION OF H^E AT 162.97 K

In the calorimetric experiments hydrogen chloride was condensed into the upper compartment of the vessel, while carbon tetrafluoride was admitted into the lower chamber.

The experiments were carried out at a temperature of 162.97 ± 0.02 K. At this temperature the second virial coefficients of the two components were estimated to be

$$B_{11}\,(162.97\,K) = -645\ cm^3\ mol^{-1}$$

$$B_{22}\,(162.97\,K) = -329\ cm^3\ mol^{-1}\ .$$

The value of the molar enthalpy of vaporization of HCℓ at the working temperature was taken as

$$\Delta H_{v,1}\,(162.97\,K) = 16880\ J\ mol^{-1}$$

this being derived from the calorimetric results of GIAUQUE and WIEBE[3], while for CF_4 use of the data of SMITH and PACE[6] gave

$$\Delta H_{v,2}\,(162.97\,K) = 10980\ J\ mol^{-1}\ .$$

The quantities of the two pure liquids mixed in the calorimeter were always such that these resulted in a mixture of the two liquid phases L^I and L^{II}. The amounts of the two components were varied so as to cover a wide range of the relative amounts of the L^I and L^{II} phases produced on mixing. The quantities sought were, of course, $H^E(L^I)$ and $H^E(L^{II})$.

To evaluate these from eqn (7.47) the following approximations have been made:

(i) the quantities $V^E(L^I)$ and $V^E(L^{II})$ were both assumed to be zero, since the two phases have compositions in the extremes of the diagram;

(ii) term ξ_3 was neglected for the usual reason, namely the absence of experimental values of $H^E(G)$ and $V^E(G)$.

Values of x_i for the phases L^I and L^{II}, and of y_i for the co-existing vapour, had to be interpolated from the estimates reached above for 159.01 K and 173.08 K. These interpolated values are

$$x_1(L^I) = 0.93(2)$$
$$x_1(L^{II}) = 0.01(0)$$
$$y_1 = 0.05(5) .$$

Of the correction terms in eqn (7.47), ξ_4 (always $\leqslant 2\ J\ mol^{-1}$) and ξ_5 ($\leqslant 1\ J\ mol^{-1}$) are almost negligible, but the vaporization corrections terms ξ_6 and ξ_7 are important. The values of Z and $1/F$ (section 7.4) for each calorimetric experiment are given in Table 14.2, together with the experimental Q_H and the calculated $\xi_{6,7}$. The experimental points fit the expression, [eqn (7.50)],

$$Z = Y/F + X \qquad \ldots (14.9)$$

with a correlation coefficient of (better than) 0.99, for $X = -185\ J\ mol^{-1}$ and $Y = +170\ J\ mol^{-1}$. The standard deviation of this fitting is

$$\sigma(Z) = \pm 28\ J\ mol^{-1} .$$

From these values, $H^E(L^I)$ and $H^E(L^{II})$ are obtained as

$$H^E(L^I) = -15\ J\ mol^{-1}$$
$$H^E(L^{II}) = 170\ J\ mol^{-1} .$$

TABLE 14.2

DATA FOR THE CALCULATION OF $H^E(L^I)$ AND $H^E(L^{II})$ FOR $HC\ell + CF_4$ AT 162.97 ± 0.02 K

n(L)/mol	1/F	Q/J	$\xi_{6,7}$/J	Z/J mol^{-1}
0.11323	5.122	20.962	- 6.839	+ 645
0.07219	4.411	17.387	- 7.768	+ 595
0.06666	2.583	14.254	- 7.386	+ 272
0.07719	2.200	13.449	- 6.754	+ 195
0.06400	1.746	12.145	- 6.880	+ 148
0.07805	1.598	9.122	- 6.049	+ 67
0.08000	1.466	9.443	- 5.736	+ 72
0.06028	1.252	5.404	- 6.335	- 15
0.07020	1.115	5.244	- 5.462	- 0

The Z versus 1/F points, and the least-squares straight line through them, are shown in Fig. 14.2.

14.5 DISCUSSION

As will be seen from Fig. 14.2, there is some scatter in the experimental points, which is not surprising in view of the very limited mutual solubility of the two liquids, especially of $HC\ell$ in CF_4. But we are reasonably confident that when CF_4 dissolves in $HC\ell$ to give a dilute solution, $H^E(L^I)$ is at least small and very possibly negative, whereas by contrast the very small amount of $HC\ell$ which dissolves in CF_4 does so with a considerable and positive $H^E(L^{II})$, so that the H^E versus mole fraction curve, if it were not interrupted by the immiscibility gap, would be very asymmetric. If the values obtained for $H^E(L^I)$ and $H^E(L^{II})$, and the corresponding x_1 values are fitted to the equation

$$H^E/RT = x_1(1 - x_1)\left[A_H + B_H(2x_1 - 1)\right] \qquad \ldots (14.10)$$

the estimate of $H^E_{\frac{1}{2}}$ for an imagined one-phase equimolar solution is

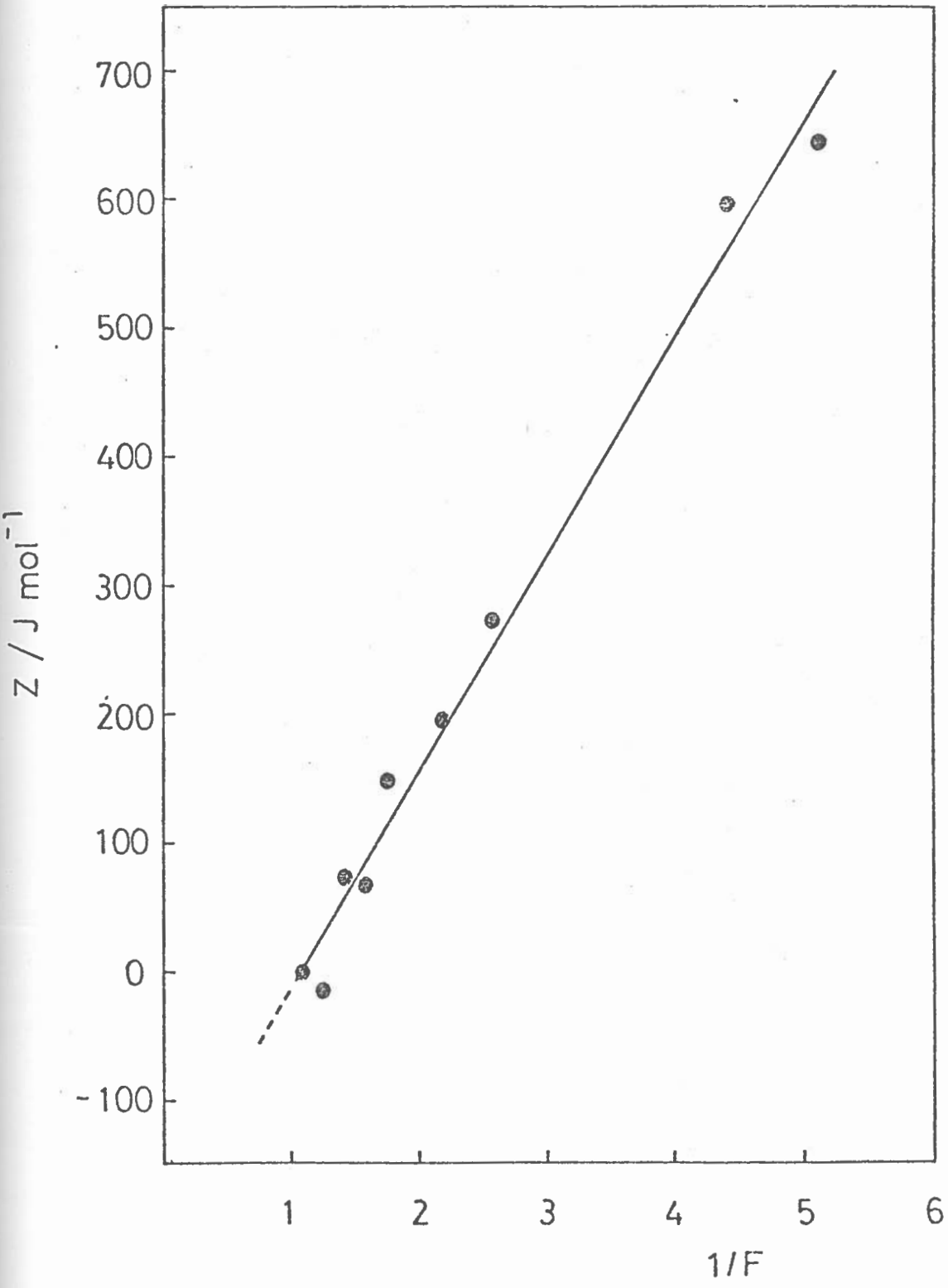

Fig. 14.2

Z versus 1/F. Full circles are experimental; line is from eqn (14.9)

$$H^E_{\frac{1}{2}} \simeq 2.0\,\text{kJ mol}^{-1} .$$

In principle, since G^E was determined at two temperatures, we could attempt to estimate the H^E values using eqn (8.3) for the two liquid mixtures in equilibrium. This method can be applied when the interval of temperatures is small, as it is indeed in the present case. However, for the result to have any worth the G^E values have to be known with great precision. In the present case the calculated excess molar Gibbs energies bear standard deviations of about ± 8 to $\pm 9\,\text{J mol}^{-1}$, and this is far above the acceptable uncertainty limites. In fact, the uncertainty in $\Delta(G^E/T)$ comes out as

$$\varepsilon\,[\Delta(G^E/T)] \simeq \pm\ 10^{-1}\ \text{J mol}^{-1}\ \text{K}^{-1} ,$$

and since

$$\Delta(1/T) \simeq 5 \times 10^{-4}\ \text{K}^{-1} ,$$

the final uncertainty in H^E would be

$$\varepsilon(H^E) = \frac{\varepsilon[\Delta(G^E/T)]}{\Delta(1/T)} \simeq \pm\ 200\ \text{J mol}^{-1} ,$$

even assuming that the temperature is known with zero error. Therefore, in this case, the calculation of H^E from eqn (8.3) and the knowledge of the G^E values is meaningless.

Having studied the three possible binary systems involving HCℓ, CF_4 and Xe, the excess properties at 159.01 K of the equimolar mixture in each of these systems are summarized in Table 14.3, to allow a quick comparison of the differences between them. (The equimolar mixture for $HCℓ + CF_4$ is, of course, hypothetical.)

TABLE 14.3

EXCESS MOLAR THERMODYNAMIC PROPERTIES (EQUIMOLAR MIXTURE) OF THE SYSTEMS $HC\ell + Xe$, $Xe + CF_4$ AND $HC\ell + CF_4$

System	$\frac{T}{K}$	$G^E_{\frac{1}{2}}$	$H^E_{\frac{1}{2}}$	$TS^E_{\frac{1}{2}}$	$V^E_{\frac{1}{2}}$
		J mol^{-1}			cm^3 mol^{-1}
$HC\ell + Xe$	159.01	698[a]			
	182.32	685[a]	813	128	
	195.47	655[a]			0.66[a]
$Xe + CF_4$	159.01	644[b]	959	315	1.94
$HC\ell + CF_4$	159.01	(1290)	(1975)	(685)	-
	173.08	(1205)			

a - From reference (7)

b - From reference (8)

14.6 REFERENCES

(1) PRICHARD, P.C., 'A comparison of some Thermodynamic Properties of Some Simple Isotopic Compounds', (Part II) Thesis, University of Oxford (1968).

(2) LEWIS, D.G., 'A Comparison of Some Thermodynamic Properties of Hydrogen Chloride and Deuterium Chloride', (Part II) Thesis, University of Oxford (1973).

(3) GIAUQUE, W.B. and WIEBE, R., J. Am. Chem. Soc., 1928, 50, 101.

(4) TERRY, M.J., LYNCH, J.T., BUNCLARK, M., MANSELL, K.R. and STAVELEY, L.A.K., J. Chem. Thermodynamics, 1969, 1, 413.

(5) PERRY, R.H. and CHILTON, C.H., 'Chemical Engineers' Handbook', 5th ed., McGraw-Hill, New York, (1973).

(6) SMITH, J.H. and PACE, E.L., J. Phys. Chem., 1969, 73, 4232.

(7) CALADO, J.C.G., KOZDON, A.F., MORRIS, P.J., PONTE, M.N.da, STAVELEY, L.A.K. and WOOLF, L.A., J. Chem. Soc., Faraday I, 1975, 71, 1372.

(8) CLANCY, P., GUBBINS, K.E., LOBO, L.Q., McCLURE, D.W. and STAVELEY, L.A.K., 1975/1979 (to be published).

CHAPTER 15

THE SYSTEM NITROUS OXIDE + ETHYLENE

15.1 INTRODUCTION

This chapter is concerned with a system in which both types of molecule lack dipole moments (at least, of any significant magnitude), but have quadrupole moments of opposite sign. The general behaviour of such systems has already been explored theoretically by GUBBINS and his collaborators[1], who showed that the mixing of such molecules could lead to negative values of all three primary excess functions. It has been known for some time that the system carbon dioxide + acetylene ($CO_2 + C_2H_2$), which falls in this category, does in fact exhibit negative azeotropy, indicative of the favourable 'association' into which such molecules can enter. TWU and GUBBINS[2] obtained good agreement between theory and experiment for the liquid-vapour curves of three systems of this general type: $CO_2 + C_2H_4$, $CO_2 + C_2H_2$ and $C_2H_4 + C_2H_6$. But as far as we are aware, measurements of the three primary excess functions for a suitable model system have not yet been made †.

As already mentioned (Chapter 10), STOGRYN and STOGRYN[4] selected for the quadrupole moment of ethylene a value of $Q(C_2H_4) = +1.5 \times 10^{-26}$ esu cm^2 $= +5.0 \times 10^{-40}$ C m^2, but the significantly higher value of $Q(C_2H_4) = +3.85 \times 10^{-26}$ esu cm^2 $= +12.8 \times 10^{-40}$ C m^2 due to SPURLING and MASON[5] has been found[2,6] to give good results in perturbation theory. In this molecule, the negative charges of the quadrupole are located at the central region of the molecule, whereas in that of nitrous oxide it is the positive

---

† Recently, after this work was completed, AZEVEDO[3], in this laboratory, measured H^E for $C_2H_4 + C_2H_6$ at 162 K. The quadrupole moment of C_2H_6 is, however, much smaller than that of N_2O.

charges which are effectively situated on or near the central nitrogen atom; $Q(N_2O) = -3.0 \times 10^{-26}$ esu cm^2 $= -10.0 \times 10^{-40}$ C m^2.[4] The sign and the magnitude of the quadrupole moments of N_2O and C_2H_4 (which are not seriously smaller numerically than those of CO_2 and C_2H_2 respectively), and also, from the practical point of view, the conformity of N_2O and C_2H_4 to general rules mentioned in previous chapters of this thesis, determined the choice made of these two components. However, it should be added that in carrying out work on this system we were aware that it is a thermodynamically unstable mixture, and while our own experiments were completed without any untoward incident, mixtures of nitrous oxide and a hydrocarbon have been known to ignite spontaneously[7]. (The pressure and temperature at which this occurred were, however, considerably higher than those at which our own measurements were made.)

We report in this chapter experimental results for G^E and V^E for the system $N_2O + C_2H_4$ at 182.32 K (the triple-point temperature of nitrous oxide). We shall see that the volume of mixing V^E has a surprising dependence on composition. The excess enthalpy H^E was measured at a slightly higher temperature (184.01 K).

15.2 DETERMINATION OF G^E, V^E AND H^E

The auxiliary information required in the evaluation of the excess functions from the experimental measurements has already been indicated (Chapter 10) as regards nitrous oxide (component 1). For the second virial coefficient of ethylene at room temperature we used unpublished results of LEE and SAVILLE[8] and those recorded by DOUSLIN and HARRISON[9]. In the light of these results the low-temperature values of B_{22} reported by EUCKEN and PARTS[10] were not considered reliable, so that we used PITZER and CURL's equation, eqn (10.1), to estimate

$$B_{22}\,(182.32\,\mathrm{K}) = -387\ \mathrm{cm^3\ mol^{-1}}\ .$$

The acentric factor

$$\omega_2 = 0.086$$

needed in the above calculation of B_{22} was derived, through eqn (10.2), using vapour pressures taken from MICHELS and WASSENAAR[11] and critical constants determined by DOUSLIN and HARRISON[9]. The expansion coefficient of liquid C_2H_4 was found to be

$$\alpha^*_{P,2} \simeq \alpha^*_{\sigma,2} = 2.7 \times 10^{-3}\ K^{-1}$$

from the molar volumes reported by MENES *et al.*[12]. This value was then used in eqn (7.20) to estimate the isothermal compressibility, giving

$$\kappa^*_{T,2} \simeq 2.2 \times 10^{-3}\ MPa^{-1} .$$

The molar enthalpy of vaporization of ethylene at 184.01 K was determined in the usual way from data of EGAN and KEMP[13] at the normal boiling point, giving

$$\Delta H_{v,2}\ (184.01\ K) = 13060\ J\ mol^{-1} .$$

The corresponding volume change on vaporization, calculated as before, is

$$\Delta V_{v,2}\ (184.01\ K) = 6930\ cm^3\ mol^{-1} .$$

15.2.1 *G^E AT 182.32 K*

The vapour pressure results are presented in Table 15.1 together with the corresponding G^E values derived by Barker's method. G^E conforms to the Redlich-Kister equation

$$G^E/RT = x_1 (1 - x_1) \left[A_G + B_G (2 x_1 - 1) \right] , \qquad \ldots (15.1)$$

with

$$A_G = 0.4457 \quad (\sigma_A = 0.0011)$$

$$B_G = 0.0674 \quad (\sigma_B = 0.0027) .$$

The value of G^E for the equimolar mixture is

$$G^E_{\frac{1}{2}} = 168.9 \pm 1.6\ J\ mol^{-1} .$$

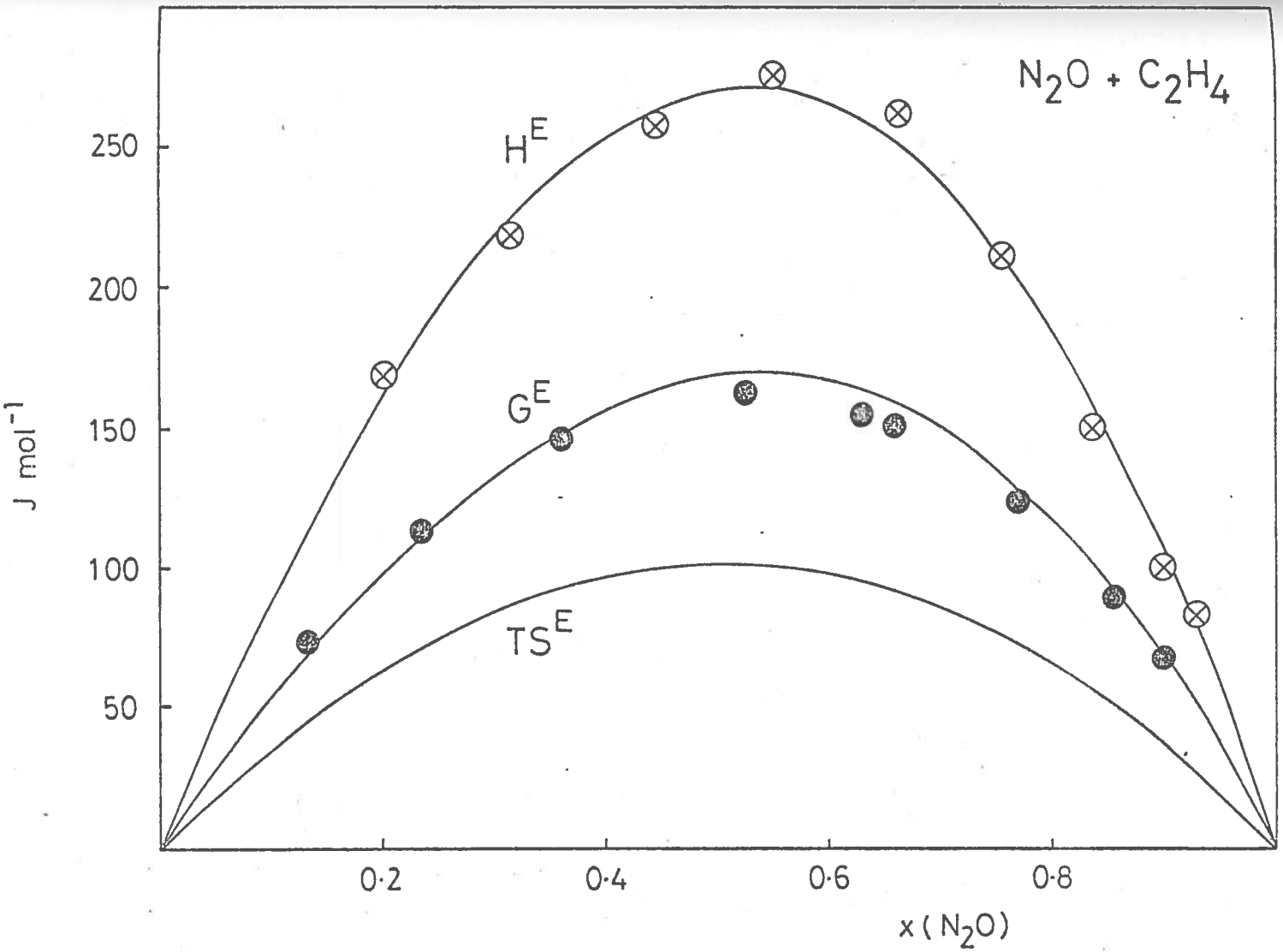

Fig. 15.1

$N_2O + C_2H_4$: G^E (182.32 K), H^E (184.01 K) and $TS^E = H^E - G^E$ as functions of composition

The experimental points and the curve obtained from eqn (15.1) are shown in Fig. 15.1.

TABLE 15.1

VAPOUR PRESSURE AND EXCESS MOLAR GIBBS ENERGY OF $N_2O + C_2H_4$ AT 182.32 K.

x_1	y_1	P/kPa	R_p/kPa	G^E/J mol^{-1}
0.0000	0.0000	205.216	-	0
0.1365	0.0886	194.499	+ 0.061	73.2
0.2380	0.1497	186.071	+ 0.017	113.2
0.3628	0.2235	175.282	+ 0.030	146.6
0.5236	0.3246	160.078	- 0.000	162.3
0.6322	0.4047	148.350	- 0.128	154.5
0.6583	0.4260	145.392	- 0.071	151.0
0.7727	0.5377	130.807	+ 0.161	123.8
0.8571	0.6521	117.540	+ 0.119	89.3
0.8968	0.7236	110.112	- 0.152	67.5
1.0000	1.0000	87.866	-	0

15.2.2 *V^E AT 182.32 K*

The molar volumes of liquid mixtures of known composition and the corresponding V^E values are given in Table 15.2. V^E is plotted against x_1 in Fig. 15.2. The shape of the curve in this figure is quite unlike any we have encountered before. It is not possible to fit the V^E values to the usual expression, eqn (6.7), with a reasonable number of parameters. Attempts to achieve a fit by introducing Myers and Scott's 'skewing parameter' D_V [corresponding to B_1 in eqn (5.36)].

$$V^E = x_1(1 - x_1)\,\frac{[A_V + B_V(2x_1 - 1) + C_V(2x_1 - 1)^2]}{1 + D_V(2x_1 - 1)}, \quad \ldots (15.2)$$

also failed. All of the curve except the small portion in the immediate neighbourhood of the minimum can be fitted by two equations, but the value of this is limited — it would help, for example, in evaluating the partial

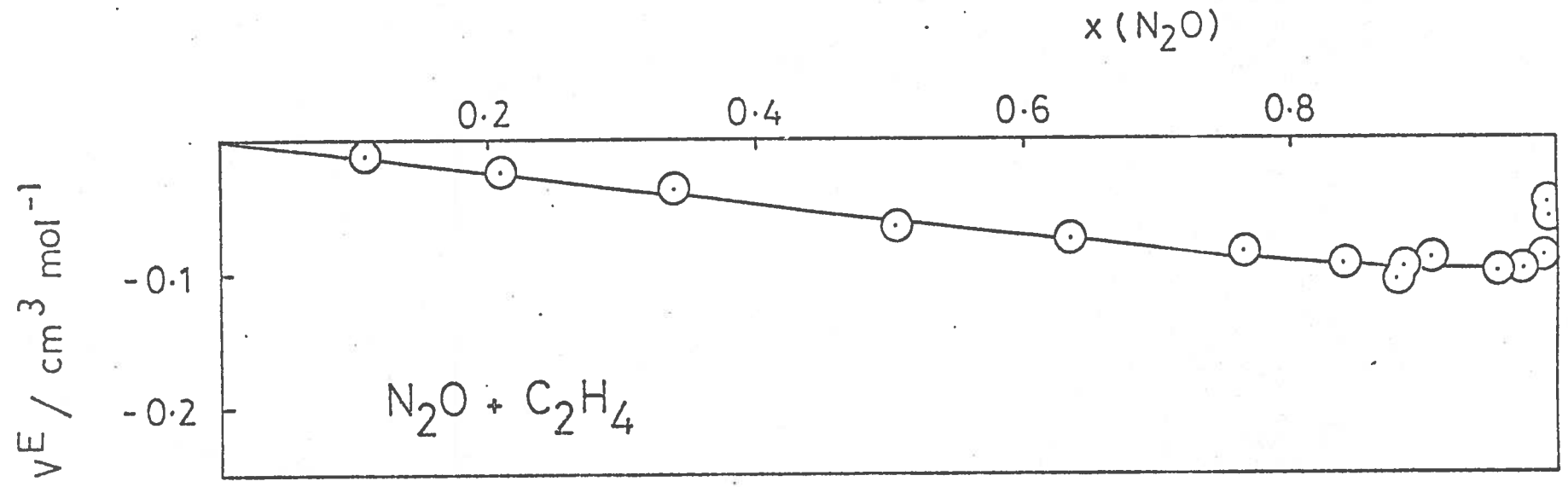

Fig. 15.2

$N_2O + C_2H_4$: V^E (182.32 K) as a function of composition.

TABLE 15.2

MOLAR VOLUMES AND EXCESS MOLAR VOLUMES OF $N_2O + C_2H_4$ AT 182.32 K

x_1	$V/cm^3\ mol^{-1}$	$V^E/cm^3\ mol^{-1}$	x_1	$V/cm^3\ mol^{-1}$	$V^E/cm^3\ mol^{-1}$
0.0000	51.104	0	0.8852	37.182	- 0.097
0.1115	49.350	- 0.011	0.9078	36.836	- 0.091
0.2133	47.747	- 0.024	0.9561	36.073	- 0.100
0.3410	45.739	- 0.038	0.9730	35.810	- 0.099
0.5049	43.152	- 0.066	0.9885	35.575	- 0.091
0.6368	41.084	- 0.075	0.9963	35.488	- 0.057
0.7652	39.069	- 0.084	0.9967	35.488	- 0.051
0.8396	37.897	- 0.094	1.0000	35.487	0
0.8825	37.216	- 0.106			

molar volumes. The two best equations appeared to be the following:

for $x_1 < 0.980$

$$V^E = x_1 \left[A'_V + B'_V x_1 + C'_V x_1^2\right] \qquad \ldots (15.3)$$

with

$$A'_V = - 0.094\ cm^3\ mol^{-1}$$

$$B'_V = - 0.101\ cm^3\ mol^{-1}$$

$$C'_V = + 0.096\ cm^3\ mol^{-1} \ ,$$

the standard deviation being

$$\sigma'(V^E) = \pm 0.005\ cm^3\ mol^{-1}$$

and

for $x_1 > 0.988$

$$V^E = x_2 \left[A''_V + B''_V x_2\right] \ , \qquad \ldots (15.4)$$

where

$$A''_V = - 15.6\ cm^3\ mol^{-1}$$

$$B''_V = 655\ cm^3\ mol^{-1}$$

with

$$\sigma''(V^E) = \pm 0.010\ cm^3\ mol^{-1} \ .$$

15.2.3 *H^E AT 184.01 K*

The H^E results obtained at a temperature of 184.01 ± 0.03 K are presented in Table 15.3, in the form adopted in previous chapters. As regards the conditions to which the tabulated H^E values apply, we estimate that for none of the mixtures studied does the difference $H^E(P_m) - H^E(0)$ exceed 0.1 J mol^{-1}. As this figure is considerably less than the precision of the H^E measurements, the values listed in Table 15.3 can be regarded as being either $H^E(P_m)$ or $H^E(0)$.

TABLE 15.3

EXCESS MOLAR ENTHALPY OF $N_2O + C_2H_4$ AT 184.01 ± 0.03 K

n_1/mol	n_2/mol	x_1	y_1	Q/J	$\psi_{6,7}$/J	$H^E(0)$/J mol^{-1}	R_H/J mol^{-1}
0.01280	0.05167	0.1993	0.1288	12.373	- 1.493	169.0	+ 7.3
0.02223	0.04798	0.3158	0.2019	16.019	- 0.737	217.7	- 7.2
0.03735	0.04585	0.4465	0.2851	21.176	+ 0.258	257.3	- 7.4
0.03955	0.03150	0.5518	0.3568	18.560	+ 1.098	275.9	+ 5.0
0.04649	0.02277	0.6638	0.4438	16.065	+ 2.156	262.0	+ 11.7
0.04651	0.01419	0.7549	0.5308	9.753	+ 3.134	210.9	- 0.5
0.04725	0.00822	0.8362	0.6313	4.184	+ 4.186	149.5	- 9.6
0.08327	0.00839	0.8973	0.7318	4.055	+ 5.184	100.2	- 8.1
0.08249	0.00477	0.9325	0.8051	1.543	+ 5.767	83.2	+ 8.7

The curve of H^E against mole fraction only shows slight asymmetry, being adequately represented by the equation

$$H^E/RT = x_1 (1 - x_1) \left[A_H + B_H (2 x_1 - 1) \right] , \qquad \ldots (15.5)$$

with

$$A_H = 0.7082$$

$$B_H = 0.0759 .$$

The standard deviation of the H^E values is

$$\sigma(H^E) = \pm 8.9 \text{ J mol}^{-1} ,$$

and for the equimolar mixture

$$H^E_{\frac{1}{2}}(0) = 270.9 \text{ J mol}^{-1} .$$

Assuming that H^E at 182.32 K is not significantly different from the measured values at 184.01 K, a combination of eqns (15.1) and (15.5) gives for the excess molar entropy S^E,

$$S^E/R = x_1 (1 - x_1) \left[A_S + B_S (2 x_1 - 1) \right] \qquad \ldots (15.6)$$

with

$$A_S = 0.2625$$

$$B_S = 0.0085 ,$$

and

$$TS^E_{\frac{1}{2}} = 102.0 \text{ J mol}^{-1} .$$

The H^E and TS^E curves are shown in Fig. 15.1.

15.3 DISCUSSION

ROWLINSON *et al.*[13] also studied the vapour-liquid equilibrium of $N_2O + C_2H_4$ but as their measurements were made at much higher temperature and pressure conditions no useful comparison can be made with our own results.

Figure 15.1 makes it apparent that the G^E experimental points in the central region of the diagram fall somewhat off (for this system, below) the curve calculated from eqn (15.1). This is in contrast with the results for all the other systems we have studied. In the present case the deviations are only slight but from time to time appreciable discrepancies have emerged from the work of several laboratories[14] between the G^E values evaluated directly from each set of measurements (i.e. vapour pressure and liquid-vapour compositions), and those calculated (through Barker's method) from the Redlich-Kister equation. These differences in the derived G^E values have been attributed to the inadequacy of the Redlich-Kister equation[15], namely to the non-orthogonality of the polynomial coefficients of A_G, B_G and C_G in eqns (AI.4) and (AI.5), Appendix (I), rather than to Barker's method in itself. We do not share this opinion. In fact,

(i) if the G^E residuals, $R_G = G^E_{exp} - G^E_{calc}$, in the central part of the diagram were due to any intrinsic shortcomings of the Redlich-Kister equation, it would not be possible to obtain better fittings of the experimental G^E values by using an equation of the same type (with slightly different parameters); and

(ii) if the reported differences were a consequence of the non-orthogonality of the coefficients of A_G, B_G and C_G, it would be reasonable to expect a decrease in such residuals by neglecting all the experimental points falling outside a composition interval of, say, $0.2 < x < 0.8$. This would follow because the x values outside such an interval provide the main contribution to the 'non-orthogonality' of the polynomial coefficients.

CALADO and SOARES[14b] themselves provided the information necessary to contradict assumption (i) above. They obtained a better representation for the $CH_4 + C_2H_4$ experimental G^E values by <u>directly</u> fitting their experimental points to a Redlich-Kister equation, rather than by minimizing the pressure residuals through Barker's method combined with the Redlich-Kister expansion for G^E. As regards assumption (ii), we have repeated the calculation for $N_2O + C_2H_4$ (using Barker's method and the Redlich-Kister equation) but excluding from the input data the three points for which the condition $0.2 < x < 0.8$ is not satisfied. As a result, not only was there no improvement in the fitting, but indeed a slight increase of the G^E residuals for the central points of the diagram was observed. It is, therefore, still possible that the reported deviations arise as a consequence of Barker's method itself. This method does in fact minimize the pressure residuals instead of the G^E residuals, and since G^E is a complex function not only of the compositions but also of the pressure, it does not immediately follow that R_G and R_P must reach simultaneously their respective minima [i.e. the values of P_{calc} that produce the minimum $\sum (R_p)^2$ may not give at the same time the minimum $\sum (R_G)^2$]. This is a complex statistical

problem, and to attempt to find the mathematical solution to it is clearly beyond the scope of the present work, so we shall not consider this subject any further. (Why such deviations, when they occur, always appear in the central region of the diagram is another matter for which such an examination might also provide the answer.)

Although the molecules of the two components have quadrupoles of opposite sign, G^E, H^E and S^E are all positive. The contrast between the almost symmetrical dependence of these functions on composition and that of V^E is very striking. The shape of this curve is extremely uncommon so that considerable care was taken in the determination of the corresponding experimental points. As will be seen from Table 15.2 several measurements of the molar volume of mixtures were carried out at low mole fractions of ethylene. These measurements were made alternately with determinations of the molar volumes of the pure components, to force any systematic errors to become apparent if there were faults in the experimental technique. The molar volumes of the pure liquids determined on this occasion are in perfect agreement with the results obtained at other stages of the author's work. It is reassuring to note the good agreement between the value of 51.098 ± 0.007 $cm^3\ mol^{-1}$ for the molar volume of pure C_2H_4 at 182.32 K, as recently obtained by HAYNES[16] using the buoyancy technique, and our own result of

$$V_2^*(182.32\,K) = 51.104 \pm 0.005\ cm^3\ mol^{-1}$$

which is the mean of four independent determinations carried out in 1976/77. The validity of our V^E results does not, of course, depend critically on the absolute accuracy of the measurements on the pure liquids, but the consistency of the latter leads us to have confidence in the reality of the results for the mixtures. Moreover, calculation of the errors associated with the measurements for the two more dilute solutions of ethylene in nitrous oxide gives an upper limit of ± 0.023 $cm^3\ mol^{-1}$ for the uncertainty

in V^E for these mixtures. This means that in the most unfavourable circumstances these two values of V^E would be still small and negative, being thus significantly different from those of neighbouring points.

The plot of V^E against mole fraction in Fig. 15.2 implies that the partial molar volume of ethylene in very dilute solution of nitrous oxide is much smaller than the molar volume of pure C_2H_4, but that as the concentration of ethylene increases the partial molar volume of this component rapidly becomes much greater, so that at mole fractions of ethylene above 0.02 it is only slightly different from the molar volume of the pure liquid. In fact, from eqn. (15.4), the partial molar volume of C_2H_4 at infinite dilution is 35.46 $cm^3\ mol^{-1}$, virtually identical with the molar volume of nitrous oxide. It has been suggested by CRAWFORD *et al.*[17], on the basis of a comparison of the melting behaviour of argon and nitrogen, that <u>liquid</u> nitrogen may have more local orientational order near the triple-point than the <u>solid</u> in the high-temperature form. STREETT[18] and WANG *et al.*[19] also found, from Monte Carlo and Molecular Dynamics calculations, that for quadrupolar diatomic molecules the minimum of the intermolecular potential energy function is deeper when the molecules tend to orientate towards each other in a T-shape (perpendicular) arrangement, in the liquid phase. This might suggest that liquid nitrous oxide, with linear molecules with a larger quadrupole moment than nitrogen, may be a still more highly structured liquid at the triple-point. Perhaps a very few ethylene molecules can then be accommodated in liquid nitrous oxide in a way which makes only about the same spatial demand per ethylene molecule as a molecule of N_2O itself. This is consistent with the interpretation given before (Chapters 10 and 13) for the behaviour of mixtures containing liquid N_2O at its own triple-point temperature.

For reasons already mentioned, we do not normally extend our H^E measurements below a mole fraction of one component of ~ 0.2. However, in

view of the interest engendered by the V^E results in solutions dilute in C_2H_4, three H^E determinations were made at $x_2 < 0.2$. The small, endothermic effect observed in this region is 'normal', so to say, and consistent with the trend of the remaining points on the H^E curve. Since no dramatic energy release is localized at or near the composition of the minimum of the V^E curve, it is plausible that the first few C_2H_4 molecules may fit into vacancies in or near small, ordered N_2O clusters until saturation of such sites. The introduction of more ethylene molecules would not, however, bring about any radical alteration of the intermolecular energy of interaction, nor perhaps of the molecular packing in the solution.

15.4 REFERENCES

(1) FLYTZANI-STEPHANOPOULOS, M., GUBBINS, K.E. and GRAY, C.G. Mol. Phys., 1975, 30, 1649.

(2) TWU, C.-H. and GUBBINS, K.E., Chem. Eng. Sci., 1978, 33, 879.

(3) AZEVEDO, E.J.S.G., 1978 (to be published).

(4) STOGRYN, D.E. and STOGRYN, A.P., Mol. Phys., 1966, 11, 371.

(5) SPURLING, T.H. and MASON, E.A., J. Chem. Phys., 1967, 46, 322.

(6)(a) TWU, C.-H., 'Perturbation Theory for High Pressure Behaviour of Liquid Mixtures', (Ph.D.) Dissertation, University of Florida, (1976).

(b) GUBBINS, K.E. and TWU, C.-H., communication to the Engineering Foundation Conference on The Estimation and Correlation of Phase Equilibria and Fluid Properties in the Chemical Industry, Pacific Grove, California, U.S.A., 1977.

(c) CLANCY, P., GUBBINS, K.E. and GRAY, C.G., Faraday Disc., 1979, 66 (in press).

(7) ROWLINSON, J.S. 1977 (private communication).

(8) SAVILLE, G., 1977/1978 (private communication).

(9) DOUSLIN, D.R. and HARRISON, R.H., J. Chem. Thermodynamics, 1976, 8, 301.

(10) EUCKEN, A. and PARTS, A., Z. physik. Chem., 1933, B20, 184.

(11) MICHELS, A. and WASSENAAR, T., Physica, 1950, 16, 221.

(12) MENES, F., DORFMÜLLER, T. and BIGELEISEN, J., J. Chem. Phys., 1970, 53, 2869.

(13) ROWLINSON, J.S., SUTTON, J.R. and WESTON, J.F., Proc. Joint Conference Thermodynamics and Transport Properties of Fluids, Inst. Mech. Eng., London, 1958.

(14)(a) CALADO, J.C.G., KOZDON, A.F., MORRIS, P.J., PONTE, M.N.da, STAVELEY, L.A.K. and WOOLF, L.A., J. Chem. Soc., Faraday I, 1975, 71, 1372.

(b) CALADO, J.C.G. and SOARES, V.A.M., J. Chem. Soc., Faraday I, 1977, 73, 1271.

(c) PARRISH, W.R. and HIZA, M.J., Adv. Cryogenic Engineering, 1978, 19, 300.

(d) WILLIAMSON, A.G. and SCOTT, R.L., J. Phys. Chem., 1961, 65, 275.

(15) KIDNAY, A.J., LEWIS, K.L., CALADO, J.C.G. and STAVELEY, L.A.K., J. Chem. Thermodynamics, 1975, 7, 847.

(16) HAYNES, W.M., Cryogenics, 1978, 18, 621.

(17) CRAWFORD, R.K., DANIELS, W.B. and CHENG, V.M., Phys. Rev., 1975, A 12, 1690.

(18) STREETT, W.B., communication to the Annual Chemical Congress, Faraday Division Symposium on Pair Interaction Between Molecules, Roy. Inst. Chem./Chem. Soc., London, 1977.

(19)(a) WANG, S.S., GRAY, C.G., EGELSTAFF, P.A. and GUBBINS, K.E., Chem. Phys. Lett., 1973, 21, 123.

(b) WANG, S.S., EGELSTAFF, P.A., GRAY, C.G. and GUBBINS, K.E., Chem. Phys. Lett., 1974, 22, 453.

CHAPTER 16

THE SYSTEM ETHYLENE + METHANE

16.1 INTRODUCTION

The system dealt with here is one in which the molecules of component 2 — ethylene, C_2H_4 — have a quadrupole, while those of component 1 — methane, CH_4 — bear an octupole. In view of the technical importance of methane and ethylene, it is not surprising that a considerable amount of work has already been carried out on liquid mixtures of these two hydrocarbons. For example, at least eight studies of the liquid-vapour equilibrium have been made, which have been briefly reviewed by CALADO and SOARES[1]. Of those investigations carried out below the critical temperature of metane (190.555 K), the three most accurate appear to be those of HSI and LU[2], who measured liquid-vapour equilibrium compositions at 148, 159 and 169 K, of MILLER, KIDNAY and HIZA[3], who determined these compositions and the total vapour pressure at 10 K intervals from 150 to 190 K, and of CALADO and SOARES themselves, who measured the total vapour pressure of the system as a function of composition at 103.94 and 115.77 K, and also the volume change on mixing, V^E, at 103.94 K.

From the results of these studies, estimates were made of the molar excess Gibbs energy G^E as a function of composition. CALADO and SOARES showed that while their own estimates of G^E for the equimolar mixture at the two lowest temperatures could be regarded as consistent with the G^E values at higher temperatures derived either from the work of HSI and LU or from that of MILLER *et al.*, the last two sets of measurements are not in good agreement with each other. To try and resolve this uncertainty in the G^E values at higher temperatures, we have measured calorimetrically the enthalpy of mixing H^E of liquid methane (admitted into the lower

chamber of the apparatus) and liquid ethylene at three temperatures: 115.77 ± 0.02, 140.12 ± 0.03 and 150.00 ± 0.05 K. Information on H^E and its temperature dependence makes it possible to predict the temperature dependence of G^E. In the following sections we report our results for H^E and apply them to an examination of the temperature dependence of G^E.

16.2 DETERMINATION OF H^E AT 115.77, 140.12 AND 150.00 K

The information at present available for the $CH_4 + C_2H_4$ system on V^E, the second virial coefficients, and to some degree on the energies of vaporization of the two components is not as accurate or reliable as could be desired. Here we will summarize the steps by which our own estimates of these quantities were reached, as well as the values used for the remaining ancillary properties needed in the calculation of H^E from the raw calorimetric data.

(i) V^E has been measured at 103.94 K by CALADO and SOARES[1], but not, as far as we are aware, at any other temperature. At 103.94 K it is small and negative ($V^E_{\frac{1}{2}} = -0.184 \pm 0.012$ cm^3 mol^{-1}). By analogy with other systems for which V^E has been determined over a temperature range we might expect V^E to increase numerically, while remaining negative, with rising temperature, so that term ψ_2 in eqn (7.14) could become an important factor in our calculations at the higher temperatures. Since ethylene does not conform to the principle of corresponding states the estimation of V^E through an equation of state seemed to be preferable to using methods based on that principle. Therefore, we have used a semi-empirical approach involving an equation of state with a van der Waals-type attraction term, and a repulsive term derived by GIBBONS[4,5] for hard convex particles of arbitrary shape. This method is explained in detail in the Appendix [Appendix (N)]. The resulting calculated values

of V^E fit the usual equation

$$V^E = x_1 (1 - x_1)[A_V + B_V (2 x_1 - 1) + C (2 x_1 - 1)^2] , \qquad \ldots (16.1)$$

with parameters, respectively,

$A_V = - 1.30$ $B_V = - 0.30$ $C_V = - 0.10$ at 116 K

$- 3.18$ $- 1.08$ $- 0.47$ at 140 K

and $- 5.70$ $- 1.75$ $- 0.70$ at 150 K ,

all these being expressed in $cm^3\ mol^{-1}$.

The density of liquid methane was taken from the paper by HAYNES and HIZA[6], and that of ethylene from the work of MENES *et al.*[7], since the more accurate data of HAYNES[8] only very recently became available, after this calculation was made. The difference between the two sets of measurements does not influence the final H^E results to any significant extent.

(ii) Measurements of the second virial coefficient from room temperature down to 155.89 K for methane, 243.6 K for ethylene, and 223.3 K for several mixtures of the two gases have been made by LEE and SAVILLE[9]. Their results show that, well within experimental error, the quantity δ_{12}, defined by eqn (5.20), in the entire interval of temperatures studied is given by the equation

$$\delta_{12}/cm^3\ mol^{-1} = 11.6 - 0.239\ T/K \qquad \ldots (16.2)$$

We have assumed that this linear relation persists to 116 K.

For methane, we have made use of the B values selected by GOODWIN[10]. Since LEE and SAVILLE's results for ethylene stop at 243.6 K, and those of DOUSLIN and HARRISON[11] stop at 238.15 K, we have calculated B for this gas using the acentric factor method of PITZER and CURL[12], eqn (10.1). It is reassuring that the value

of B_{22} — the second virial coefficient of C_2H_4 — so obtained at 243.6 K agrees within 2% with the experimental values in both references[9.11]. The value of ω needed in the calculation of B_{22} was obtained as explained in Chapter 15.

(iii) The vaporization corrections are particularly important for the more volatile component (CH_4) at the higher temperatures. Enthalpies of vaporization ΔH_v have been tabulated by GOODWIN[10]. However, our calorimeter can be used to measure vaporization energies directly, simply by having one compartment initially evacuated and closed while the other contains a sample of the liquefied gas. We have therefore measured this quantity for liquid methane at 140.09 and 149.98 K in this way. At the lower temperature, our result of

$$\Delta H_{v,1}\,(140.09\,\mathrm{K}) = 7000\ \mathrm{J\ mol^{-1}}$$

is in fair agreement with the value obtained from GOODWIN's enthalpy compilation of 7139 J mol^{-1}. At 149.98 K the discrepancy is rather larger, the two values being

$$\Delta H_{v,1}\,(149.98\,\mathrm{K}) = 6310\ \mathrm{J\ mol^{-1}} \quad \text{(measured)}$$

and $6612\ \mathrm{J\ mol^{-1}}$ (GOODWIN).

At 115.77 K [10]

$$\Delta H_{v,1}\,(115.77\,\mathrm{K}) = 8079\ \mathrm{J\ mol^{-1}}\ .$$

The enthalpy of vaporization of ethylene was estimated, in the usual way, from EGAN and KEMP's[13] experimental value at the normal boiling point of this substance, giving

$$\Delta H_{v,2}\,(115.77\,\mathrm{K}) = 15440\ \mathrm{J\ mol^{-1}}$$

$$\Delta H_{v,2}\,(140.12\,\mathrm{K}) = 14550\ \mathrm{J\ mol^{-1}}$$

$$\Delta H_{v,2}\,(150.00\,\mathrm{K}) = 14200\ \mathrm{J\ mol^{-1}}\ .$$

(iv) For methane, the expansion coefficient α_P^* and the isothermal compressibility κ_T^* have been calculated from the velocity of sound data tabulated by GOODWIN[10]. The values so obtained,

$\alpha^*_{P,1} = 3.6 \times 10^{-3}\ K^{-1}$ $\quad \kappa^*_{T,1} = 2.4 \times 10^{-3}\ MPa^{-1}$ at 115.77 K,

$4.9 \times 10^{-3}\ K^{-1}$ $\quad 4.8 \times 10^{-3}\ MPa^{-1}$ at 140.12 K,

and $5.9 \times 10^{-3}\ K^{-1}$ $\quad 6.8 \times 10^{-3}\ MPa^{-1}$ at 150.00 K,

are only slightly higher than those presented in ROWLINSON's[14] book. For ethylene, the approximate methods of estimation described in Chapter 7 have been used, $\alpha^*_{P,2}$ being evaluated from the density measurements of MENES *et al.*[7]:

$\alpha^*_{P,2} \simeq 2.0 \times 10^{-3}\ K^{-1}$ $\quad \kappa^*_{T,2} \simeq 0.7 \times 10^{-3}\ MPa^{-1}$ at 115.77 K,

$2.2 \times 10^{-3}\ K^{-1}$ $\quad 1.1 \times 10^{-3}\ MPa^{-1}$ at 140.12 K,

and $2.3 \times 10^{-3}\ K^{-1}$ $\quad 1.3 \times 10^{-3}\ MPa^{-1}$ at 150.00 K.

H^E at 115.77 K was determined as a function of composition using G^E values from the work of CALADO and SOARES[1], and H^E at 150.00 K was first estimated using a provisional value of $G^E_{\frac{1}{2}}$ taken from MILLER *et al.*[3]. Assuming $H^E_{\frac{1}{2}}$ to be a linear function of temperature between 115.77 and 150.00 K, $G^E_{\frac{1}{2}}$ at 140.12 K was then estimated and H^E determined as a function of composition at this temperature. With these provisional estimates of H^E as a function of composition at the three temperatures improved expressions for G^E at 140.12 and 150.00 K were then obtained, which were in turn used to generate new H^E values. The process was repeated until self-consistency was obtained. The changes made in the original H^E values by this subsequent recycling are, however, small, in no case exceeding 15 J mol^{-1}.

In Table 16.1 we present values of $H^E(0)$, the enthalpy of mixing at zero pressure, calculated using our directly determined values of the

TABLE 16.1

EXCESS MOLAR ENTHALPY H^E FOR $CH_4 + C_2H_4$

T/K	n_1/mol	n_2/mol	x_1	Q/J	$\psi_{6,7}{}^a/J$	$H^E(0)^a$ / J mol^{-1}	$H^E(0)^b$ / J mol^{-1}	$R_H{}^a$ / J mol^{-1}
115.77	0.01820	0.05710	0.2368	+ 7.105	+ 5.169	163.8		- 1.6
± 0.02	0.01764	0.03342	0.3364	+ 7.427	+ 3.671	219.9		+ 6.7
	0.03249	0.04197	0.4309	+ 15.693	+ 2.710	249.4		+ 6.2
	0.03747	0.03554	0.5076	+ 16.151	+ 1.869	249.3		- 6.3
	0.03839	0.03268	0.5345	+ 15.641	+ 1.579	244.9		- 12.2
	0.03030	0.01585	0.6483	+ 10.993	+ 0.329	250.8		+ 5.0
	0.05708	0.01366	0.8039	+ 13.671	- 0.815	184.3		+ 4.6
140.12	0.01815	0.04222	0.2779	- 7.745	+ 18.619	181.0	173.4	+ 0.9
± 0.03	0.02631	0.04149	0.3649	- 0.716	+ 14.798	209.3	203.9	+ 3.8
	0.03514	0.03568	0.4753	+ 4.400	+ 10.167	209.4	205.9	- 8.3
	0.04847	0.02763	0.6201	+ 10.905	+ 4.390	206.1	204.7	+ 4.7
	0.05545	0.01082	0.8248	+ 11.444	- 3.877	119.2	120.7	- 0.6
150.00	0.02148	0.04630	0.2884	- 17.636	+ 28.668	159.1	134.7	+ 1.9
± 0.05	0.03277	0.03095	0.4789	- 5.512	+ 16.374	169.8	154.7	- 5.7
	0.03242	0.02140	0.5600	- 2.315	+ 11.423	172.4	159.5	+ 5.7
	0.04548	0.01332	0.7453	+ 6.283	+ 0.202	112.5	112.2	- 4.3
	0.05904	0.00485	0.9136	+ 14.300	- 11.137	51.3	61.9	+ 7.0
	0.04685	0.00283	0.9313	+ 13.986	- 12.390	33.4	49.6	- 2.1

a - Using $\Delta H_{v,1}$ from Ref. (10)

b - Using $\Delta H_{v,1}$ from this work

energy of vaporization of methane, as well as those obtained from GOODWIN's recommended $\Delta H_{v,l}$ values. The difference between $H^E(P_m)$ and $H^E(0)$ is always less than $0.5\,J\,mol^{-1}$. At the two higher temperatures, the magnitude of the vaporization corrections is much higher than at 115.77 K. The uncertainty in $\Delta H_{v,l}$ is certainly the chief contributor to the uncertainty in our final values of H^E.

$H^E(0)$ is plotted against the mole fraction of methane in Fig. 16.1. In this plot, (and from hereon in this Chapter) we use, for consistency, the estimates of $H^E(0)$ identified in Table 16.1 by superscript 'a', i.e. that based on the values of $\Delta H_{v,l}$ taken from GODDWIN's work.

The escess enthalpy fits the equation

$$H^E(0) = x_1 (1 - x_1)[A_H + B_H (2 x_1 - 1)] \qquad \ldots (16.3)$$

with the following values of A_H and B_H (in $J\,mol^{-1}$):

A_H = 1019.3 B_H = 197.6 at 115.77 K,

869.9 − 62.7 at 140.12 K,

and 696.0 − 164.6 at 150.00 K.

The standard deviations of these fittings are, respectively,

$$\sigma(H^E) = \pm 8.0 \text{ J mol}^{-1} ,$$

$$\pm 6.0 \text{ J mol}^{-1} ,$$

and $$\pm 6.0 \text{ J mol}^{-1} .$$

If the values of A_H and B_H at the three temperatures are fitted to quadratic expressions in the temperature,

$$A_H = A_{H0} + A_{H1} T + A_{H2} T^2 , \qquad \ldots (16.4)$$

and

$$B_H = B_{H0} + B_{H1} T + B_{H2} T^2 , \qquad \ldots (16.5)$$

then,

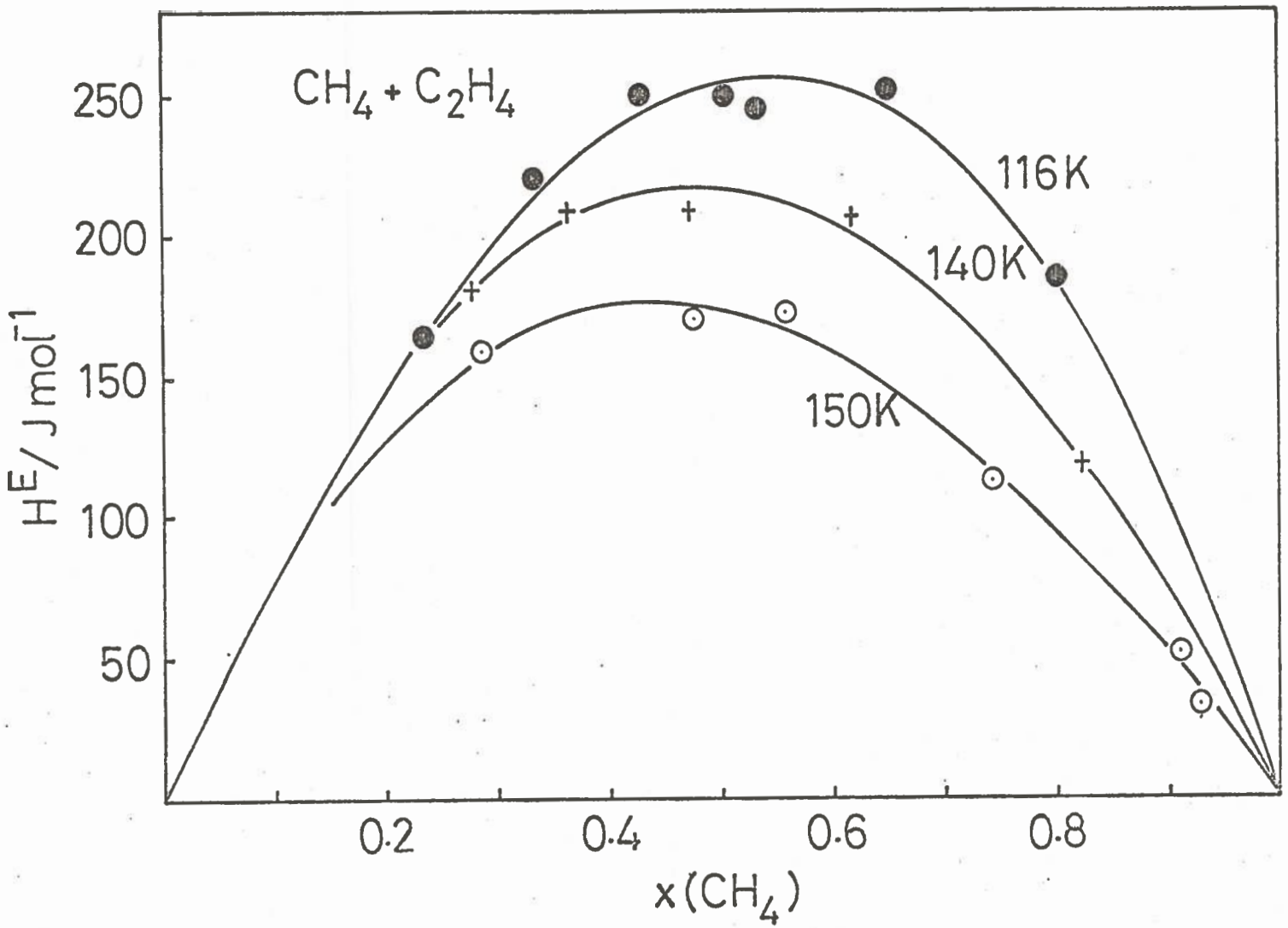

Fig. 16.1
$CH_4 + C_2H_4$: H^E as a function of composition at three temperatures (115.77, 140.12 and 150.00 K)

$A_{H0} = -3702.7\ J\ mol^{-1}$; $B_{H0} = 1613.5\ J\ mol^{-1}$

$A_{H1} = 79.559\ J\ mol^{-1}\ K^{-1}$; $B_{H1} = -13.503\ J\ mol^{-1}\ K^{-1}$

$A_{H2} = -0.3349\ J\ mol^{-1}\ K^{-2}$; $B_{H2} = 0.0110\ J\ mol^{-1}\ K^{-2}$

$H^E(0)$ can, then, be expressed as a function of both temperature and composition:

$$H^E(0) = x_1(1-x_1)[(A_{H0} + A_{H1}T + A_{H2}T^2) + (B_{H0} + B_{H1}T + B_{H2}T^2)(2x_1 - 1)] . \quad \ldots (16.6)$$

16.3 DISCUSSION

Values of H^E have recently been reported by MILLER and STAVELEY[15] for other binary mixtures of the general type 'octupolar molecules + quadrupolar molecules' involving methane and a second component other than ethylene, namely ethane and propane. It is perhaps interesting to note that $H^E_{\frac{1}{2}}$ at $T \simeq 112\ K$ for these systems varies according to the series

$$C_2H_4 > C_3H_8 > C_2H_6 .$$

The quadrupole moment of propane does not appear to have been measured yet but it is not unreasonable to accept that it may be larger than that of ethane, so that the $H^E_{\frac{1}{2}}$ values for the three mixtures seem to be arranged in the same order as the quadrupole moments of the second species present in these systems. H^E for the system $CH_4 + N_2$ has also been determined[16,17] at several temperatures, giving for $T \simeq 112\ K$ a value of $H^E_{\frac{1}{2}}$ which is about the same as that for $CH_4 + C_2H_6$. However, 112 K is sufficiently close to the critical temperature of nitrogen to make any comparison clearly pointless.

Use of equation (16.6) above 150 K means an extrapolation of uncertain reliability. However, the course taken by $H^E_{\frac{1}{2}}$ with rising temperature is similar to that found for the $Ar + CH_4$ [18] and $N_2 + CH_4$ [16] systems at

the saturation vapour pressure. For these systems $H^E_{\frac{1}{2}}$ becomes zero a few degrees ($\sim$ 14 K for $Ar + CH_4$ and $\sim$ 8 K for $N_2 + CH_4$) below the critical temperature of the more volatile component (Ar and N_2, respectively), and there are grounds for thinking that the same is true of the $Ar + Kr$ system (Chapter 8). According to eqn (16.6), $H^E_{\frac{1}{2}}$ becomes zero at 174.0 K, $\sim$ 17 K below the CH_4 critical point, so perhaps this equation gives a reasonable representation of the course of H^E above 150 K.

By combining eqn (16.6) with the general thermodynamic relation (8,3) we obtain the corresponding expression for G^E as a function of x_1 and T:

$$G^E = x_1 (1 - x_1)[(A_{H0} - A_{H1} T \ln T - A_{H2} T^2 + A_{H3} T) + (B_{H0} - B_{H1} T \ln T - B_{H2} T^2 + B_{H3} T)(2 x_1 - 1) + C_{H3} T (2 x_1 - 1)^2] \quad \ldots (16.7)$$

since, in general, the isothermal fitting of G^E as a function of the mole fraction involves a term in $(2 x_1 - 1)^2$. To determine the parameters A_{H3}, B_{H3} and C_{H3}, one experimental expression for G^E as a function of composition must be assumed and we have taken for this purpose the G^E results of CALADO and SOARES[1] at 115.77 K. We then obtain the following values for the parameters (in J mol^{-1} K^{-1}):

$$A_{H3} = 378.473 \qquad B_{H3} = -76.082 \qquad C_{H3} = 0.27 .$$

$G^E_{\frac{1}{2}}$, as derived from eqns (16.7), is plotted against temperature in Fig. 16.2 in which are also shown the experimental values of $G^E_{\frac{1}{2}}$ resulting[19] from the work of CALADO and SOARES[1], HSI and LU[2], MILLER *et al*[3], and VOLOVA[20].

It is apparent that our equation for G^E gives better agreement with the results of MILLER *et al.* than with those of HSI and LU. (VOLOVA's $G^E_{\frac{1}{2}}$

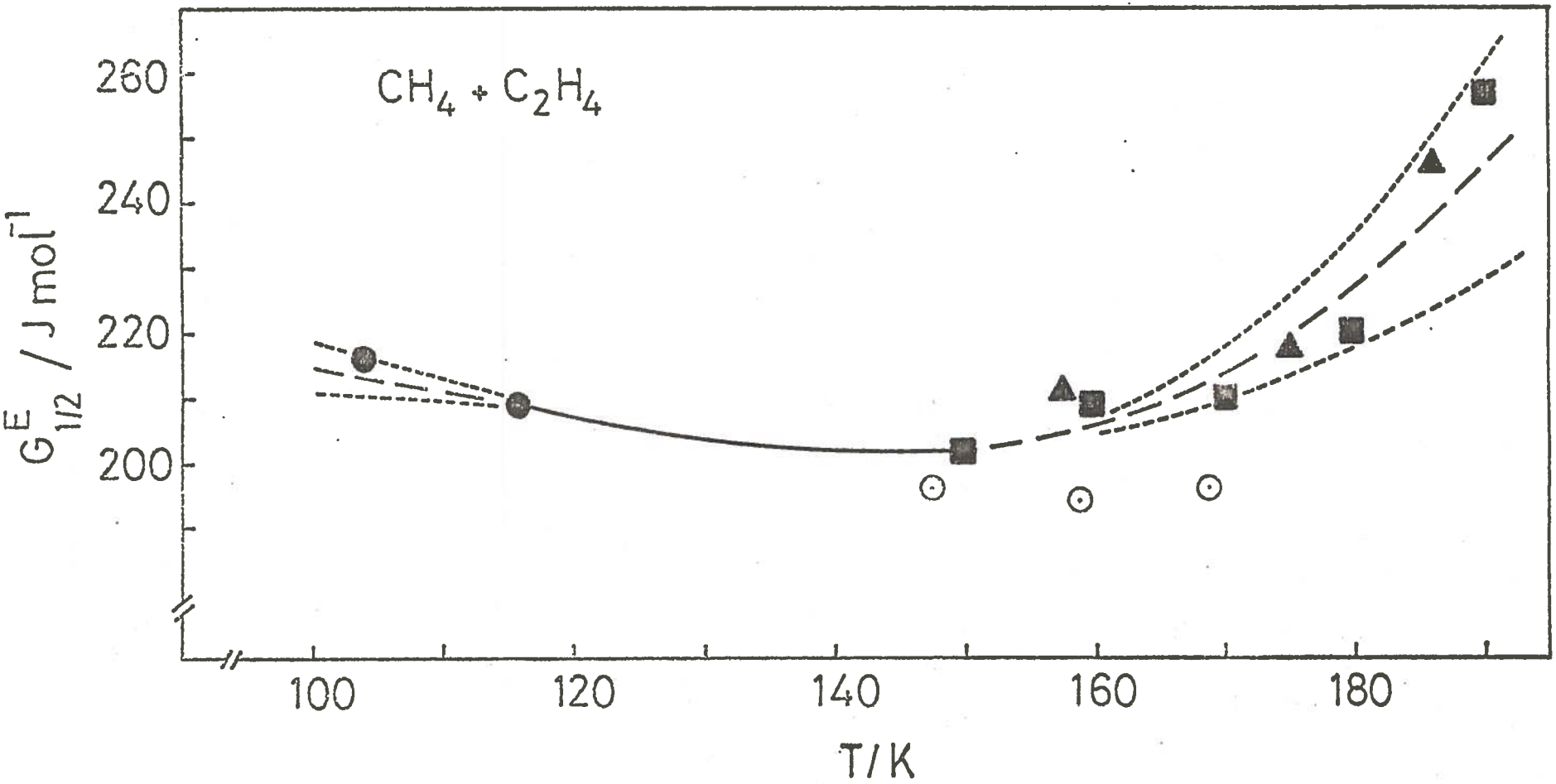

Fig. 16.2

$CH_4 + C_2H_4$: $G^E_{\frac{1}{2}}$ as a function of temperature. Full circles, Ref. (1); open circles, Ref. (2); full squares, Ref. (3); full triangles, Ref. (20). Full line from eqn (16.7), this work; long-dashed line from eqn (16.7) in region of extrapolation; short-dashed lines are limits of uncertainty.

values at 127.1 and 143.1 K are too high to be represented in Fig. 16.2).

However we note that MILLER *et al.* in evaluating G^E from their experimental results for the composition of coexisting liquid and vapour phases and for the total vapour pressure, only corrected for the non-ideality of the vapour phase as far as the second virial coefficient. From ~ 150 K upwards it would seem to us to be desirable to incorporate third virial coefficients C_{ijk} into the calculation. CALADO[21] has estimated the required C_{ijk} values by the procedure suggested by CHUEH and PRAUSNITZ[22]. The effect on $G^E_{\frac{1}{2}}$ of considering terms involving the third virial coefficient is in all cases to increase it — by 2.8, 4.5, 7.5, 10.8, and 16.7 J mol^{-1} at, respectively, 150, 160, 170, 180 and 190 K. If these corrections are added to the $G^E_{\frac{1}{2}}$ estimates from the work of MILLER *et al.*, some of the resulting values lie somewhat above our suggested 'upper limit' curve. [The limiting curves in Fig. 16.2 correspond to considering the combined effect of the uncertainty in $G^E_{\frac{1}{2}}$ at 115.77 K and the two most extreme combinations of the uncertainties in our experimental $H^E_{\frac{1}{2}}$ values.]

We consider that Fig. 16.2 and eqn (16.7) summarize all available information on the excess thermodynamic functions of the liquid methane + liquid ethylene system below the methane critical temperature.

16.4 REFERENCES

(1) CALADO, J.C.G. and SOARES, V.A.M., J. Chem. Soc., Faraday I, 1977, 73, 1271.

(2) HSI, C. and LU, B.C.-H., Can. J. Chem. Eng., 1971, 49, 140.

(3) MILLER, R.C., KIDNAY, A.J. and HIZA, M.J., J. Chem. Thermodynamics, 1977, 9, 167.

(4) GIBBONS, R.M., Mol. Phys., 1969, 17, 81.

(5) GIBBONS, R.M., Mol. Phys., 1970, 18, 809.

(6) HAYNES, W.M. and HIZA, M.J., J. Chem. Thermodynamics, 1977, 9, 179.

(7) MENES, F., DORFMÜLLER, T. and BIGELEISEN, J., J. Chem. Phys., 1970, 53, 2869.

(8) HAYNES, W.M., Cryogenics, 1978, 18, 621.

(9) SAVILLE, G., 1977/1978 (private communication).

(10) GOODWIN, R.D., 'The Thermophysical Properties of Methane from 90 to 500 K at Pressures to 700 bar', NBS Tech. Note 653 (1974).

(11) DOUSLIN, D.R. and HARRISON, R.H., J. Chem. Thermodynamics, 1976, 8, 301.

(12) PITZER, K.S. and CURL, Jr, R.F., J. Am. Chem. Soc., 1957, 79, 2369.

(13) EGAN, C.J. and KEMP, J.D., J. Am. Chem. Soc., 1937, 59, 1264.

(14) ROWLINSON, J.S., 'Liquids and Liquid Mixtures', 2nd ed., Buttwerworth, London (1969).

(15) MILLER, R.C. and STAVELEY, L.A.K., Adv. Cryogenic Eng., 1976, 21, 493.

(16) McCLURE, D.W., LEWIS, K.L., MILLER, R.C. and STAVELEY, L.A.K., J. Chem. Thermodynamics, 1976, 8, 785.

(17) LEWIS, K.L., MOSEDALE, S.E. and WORMALD, C.J., J. Chem. Thermodynamics, 1977, 9, 121.

(18)(a) LEWIS, K.L., SAVILLE, G. and STAVELEY, L.A.K., J. Chem. Thermodynamics, 1975, 7, 389.

(b) KIDNAY, A.J., LEWIS, K.L., CALADO, J.C.G. and STAVELEY, L.A.K., J. Chem. Thermodynamics, 1975, 7, 847.

(c) MOSEDALE, S.E. and WORMALD, C.J., J. Chem. Thermodynamics, 1977, 9, 483.

(19) SOARES, V.A.M., 'Estudo Termodinâmico de Misturas Líquidas Binárias Contendo Etileno', Tese de Doutoramento, Inst. Sup. Técnico, Lisboa (1976).

(20) VOLOVA, L.M., Zhur. fiz. Khim., 1940, 14, 268.

(21) LOBO, L.Q., CALADO, J.C.G. and STAVELEY, L.A.K., communication to the 71st A.I.Ch.E. Annual Meeting, Miami, Florida, 1978 (to be published).

(22) CHUEH, P.L. and PRAUSNITZ, J.M., A.I.Ch.E. Journal, 1967, 13, 896.

CHAPTER 17

THE VAPOUR PRESSURE OF CARBON TETRAFLUORIDE

17.1 INTRODUCTION

Carbon tetrafluoride is a compound with a long liquid range. Its triple-point temperature is 89.56 K and the critical temperature is 227.5 K. It is, of course, non-flammable and chemically relatively inert. It is therefore not unlikely that it will find increasing use in low-temperature research, for example as the liquid in a vapour pressure thermometer, or as the bath fluid in a cryostat. It would clearly be helpful to potential users to have reliable information on its vapour pressure over as wide a range of temperature as possible. Such users would include those applying perturbation theory to the prediction of phase equilibria in fluid mixtures. In fact, one of the initial steps in such treatment is to determine the parameters n, ε and σ of the potential energy of interaction of the pure components, and this is accomplished by fitting to liquid density and/or vapour pressure experimental data. Although the theory seems to be less sensitive to the latter[1], the lack of liquid density data for CF_4 above 185 K makes it desirable, for the purpose of applying the theory to systems of which carbon tetrafluoride is one component, to have vapour pressure information above that temperature, namely to the critical point.

In the study of the system $HC\ell + CF_4$ (Chapter 14) we measured the vapour pressure of the second component at the triple-point temperature of $HC\ell$ and also of C_2F_6. This suggested to us that it would be worthwhile to determine its vapour pressure at the triple-point temperature of other substances, chosen because these temperatures have already been carefully measured, and also because they are suitably spaced over as much of the

liquid range of carbon tetrafluoride as possible. With the all-glass apparatus available, the practical upper limit of the vapour pressure measurements was ~ 0.5 MPa. The technique has been currently used in the investigations of the thermodynamic properties (namely, vapour pressure) of binary liquefied gas mixtures carried out in this laboratory, but does not seem to have been applied before to a systematic study of the vapour pressure of a pure substance spanning a wide temperature range.

We accordingly measured the vapour pressure of carbon tetrafluoride at the triple-point temperatures of ethylene, krypton, n-butane, hydrogen chloride, xenon and hexafluoroethane. We also determined the small triple-point pressure of CF_4 itself. To bridge the gap between the triple-point temperatures of n-butane (134.84 K) and hydrogen chloride (159.01 K) we attempted to determine the vapour pressure at the triple-point temperature of boron trifluoride (144.71 K), but for reasons given below the value obtained was not used in establishing the final vapour pressure equation. Attempts were also made to use *trans*-2-butane (triple-point temperature 167.61 K [2]) as a cryostat material. However, even after repeated fractionation, this froze to what appeared to be a glass, which failed to melt sharply.

Since the triple-point temperatures had been determined at different times in different laboratories, it was necessary to convert these to the same scale, the obvious choice for which seemed to be IPTS - 68. It will be apparent that while these corrected temperatures may differ in their accuracy, at least there can scarcely be any systematic error in the temperatures as a whole.

We report in this chapter our vapour pressure results and the values of the temperatures at which they were determined corrected to IPTS - 68. We show that our results can be satisfactorily represented by the WAGNER

equation[3], and we compare them with previously published vapour pressure values.

17.2 RESULTS AND DISCUSSION

Different schemes had to be adopted to convert the triple-point temperature T_t given in the literature to the common IPTS-68 scale.

(i) T_t for carbon tetrafluoride was measured by SMITH and PACE[4] and by SIMON *et al.*[5] with NBS-calibrated thermometers, so the conversion to IPTS-68 was simply made using the comparison tables given by BEDFORD *et al.*[6].

(ii) LOVEJOY[7] determined T_t for krypton and xenon on IPTS-48. His values were corrected to IPTS-68 using the tables presented by DOUGLAS[8]. Another value of T_t for krypton was obtained from the work of BEAUMONT *et al*[9] after deducting 6 mK from the original value, as recommended by LOVEJOY.

(iii) The original T_t values for ethylene[10], n-butane[11] and hexafluoroethane[12], and also that for hydrogen chloride given by GIAUQUE and WIEBE[13], were corrected to IPTS-68 using the procedure due to HOGE[14], which was later advocated by HUST[15], and also used by ZIEGLER *et al.*[16]. This requires that the original determination should have been made on a scale on which two sufficiently widely separated reference temperatures had been determined. For these two temperatures we chose the triple-point of water T_w and the normal-point of oxygen T_o. The correction ΔT which must be added to a temperature T^A as originally determined to give the corresponding temperature T^{68} on IPTS-68 is

$$\Delta T = \frac{(T_w^{68} - T_w^A) - (T_o^{68} - T_o^A)}{(T_w^{68} - T_o^{68})} (T^A - T_o^{68}) + (T_o^{68} - T_o^A). \quad \ldots (17.1)$$

T_t for carbon tetrafluoride, as determined by POOL *et al.*[17] using a liquid oxygen vapour pressure thermometer, was converted to IPTS-68 in the same way.

The only T_t value which had been directly measured on IPTS-68 was that for hydrogen chloride published by CHIHARA and INABA[18]. This is ~ 0.08 K higher than that derived from GIAUQUE and WIEBE's work, and we adopted a mean of the two values.

The results are shown in Table 17.1, in which are recorded the original T_t values, the corresponding IPTS-68 values, the literature values as well as our own results for the various triple-point pressures, and the vapour pressure of carbon tetrafluoride at the various triple points. Each vapour pressure value, for which the standard deviation is also recorded, is a mean of at least thirty observations.

We fitted our vapour pressure results to several equations, which included the Antoine equation, Chebyshev polynomials, and the equation proposed by GOMEZ-NIETO and THODOS[19], namely

$$\ln P_R = A + B/T_R^m + C T_R^7, \qquad \ldots (17.2)$$

where P_R and T_R are the reduced pressure and temperature. [An equation similar to eqn (17.2) but with the last term replaced by $C T_R^n$, n being variable, was also tried.] We shall not enlarge on these trials, since it was subsequently found that the equation proposed by WAGNER[3] was clearly superior to any of the other equations. This equation is

$$\ln P = \ln P_c + (A_1 \tau + A_2 \tau^{1.5} + A_3 \tau^3 + A_4 \tau^6)/T_R \qquad \ldots (17.3)$$

with

$$A_1 = -6.7651056$$
$$A_2 = 1.0777437$$
$$A_3 = -1.7490971$$
$$A_4 = -2.5845119$$

TABLE 17.1

VAPOUR PRESSURE OF CF_4

TRIPLE-POINT CHARACTERISTICS OF CRYOGENIC SUBSTANCES						CF_4 VAPOUR PRESSURE[a] P/kPa	ΔP/kPa
SUBSTANCE	TEMPERATURE			PRESSURE			
	Ref.	T^A/K	T^{68}/K	Ref.	P/kPa		
CF_4	4	89.56	89.568	22	0.107		
	5	89.547	89.556	5	0.107 ± 0.001		
	17	89.569 ± 0.003	89.567	23	0.107 ± 0.004		
	Selected		89.56	This work[a]	0.109 ± 0.013	0.109 ± 0.013	- 0.000
C_2H_4	10	103.95 ± 0.05	104.007	29	0.123		
	Selected		104.01	This work[a]	0.125 ± 0.007	1.465 ± 0.012	+ 0.000
Kr	7	115.770 ± 0.001	115.762	30	72.994 ± 0.004		
	9	115.776	115.762	31	72.995 ± 0.004		
	Selected		115.76	This work	72.978 ± 0.016	7.013 ± 0.015	+ 0.001
$n\text{-}C_4H_{10}$	11	134.87 ± 0.05	134.843	32	(~ 0.001)		
	Selected		134.84	This work	-	46.074 ± 0.065	- 0.074
BF_3	33	144.46	?	31	8.343 ± 0.004		
	34	144.79	?				
	Selected		(144.71)	This work	8.342 ± 0.016	(98.216 ± 0.020)	(+ 0.017)
HCl	13	158.91 ± 0.05	158.969	35	13.811 ± 0.004		
	18	159.052 ± 0.05	159.052	36	13.799 ± 0.004		
	Selected		159.01	This work	13.807 ± 0.005	244.500 ± 0.024	+ 0.511
Xe	7	161.381 ± 0.001	161.392	35	81.684 ± 0.003		
				36	81.661 ± 0.003		
	Selected		161.39	This work	81.667 ± 0.004	279.321 ± 0.023	+ 0.246
C_2F_6	12	173.10 ± 0.05	173.077	-	-		
	Selected		173.08	This work	26.259 ± 0.004	508.613 ± 0.033	- 1.130

a - Readings with Texas Instruments gauge

and where $\tau = (1 - T_R)$, and P_c and $T_R = T/T_c$ are the critical pressure and the reduced temperature respectively. The merits of the WAGNER equation have been thoroughly examined by AMBROSE[20], who has drawn attention to its reliability over a wide temperature range. For P_c and T_c, the critical pressure and temperature of CF_4, we took the values of 3.742 MPa and 227.5 K respectively[21].

In fitting our results to eqn (17.3) it seemed desirable to weight the points, even though this had to be done arbitrarily. Thus, the T_t values of Kr and Xe had clearly been determined with great care by LOVEJOY[7], with the object of establishing them as fixed thermometric points, and these were given the highest weighting factor of five. All other sets of values were given a weight of two, except for those for the critical point of carbon tetrafluoride and the triple-point of hydrogen chloride, which were given a weight of one — in the case of HCℓ because of the difference just mentioned in the two T_t values. The success of the WAGNER equation in fitting the experimental data is indicated by the values of the pressure residuals

$$\Delta P = P(\text{obs}) - P(\text{calc})$$

given in Table 17.1. We may note that the ΔP for the hydrogen chloride triple-point would virtually vanish if we adopted the Japanese[18] value of 159.052 K for T_t. The value given by eqn. (17.3) for the normal boiling-point of CF_4 is 145.16 K.

There have been several previous studies of the vapour pressure of carbon tetrafluoride as a function of temperature below the normal boiling-point[4,5,22-24], but none, as far as we are aware, above. The results of these studies are compared graphically with our work in Fig. 17.1. In this comparison, wherever possible allowance was made for the difference between the temperature scale used by the authors and IPTS-68. This correction

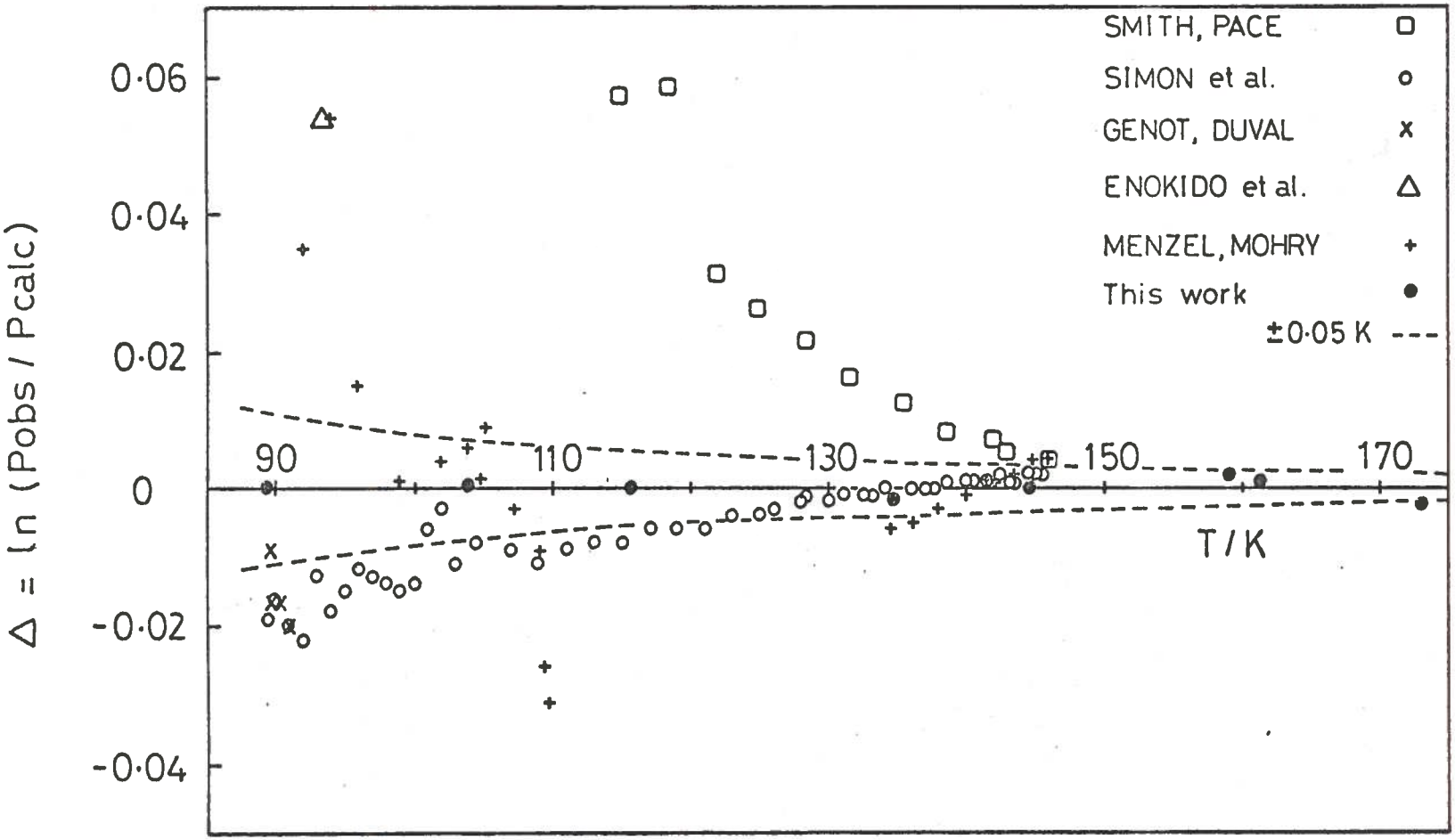

Fig. 17.1
Deviation plot for the vapour pressure of CF_4 as a function of temperature

was applied to the results given in references (4, 5 and 24). The results in closest agreement with our own are those of SIMON *et al.*[5], though there appears to be a shift in the relation between their temperature scale and ours of ~ 0.1 K over the range covered in their experiments.

Our measured value of the vapour pressure of carbon tetrafluoride at the triple-point of boron trifluoride was 98.216 ± 0.020 kPa. Our sample of this substance had been fractionated, and melted with a triple-point pressure of 8.342 ± 0.016 kPa. There are two published estimates of T_t, one being 144.46 K (EUCKEN and SCHRÖDER[33]) and the other 144.79 K (KOSTRYUKOV *et al.*[34]). In neither case is sufficient information given about the temperature scales used to be able to correct the measured T_t values to IPTS-68 with reasonable certainty. Two further complicating factors are that it is possible that the sample used by EUCKEN and SCHRÖDER was somewhat impure, and that, as suggested by CALADO and STAVELEY[31], there may be two crystalline phases of BF_3 with triple-points close together. For these reasons we rejected the measurements made at the triple-point of boron trifluoride in evaluating the parameters of the WAGNER equation. However, our measured value of the vapour pressure of carbon tetrafluoride at the boron trifluoride triple-point, together with eqn (17.3), gives 144.71 K for the triple-point temperature, in close agreement with 144.70 K as estimated by CALADO and STAVELEY for the solid phase of lower melting-point.

From eqn (17.3), the value of $(d\,\ell n\,P/dT)$ at the normal boiling-point of carbon tetrafluoride is $7.01634 \times 10^{-2}\ K^{-1}$. The enthalpy of vaporization is $\Delta H_v = 11814\ J\ mol^{-1}$ [25], and the molar volume of the liquid as interpolated from the results of TERRY *et al.*[26] is 54.675 $cm^3\ mol^{-1}$ (after a correction of -0.4% has been applied; cf. Chapter 11). Use of these figures and the Clapeyron equation,

$$\frac{PV^G}{RT} = \frac{\Delta H_v}{RT^2 \left(1 - \frac{V^L}{V^G}\right)\left(\frac{d\,\ell n\,P}{dT}\right)} \quad , \qquad \ldots (17.4)$$

following the method suggested by CURTISS and HIRSCHFELDER[27], leads (after recycling) to a value of the second virial coefficient B at 145.16 K of -395 cm^3 mol^{-1}. The same procedure would give B values of -306 cm^3 mol^{-1} and -430 cm^3 mol^{-1} if the vapour pressure equations of SMITH and PACE[4] and SIMON *et al.*[5], respectively, had been used. No direct measurements of B at temperatures as low as this appear to have been made. However, LANGE and STEIN[25] determined B from 203 to 368 K, and DOUSLIN *et al.*[28] from 273 to 623 K. We fitted the B values to the equation

$$B/V_c = \sum_i a_i \, T_R^i \qquad \ldots (17.5)$$

where V_c is the critical volume. Experience of this form of B vs T equation with other substances had shown that its use for extrapolation to lower temperatures produced reasonably reliable values. Such extrapolation for carbon tetrafluoride gave B (145.16 K) = -397 cm^3 mol^{-1}. The close agreement with our indirect estimate given above may well be partly fortuitous, but at least it can be said that our vapour pressure equation (17.3) is consistent with the presently available virial coefficient data.

17.3 REFERENCES

(1) GIBBS, G.M., communication to the Conference on Chem. Thermodynamic Data on Fluids and Fluid Mixtures, NPL, Teddington, U.K., 1978.

(2) GUTTMAN, L. and PITZER, K.S., J. Amer. Chem. Soc., 1945, 67, 324.

(3) WAGNER, W., Cryogenics, 1973, 13, 470.

(4) SMITH, J.H. and PACE, E.L., J. Phys. Chem., 1969, 73, 4232.

(5) SIMON, M., KNOBLER, C.M. and DUNCAN, A.G., Cryogenics, 1967, 7, 138.

(6) BEDFORD, R.E., DURIEUX, M., MUIJLWIJK, R. and BARBER, C.R., Metrologia, 1969, 5, 47.

(7) LOVEJOY, D.R., Nature, 1963, 197, 353.

(8) DOUGLAS, T.B., J. Res. Nat. Bur. Stand., 1969, 73A, 451.

(9) BEAUMONT, R.H., CHIHARA, H. and MORRISON, J.A., Proc. Phys. Soc. (London), 1961, 78, 1462.

(10) EGAN, C.J. and KEMP, J.D., J. Am. Chem. Soc., 1937, 59, 1264.

(11) ASTON, J.G. and MESSERLY, G.H., J. Am. Chem. Soc., 1940, 62, 1917.

(12) PACE, E.L. and ASTON, J.G., J. Am. Chem. Soc., 1948, 70, 566.

(13) GIAUQUE, W.F. and WIEBE, R., J. Am. Chem. Soc., 1928, 50, 101.

(14) HOGE, H.J., J. Res. Nat. Bur. Stand., 1950, 44, 321.

(15) HUST, J.G., Cryogenics, 1969, 9, 443.

(16) ZIEGLER, W.T., YARBROUGH, D.W. and MULLINS, J.C., Tech. Rep. No.1, Project No. A-764, Georgia Inst. Tech., Atlanta, Georgia, 1964.

(17) POOL, R.A.H., SAVILLE, G., HERRINGTON, T.M., SHIELDS, B.D.C. and STAVELEY, L.A.K., Trans. Faraday Soc., 1962, 58, 1692.

(18) CHIHARA, H. and INABA, A., J. Chem. Thermodynamics, 1976, 8, 915.

(19) GOMEZ-NIETO, M. and THODOS, G., A.I.Ch.E. Journal, 1977, 23, 904.

(20) AMBROSE, D., J. Chem. Thermodynamics, 1978, 10, 765.

(21) Engineering Sciences Data Unit, Index 1977-78, London, 1977, 248.

(22) GÉNOT, B. and DUVAL, X., J. Chim. Phys., 1970, 67, 1332.

(23) ENOKIDO, H., SHINODA, T. and MASHICO, Y., Bull. Chem. Soc. Japan, 1969, 42, 3415.

(24) MENZEL, W. and MOHRY, F., Z. anorg. u. allg. Chem., 1930, 210, 257.

(25) LANGE, Jr., H.B. and STEIN, F.P., J. Chem. Eng. Data, 1970, 15, 56.

(26) TERRY, M.J., LYNCH, J.T., BUNCLARK, M., MANSELL, K.R. and STAVELEY, L.A.K., J. Chem. Thermodynamics, 1969, 1, 413.

(27) CURTISS, C.F. and HIRSCHFELDER, J.O., J. Chem. Phys., 1942, 8, 491.

(28) DOUSLIN, D.R., HARRISON, R.H., MOORE, R.T. and McCULLOUGH, J.P., J. Chem. Phys., 1961, 35, 1357.

(29) BIGELEISEN, J., FUKS, S., RIBNIKAR, S.V. and YATO, Y., J. Chem. Phys., 1977, 66, 1689.

(30) DAVIES, R.H., DUNCAN, A.G., SAVILLE, G. and STAVELEY, L.A.K., Trans. Faraday Soc., 1967, 63, 855.

(31) CALADO, J.C.G. and STAVELEY, L.A.K., Trans. Faraday Soc., 1971, 67, 1261.

(32) TICKNER, A.W. and LOSSING, F.P., J. Phys. and Colloid Chem., 1951, 55, 733.

(33) EUCKEN, A. and SCHRÖDER, E., Z. physik. Chem., 1938, 41B, 307.

(34) KOSTRYUKOV, U.N., SAMORUKOV, O.P. and STRELKOV, P.G., Zhur. Fiz. Khim., 1958, 32, 1354.

(35) CALADO, J.C.G., KOZDON, A.F., MORRIS, P.J., da PONTE, M.N., STAVELEY, L.A.K. and WOOLF, L.W., J. Chem. Soc., Faraday I, 1975, 71, 1372.

(36) CALADO, J.C.G., GRAY, C.G., GUBBINS, K.E., PALAVRA, A.M.F., SOARES, V.A.M., STAVELEY, L.A.K. and TWU, C.-H. J. Chem. Soc., Faraday I, 1978, 74, 893.

PART 5

CONCLUSIONS

CHAPTER 18 - FINAL COMMENTS

CHAPTER 18

FINAL COMMENTS

Although the full implications of this work cannot be apparent until further theoretical work has been carried out, we shall try to draw some preliminary conclusions from the information available.

A brief comment can be made on the perturbation theory results of GUBBINS and co-workers. For systems with quadrupolar or octupolar components, even though one has to use experimental values of $G^E_{\frac{1}{2}}$ and $V^E_{\frac{1}{2}}$ to fix the two correction parameters k_{12} and j_{12} of the Lorentz-Berthelot rules, at least the theory than predicts the asymmetry of the plots of G^E and V^E against composition more or less correctly, and above all one gets good calculated values for the most sensitive function H^E. The failure of theory to give values of H^E in agreement with experiment in the case of Xe + HCℓ might be said to be yet another demonstration of the superior value of the excess enthalpy as an effective testing function when compared with G^E and V^E, whose values are well reproduced by the theory. It is therefore hoped that the experimental H^E results for eight of the binary systems reported in this thesis will help to improve some aspects of the theory, once calculations have been made for the whole set. Further experimental research in this field will, however, be needed, especially on systems involving at least one strongly dipolar component.

The apparent success of perturbation methods in reproducing the excess thermodynamic functions for most of the cases already studied should nevertheless, not be allowed to conceal its main limitation, for as long as empirical deviation parameters, k_{ij} and j_{ij}, are required to force agreement with experiment, the theory cannot be regarded as predictive in the sense that the properties of a mixture can be accurately calculated using only information about the two pure components. Moreover, the relative

importance of the several anisotropic terms in the potential function is still not completely established. It is, therefore, to be expected that the research effort in this field will probably develop in two main directions:

(i) determination of deviation parameters (in particular k_{ij}) either from independent experimental sources (such as second virial coefficients), or from simple correlation procedures (in which case more experimental information on the excess functions will be needed);

(ii) theoretical investigations on multibody interactions (and on the role of hydrogen bonding).

Moreover, since no additional deviation parameters should be required to extend the theory to the prediction of the excess functions of ternary and multicomponent systems, experimental work in this area will provide further scope for comparison.

Qualitative deductions about any order or structure which may exist in liquid mixtures of molecularly simple species, made on the basis of the measured values of the excess thermodynamic functions, are of little reliability unless supported by additional information from appropriate sources — such as neutron scattering and spectroscopic techniques — which can yield more direct insight into the molecular packing in the solution. However, as far as we are aware, such studies have not yet been made for any of the mixtures studied in the present work.

Results for the systems so far studied show that, in spite of the guidance given by the generalized perturbation treatment of TWU, GUBBINS and GRAY[1], no useful general correlation can be made between the strength of the dipole or multipole and the non-ideality of a system. For example, if one considers the $G^E_{\frac{1}{2}}$ values (at 182 K) for the binary liquid mixtures of which xenon is one component (Table 18.1) there is no apparent correlation

TABLE 18.1

$G^E_{\frac{1}{2}}$ at 182 K FOR BINARY MIXTURES INVOLVING XENON (COMPONENT 1)[a]. [ε_{11}/k = 231.52 K; σ_{11} = 0.3961 nm [b]]

Component 2	(ε_{22}/k)/K	σ_{22}/nm	μ_2^*	Q_2^*	Ω_2^*	$G^E_{\frac{1}{2}}$/J mol^{-1}
Kr	167.8 [c]	0.3613 [c]	-	-	-	120 [d]
HCℓ	191.4 [e]	0.3641 [e]	0.95	0.92	-	685 [f]
C_2H_6	251.8 [c]	0.4346 [c]	-	0.09	-	- 30 [g]
C_2H_4	232.2 [c]	0.4168 [c]	-	0.61	-	136 [h]
N_2O	265.5 [b]	0.3762 [b]	0.12	0.67	-	448 [b]
C_2F_6	266.0 [i]	0.4904 [i]	-	(0.098 Q)	-	597 [i]
CF_4	206.7 [j]	0.4193 [j]	-	-	0.13	599 [j]

(a) Reduced electric moments [Ref. (1)]:

$\mu^* = \mu/(\varepsilon\sigma^3)^{\frac{1}{2}}$; $Q^* = Q/(\varepsilon\sigma^5)^{\frac{1}{2}}$; $\Omega^* = \Omega/(\varepsilon\sigma^7)^{\frac{1}{2}}$.

Values calculated using μ, Q and Ω from previous Chapters.

(b) From Chapter 10

(c) From Ref. (2)

(d) From Ref. (3) and eqn (8.3), using $H^E = 72.5$ J mol^{-1}, Ref. (4).

(e) From Ref. (5).

(f) From Ref. (6).

(g) From Ref. (7).

(h) From Ref. (8) and eqn (8.3), using $H^E \simeq 230$ J mol^{-1}, ref. (9).

(i) From Chapter 12 and Ref. (10).

(j) From Chapter 11.

between $G^E_{\frac{1}{2}}$ and the reduced electric moments of every second component in such mixtures. In fact, if among these mixtures those of the type non-polar + quadrupolar are selected for a closer examination the relation between the $G^E_{\frac{1}{2}}$ values is

$$G^E(C_2F_6) > G^E(N_2O) \gg G^E(C_2H_4)[\simeq G^E(Kr)] > G^E(C_2H_6)$$

while that of the reduced quadrupole moment of the second components involved is

$$Q^*(N_2O) \simeq Q^*(C_2H_4) \gg Q^*(C_2H_6)[> Q^*(Kr) = 0] .$$

(A quadrupole moment larger than ~ 7 to 8×10^{-26} esu cm^2 would be required for C_2F_6 to obtain a value of Q^* larger than that of N_2O.)

The situation is similar when both components bear non-zero multipole moments. Thus, on the one hand one might expect from the results in Ref. (1) that $HC\ell + N_2O$ and $N_2O + C_2H_4$ should be less non-ideal mixtures (as they actually are) than those formed by any one of these substances with a second, non-polar component like xenon. But, on the other hand, the $HC\ell + CF_4$ system shows quite the opposite behaviour, being so imperfect that the two liquids are in fact only partially miscible.

18.1 REFERENCES

(1) TWU, C.-H., GUBBINS, K.E. and GRAY, C.G., Mol. Phys., 1975, 29, 713.

(2) TWU, C.-H. and GUBBINS, K.E., Chem. Eng. Sci., 1978, 33, 879.

(3) CALADO, J.C.G. and STAVELEY, L.A.K., Trans. Faraday Soc., 1971, 67, 289.

(4) LEWIS, K.L. and STAVELEY, L.A.K., 1975 (unpublished results).

(5) CLANCY, P., GUBBINS, K.E. and GRAY, C.G., Faraday Disc., 1979, 66, in press.

(6) CALADO, J.C.G., KOZDON, A.F., MORRIS, P.J., da PONTE, M.N., STAVELEY, L.A.K. and WOOLF, L.A., J. Chem. Soc., Faraday I, 1975, 71, 1372.

(7) CALADO, J.C.G., AZEVEDO, E.J.S.G. and SOARES, V.A.M., communication to the 71st A.I.CH.E. Annual Meeting, Miami, Florida, 1978.

(8) CALADO, J.C.G. and SOARES, V.A.M., J. Chem. Thermodynamics, 1977, 9, 911.

(9) CALADO, J.C.G., da PONTE, M.N., SOARES, V.A.M. and STAVELEY, L.A.K., J. Chem. Thermodynamics, 1978, 10, 35.

(10) ALDERSLEY, S.C., LOBO, L.Q. and STAVELEY, L.A.K., J. Chem. Thermodynamics, 1979, 11, in press.

PART 6

APPENDICES

APPENDIX (A) - MERCURY CAPILLARY DEPRESSIONS

APPENDIX (B) - PRESSURE CONVERSION FACTORS

APPENDIX (C) - CALIBRATED VOLUMES IN THE G^E AND V^E APPARATUS

APPENDIX (D) - CALIBRATION OF TEXAS INSTRUMENTS PRESSURE GAUGES

APPENDIX (E) - ERROR IN THE OVERALL COMPOSITION OF THE MIXTURES

APPENDIX (G) - CALIBRATION OF THE AUXILIARY COPPER RESISTANCE THERMOMETERS

APPENDIX (H) - CALIBRATION OF THE CALORIMETER COPPER RESISTANCE THERMOMETER

APPENDIX (I) - SOME PROPERTIES OF THE REDLICH-KISTER EQUATION

APPENDIX (J) - BARKER'S METHOD FOR THE EVALUATION OF G^E

APPENDIX (K) - ERRORS IN G^E

APPENDIX (L) - ERRORS IN V^E

APPENDIX (M) - ERRORS IN H^E

APPENDIX (N) - ESTIMATION OF V^E FOR $CH_4 + C_2H_4$

APPENDIX (A)

MERCURY CAPILLARY DEPRESSIONS

Capillary depressions (mm) for mercury menisci [1]

Tube diameter/mm	Meniscus height / mm								
	0.2	0.4	0.6	0.8	1.0	1.2	1.4	1.6	1.8
10	0.062	0.125	0.185	0.240	0.285	0.320	0.350	0.375	0.395
11	0.047	0.092	0.138	0.181	0.217	0.243	0.265	0.285	0.303
12	0.036	0.070	0.105	0.138	0.165	0.187	0.203	0.218	0.231
13	0.028	0.054	0.080	0.106	0.127	0.145	0.157	0.169	0.179
14	0.021	0.042	0.062	0.082	0.098	0.112	0.123	0.132	0.140
15	0.017	0.033	0.049	0.064	0.077	0.088	0.097	0.104	0.110
16	0.013	0.026	0.038	0.050	0.060	0.069	0.076	0.082	0.088
17	0.011	0.021	0.030	0.039	0.047	0.054	0.060	0.066	0.071
18	0.009	0.016	0.024	0.031	0.037	0.043	0.048	0.052	0.056
19	0.007	0.013	0.019	0.025	0.030	0.034	0.038	0.042	0.045

(1) KISTEMAKER, J., Physica, 1945, 11, 277

APPENDIX (B)

PRESSURE CONVERSION FACTORS

Pressure conversion factors, f, to 'international millimetres of mercury' as a function of temperature (t/°C), for Oxford[(a)].

t/°C	f	t/°C	f	t/°C	f
15.0	0.99784	19.0	0.99716	23.0	0.99648
.2	81	.2	12	.2	45
.4	0.99777	.4	0.99709	.4	41
.6	74	.6	05	.6	0.99638
.8	71	.8	02	.8	34
16.0	0.99768	20.0	0.99699	24.0	31
.2	64	.2	96	.2	0.99627
.4	61	.4	92	.4	24
.6	0.99757	.6	0.99689	.6	20
.8	54	.8	85	.8	0.99617
17.0	50	21.0	83	25.0	14
.2	0.99747	.2	0.99679	.2	11
.4	43	.4	76	.4	0.99607
.6	40	.6	72	.6	04
.8	0.99737	.8	0.99669	.8	0.99600
18.0	33	22.0	65	26.0	0.99597
.2	30	.2	62		
.4	0.99726	.4	0.99659		
.6	22	.6	55		
.8	0.99719	.8	52		

(a) Latitude: 51°46'. Correction for height above sea-level is less than - 0.005 mm Hg.

APPENDIX (C)

CALIBRATED VOLUMES IN THE G^E AND V^E APPARATUS

Reference: Figure 3.1

Volume of pyknometer	$V_{pk}(159.01\ K) = 2.2016 \pm 0.0004\ cm^3$ $V_{pk}(182.32\ K) = 2.2026 \pm 0.0002\ cm^3$	
Cross-section of pyknometer stem	$\phi = 0.02076\ cm^2$	[Not verified]
Volume of gas storage globes	$V_M = 2667.8\ cm^3$ (left) $V_N = 2664.5\ cm^3$ (right)	
Volume of vessel (E)	$V_E = 12.244 \pm 0.002\ cm^3$	[Not verified]
Volume defined by (1) and etch mark	$V_{gr} = 1.425\ cm^3$	[Not verified]
Volume defined by (1),(2), (4), (B), (D)	$V_{R1} = 9.76\ cm^3$	
Volume of left-hand limb of (J), to (10)	$V_J = (1.06 + 0.076\ h)\ cm^3$ h ≡ drop in height (cm) of left-hand mercury meniscus when pressure increases from zero to P.	
Volume defined by (1), (4), (7), (10), (11), (13), (14), (B), (D)	$V'_{R2} = 37.14\ cm^3$ $V_{R2} \equiv V'_{R2} + V_J$ $V_{R2} = (38.20 + 0.076\ h)\ cm^3$	

APPENDIX (D)

CALIBRATION OF TEXAS INSTRUMENTS PRESSURE GAUGES

$$P/\text{torr} = K_p P_g \qquad K_p = \sum_i a_i P_g^i$$

(i) Model 145-01, Capsule Type 1, No. 6094

$$a_0 = 9.91645$$

$$a_1 = 0.00163$$

(ii) Model 145-0, Capsule Type 1, No. 6491

$$a_0 = 8.5274$$

$$a_1 = -0.5361 \times 10^{-3}$$

$$a_2 = 4.6975 \times 10^{-6}$$

$$a_3 = -1.5690 \times 10^{-8}$$

$$a_4 = 1.8828 \times 10^{-11}$$

(iii) Model 140B, Capsule Type 1, No. 4018

$$a_0 = 51.617$$

APPENDIX (E)

ERROR IN THE OVERALL COMPOSITION OF THE MIXTURES

The uncertainty affecting a derived variable is assessed from the knowledge of the errors in the measured quantities of which that variable is a function. Usually only an upper limit of that uncertainty can be directly calculated. Such a limit is calculated below for the overall composition of the mixture in the pyknometer for a vapour pressure experiment. For simplicity, the mixture is supposed to be equimolar ($x_1 = x_2 = 0.5$). In this calculation both the absolute error, ε_K, and the relative error, $\Delta K = \varepsilon_K / K$, associated with variable K will be used.

For an actual experiment the quantities in the measurements and their respective uncertainties (hereby treated as absolute errors) are of the following orders of magnitude:

Volume of the thermostatted globe	$V_{gl} \sim (2500.0 \pm 0.1)\ cm^3$
Volume of the dead-space	$V_{ds} \sim (40.00 \pm 0.01)\ cm^3$
Temperature of the thermostat tank	$T_w \sim (300.00 \pm 0.01)\ K$
Temperature of air (room)	$T_r \sim (300.00 \pm 0.05)\ K$
Second virial coefficients	$B_w \sim B_r \sim (200 \pm 2)\ cm^3\ mol^{-1}$
Pressure of the gas	$P \sim (50.000 \pm 0.002)\ kPa$

The initial (or final) number of moles, $n^{I,F}$, of one gaseous component is given by equation (5.38), so that the associated error is[1]:

$$\varepsilon_{nI} \simeq \varepsilon_{nF} \sim 7.5 \times 10^{-6}\ mol.$$

Therefore, as the number of moles n_1 of component 1 condensed into the pyknometer is given by the difference

$$n_1 = n^I - n^F \quad (\sim 2 \times 10^{-2}\ mol),$$

the uncertainty in n_1 is

$$\varepsilon_{n_1} = \varepsilon_{nI} + \varepsilon_{nF} \sim 2\,\varepsilon_{nI}\ .$$

Now, the overall mole fraction of 1 in the pyknometer is

$$x = n_1/(n_1 + n_2)$$

and consequently

$$\Delta x = \Delta n_1 + \Delta(n_1 + n_2) \simeq \Delta n_1 + \Delta(2\,n_1) \simeq 2(\Delta n_1) \ .$$

Therefore

$$\varepsilon_x = x\,\Delta x \simeq 2\,x\,\Delta n_1 \simeq 2x(2\,\varepsilon_{nI}/n_1)$$
$$\sim 7.5 \times 10^{-4} \ ,$$

that is, the error affecting the mole fraction x is of the order of 'a few parts in 10^4.'

(1) TOPPING, J., 'Errors of Observation and their Treatment', 4th edition, Chapman & Hall, London (1972), p.20.

APPENDIX (F)

CALIBRATED VOLUMES IN THE H^E APPARATUS

Reference: Figure 4.2.

Volume of gas storage globes

V_{G1} = 5417.4 cm^3 (upper supply line)

V_{G2} = 5317.3 cm^3 (lower supply line)

Volume of lower section of manometer (U), between contacts

V_U = 13.109 ± 0.002 cm^3

Volume defined by (11), (13), (24), (15) and (17)

V_{r1} = 85.02 cm^3 (upper line)

Volume defined by (21), (23), (14), (25) and (27)

V_{r2} = 78.74 cm^3 (lower line)

Volume defined by (12), (13), (24), (15) and (17)

V_{L1} = 66.16 cm^3 (upper line)

Volume defined by (22), (23), (14), (25) and (27)

V_{L2} = 63.77 cm^3 (lower line)

$$V_{I1} = V_{F1} = V_{G1} + V_{r1} = 5483.6 \text{ cm}^3$$
$$V_{I2} = V_{F2} = V_{G2} + V_{r2} = 5381.1 \text{ cm}^3$$

Volume of calorimeter compartments

at 290.25 K: V_I = 3.17 cm^3 (upper chamber)

at 290.55 K: V_{II} = 8.70 cm^3 (lower chamber)

Volume of calorimeter compartments at low temperatures (exttapolated from values at room temperature through copper linear expansion coefficient data[1])

from 116 K to 163 K	V_I = 3.15 cm^3
from 175 K to 184 K	V_I = 3.16 cm^3
at 116 K	V_{II} = 8.64 cm^3
from 140 K to 150 K	V_{II} = 8.65 cm^3
from 163 K to 184 K	V_{II} = 8.66 cm^3

(1) RUBIN, T., ALTMAN, H.W. and JOHNSTON, H.L., J. Am. Chem. Soc., 1954, 76. 5289.

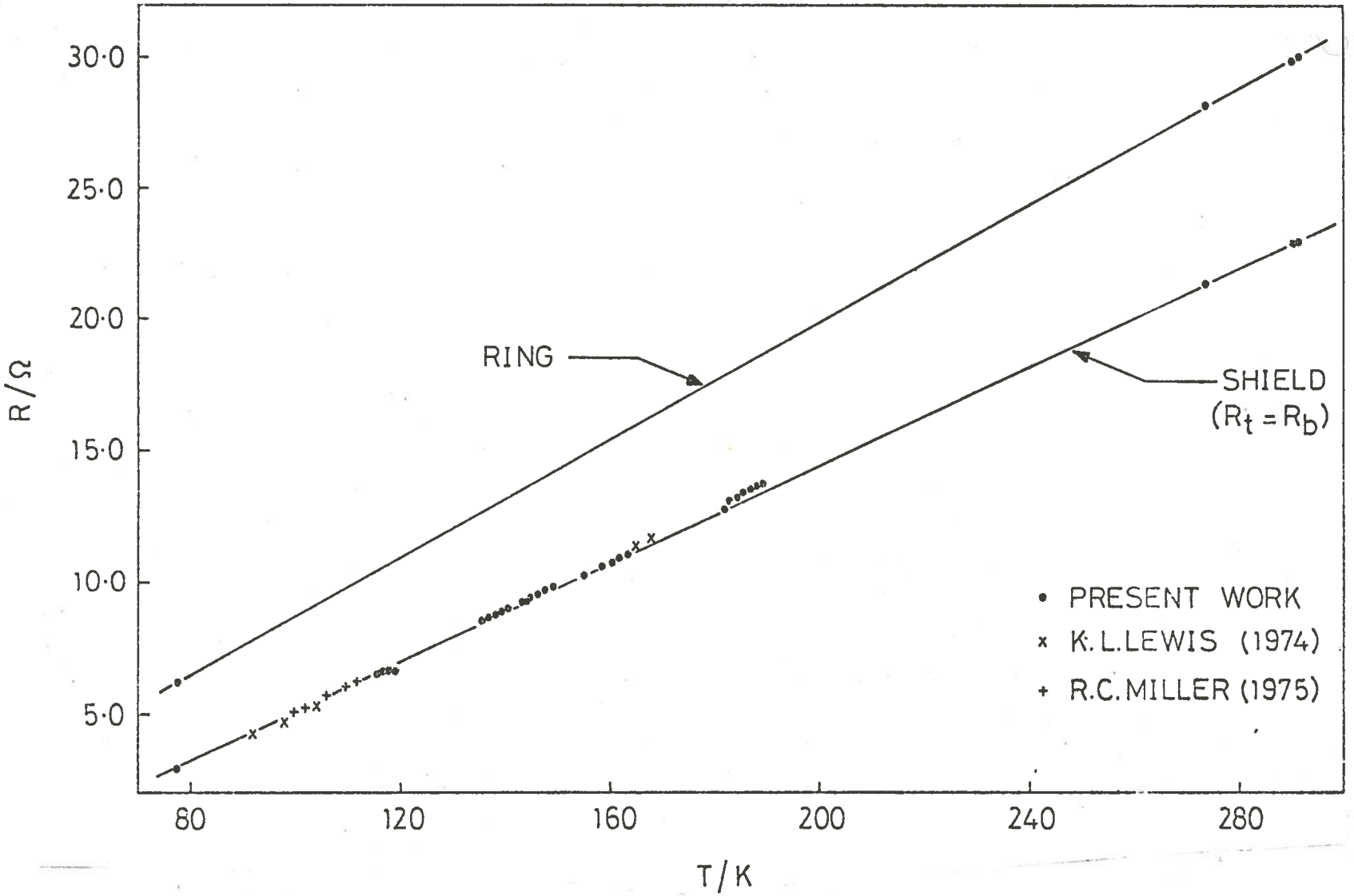

Fig. AG.1. Calibration lines of the auxiliary copper resistance thermometers in the calorimeter

APPENDIX (H)

CALIBRATION OF THE CALORIMETER COPPER RESISTANCE THERMOMETER

$$R_T/\Omega = \sum_{i=0}^{3} a_i (T/K)^i \qquad (\sigma = \text{standard deviation})$$

(i) Calibration with krypton. (Vapour pressure equation from MICHELS *et al*[1]).

$$116.01\ K \leqslant T \leqslant 118.85\ K$$

$a_0 = 13.2205$ $\qquad$ $a_2 = 0.137440 \times 10^{-2}$

$a_1 = -0.203947$ $\qquad$ $a_3 = 0$

$$\sigma = \pm 2.8\ m\Omega \doteqdot \pm 0.02\ K.$$

(ii) Calibration with carbon tetrafluoride. (Vapour pressure equation from SMITH and PACE[2]).

$$135.45\ K \leqslant T \leqslant 148.82\ K$$

$a_0 = -1.12891$ $\qquad$ $a_2 = 0.197173 \times 10^{-3}$

$a_1 = 0.573655 \times 10^{-1}$ $\qquad$ $a_3 = 0$

$$\sigma = \pm 1.2\ m\Omega \mathrel{\hat{=}} \pm 0.01\ K$$

(iii) Calibration with ethane. (Vapour pressure equation from GOODWIN *et al.*[3]).

(a) $155.34\ K \leqslant T \leqslant 163.70\ K$

$a_0 = -104.993$ $\qquad$ $a_2 = -0.381601 \times 10^{-2}$

$a_1 = 1.34662$ $\qquad$ $a_3 = 0$

$$\sigma = \pm 4.6\ m\Omega \mathrel{\hat{=}} \pm 0.04\ K$$

(b) $180.72\ K \leqslant T \leqslant 187.35\ K$

$a_0 = -4200.53$ $\qquad$ $a_2 = -0.367886$

$a_1 = 68.1614$ $\qquad$ $a_3 = 0.662907 \times 10^{-3}$

$$\sigma = \pm 1.8\ m\Omega \mathrel{\hat{=}} \pm 0.01\ K$$

(1) MICHELS, A., WASSENAAR, T. and ZWIETERING, T.N., Physica, 1952, 18, 63.

(2) SMITH, J.H. and PACE, E.L., J. Phys. Chem., 1969, 73, 4232

(3) GOODWIN, R.D., RODER, H.M. and STRATY, G.C., 'Thermophysical Properties of Ethane, from 90 to 600K at Pressures to 700 bar', N.B.S. Tech. Note 684, (1976).

APPENDIX (I)

SOME PROPERTIES OF THE REDLICH-KISTER EQUATION (5.37)

In the Redlich-Kister expansion

$$G^E/RT = x_1(1-x_1)[A_G + B_G(2x_1 - 1) + C_G(2x_1 - 1)^2], \qquad (5.37)$$

the first term is symmetric in x_1 thus giving a parabola when G^E is plotted against x_1; the term in B_G is assymetric and therefore tends to skew the parabola towards either one component or the other; the third term flattens or sharpens the parabola, since it has two symmetrically located maxima or minima in the interval $0 < x_1 < 1$. The combination of these terms gives considerable flexibility to equation (5.37).

SHAIN and PRAUSNITZ[1] discussed the relative values of the parameters A_G, B_G and C_G which are compatible with complete miscibility.

Since

$$RT \ln \gamma_i = \mu_i^E = G_i^E$$

$$= \left[\frac{\partial(nG^E)}{\partial n_i}\right]_{P,T,n_j} \qquad \ldots (AI.1)$$

the activity coefficients are readily obtained from equation (5.37):

$$\ln \gamma_1 = a_1 x_2^2 + b_1 x_2^3 + c_1 x_2^4 \qquad \ldots (AI.2)$$

$$\ln \gamma_2 = a_2 x_1^2 + b_2 x_1^3 + c_2 x_1^4 \qquad \ldots (AI.3)$$

where

$$a_1 = A_G + 3B_G + 5C_G \qquad a_2 = A_G - 3B_G + 5C_G$$

$$b_1 = -4(B_G + 4C_G) \qquad b_2 = 4(B_G - 4C_G)$$

$$c_1 = 12C_G \qquad c_2 = c_1$$

These relations lead to the following alternative forms of equations (AI.2) and (AI.3):

$$\ln \gamma_1 = A_G x_2^2 - B_G x_2^2(1 - 4x_1) + C_G x_2^2(1 - 8x_1 + 12x_1^2) \quad \ldots \text{(AI.4)}$$

$$\ln \gamma_2 = A_G x_1^2 + B_G x_1^2(1 - 4x_2) + C_G x_1^2(1 - 8x_2 + 12x_2^2) \quad \ldots \text{(AI.5)}$$

In these equations, the coefficients of A_G, B_G and C_G are not orthogonal functions but the cross integrals are small, of the order of 0.07 or less; this means that A_G, B_G and C_G are only slightly altered when extra terms are successively introduced in equation (5.37).

(1) SHAIN, S.A. and PRAUSNITZ, J.M., Chem. Eng. Sci., 1963, 18. 244.

APPENDIX (J)

BARKER'S METHOD FOR THE EVALUATION OF G^E

From equation (5.31) and its counterpart for component 2 the following relationships are obtained

$$y_1 P = \gamma_1 x_1 P_1^* \exp\left[-\left(\sum_{n=1}^{9} \tau_{1,n}\right)\Big/ RT\right] \qquad \ldots \text{(AJ.1)}$$

$$y_2 P = \gamma_2 x_2 P_2^* \exp\left[-\left(\sum_{n=1}^{9} \tau_{2,n}\right)\Big/ RT\right] \qquad \ldots \text{(AJ.2)}$$

so that we can write

$$P = \gamma_1 x_1 P_1' + \gamma_2 x_2 P_2' \qquad \ldots \text{(AJ.3)}$$

where

$$P_1' = P_1^* \exp\left[-\left(\sum_{n=1}^{9} \tau_{1,n}\right)\Big/ RT\right] \qquad \ldots \text{(AJ.4)}$$

and

$$P_2' = P^* \exp\left[-\left(\sum_{n=1}^{9} \tau_{2,n}\right)\Big/ RT\right] \qquad \ldots \text{(AJ.5)}$$

are, as it were, 'corrected' vapour pressures of the components 1 and 2, respectively.

Equation (AJ.3) shows that a calculated value for the total pressure of the mixture, $P_{calc} \equiv P$, can be obtained from a knowledge of the activity coefficients and the physical data involved in the calculation of terms $\tau_{i,n}$.

BARKER[1] derived a numerical method for minimizing the pressure residuals

$$R_P = P_{exp} - P_{calc} \qquad (5.54)$$

by adjusting the parameters A_G, B_G and C_G which appear in the Redlich-Kister equation (5.37) [or in (AI.4) and (AI.5)]. The calculation involves a successive approximation procedure. It starts by assuming $B_G = C_G = 0$

and using α, given by equation (5.52), as a first approximate value for A_G. Using the values of x_1 and y_1 obtained according to the process described in section 5.3, approximate activity coefficients γ_1 and γ_2 are calculated through equations (5.48) and (5.50), and then a first value for P_{calc} is obtained by means of equation (AJ.3). The total pressure P also appears in the right-hand side of equations (AJ.4) and (AJ.5) but, in practice, it can be replaced by the experimental vapour pressure, P_{exp}.

From equation (AJ.3) the derivative $(\partial P/\partial A_G)$ is

$$\frac{\partial P}{\partial A_G} = P'_1 x_1 \frac{\partial \gamma_1}{\partial A_G} + P'_2 x_2 \frac{\partial \gamma_2}{\partial A_G} \qquad \ldots \text{(AJ.6)}$$

so that the calculation of $(\partial\gamma_1/\partial A_G)$ and $(\partial\gamma_2/\partial A_G)$, from equations (AI.4) and (AI.5), gives:

$$\frac{\partial P}{\partial A_G} = \gamma_1 P'_1 x_1 x_2^2 + \gamma_2 P'_2 x_2 x_1^2 \qquad \ldots \text{(AJ.7)}$$

$$\frac{\partial P}{\partial B_G} = -\gamma_1 P'_1 x_1 (1 - 4x_1) x_2^2 + \gamma_2 P'_2 x_2 (1 - 4x_2) x_1^2 \qquad \ldots \text{(AJ.8)}$$

$$\frac{\partial P}{\partial C_G} = \gamma_1 P'_1 x_1 (1 - 8x_1 + 12x_1^2) x_2^2 + \gamma_2 P'_2 x_2 (1 - 8x_2 + 12x_2^2) x_1^2 \qquad \ldots \text{(AJ.9)}$$

It is now required to find the 'changes δA, δB and δC in A_G, B_G and C_G which will most nearly reduce the pressure residuals to zero, by fitting by least squares to the equation'[1]

$$\left(\frac{\partial P}{\partial A_G}\right)\delta A + \left(\frac{\partial P}{\partial B_G}\right)\delta B + \left(\frac{\partial P}{\partial C_G}\right)\delta C = R_P \quad . \qquad \ldots \text{(J.10)}$$

This is effected by solving the normal equations

$$\left.\begin{aligned}
&\delta A \sum (\partial P/\partial A_G)^2 + \delta B \sum (\partial P/\partial A_G)(\partial P/\partial B_G) + \\
&\qquad + \delta C \sum (\partial P/\partial A_G)(\partial P/\partial C_G) = \sum R_P (\partial P/\partial A_G) \\
&\delta A \sum (\partial P/\partial A_G)(\partial P/\partial B_G) + \delta B \sum (\partial P/\partial B_G)^2 + \\
&\qquad + \delta C \sum (\partial P/\partial B_G)(\partial P/\partial C_G) = \sum R_P (\partial P/\partial B_G) \\
&\delta A \sum (\partial P/\partial A_G)(\partial P/\partial C_G) + \delta B \sum (\partial P/\partial B_G)(\partial P/\partial C_G) + \\
&\qquad + \delta C \sum (\partial P/\partial C_G)^2 = \sum R_P (\partial P/\partial C_G)
\end{aligned}\right\} \quad \ldots \text{(AJ.11)}$$

where the summations are taken over all the experimental points.

The calculation is then recycled by using as new values of A_G, B_G and C_G the initial values altered by δA, δB and δC;

$$\alpha \rightarrow \alpha + \delta A$$

$$0 \rightarrow \delta B$$

$$0 \rightarrow \delta C$$

and the process is repeated [using now equations (AI.4) and (AI.5) to calculate γ_1 and γ_2] until A_G, B_G and C_G do not change significantly.

The standard deviation σ_A of A_G is given by

$$\sigma_A = \left[\frac{\Delta A}{\Delta} \frac{\sum R_P^2}{N - M}\right]^{\frac{1}{2}} \quad \ldots \text{(AJ.12)}$$

where N is the number of experimental points, M(= 3, in this case) is the number of parameters in the Redlich-Kister equation, Δ is the determinant of the system of normal equations (AJ.11), and ΔA is the minor complementary of element (1,1) in the determinant Δ.

Similar expressions hold for σ_B and σ_C.

The value of A_G is used to recalculate the liquid and vapour mole fractions and these can be fed back in the calculation of G^E, but usually

only very minor changes are obtained.

This method is obviously suited for using computational techniques. The calculations for this thesis were carried out on the University ICL 1906 A computer.

(1) BARKER, J.A., Austral. J. Chem., 1953, 6, 207

APPENDIX (K)

ERRORS IN G^E

The final error in the G^E determination is a function of the uncertainties affecting the experimental measurements, the quality of the physical data used in the evaluation of the different terms in equation (5.32), and the assumptions made in the calculations.

As indicated in the main text, the magnitude of terms $\tau_{i,n}$ increases with the vapour pressure of the mixture. Since the upper limiting pressure which the apparatus can stand is ~ 0.5 MPa most systems are studied under quite low pressure conditions. An equimolar mixture ($x_1 \sim y_1 = 0.5$) of vapour pressure $P \sim 250$ kPa is therefore adopted as the basis for the discussion which follows. Exceptions will be dealt with in future chapters.

The uncertainty in the experimental measurements, i.e. in the vapour pressure and composition determinations, constitutes the main source of error in G^E since those variables have a strong influence upon the leading terms $\tau_{i,0}$ of (5.32). Errors of ± 0.1 kPa in the pressure and of $\pm 5 \times 10^{-4}$ in the compositions will cause G^E to be in error by as much as $\pm 0.5\ J\,mol^{-1}$ in each case. This figure corresponds to changes in $\tau_{i,0}$ alone, the contribution from the remaining terms being $\pm 0.0\ J\,mol^{-1}$.

The assumption that all terms involving P^2 (or higher powers of P) are negligible is absolutely legitimate in the present case. In fact $\tau_{i,3}$ is the most important of these terms and for third virial coefficients of the order of $\pm 7000\ cm^6\,mol^{-2}$ an error in G^E of much less than $\pm 0.1\ J\,mol^{-1}$ will result from uncertainties as large as 100% in the C_{iii} values or $\pm 10\ cm^3\,mol^{-1}$ for the B_{ii} values. Terms $\tau_{1,5}$ contribute to the overall value of G^E by $\sim 0.1\ J\,mol^{-1}$, thus having a negligible influence in the final result. The same cannot be said of terms $\tau_{i,2}$ which involve the

quantity δ_{12}. This is usually positive, and if it is considered to be of moderate magnitude, say $+15\,cm^3\,mol^{-1}$, G^E will be affected by as much as $+1.0\,J\,mol^{-1}$ when the 'naive formula' is used.

The above discussion leaves the second virial coefficients as the only matter requiring comment among the data used in the calculations. Uncertainties of $\pm 5\,cm^3\,mol^{-1}$ in the B_{ii} values lead to errors of about $\pm 0.3\,J\,mol^{-1}$ in G^E and this is always smaller than the standard deviation in the Redlich-Kister fitting.

However, it should be noted that second virial coefficients are also used in the evaluation of the compositions, having thus an indirect influence on the final G^E values. Assuming that all terms but $\tau_{i,0}$ and $\tau_{i,1}$ are negligible, by differentiating (5.34) the relationship

$$\frac{\partial y_1}{\partial B_{11}} \simeq -y_1 \frac{(P - P_1^*)}{RT} \qquad \ldots \text{(AK.1)}$$

is obtained. Considering the expression written in terms of finite differences and taking the latter as the errors associated with the corresponding variables, one obtains:

$$\frac{\varepsilon_y}{y} \simeq \frac{(P - P_i^*)}{RT} \varepsilon_B \qquad \ldots \text{(AK.2)}$$

$$\sim 10^{-4} \varepsilon_B \ .$$

On the other hand, by a similar procedure equation (5.48), (taken as a first approximation), gives:

$$\frac{\varepsilon_y}{y} \simeq \left[2\alpha(x_1 - 1) - 1\right] \frac{\varepsilon_x}{x} \qquad \ldots \text{(AK.3)}$$

or

$$\frac{\varepsilon_y}{y} \sim 2 \frac{\varepsilon_x}{x}$$

since $\alpha \sim 1$. Therefore, if one aims at an error of not more than a few parts in 10^4 for the liquid and vapour phase mole fractions, the second virial coefficients must be known to within a few $cm^3\,mol^{-1}$.

APPENDIX (L)

ERRORS IN V^E

The definition of excess molar volume, equation (6.6), shows that the errors in V^E arise from the uncertainty in the determination of the molar volume of the liquid mixture, from that of the pure components, and also from the error associated with the compositions x_i. Since V^E is always a small quantity when compared with the two terms from whose difference it is obtained, it is worthwhile to discuss this matter in some detail.

Accepting the principle of superposition of errors, an upper limit of the absolute error affecting the excess molar volume, ε_{V^E}, will be given by

$$|\varepsilon_{V^E}| \leq |\varepsilon_V| + |\varepsilon_{V^{id}}| \quad . \qquad \ldots \text{(AL.1)}$$

In the following calculations it will be assumed that the molar volumes of the two pure liquids are of the order of $35-45\ cm^3\ mol^{-1}$ and that the binary mixture is equimolar, $x_1 = x_2 = x = 0.5$. This means that about 3×10^{-2} mol of each component are needed to fill the pyknometer ($V_{pk} \sim 2\ cm^3$) with the mixture.

The molar volume of the mixture is given by the quotient between the volume of the liquid in the pyknometer ($V^L \simeq V_{pk}$) and the total number of moles of mixture ($n \simeq 6 \times 10^{-2}$ mol), and therefore

$$|\varepsilon_V| \leq \frac{1}{n} |\varepsilon_{V^L}| + \frac{V^L}{n^2} |\varepsilon_n| \qquad \ldots \text{(AL.2)}$$

where $|\varepsilon_{V^L}|$, obtained from equation (6.5), is given by

$$|\varepsilon_{V^L}| \leq |\varepsilon_{V_{pk}}| + |(h_m - h_r)||\varepsilon_\phi| + 2\phi\ |\varepsilon_h| , \qquad \ldots \text{(AL.3)}$$

so that

$$|\varepsilon_{V^L}| \simeq |\varepsilon_{V_{pk}}| \sim 3 \times 10^{-4}\ cm^3 .$$

The error in the calculation of the number of moles has already been obtained,

in Appendix (E). In the present case it is $\varepsilon_n \leq 3 \times 10^{-5}$ mol, since two components have to be admitted in the pyknometer. Then, $|\varepsilon_V| \leq 0.021\ \mathrm{cm^3\,mol^{-1}}$. The second term in the right-hand side of equation (6.6) can be written as

$$V^{id} = V_2^* + (V_1^* - V_2^*)\, x_1$$

$$= V^* + (\delta V^*)\, x\ , \qquad \ldots \text{(AL.4)}$$

giving

$$|\varepsilon_{V^{id}}| \leq 2|\varepsilon_{V^*}| + |(\delta V^*)||\varepsilon_x|\ . \qquad \ldots \text{(AL.5)}$$

The value of $|\varepsilon_x|$ is $\sim 7.5 \times 10^{-4}$, as obtained from Appendix (E), and the difference δV^* will be assumed to be $\sim 10\ \mathrm{cm^3\,mol^{-1}}$, a representative figure for the systems studied. The error in the molar volume of a pure component ε_{V^*} is calculated in the same way as ε_{V^L}, noting that for a pure substance $\varepsilon_n \sim 1.5 \times 10^{-5}$ mol. The evaluation gives $|\varepsilon_{V^*}| \leq 0.013\ \mathrm{cm^3\,mol^{-1}}$. Therefore, $|\varepsilon_{V^{id}}| \leq 0.034\ \mathrm{cm^3\,mol^{-1}}$, thus giving $|\varepsilon_{V^E}| \leq 0.055\ \mathrm{cm^3\,mol^{-1}}$. As said, this is an upper limit for the uncertainty in V^E, obtained by assuming the most unfavourable combination of the sources of error. In a real case, however, there will be some degree of mutual cancellation, so that the actual value of the final error affecting V^E will be, in general, somewhat less than the calculated upper limit.

Perhaps a more realistic figure can be obtained as follows. By averaging the standard deviations of more than twenty experimental molar volumes of five of the pure substances studied (Xe, $HC\ell$, N_2O, C_2H_4 and CF_4) the result is $\sigma(V^*) = \pm 0.005\ \mathrm{cm^3\,mol^{-1}}$. This can be taken as the statistical error in the determination of V^*. If it is assumed that the other terms contributing to ε_{V^E} are reduced in the same proportion, the uncertainty in V^E changes to

$$\varepsilon_{V^E} \simeq 0.020\ \mathrm{cm^3\,mol^{-1}}$$

which is probably a better estimate of the final error. In fact, this value is much closer to the standard deviations obtained on fitting the experimentally determined excess molar volumes to an equation of the type of (6.7), which are of the order of $0.010\ \mathrm{cm^3\,mol^{-1}}$.

APPENDIX (M)

ERRORS IN H^E

The composition of the mixture can usually be calculated to within a few parts in 10^4. The main factors which determine the magnitude of this error are the uncertainties in the measurement of the temperature and pressure of the gas in the calibrated storage globes (G_1 and G_2, Fig. 4.2). Combined deviations of ± 0.05 K and ± 6 Pa in these variables produce an error of less than $\pm 3 \times 10^{-4}$ in the composition of the final liquid mixture, for $0.2 \leqslant x \leqslant 0.8$.

The uncertainty in the calibration of the volume of the two cavities in the mixing vessel, which can affect the calculated distribution of the components between liquid and vapour (and hence the final value of H^E), only becomes important at pressures near the practical upper limit ($\sim$ 1.2 MPa). Even in this case an error of ± 0.05 cm^3 in the volume of the smaller (upper) compartment introduces deviations of less than ± 0.6 J mol^{-1} in H^E and of about $\pm 3 \times 10^{-4}$ in the composition of the liquid phase.

In the calculation of H^E the results from other experiments, namely those concerned with P_m and G^E, are used. An error of ± 0.5 kPa in the value of the vapour pressure of the mixture has no influence upon either H^E or the calculated composition of the liquid mixture in the calorimeter. If the experimental G^E are considered to be uncertain by as much as 1.5 J mol^{-1}, which is the order of the largest standard deviation encountered in the present work, errors of less than $\pm 10^{-4}$ in the composition of the liquid, and as low as ± 0.6 J mol^{-1} in H^E will result for the equimolar mixture (under the highest working pressure conditions).

Both the quality of the data used in the evaluation of the correction terms ψ_2 to ψ_7 of eqn (7.14), and the uncertainty in the experimental

determination of the quantity Q_H can be responsible for errors affecting the final values of the excess enthalpy H^E. Since the total amount of liquid mixture, n(L), is in most cases of the order of 10^{-1} mol the error in Q_H is multiplied by a factor of ~ 10 on calculating H^E. However, the energy supplied to the calorimeter, being a function of the potentials V_1 and V_2 and of the time t (as shown by eqn (4.4)), can be very accurately determined. In fact, taking a representative experiment, errors as large as 3×10^{-5} V in V_1 and V_2, and 5×10^{-3} s in t together introduce only an uncertainty of less than 10^{-2} J in the value of Q_H. Therefore, the main source of the uncertainty in Q_H will probably arise from the graphical method used to work out the correction for the uncompensated ΔT (and the energy of friction on opening the central valve), Fig. 4.8. It is difficult to assess the magnitude of this error since it can vary widely from case to case according to the ability of the experimentalist to achieve an acceptable value of ΔT in as short a time as possible after opening the central valve. It can be said, however, that whenever such uncertainties contribute to Q_H by more than, say, ± 0.3 J (corresponding to an error of $\sim \pm 4$ J mol^{-1} in H^E) the run ought to be discarded. This is, of course, a limiting situation very seldom encountered in practice. It is usually possible, after some experience, to operate in such a way as to keep the uncertainty well below this limit.

It remains to discuss the errors associated with the correction terms ψ_2 to ψ_7, among which the leading ones are the vaporization corrections, ψ_6 and ψ_7. In these last two, the $P\Delta V_v$ quantities are generally much smaller than the corresponding ΔH_v. Only for experiments carried out at temperatures near the critical point of any one of the two components is $P_i^* \Delta V_{v,i}$ likely to contribute significantly. Such conditions were, however, uncommon in our work, most of the heat of mixing experiments being carried out slightly above the triple-point temperature of one of the pure

liquids, with the other component being never too far from its normal boiling point. In these conditions accurate values of ΔH_v for both substances at or near the temperature of the experiment are usually available. Temperature corrections may have to be applied to ΔH_v over small temperature intervals, but, again, the uncertainty introduced by this is small. Therefore, it can be considered that the errors in the enthalpies of vaporization are of the order of magnitude of those reported in the literature for the experimental determination of ΔH_v. This quantity is usually known to better than $\pm 30\,J\,mol^{-1}$, an error which causes deviations not larger than $\pm 0.2-0.3\,J\,mol^{-1}$ in H^E if the total pressure of the mixture is of the order of 0.2-0.3 MPa. The magnitude of ψ_6 and ψ_7 (and also that of their respective uncertainties) rapidly increases with increasing temperature, due to the larger amounts of substance transferred from one phase to the other (larger δn_i). Under extreme conditions (i.e., when the vapour pressure of the more volatile component is of the order of 1.2 MPa, and the relative volatility of the two pure liquids is large, say, ~ 10) the errors affecting terms ψ_6 and ψ_7 can reach $\pm 3-4\,J\,mol^{-1}$.

As for the other terms, the overall contribution of ψ_2 to ψ_4 to the final value of H^E seldom exceeds $\sim 2\,J\,mol^{-1}$ for $P_m \sim 0.2-0.3$ MPa, so that errors of ± 20% in V^E and ± 100% in $\alpha^*_{P,i}$ never cause deviations in H^E larger than $\sim \pm 0.5\,J\,mol^{-1}$.

Term ψ_5 results from the addition of two quantities relating to each of the pure components. Except in the vicinity of an azeotrope these two quantities bear opposite signs, thus partly cancelling each other. At low pressures, errors of 2% in the second virial coefficients have a negligible effect on H^E or on the compositions. However, at higher pressures the relative importance of ψ_5 increases due to the larger amount of material in the vapour phase, so that the same uncertainty in B_{ii} gives rise to larger deviations in H^E (up to about $\pm 3\,J\,mol^{-1}$) and also in the calculated composition of the liquid (of about $\pm 10^{-4}$).

In short, it can be said that under low-pressure conditions ($P_m \sim 0.2$ MPa) H^E can usually be determined to within ± 3-$4\ J\ mol^{-1}$, 75% of this error arising from instrumental factors. At higher pressures the uncertainty in H^E rises to about three times this value, mainly due to the increasing influence of the errors in the data needed for the calculation of the correction terms, which can be responsible for more than 50% of the total uncertainty in H^E. In both cases the composition of the liquid can be calculated to within a few parts in 10^4.

The final uncertainty in the experimental values of the excess enthalpy is of the order of magnitude of the standard deviation of the fitting of H^E as a function of composition.

APPENDIX (N)

ESTIMATION OF V^E FOR $CH_4 + C_2H_4$

In recent publications[1,2] methods based on the FRISCH-LONGUET-HIGGINS-WIDOM (FLHW) equation of state for an hard-sphere fluid[3] have been used to estimate volume changes on mixing.

RODOSEVICH and MILLER[2] added to the basic equation of state a third parameter c, essentially a shape factor, so that

$$\frac{PV}{RT} = c\left[\frac{1+Y+Y^2}{(1-Y)^3}\right] - \frac{a}{RTV} , \qquad \ldots (AN.1)$$

where

$$Y = b/4V . \qquad \ldots (AN.2)$$

For spherically symmetrical molecules $c = 1$, while for r-mer-like species, namely the normal alkanes, c can be assessed from knowledge of the molecular structure[2]. It can also be expressed in terms of the acentric factor:

$$c = (10/3)\,\omega + (7/6) . \qquad \ldots (AN.3)$$

RODOSEVICH and MILLER used the theory of SNIDER and HERRINGTON[4] to evaluate the parameters a and b (regarded as independent of temperature) from experimental values of the liquid molar volumes of the pure components and their enthalpies of vaporization. Thus, the expression

$$\frac{\Delta H_v}{RT} = c\left[\frac{1+Y+Y^2}{(1-Y)^3}\right] + 1 - \frac{2PV}{RT} \qquad \ldots (AN.4)$$

was used together with eqn (AN.1) to estimate a and b. Once the parameters for the pure components (a_{ii}, b_{ii}, and c_{ii}) had been obtained, values of a, b and c for the liquid mixture were determined by using the van der Waals mixing rules:

$$a = \sum_i \sum_j x_i\, x_j\, a_{ij} \qquad \ldots (AN.5)$$

$$b = \sum_i \sum_j x_i\, x_j\, b_{ij} \qquad \ldots (AN.6)$$

$$c = \sum_i \sum_j x_i\, x_j\, c_{ij} , \qquad \ldots (AN.7)$$

the cross-parameters being evaluated from the expressions

$$b_{ij} = \left[\tfrac{1}{2}\left(b_{ii}^{\frac{1}{3}} + b_{jj}^{\frac{1}{3}}\right)(1 + j_{ij})\right]^3 \qquad \ldots \text{(AN.8)}$$

$$a_{ij} = (a_{ii}\, a_{jj})^{\frac{1}{2}} \left(b_{ij}^2 / b_{ii}\, b_{jj}\right)^{\frac{1}{2}} (1 - k_{ij}) \qquad \ldots \text{(AN.9)}$$

$$c_{ij} = \tfrac{1}{2}\left(c_{ii} + c_{jj}\right) . \qquad \ldots \text{(AN.10)}$$

In these equations j_{ij} and k_{ij} are the parameters expressing the deviations from the Lorentz-Berthelot rules (Chapter 9). They can be evaluated by using experimental values of either $V_{\frac{1}{2}}^E$ and $G_{\frac{1}{2}}^E$ or $V_{\frac{1}{2}}^E$ and $H_{\frac{1}{2}}^E$. It should be noted that the two fittings usually give different sets of j_{ij}, k_{ij} values, which means that by this method estimate of the third of the primary excess functions (H^E or G^E, respectively) cannot be accurately made from the knowledge of the other two. [Evidence for this is provided, for instance, by the results for $CH_4 + N_2$ in Refs (2) and (5).]

In their paper on $CH_4 + C_2H_4$, CALADO and SOARES[1] used a blend of the method proposed by RODOSEVICH and MILLER[2] and an approach based on the equation of state for hard convex bodies of arbitrary shape developed by GIBBONS[6,7].

This equation is

$$\frac{PV}{RT} = \left[\frac{3 + (3\phi_s - 6)Y + (3 - 3\phi_s + \phi_s^2)Y^2}{3(1 - Y)^3}\right] - \frac{a}{RTV} , \qquad \ldots \text{(AN.11)}$$

where Y is given by eqn (AN.2), and ϕ_s is a shape factor which can be calculated from the geometry of the individual molecules of the pure components. For spherical molecules $\phi_s = 3$, so that in this case eqns (AN.11) and (AN.1) both reduce to the orginal FLHW equation. For pure components, b and ϕ_s can be estimated from correlations due to BIENKOWSKI and CHAO[8]:

$$b = 4V_c(0.544046 - 0.010218\, T_R)^3 \qquad \ldots \text{(AN.12)}$$

$$\phi_s = 3 + 0.5600\,(V_c/b)\left[1 - \exp(-8.78\,\omega)\right] , \qquad \ldots \text{(AN.13)}$$

where $T_R = T/T_c$ is the reduced temperature. [ϕ_s is actually γ/α in the notation of Ref. (8).] The parameter a is then obtained from eqn (AN.11) and experimental information on the molar volume of the pure liquids. This method can be applied to estimate the molar volume of liquid mixtures by using the combination rules (AN.5) - (AN.10), with the last of these equations written in terms of the appropriate shape factor, ϕ_s.

The two methods just described are quite similar, so that one might expect equivalent results from both. However, it is well known that the main deficiency in the use of equations of state for the estimation of excess properties is that they can become quite inaccurate when extrapolation is made to temperature (or pressure) regions far from those at which the empirical parameters were calculated to fit the experimental information. In the present case we aimed at the estimation of V^E for liquid mixtures of $CH_4 + C_2H_4$ at temperatures up to 150 K from the knowledge of the experimental results at ~104 K. Therefore, it seemed desirable to compare the experimental V^E values with those evaluated from the two above mentioned methods of estimation, since any slight differences that might be apparent at 104 K would certainly become more important at 140 and 150 K.

BLINOWSKA, HERRINGTON and STAVELEY[9] pointed out that agreement between estimated and experimental values of the excess functions would be improved if the parameters a and b in the SNIDER-HERRINGTON equation of state were regarded as temperature dependent. It also seemed preferable to use ΔH_v^0 — the molar enthalpy of vaporization to give the infinitely dilue, perfect gas — instead of the value ΔH_v at the saturation vapour pressure and the normal boiling point. ΔH_v^0 is readily obtained from the knowledge of ΔH_v and the virial coefficients.

In estimating V^E by the method proposed by RODOSEVICH and MILLER we have therefore replaced ΔH_v by ΔH_v^0 in eqn (AN.4). Moreover, the

enthalpies of vaporization were calculated at the temperature of interest (104 K) rather than at the normal boiling point of the two components. The information required for this was taken from GOODWIN's report[10] and from EGAN and KEMP[11], respectively, for methane and ethylene. The liquid molar volumes and vapour pressures necessary to evaluate a_{ii} and b_{ii} were those measured by CALADO and SOARES[1]. As regards the shape factor c, we considered[2] $c_{11} = 1.00$, and for ethylene $c_{22} = 1.45$ as calculated from eqn (AN.3) using $\omega_2 = 0.086$. The complete set of parameters for the pure liquids at 104 K is then:

$$a_{11} = 2.813 \times 10^5 \text{ J cm}^3 \text{ mol}^{-2} \qquad b_{11} = 63.848 \text{ cm}^3 \text{ mol}^{-1} \qquad c_{11} = 1.00$$

$$a_{22} = 6.438 \times 10^5 \text{ J cm}^3 \text{ mol}^{-2} \qquad b_{22} = 81.813 \text{ cm}^3 \text{ mol}^{-1} \qquad c_{22} = 1.45 \text{ .}$$

The deviation parameters needed to evaluate a_{12} and b_{12} were obtained as follows: $k_{12} = 0.040$ was simply taken from Ref. (1), while a value of $j_{12} = -0.002$ was found necessary to reproduce the experimental $V^E_{\frac{1}{2}}$. The V^E results obtained by this method are represented in Fig. AN.1, curve B.

On applying the second technique the following values were found for the parameters:

$$a_{11} = 2.511 \times 10^5 \text{ J cm}^3 \text{ mol}^{-2} \qquad b_{11} = 60.339 \text{ cm}^3 \text{ mol}^{-1} \qquad \phi_{s,1} = 3.100$$

$$a_{22} = 5.519 \times 10^5 \text{ J cm}^3 \text{ mol}^{-2} \qquad b_{22} = 82.625 \text{ cm}^3 \text{ mol}^{-1} \qquad \phi_{s,2} = 3.471$$

and

$$k_{12} = 0.040 \qquad\qquad j_{12} = +0.004 \text{ .}$$

The estimated V^E are shown, curve A, in Fig. AN.1, where the experimental points of CALADO and SOARES[1] are also included.

It is apparent from the figure that the method of RODOSEVICH and MILLER gives, in the present case, the asymmetry of the curve in the wrong direction, and therefore it was not selected to estimate V^E at the higher temperatures. For this purpose we accordingly preferred the method based

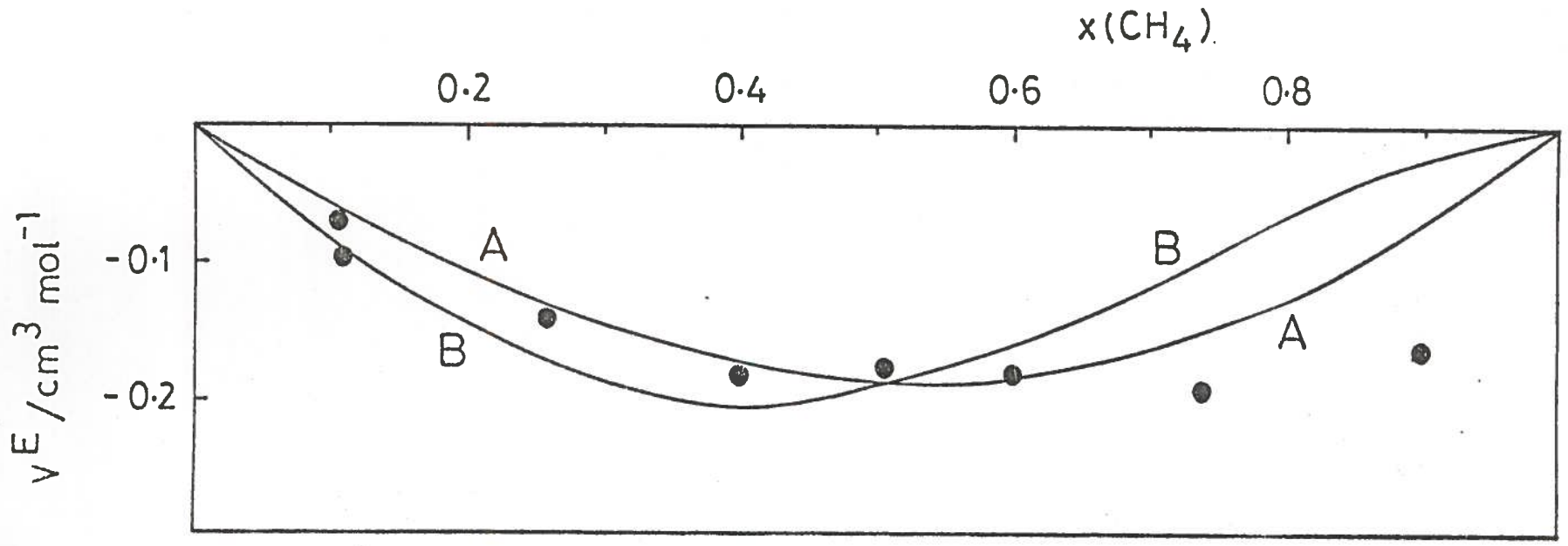

Fig. AN.1

$CH_4 + C_2H_4$: V^E (104 K) as a function of composition. Points are experimental [Ref. (1)] and lines are calculated.

on GIBBONS' equation of state. On using it, however, all the parameters were considered temperature dependent. This was made possible by the existence of data for the molar volume[1,10,12,13] and vapour pressure[1,10,11] of the two components at the temperatures of interest: 116, 140 and 150 K. The values of the parameters for the two pure liquids were calculated as indicated in Table AN.1.

TABLE AN.1

PARAMETERS OF EQN (AN.11) FOR THE PURE COMPONENTS

T/K	116	140	150
$a_{11} \times 10^{-5}$/J cm^3 mol^{-2}	2.588	2.676	2.690
$a_{22} \times 10^{-5}$/J cm^3 mol^{-2}	5.780	6.145	6.261
b_{11} / cm^3 mol^{-1}	59.880	58.970	58.593
b_{22} / cm^3 mol^{-1}	82.426	82.029	81.864
$\phi_{s,1}$	3.101	3.102	3.103
$\phi_{s,2}$	3.472	3.475	3.476

The estimated excess molar volumes V^E at the three temperatures were, finally, fitted to the equation

$$V^E = x_1 (1 - x_1) [A_V + B_V (2 x_1 - 1) + C_V (2 x_1 - 1)^2]$$

the values of A_V, B_V and C_V being indicated in Section 16.2 of the main text.

(1) CALADO, J.C.G. and SOARES, V.A.M., J. Chem. Soc., Faraday I, 1977, 73, 1271.

(2) RODOSEVICH, J.B. and MILLER, R.C., Adv. Cryogenic Eng., 1974, 19, 339.

(3) LONGUET-HIGGINS, H.C. and WIDOM, B., Mol. Phys., 1964, 8, 549.

(4) SNIDER, N.S. and HERRINGTON, T.M., J. Chem. Phys., 1967, 47, 2248.

(5) McCLURE, D.W., LEWIS, K.L., MILLER, R.C. and STAVELEY, L.A.K., J. Chem. Thermodynamics, 1976, 8, 785.

(6) GIBBONS, R.M., Mol. Phys., 1969, 17, 81.

(7) GIBBONS, R.M., Mol. Phys., 1970, 18, 809.

(8) BIENKOWSKI, P.R. and CHAO, K.-C., J. Chem. Phys., 1975, 63, 4712.

(9) BLINOWSKA, A., HERRINGTON, T.M. and STAVELEY, L.A.K., Cryogenics, 1973, 13, 85.

(10) GOODWIN, R.D., 'The Thermophysical Properties of Methane from 90 to 500 K and Pressures to 700 bar', NBS Tech Note 653, 1974.

(11) EGAN, C.J. and KEMP, J.D., J. Am. Chem. Soc., 1937, 59, 1264.

(12) CALADO, J.C.G., PONTE, M.N.da, SOARES, V.A.M. and STAVELEY, L.A.K., J. Chem. Thermodynamics, 1978, 10, 35.

(13) MENES, F., DORFMÜLLER, T. and BIGELEISEN, J., J. Chem. Phys., 1970, 53, 2869,